EP2DS.20
MSS.16
Wrocław 2013

20th International Conference on

Electronic Properties of Two-Dimensional Systems

and

16th International Conference on

Modulated Semiconductor Structures

Abstracts

plenary – invited – contributed talks

1 – 5 July 2013

Wrocław University of Technology Congress Centre
Wrocław, Poland

Dear Participants of EP2DS-20 and MSS-16,

Welcome to the joint conferences on *Electronic Properties of Two-Dimensional Systems (EP2DS)* and *Modulated Semiconductor Structures (MSS)*, organized by the Institute of Physics Wrocław University of Technology, in collaboration with the Institute of Physics, Polish Academy of Sciences.

The meeting has long tradition, reaching back to the first EP2DS conference organized by Professors John J. Quinn and Phillip J. Stiles at Brown University in 1976. It has been usually organized once in two years, alternately in America, Asia, and Europe. The last three editions took place in Genova, Italy (2007), Kobe, Japan (2009) and Tallahassee, USA (2011), and this year we have a privilege to host it for the first time in Poland.

Both conferences have established high reputation in the broad area of low-dimensional physics. EP2DS traditionally emphasizes fundamental physics, including transport and optical properties of electronic states in low-dimensional systems including graphene, nanotubes, and dielectric interfaces, while MSS addresses synthesis, processing and applications of modulated materials and novel systems including a broader range of carbon-based, hybrid, modulated organic, spintronic, and biologically based structures.

The topics highlighted by the 8 *plenary lectures* include fractional quantum Hall effect, graphene, topological insulators, quantum dots, condensates, and spintronics. *Special joint session* will also be devoted to Majorana fermions.

The conference host, *Wrocław University of Technology*, is a leading Polish university, ranked in the top five nationwide in academic quality and prestige.

The 1000 years old City of Wrocław, with the population over 600 000, is the capital of the south-western province of Poland “Lower Silesia”. It is majestically situated on 12 islands on river Odra, linked by over 150 bridges. It is also the third largest Polish educational centre, with 170 000 students and 6 300 academic staff in 30 colleges, including Wrocław University of Technology as the largest one.

The Conference is proud of the Honorary Patronage of Polish Ministry of Science and Higher Education, National Centre for Research and Development, National Science Centre, Polish Physical Society, and Rector of Wrocław University of Technology. We also gratefully acknowledge financial support from Polish Ministry of Science and Higher Education, International Union of Pure and Applied Physics, and U.S. Army. The list of sponsors includes Comef, Newport, attocube, Raith, Hamamatsu Photonics Deutschland, SPS-Europe, Scontel, and PGE GiEK.

We look forward to welcoming you in Wrocław and wish you all a fruitful meeting and enjoyable time!

Jan Misiewicz   Arkadiusz Wójs   Jacek Kossut   Tomasz Dietl

Committees

Organizers

Jan Misiewicz – Conference Chair
(*Institute of Physics, Wrocław University of Technology*)

Arkadiusz Wójs – Program Chair
(*Institute of Physics, Wrocław University of Technology*)

Jacek Kossut – EP2DS Chair
(*Institute of Physics , Polish Academy of Sciences, Warsaw*)

Tomasz Dietl – MSS Chair
(*Institute of Physics , Polish Academy of Sciences, Warsaw*)

International Advisory Committee

Gerhard Abstreiter	(*Germany*)
Gunther Bauer	(*Austria*)
Fabio Beltram	(*Italy*)
Sankar Das Sarma	(*USA*)
Lloyd W. Engel	(*USA*)
Klaus Ensslin	(*Switzerland*)
Vladimir Fal'ko	(*UK*)
Alfred Forchel	(*Germany*)
Christian Glattli	(*France*)
M. Zahid Hasan	(*USA*)
Moty Heiblum	(*Israel*)
Yoshiro Hirayama	(*Japan*)
Tae-Won Kang	(*South Korea*)
Belita Koiller	(*Brazil*)
Leo P. Kouwenhoven	(*Netherlands*)
Steven G. Louie	(*USA*)
Charles Marcus	(*Denmark*)
Bruce D. McCombe	(*USA*)
Aron Pinczuk	(*USA*)
John J. Quinn	(*USA*)
C. N. R. Rao	(*India*)
David A. Ritchie	(*UK*)
Michelle Y. Simmons	(*Australia*)
Maurice Skolnick	(*UK*)
Robert A. Suris	(*Russia*)
Carlos Tejedor	(*Spain*)
Paul Voisin	(*France*)
Klaus von Klitzing	(*Germany*)
Enge Wang	(*China*)
Robert M. Westervelt	(*USA*)
Qi-Kun Xue	(*China*)
Hou Zhi Zheng	(*China*)

EP2DS Program Committee

Jacek Kossut (Chair)	*Polish Academy of Sciences, Warsaw, Poland*
Manfred Bayer	*Technische Universität Dortmund, Germany*
Rolf J. Haug	*Leibniz Universität Hannover, Germany*
Philip Hofmann	*Aarhus University, Denmark*
Igor Kukushkin	*Russian Academy of Sciences, Chernogolovka, Russia*
Patricia Lustoza de Souza	*Pontifícia Universida de Católica, Rio de Janeiro, Brasil*
Alberto Morpurgo	*Université de Genève, Switzerland*
Daniela Pfannkuche	*Universität Hamburg, Germany*
Marek Potemski	*Grenoble High Magnetic Field Laboratoy, France*
Andrew Sachrajda	*National Research Council, Ottawa, Canada*
Mansour Shayegan	*Princeton University, USA*
Steven H. Simon	*University of Oxford, UK*
Adiel Stern	*Weizmann Institute of Science, Rehovot, Israel*
Seigo Tarucha	*University of Tokyo, Japan*
Arkadiusz Wójs	*Wrocław University of Technology, Poland*

MSS Program Committee

Tomasz Dietl (Chair)	*Polish Academy of Sciences, Warsaw, Poland*
Alexander V. Chaplik	*Russian Academy of Sciences, Novosibirsk, Russia*
Scott A. Crooker	*Los Alamos National Laboratory, USA*
Łukasz Cywiński	*Polish Academy of Sciences, Warsaw, Poland*
Jonathan Finley	*Technische Universität München, Germany*
Jean-Michel Gerard	*Service de Physique des Matériaux et des Microstructures (CEA/INAC/SP2M) Grenoble, France*
Shingo Katsumoto	*University of Tokyo, Japan*
Junichiro Kono	*Rice University, Houston, USA*
Hideo Ohno	*Tohuku University, Sendai, Japan*
Amalia Patane	*University of Nottingham, UK*
Raimundo Rocha dos Santos	*Universida de Federal do Rio de Janeiro, Brazil*
Ludvik Smrcka	*Akademie věd České republiky, Prague, Czech Republic*
Marzena Szymanska	*University of Warwick, Coventry, UK*
Alexander Tartakovskii	*University of Sheffield, UK*
Luis Vina	*Universidad Autónoma de Madrid, Madrid, Spain*

Local Committee

Jan Misiewicz (Chair)	*Institute of Physics, Wrocław University of Technology*
Adam Babiński	*Institute of Physics, University of Warsaw*
Leszek Bryja	*Institute of Physics, Wrocław University of Technology*
Paweł Machnikowski	*Institute of Physics, Wrocław University of Technology*
Paweł Podemski	*Institute of Physics, Wrocław University of Technology*
Katarzyna Roszak	*Institute of Physics, Wrocław University of Technology*
Grzegorz Sęk	*Institute of Physics, Wrocław University of Technology*
Piotr Sitarek	*Institute of Physics, Wrocław University of Technology*

Patronage

Ministry of Science and Higher Education, Poland

National Centre for Research and Development, Poland

National Science Centre, Poland

Polish Physical Society

Rector of Wrocław University of Technology, Poland

Financial Support

Ministry of Science and Higher Education, Poland

International Union of Pure and Applied Physics

U.S. Army Forward Element Command – Atlantic

Sponsors

COMEF Scientific & Research Equipment, Poland and Newport, Germany

attocube systems AG, Germany

Raith GmbH, Germany

Hamamatsu Photonics Deutschland GmbH, Germany

SPS-Europe B.V., The Netherlands

Scontel, Russia

PGE Górnictwo i Energetyka Konwencjonalna S.A., Poland

Social Program

The following special attractions are offered free of charge to all registered participants and accompanying persons.

Guided city excursions (Wednesday, 13.30 – 16.15)

We propose a few guided excursions around the most interesting places in Wrocław, e.g.:

The oldest part of the city: The Old Town includes the Gothic St. John's Cathedral, the Renaissance houses near the Market Square, the Baroque university and lots of fine examples of Art Nouveau and Functionalism.

The Centennial Hall and the Japanese Garden: The Centennial Hall is the most famous work of Wrocław Modernism. It was listed as a UNESCO World Heritage Site in 2006. The Japanese Garden located within Szczytnicki Park is one of the few traces of the 1913 World's Fair that was held in Wroclaw.

The Quarter of Tolerance: The Quarter of Four Temples also known as The Quarter of Tolerance is an old part of the city, where four religions coexist: Lutheran Protestantism, Orthodox Christianity, Catholicism and Judaism.

Conference Banquet (Wednesday, 19.30 – 21.00)

The Conference Banquet will take place in the splendid City Hall at the heart of our historic Market Square.

Music Concert (Thursday, 20.00 – 21.00)

The Music Concert is planned in Wrocław's magnificent Opera House located within walking distance of Market Square. Soloists of the opera will present the specially chosen repertoire.

Additional attractions are also available at modest fees (detailed information is available at registration desks).

1 July (Monday)

Wrocław University of Technology Main Building

1 July (Monday)

8.30	**Official Opening of the Conference** **Tadeusz Więckowski**, Rector of Wrocław University of Technology

Plenary Session 1

9.00 – 9.45	**MoPlenary1** **James P. Eisenstein** (*Caltech, USA*) Recent results from single and double layer quantum Hall systems
9.45 – 10.30	**MoPlenary2** **Takao Someya** (*University of Tokyo, Japan*) Ultraflexible and stretchable organic devices

Plenary Session 2

11.00 – 11.45	**MoPlenary3** **Jainendra K. Jain** (*Penn State University, USA*) Fractional quantum Hall effect: What's new
11.45 – 12.30	**MoPlenary4** **Shoucheng Zhang** (*Stanford University, USA*) Completion of the quantum Hall trio

EP2DS Session 1

14.00 – 14.30 **MoIE1**
Ursula Wurstbauer
(*Columbia University, USA; TU Munich, Germany*)
Coexistence of phases and gapped excitations in the second LL: Fundamental insights from inelastic light scattering

14.30 – 14.45 **MoOE1**
Trevor D. Rhone, Lars Tiemann, Koji Muraki
(*NTT Corporation, Japan; JST, Japan*)
NMR reveals maximum spin polarization in the presence of Wigner crystal domains at $\nu \sim 3$

14.45 – 15.00 **MoOE2**
Junichiro Hayakawa[1], Koji Muraki[2], Go Yusa[1]
([1]*Tohoku University;* [2]*NTT Corporation, Japan*)
Real-space imaging of fractional quantum Hall effect

15.00 – 15.15 **MoOE3**
I. Gurman, R. Sabo, M. Heiblum, V. Umansky, D. Mahalu
(*Weizmann Institute of Science, Israel*)
Extracting net current from an upstream neutral mode in the fractional quantum Hall regime

MSS Session 1

14.00 – 14.15 **MoOM1**
B. Schwarz, P. Reininger,W. Schrenk, H. Detz, O. Baumgartner, T. Zederbauer, A.M. Andrews, H. Kosina, G. Strasser
(*Vienna University of Technology, Austria*)
Monolithically integrated quantum cascade laser and detector

14.15 – 14.30 **MoOM2**
G. Cerulo[1], V. Liverini[1], P. Friedli[2], H. Sigg[2], *Faist*[1]
([1]*Institute of Quantum Electronics;* [2]*Paul Scherrer Institute, Switzerland*)
Optically driven current turnstile based on self-assembled semiconductor quantum dots

14.30 – 14.45 **MoOM3**
C. Sturm[1,2], D. Tanese[1], H.S. Nguyen[1], H. Flayac[3], E. Gallopin[1], A. Lemaître[1], I. Sagnes[1], D. Solnyshkov[3], A. Amo[1], G. Malpuech[3], J. Bloch[1] ([1]*LPN/CNRS-Marcoussis, France;* [2]*Universität Leipzig, Germany;* [3]*Clermont Université, Université Blaise Pascal, France*)
All-optical controlled polariton Mach-Zehnder interferometer

14.45 – 15.15 **MoIM1**
Y. Arakawa[1], M. Holmes[1], P. Podemski[2], K. Choi[1], M. Arita[1], S. Kako[1] ([1]*University of Tokyo, Japan;* [2]*Wrocław University of Technology, Poland*)
Advances in GaN quantum dots for coherent control

EP2DS Session 2

15.45 – 16.15 **MoIE2**
Tomasz Story
(*Polish Academy of Sciences, Poland*)
Topological crystalline insulator states in $Pb_{1-x}Sn_xSe$

16.15 – 16.30 **MoOE4**
S. Wiedmann[1], C. Brüne[2], A. Jost[1], F. Chiappini[1], C. Thienel[2], C. Ames[2], P. Leubner[2], U. Zeitler[1], J. C. Maan[1], H. Buhmann[2], L.W. Molenkamp[2]
([1]*Radboud University Nijmegen, The Netherlands;* [2]*Universität Würzburg, Germany*)
Ambipolar surface quantum Hall effect in the 3D TI strained HgTe

16.30 – 16.45 **MoOE5**
G. Springholz[1], J. Sanchez Barriga[2], H. Steiner[1], R. Kirchschlager[1], G. Bauer[1], A. Varykhalov[2], O. Rader[2], E. Schierle[2], E. Weschke[2], O. Caha[3], V. Holy[4]
([1]*Johannes Kepler University, Austria;* [2]*Helmholtz-Zentrum Berlin, Germany,* [3]*Masaryk University, Czech Republic;* [4]*Charles University Prague, Czech Republic*)
Dirac point band gap opening in ferromagnetic Mn-doped topological insulators of the bismuth chalcogenides

16.45 – 17.00 **MoOE6**
S.-J. Choi, S. Park, H.-S. Sim
(*Korea Advanced Institute of Science and Technology, Daejeon*)
Local and tunable geometric phase of Dirac fermions in a topological junction

MSS Session 2

15.45 – 16.00 **MoOM4**
J. Fischer[1], I. Lederer[1], A. Chernenko[2], S. Brodbeck[1], A. Rahimi-Iman[1], M. Amthor[1], C. Schneider[1], M. Kamp[1], S. Höfling[1]
([1]*Universität Würzburg, Germany;* [2]*Russian Academy of Sciences, Chernogolovka*)
Magnetic field pecularities of three distinct excitation regimes of a quantum-well microcavity

16.00 – 16.15 **MoOM5**
B. Askenazi[1], A. Delteil[1], A. Vasanelli[1], Y. Todorov[1], G. Beaudoin[2], I. Sagnes[2], C. Sirtori[1]
([1]*Univ. Paris Diderot, Sorbonne Paris Cité;* [2]*CNRS, Marcoussis, France*)
Ultrastrong light-matter coupling with multisubband plasmons

16.15 – 16.30 **MoOM6**
C. Antón[1], G. Tosi[1], M.D. Martín[1], Z. Hatzopoulos[2,3], G. Konstantinidis[2], P. Eldridge[2], P.G. Savvidis[2,3], L. Viña[1]
([1]*Universidad Autónoma de Madrid, Spain;* [2]*FORTH-IESL, Greece;* [3]*University of Crete, Greece*)
Implementation of an *AND* gate with Bose-Einstein polariton condensates

16.30 – 17.00 **MoIM2**
L. Dominici[1,2], D. Ballarini[1,2], M. De Giorgi[1,2], E. Cancellieri[3], A. Bramati[3], G. Gigli[1,2], F.P. Laussy[4], D. Sanvitto[1,2]
([1]*CBN Lecce, Italy;* [2]*NNL – CNR, Lecce, Italy;* [3]*LKB, ENS et CNRS, Paris, France;* [4]*Universidad Autonoma de Madrid, Spain*)
Fluids of polariton condensates: from a drop in a quantum pond to optical gates

Recent results from single and double layer quantum Hall systems

J.P. Eisenstein
Caltech

This talk will review some of our most recent experiments [1-4] on high mobility 2D electron systems in the fractional quantized Hall effect (FQHE) regime. For the case of single layer 2D systems the focus will be on transport phenomena in the N=1, or first-excited Landau level. In particular, I will describe experiments which demonstrate that the fate of the $\nu = 5/2$ FQHE state in tilted magnetic fields depends sensitively on the width of the quantum well confining the electrons and on the relative alignment of the Landau levels emanating from the various electric subbands of the quantum well. I will also present evidence for a FQHE state at $\nu = 7/3$ which simultaneously exhibits both a robust quantized Hall plateau and a strongly anisotropic longitudinal resistance.

In double layer 2D systems I will describe recent experiments on the excitonic QHE state at total Landau level filling $\nu_T = 1$. These experiments, done in Corbino geometries, have convincingly demonstrated that while the bulk of the 2D system is opaque to charged quasiparticle transport, it is essentially transparent to neutral exciton transport. This distinction is manifested by the very large electrical resistance encountered when *parallel* currents in the two layers attempt to cross the bulk in contrast to the very small resistance encountered by *antiparallel* currents. Among other things, the ready transport of excitons across the bulk leads to the curious phenomenon of "perfect Coulomb drag" in which a bulk current in one layer spontaneously generates an equal, but oppositely directed, bulk current in the other layer even though the layers are electrically isolated.

This work represents a collaboration with Vaclav Cvicek, Aaron Finck, Debaleena Nandi, Loren Pfeiffer, Ken West, and Jing Xia. Support from the US Department of Energy and National Science Foundation is gratefully acknowledged.

1. Jing Xia, Vaclav Cvicek, J.P. Eisenstein, L.N. Pfeiffer and K.W. West, Phys. Rev. Lett. **105**, 176807 (2010).
2. Jing Xia, J.P. Eisenstein, L.N. Pfeiffer and K.W. West, Nature Physics **7**, 845 (2011).
3. A.D.K. Finck, J.P. Eisenstein, L.N. Pfeiffer and K.W. West, Phys. Rev. Lett. **106**, 236807 (2011).
4. D. Nandi, A.D.K. Finck, J.P. Eisenstein, L.N. Pfeiffer and K.W. West, Nature **488**, 481 (2012).

Ultraflexible and stretchable organic devices

Takao Someya [1,2] **and Tsuyoshi Sekitani** [1,2]

[1] *School of Engineering, The University of Tokyo, 3-7-1 Hongo, Bunkyo-ku, Tokyo, Japan*
[2] *The Exploratory Research for Advanced Technology (ERATO), JST, Tokyo, Japan*

We have succeeded in manufacturing ultraflexible organic thin-film transistors, organic light-emitting diodes, and organic photovoltaic cells on ultrathin plastic film with the thickness as small as approximately 1 µm. These novel organic devices are much lighter than bird's feathers. First, we have demonstrated polymer-based photovoltaic devices on plastic foil substrates of 1.2 µm thick, with equal power conversion efficiency to their glass-based counterparts [1]. They can reversibly withstand extreme mechanical deformation and have unprecedented solar cell specific weight. Instead of a single bend, we were able to form a random network of folds within the device area. Then, we have manufactured organic transistors on ultrathin plastic films in order to achieve sharp bending radius less than 50 µm [2,3]. Bending cycle experiments will be presented to show the mechanical durability. Moreover, the issues and the future prospect of flexible organic devices such as thin-film transistors, photovoltaic cells, and memories will be addressed. In particular, the recent progress on reliability tests of organic devices, including thermal stability at 250 ºC, multiple bending cycles, stability in air, boiling water, and saline, will be presented [4]. Furthermore, ultraflexible and stretchable electronic systems have been exploited for biomedical applications such as medical catheters and implantable devices.

Figure 1: (Left) Stretchable integrated circuits based organic field-effect transistors. (Centre) Ultraflexible organic photovoltaic cell manufactured on a 1 µm-thick plastic film. (Right) Medical catheter with helical organic transistors integrated circuits.

[1] M. Kaltenbrunner, M. S. White, E. D. Glowacki, T. Sekitani, T. Someya, N. S. Sariciftci, S. Bauer, Nature Communications 3, 770 (2012).
[2] T. Sekitani, U. Zschieschang, H. Klauk, T. Someya, Nature Material 9, 1015 (2010).
[3] M. Kaltenbrunner, T. Sekitani, J. Reeder, T. Yokota, K. Kuribara, T. Tokuhara, M. Drack, R. Schwödiauer, I. Graz, S. Bauer-Gogonea, S. Bauer, and T. Someya (in press).
[4] K. Kuribara, H. Wang, N. Uchiyama, K. Fukuda, T. Yokota, U. Zschieschang, C. Jaye, D. Fischer, H. Klauk, T. Yamamoto, K. Takimiya, M. Ikeda, H. Kuwabara, T. Sekitani, Y-L. Loo, T. Someya, Nature Communications 3, 723 (2012).

Fractional quantum Hall effect: What's new

Jainendra K. Jain

Penn State University

After a brief review of the current status of the fractional quantum Hall effect (FQHE) and open problems, I will report on recent progress on the following topics [1, 2, 3, 4]:
Anti-Pfaffian pairing at 3/8: (In collaboration with S. Mukherjee, S.S. Mandal and A. Wójs [1].) We predict [1] that an incompressible fractional quantum Hall state is likely to form at $\nu = 3/8$ as a result of a chiral p-wave pairing of fully spin polarized composite fermions carrying four quantized vortices, and that the pairing is of the anti-Pfaffian kind. Experimental ramifications include quasiparticles with non-Abelian braid statistics and upstream neutral edge modes.
Phase diagram of two-component FQHE: (In collaboration with A.C. Archer [2].) Because of FQHE in graphene and AlAs quantum wells, there is renewed interest in the physics of FQHE for multi-component systems, where the components can be spin and/or valley/subband indices. We calculate the phase diagram of two component fractional quantum Hall effect as a function of the spin/valley Zeeman energy and *continuous* filling factor, which reveals new phase transitions and phase boundaries spanning many fractional plateaus. This phase diagram is relevant to fractional quantum Hall effect in graphene and in GaAs and AlAs quantum wells, when either the spin or the valley degree of freedom is active. Good agreement is found with experiment in AlAs and graphene.
Unconventional mechanism for FQHE at 4/11, 5/13: (In collaboration with S. Mukherjee, S.S. Mandal and A. Wójs [3].) The origin of the FQHE states at 4/11 and 5/13, evidence for which was seen a decade ago by Pan *et al.* (Phys. Rev. Lett. **90**, 016801, 2003), has remained controversial. We show [3] that these represent a new class of FQHE states, originating because of a peculiar interaction between composite fermions that suppresses occupation of pairs with relative angular momentum *three* rather than one. This confirms the mechanism proposed by Wójs, Yi and Quinn (Phys. Rev. B **69**, 205322, 2004). We make quantitative predictions for experiments, including a spin transition as a function of the Zeeman energy.
Composite fermion crystals: (In collaboration with A.C. Archer and K. Park [4].) We determine quantitatively the phase diagram of the crystal phase at low fillings, and find a rich variety of crystals of composite fermions. In particular, we convincingly show that the crystal between 1/5 and 2/9 is a "type-I crystal" of composite fermions carrying two vortices. We evaluate the dispersions of the magnetophonons and magnetoplasmons of the crystals, as well as their shear modulus, which shows discontinuity at the phase boundaries. Possible experimental signatures of the phase diagram are considered.

[1] S. Mukherjee, S. S. Mandal, A. Wójs, and J. K. Jain, Phys. Rev. Lett. **109**, 256801 (2012).
[2] A. C. Archer and J. K. Jain, Phys. Rev. Lett., in press.
[3] S. Mukherjee, S. S. Mandal, A. Wójs, and J. K. Jain, unpublished.
[4] A. C. Archer, K. Park and J. K. Jain, unpublished.

Completion of the quantum Hall trio

Shoucheng Zhang

Department of Physics, Stanford University, Stanford, CA 94305-4045, USA

In this talk, I shall give an overview of current research on topological insulators, with a focus on the discovery of the quantum spin Hall effect and the quantum anomalous Hall effect

INVITED

MoIE1

Coexistence of Phases and Gapped Excitations in the Second LL: Fundamental Insights from Inelastic Light Scattering*§

U. Wurstbauer [1,2]
[1] *Department of Physics, Columbia University, New York, USA*
[2] *Walter Schottky Institute and Department of Physics, TU Munich, Munich, Germany*

The competition between quantum phases that dictates the physics in the second Landau level (SLL) results in striking phenomena. Our work explores this fascinating interaction physics by measurements of low-lying neutral excitation modes in the SLL from resonant inelastic light scattering experiments. We focus here on the marked differences of the low-lying collective excitation spectra of the highly enigmatic even-denominator state at Landau level filling $\nu=5/2$, widely believed to support non-Abelian quasi-particle excitations, with those measured in states in the range $5/2>\nu>2$. In the comparisons of observed quasi-particle excitations from different quantum phases we emphasize the results for the state at 5/2 and odd-denominator state at $\nu=7/3=2+1/3$.

Whereas clear low-lying gapped excitations with energies of less than 0.1meV are observable exactly at filling factors representing incompressible FQHE states, these gapped modes completely collapse by very small changes in filling factor of $|\Delta\nu|<0.01$ [1].

The spectra at 5/2 reveal a band of gapped modes with peak intensity at energy of 0.07meV [1]. These modes are interpreted as a roton minimum in the wave vector dispersion of spin-conserving excitations. The intensity of the roton band significantly diminishes by increasing the temperature to 250mK and it fully collapses for T>250mK [1]. This temperature dependence is consistent with activated magneto-transport of the incompressible quantum fluid at 5/2. A long wavelength spin wave mode (SW) is seen at the bare Zeeman energy, indicating that there is non-zero spin-polarization.

The most significant difference for the incompressible fluids away from 5/2 such as 2+1/3 are the coexistence of a gapped lowest energy mode together with a broader band at energies above 0.2meV and a continuum of low-lying excitations. We interpret the coexistence of excitation modes as direct evidence of coexistence and competition of different phases in the second LL. This interpretation is supported by a striking temperature dependence of these modes. The disappearance of the gapped modes by small deviations in filling factor found for $\nu=5/2$ and 2+1/3 and also evident for weaker states at 2+2/5 and 2+3/8 demonstrates a transition from an incompressible quantum Hall fluid to compressible states at very close filling factors.

(*) Research supported by the U.S. National Science Foundation and the Alexander von Humboldt Foundation (Germany).
(§) This work is in collaboration with A. Pinczuk, A. L. Levy, K. W. West. Loren N. Pfeiffer, S. Mondal, J. Watson, and M. J. Manfra.

[1] U. Wurstbauer, K.W. West, L. N. Pfeiffer, and A. Pinczuk, Phys. Rev. Lett. **110**, 026801 (2013).

Monday
Tuesday
Wednesday
Thursday
Friday

MoOE1

Monday Tuesday Wednesday Thursday Friday

NMR reveals maximum spin polarization in the presence of Wigner crystal domains at $\nu \sim 3$

Trevor D. Rhone[1,2], **Lars Tiemann**[1,2], **Koji Muraki**[1,2]

[1] *NTT Basic Research Laboratories, NTT Corporation, 3-1 Morinosato-Wakamiya, Atsugi, 243-0198, Japan*
[2] *ERATO Nuclear Spin Electronics Project, Japan Science and Technology Agency (JST)*

We probe the spin signatures of a two-dimensional electron system (2DES), confined to a GaAs quantum well, around filling factor three ($\nu \sim 3$) using resistively detected nuclear magnetic resonance (RD-NMR) spectroscopy at millikelvin temperatures. Whereas the existence of spin textures, known as skyrmions, around $\nu \sim 1$ in the lowest Landau level (LL) is well established, an understanding of the spin degrees of freedom for its higher-LL counterparts remains elusive. Although activation gap measurements in tilted fields showed the lowest-energy charged excitation at $\nu = 3$ to be a single spin flip, i.e., not skyrmions [1], recent light scattering experiments performed in the millikelvin temperature regime on ultra-high-mobility samples reveal a rapid collapse of the spin wave for $\nu \leq 3$, suggesting a loss of full spin polarization [2]. We attempt to clarify the nature of spin properties at $\nu \sim 3$ using NMR, a direct probe of the electron spin polarization. Measurements of spin-lattice relaxation time, T_1, which is a sensitive probe of spin textures, find very long T_1 at $\nu \sim 3$, indicating the absence of skyrmions. This interpretation is corroborated by Knight shift measurements, which highlight the existence of maximum spin polarization away from $\nu = 3$. Surprisingly, NMR spectroscopy also reveals that quasiparticles (quasiholes) of the $\nu = 3$ quantum Hall ferromagnet form Wigner crystal (WC) domains at $\nu > 3$ ($\nu < 3$).

A simulation of NMR spectra [3], based on a uniform 2DES model, matches experimental spectra exceedingly well around $\nu = 2.7$, 3.0 and 3.3. However, the uniform 2DES model breaks down around $\nu = 3 \pm 0.1$, where striking anomalies in the RD-NMR spectral line shape emerge. The anomalies manifest from broadening of NMR spectra, suggesting inhomogeneity in the in-plane local electron density. Using a model that describes the periodic lattice of a WC [4], we can fabricate simulations which match anomalous spectra remarkably well. As a result, we interpret the anomalous NMR spectra around $\nu = 2.9$ and 3.1 as emerging from the presence of domains of WC phases. Our simulation allows us to extract a crystal domain size of ~ 2 μm, provide a measure of electron-electron correlations not explicitly included in the ansatz wave function [4] and to show that the 2DES remains at maximum spin polarization for $2.7 \leq \nu \leq 3.3$ in the presence of translational symmetry breaking.

[1] A. Schmeller, J. P. Eisenstein, L. N. Pfeiffer, and K. W. West, Phys. Rev. Lett. **75**, 4290 (1995).
[2] T. D. Rhone, et. al., Phys. Rev. Lett. **106**, 196805 (2011).
[3] L. Tiemann, G. Gamez, N. Kumada, and K. Muraki, Science **335**, 828 (2012).
[4] K. Maki and X. Zotos, Phys. Rev. B **28**, 4349 (1983).

Real-space imaging of fractional quantum Hall effect

Junichiro Hayakawa [1], Koji Muraki [2] and Go Yusa [1]

[1] *Department of Physics, Tohoku University*
[2] *NTT Basic Research Laboratories, NTT Corporation*

Electrons in semiconductors usually behave like gas. However, in a special case when electrons are confined two-dimensionally under strong perpendicular magnetic field at low temperatures, they behave as incompressible quantum liquid—the fractional quantum Hall (FQH) effect. The FQH is a quantum mechanical manifestation of macroscopic behavior of electrons, in which longitudinal resistance reduces to zero and the Hall resistance is quantized to a universal values irrespective of the microscopic details of the sample interior as the same as the Integer quantum Hall effect.

In this paper, we present real-space images of FQH liquids by spin-resolved scanning optical microscopy and spectroscopy. Our scanning optical microscopy apparatus collects light from the two-dimensional electron system (2DES) under illumination, where each photo-excited hole binds to two electrons, forming a trion. Using appropriate optics, we performed polarization-selective photoluminescence (PL) spectroscopy of trions in a microscopic region with size comparable to the diffraction limit of light.

We show two distinctive spatial patterns: first, for a non-degenerate fully-spin polarized FQH state, compressible and incompressible FQH liquids are formed subjected to the intrinsic disorder potential, and the spatial pattern directly reflects the disorder (short-range patterns). Secondly, when differently spin-polarized FQH liquids are degenerate, real-space images show domain structures with spontaneous quasi-long-range order (long-range patterns). The two-dimensional random-field Ising model theoretically reproduced the long-range patterns from the short-range patterns [1].

Our imaging method relies on introducing trions, *i.e.*, a photo-excited hole that effectively correlates with electrons, as an internal probe. This allows for imaging genuine FQH liquids that could not be accessed through scanning probe-type microscopy. This technique can shed new light on various aspects from a microscopic viewpoint for diverse range of many-body systems not limited to FQH systems.

[1] J. Hayakawa, K. Muraki, G. Yusa, *Nature Nano*. **8**, 31 (2013).

Monday

Tuesday

Wednesday

Thursday

Friday

Extracting Net Current from an Upstream Neutral Mode in the Fractional Quantum Hall Regime

I. Gurman[§], R. Sabo[§], M .Heiblum, V. Umansky, D. Mahalu

Braun Center for Submicron Research, Dept. of Condensed Matter physics,

Weizmann Institute of Science, Rehovot 76100, Israel

[§] Both authors equally contributed to this work

Upstream neutral modes, counter propagating to charge modes and carrying energy without net charge, had been predicted to exist in some of the fractional quantum Hall states and were recently observed via noise measurements. Understanding such modes will assist in identifying the wavefunction of these states, as well as shedding light on the role of Coulomb interactions within edge modes. In this work, performed mainly in the $\nu = {}^{2}/_{3}$ state, we placed a quantum dot a few micrometers upstream of an ohmic contact, which served as a 'neutral modes source'. We showed the neutral modes heat the input of the dot, causing a net thermo-electric current to go through it. Heating of the electrons led to a decay of the neutral mode, manifested in the vanishing of the thermo-electric current at $\mathrm{T} > 110\mathrm{mK}$. This setup provides a straightforward method to investigate upstream neutral modes without turning to the more cumbersome noise measurements.

Monolithically integrated quantum cascade laser and detector

B. Schwarz[1], P. Reininger[1], W. Schrenk[1], H. Detz[1], O. Baumgartner[2], T. Zederbauer[1], A. M. Andrews[1], H. Kosina[2] and G. Strasser[1]

[1]*Institute for Solid State Electronics and Center for Micro- and Nanostructures, Vienna University of Technology, Vienna, Austria*
[2]*Institute for Microelectronics, Vienna University of Technology, Vienna, Austria*

Quantum cascade lasers (QCLs) are known as one of the most important and influential sources in the mid-infrared region. In the so called “fingerprint” region (3-20μm) most molecules have their resonances, that can be observed by optical absorption or a change of the refractive index of the chemical substance. The miniaturization of spectroscopic setups is a fascinating research topic, gaining momentum during the last couple of years. Many chip-scale sensing concepts have been demonstrated utilizing quantum cascade lasers. However, all of these concepts have been demonstrated with external optics and detectors.

We have recently demonstrated a quantum cascade device that can act as both laser and detector over the same wavelength range [1]. Simply by changing the applied bias, the structure switches between lasing (58kV/cm) and detection (0kV/cm). Based on this bi-functional active region, we have integrated a laser and a detector on the same chip [2], as illustrated in Fig. 1 (left). We have observed an on-chip detector signal of 191.5mV at room-temperature. The light power versus current density plot of the laser, comparing the on-chip detector with an external DTGS detector is shown in Fig. 1 (right). By separating the contacts of the laser and the detector we were able to reduce the electric cross-talk below 2mV at laser threshold.

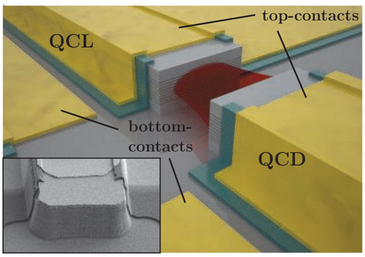

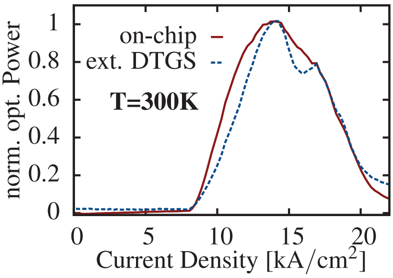

Fig. 1 Sketch of the monolithically integrated laser and detector (left) [2]. The inset shows the etched laser facet. Optical power of the laser measured with the on-chip detector at the back facet and with an external DTGS with a lens at the front facet (right). We have observed a peak detector signal of 191.5mV at room-temperature.

By combining QCLs with detector capabilities, we introduce an alternative way to develop more compact monolithic systems for mobile chemical fingerprinting, without any external detector and lens and without wafer bonding on a different technology platform. The structure can be used as a mid-infrared sensor when combined with microfluidic channels, or alternatively to monitor the power of QCLs. Due to the relative broad gain, our active region can be combined with single mode cavity arrays to give spectral resolved information of different chemical substances with greater selectivity.

[1] B. Schwarz, P. Reininger, H. Detz, T. Zederbauer, A. M. Andrews, S. Kalchmair, W. Schrenk, O. Baumgartner, H. Kosina, and G. Strasser, Appl. Phys. Lett. **101**, 191109 (2012).

[2] B. Schwarz, P. Reininger, H. Detz, T. Zederbauer, A. M. Andrews, W. Schrenk and G. Strasser, Sensors **13**, 2196 (2013).

MoOM2

Optically driven current turnstile based on self-assembled semiconductor quantum dots

G. Cerulo [1], V. Liverini [1], P. Friedli [2], H. Sigg [2] and J. Faist[1]

[1] *Institute of Quantum Electronics, ETH-Honggerberg, CH-8093, Zurich, Switzerland*

[2] *Paul Scherrer Institute, Laboratory for Micro- and Nanotechnology 5232 Villigen PSI, Switzerland*

We studied two structures based on a plane of *InAs/GaAs* self-assembled quantum dots (QDs) coupled through a *GaAs/AlGaAs/GaAs* multi-barrier structure to an *InGaAs* quantum well (QW). The latter, filled with the electrons from the *n+* doped *GaAs* top contact layer, works as a reservoir of electrons. The QDs, filled up to the *s* level, are ionized by mid-infrared optical radiation and refilled by the electrons from the QW, which tunnel through the *GaAs/AlGaAs/GaAs* multi-barrier [1]. The electrons, optically excited from the s-level to the continuum, are swept away by the built-in potential, toward the bottom contact, giving rise to a current [2]. Two devices have been characterized with two different QD densities $n_D=2\cdot 10^{10}cm^{-2}$ and $n_D=3\cdot 10^{9}cm^{-2}$, respectively. The density was estimated by SEM on two reference samples grown in similar conditions (see Fig. 1a). To prove the turnstile operation, the devices were excited by pulsed radiation (100ps) @ $\lambda=6.8\mu m$ (*s→continuum*) (see Fig. 1b), with a pulse rate $f=1kHz$. To remove the contribution coming from the spectral overlapping between *s and p* levels of the QDs, the current measured @ $\lambda=10\mu m$ (*p→continuum*) was subtracted from the current @ $\lambda=6.8\mu m$ [3]. In saturation conditions, when all the QDs get ionized by the incident radiation, the contribution of the electrons from the *s* level is $I=2\cdot N_D\cdot f\cdot e$; where N_D is the number of QDs and *e* the charge of the electron. The current density obtained after the subtraction operation is shown in Fig 1c, as a function of the applied bias. In correspondence of the plateau, because of the proportionality relationship, we could estimate the QD density for the two devices: $n_D=1.60\times 10^{10}cm^{-2}$ and $n_D=1.85\times 10^{9}cm^{-2}$, respectively. These values are in a good agreement with those obtained from the preliminary SEM characterization, proving the turnstile working principle of the two devices.

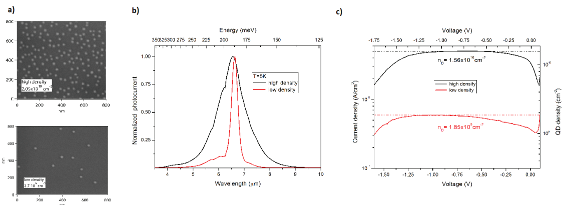

Fig. 6 (a) SEM pictures of the two reference samples; (b) Photocurrent spectra of the two devices based on high density (black), and the low density (red) QDs; (b) Photocurrent density measured exciting @ *6.8μm* at a pulse rate of 1 *KHz* (T=5K) for the electron pump based on high density (black) and low density (red) self-assembled QDs.

[1] G.Cerulo, L. Nevou, V. Liverini, F. Castellano and J. Faist, *J. Appl. Phys.* **112**, p. 043702 (2012)
[2] L. Nevou, V. Liverini, F. Castellano, A. Bismuto and J. Faist, *Applied Physics Letters* **97**(2) p.023505 (2010).
[3] L. Nevou, V. Liverini, P. Friedli, F. Castellano, A. Bismuto, H. Sigg, F. Gramm, E. Muller and J. Faist, *Nature Physics* **7**(5) p.423 (2011).

All-optical controlled polariton Mach-Zehnder interferometer

C. Sturm[1,2], D. Tanese[1], H.S. Nguyen[1], H. Flayac[3], E. Gallopin[1], A. Lemaître[1], I. Sagnes[1], D. Solnyshkov[3], A. Amo[1], G. Malpuech[3] and J. Bloch[1]

[1] *Laboratoire de Photonique et de Nanostructures, LPN/CNRS, Route de Nozay 91460 Marcoussis, France*
[2] *Universität Leipzig, Inst. für Experimentelle Physik II, Linnéstr. 5, 04103 Leipzig, Germany*
[3] *Institut Pascal, PHOTON-N2, Clermont Université, Université Blaise Pascal, CNRS, 24 avenue des Landais, 63177 Aubière Cedex, France*

Optical switches and modulators are key components in the next generation of all-optical logic elements. One of the main ingredients in their implementation is the achievement of the phase control of the optical signal. This can be done by modulating the optical index of the guiding material and using slow light effects, for instance in photonic crystal structures [1,2]. However, non-linearities are small in conventionally used materials and architectures, and phase modulations require high optical powers. In this work we show that a giant phase modulation can be achieved using both the strong non-linearity of cavity polaritons and their small in-plane group velocity. These effects are used to implement the first exciton-polariton Mach-Zehnder interferometer (MZI), based on a 1D waveguide structure etched on a high quality GaAs microcavity (Fig.1a) [4].

A coherent polariton flow is resonantly injected in the input waveguide of the MZI at T = 10K. This splits in two in the arms of the interferometer, which are then rejoined and interfere at the output (Fig. 1b). The relative phase between the two arms is controlled by a non-resonant laser placed on one of the arms. This control beam locally creates an exciton population, inducing a local blueshift of the polariton bands due to the exciton-polariton repulsive interaction [6-8] and slowing down the polariton flow. Therewith, this control beam induces a phase shift $\delta\phi$ with respect to the other arm (Fig.1a).

A phase shift up to 2π is obtained in a region of a few µm, that allows switching off and on the output (Fig. 1c), allowing to modulate the transmission by one order of magnitude. The figure of merit for this prototype MZI, the modulated region length times the power for a π phase shift, is significantly lower than for conventional already optimized systems based on photonic crystals. Beside the modulation of the transmission, also the linear degree of polarization of the output can be controlled by the presented polariton MZI.

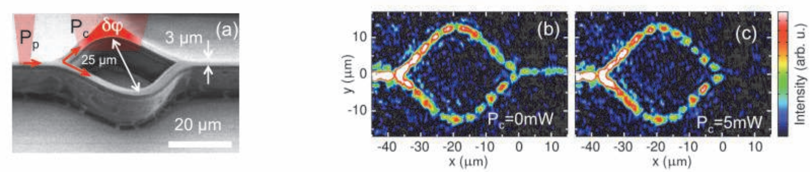

Figure 1 a) Scanning electron microscopy image of the MZI. The excitation laser and control laser are denoted by P_p and P_c, respectively, whereas the arrows indicate the polariton flow. (b and c) Spatially resolved polariton emission for different powers of the control laser.

[1] K. Nozaky *et al.,* Nature Photonics **4**, 477 (2010).
[2] B. Toshihiko, Nature Photonics, **2**, 447 (2008).
[3] C. Sturm *et al.*, submitted.
[4] E. Wertz *et al.*, Phys. Rev. Lett. **109**, 216404 (2012).
[5] T. Gao *et al.*, Phys. Rev. B **85**, 235102 (2012).
[6] G. Tosi *et al.*, Nature Physics **8**, 190 (2012).

MoIM1

INVITED

Advances in GaN quantum dots for coherent control

Yasuhiko Arakawa[1,2], Mark Holmes[1], Pawel Podemski[1,3], Kihyun Choi[1], Munetaka Arita[1], and Satoshi Kako[1]

[1]*Institute of Industrial Science, the University of Tokyo*
[2]*Institute for Nano Quantum Information Electronics, the University of Tokyo*
[3]*Institute of Physics, Wrocław University of Technology, Poland*

To date, the majority of quantum dot coherent control experiments have been performed on QDs formed in the III-As semiconductor system, with which a 2-qubit CROT logic gate has also been realized using exciton and biexciton states. However, there have been no reports on the successful coherent optical manipulation of III-Nitride QDs, which emit in the UV to visible regions. The III-Nitride system is promising as it can sustain room-temperature stable excitons in single GaN QDs; a property which enabled the realization of a single photon emitter operating at 200K [1].

Recently, in order to control the site of such QDs, we have developed the selective area growth of nanowires containing single QDs [2] by metal organic chemical vapor deposition (MOCVD). Our high-quality GaN QDs exhibit a very large biexciton binding-energy [3], fine structure splitting [4], and a strong phonon interaction [5]. Moreover, the presence of the excited states in single GaN QDs was evidenced by means of photoluminescence excitation (PLE) measurements [6].

In this presentation, we discuss recent progress in the growth and optical properties of site-controlled GaN quantum dots in GaN/AlGaN nanowires, including the experimental observation of excited state Rabi rotation, where damped oscillation has been observed in the power dependent spectra of the quantum dot ground state upon resonant pumping of an excited state [7].

This work was supported by Project for Developing Innovation Systems of the Ministry of Education, Culture, Sports, Science and Technology (MEXT).

[1] S. Kako, C. Santori, K. Hoshino, S. Gotzinger, Y. Yamamoto, and Y. Arakawa, Nat. Mater. **5**, 887 (2006).
[2] K. Choi, M. Arita, and Y. Arakawa, J. Cryst. Growth **357**, 58 (2012).
[3] K. Choi, M. Arita, S. Kako, Y. Arakawa et al., J. Cryst. Growth **370** 328 (2013)
[4] C. Kindel, S. Kako, T. Kawano, Y. Arakawa et al. Phys. Rev. B **81**, 241309 (2010)
[5] I. A. Ostapenko, G. Hoenig, S. Rodt, A. Schliwa, A. Hoffmann, D. Bimberg, S. Kako, Y. Arakawa, et al., Phys. Rev. B **85**, 081303 (2012)
[6] P. Podemski, M. Holmes, S. Kako, M. Arita,Y. Arakawa Appl. Phys. Express **6**, 012102 (2013)
[7] M. Holmes S. Kako, K. Choi, P. Podemski, M. Arita, and Y. Arakawa, Phys. Rev. Lett., to be published.

INVITED

Topological crystalline insulator states in $Pb_{1-x}Sn_xSe$

T. Story

Institute of Physics, Polish Academy of Sciences, Warsaw, Poland

Topological crystalline insulators (TCIs) constitute a new class of quantum materials recently proposed theoretically [1,2]. These materials exhibit the electronic properties characteristic for topological insulators with topologically protected Dirac-like metallic surface states crossing the bulk semiconductor band gap. In contrast to canonical topological insulators in the TCIs the topological protection is warranted not by time-reversal symmetry but by specific crystalline symmetries. The TCIs enrich the spectrum of electronic topological materials and provide new ways of controlling topological states, e.g., by applying perturbations lowering crystalline symmetry. The first material that has been theoretically identified as the TCI is SnTe [2]. Experimentally, the TCI states have been observed so far in n-$Pb_{1-x}Sn_xSe$ [3], p-SnTe [4], and p-$Pb_{1-x}Sn_xTe$ [5]. These are IV-VI narrow-gap semiconductors exhibiting the inverted band structure ordering and well known for their thermoelectric and infrared optoelectronic applications.

Our recent results will be presented on growth of bulk monocrystals by self-selecting vapor growth method, surface electronic structure investigations by angle-resolved photoemission spectroscopy (ARPES), and magneto-transport studies of $Pb_{1-x}Sn_xSe$ ($x \leq 0.3$) [3]. $Pb_{1-x}Sn_xSe$ as well as $Pb_{1-x}Sn_xTe$ are IV-VI semiconductor substitutional alloys undergoing a band inversion at a specific tin content, x_c, and temperature, T_C. For $x > x_c$ the trivial band ordering observed in PbSe and PbTe is replaced by the inverted one (SnTe-like). In the inverted band structure regime we found in the ARPES spectra clear signatures of Dirac-like topological in-gap states centered in the vicinity of the X point of the (001) surface Brillouin zone. In the $Pb_{0.77}Sn_{0.23}Se$ monocrystal we observed additionally a temperature-driven topological phase transition from a trivial insulator to a TCI (for temperatures below the inversion point $T_C \approx 150$ K). Our spin-resolved ARPES experiments enabled us to reveal a characteristic double-vortical spin polarization texture around the X point in the TCI phase of $Pb_{0.73}Sn_{0.27}Se$. All the key ARPES experimental observations agree well with model tight-binding band structure calculations taking into account strong relativistic effects [6].

Work supported in part by the European Regional Development Fund (Innovative Economy grant POIG.01.01.02-00-108/09), and the Polish National Science Centre (grant 2011/03/B/ST3/02659).

[1] L. Fu, Phys. Rev. Lett. **106**, 106802 (2011).
[2] T.H. Hsieh, H. Lin, J. Liu, W. Duan, A. Bansil, L. Fu, Nature Commun. **3**, 982 (2012).
[3] P. Dziawa, B.J. Kowalski, K. Dybko et al., Nature Materials **11**, 1023 (2012).
[4] Y. Tanaka, Z. Ren, T. Sato et al., Nature Physics **8**, 800 (2012).
[5] S.-Y. Xu, C. Liu, N. Alidoust et al., Nature Commun. **3**, 1192 (2012).
[6] B.M. Wojek, R. Buczko, S. Safaei et al, Phys. Rev. **B 87**, 115106 (2013).

MoOE4

Monday
Tuesday
Wednesday
Thursday
Friday

Ambipolar surface quantum Hall effect in the 3D TI strained HgTe

S. Wiedmann[1], C. Brüne[2], A. Jost[1], F. Chiappini[1], C. Thienel[2], C. Ames[2], P. Leubner[2], U. Zeitler[1], J. C. Maan[1], H. Buhmann[2], and L. W. Molenkamp[2]

[1] *Radboud University Nijmegen, Institute for Molecules and Materials and High Field Magnet Laboratory, Toernooiveld 7, 6525 ED Nijmegen, The Netherlands*
[2] *Faculty for Physics and Astronomy and Röntgen Center for Complex Material Systems, Universität Würzburg, Am Hubland, D-97074, Würzburg, Germany*

Topological insulators (TIs) are a new class of materials which are only conducting at their edge (2D TIs) or at their surface (3D TIs) [1]. These states are chiral, spin polarized and form a 2D electron system of Dirac fermions on the surface of a 3D TI, and, as in graphene, are described by the Dirac-Weyl equation, for massless relativistic particles.
The band structure of HgTe exhibits an energetic inversion of the Γ_6 and Γ_8 band order. Since HgTe is a semimetal, the Dirac-like surface states can only be probed if strain is applied, which leads to a gap opening between the light-hole and the heavy-hole band. Recently, experiments on strained HgTe have shown the surface quantum Hall (SQH) effect for electrons thereby proving the 2D nature of this system [2].

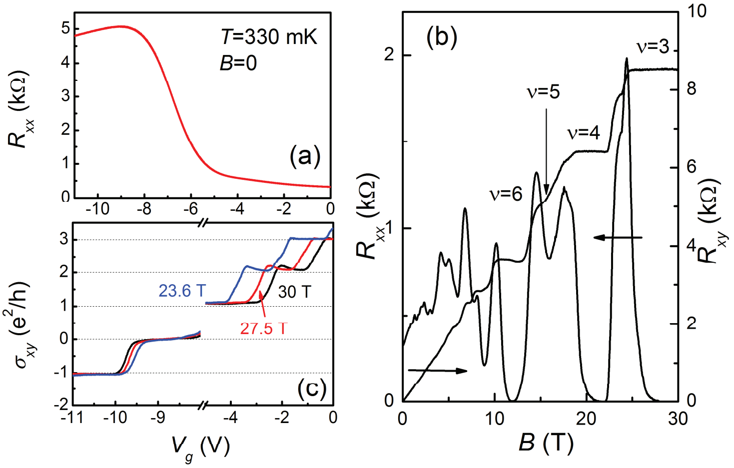

Figure 1: Magneto-transport measurements in a 3D TI: (a) Gatesweep at 0 T. (b) B-sweep at V_g=0 exhibits SQH effect for electrons. (c) Hall conductivity at high B shows the transition from electrons (ν=1) to holes (ν=-1).

We will present magnet-transport experiments where we observe the ambipolar SQH effect for the first time. The electric field effect (top-gate on the sample) enables us to tune the Fermi energy from the conduction to the valence band, i.e., through the bulk band gap, see figure 1(a, c). Furthermore, we discuss the properties of surface transport, such as the Berry phase, odd and even integer SQH effect, and address the physics of the charge neutrality point in order to demonstrate that high-quality strained 3D HgTe is an ideal material to probe surface states and properties of 3D TIs.

[1] X.-L. Qi and S.-C. Zhang, Rev. Mod. Phys. **83**, 1057 (2011); M. Z. Hasan and C. L. Kane, Rev. Mod. Phys. **82**, 3045 (2010).
[2] C. Brüne, C. X. Liu, E. G. Novik, E. M. Hankiewicz, H. Buhmann, Y. L. Chen, X. L. Qi, Z. X. Shen, S. C. Zhang, and L. W. Molenkamp, Phys. Rev. Lett. **106**, 126803 (2011).

Dirac point band gap opening in ferromagnetic Mn-doped topological insulators of the bismuth chalcogenides

G. Springholz,[1] J. Sanchez Barriga,[2] H. Steiner,[1] R. Kirchschlager,[1] G. Bauer,[1] A. Varykhalov,[2] O. Rader,[2] E. Schierle,[2] E. Weschke,[2] O. Caha[3] and V. Holy[4]

[1] *Institut for Semiconductor Physics, Johannes Kepler University, A-4040 Linz, Austria*
[2] *Helmholtz-Zentrum Berlin, BESSY II, D-12489 Berlin, Germany*
[3] *Masaryk University, Kotlarska 2, 611 37 Brno, Czech Republic*
[4] *Charles University Prague, 121 16, Praha, Czech Republic*

Topological insulators behave in bulk like ordinary insulators but exhibit a gapless Dirac like surface state that is topologically "protected" by time-reversal symmetry and immune to surface impurities [1]. A magnetic field perpendicular to the surface breaks the time reversal symmetry and opens a gap in the surface state. For 3D topological insulators, such as Bi_2Se_3 and Bi_2Te_3, a similar behavior is expected for ferromagnetic impurities like Mn [2] or Fe [3] and novel phenomena like topological magneto-electric effect, quantum anomalous Hall effect, half-integer charges at magnetic domain boundaries etc. are expected to occur [1].

Here, we present studies on Mn doped Bi_2Se_3 and Bi_2Te_3 combining a wide range of techniques to clarify the origin of the lifting of the degeneracy and gap opening induced by Mn incorporation. The samples were grown by molecular beam epitaxy and protected from oxidation by Se capping for subsequent synchrotron investigations. X-ray studies indicate a maximum solubility of Mn of about 8 % without strong structural degradation. As demonstrated by SQUID magnetometry and x-ray magnetic circular dichroism, $Bi_{2-2x}Mn_{2x}Se_3$ becomes ferromagnetic at low temperatures, with a Curie temperature of around 10 K for x_{Mn} = 8%.

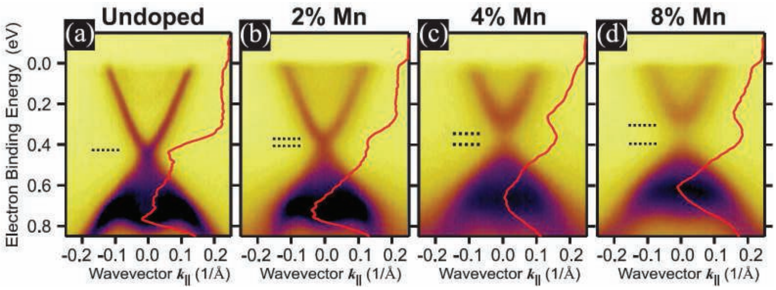

Figure 1: Mn-concentration dependent angle-resolved photoemission (ARPES) 2D maps of epitaxial $Bi_{2-2x}Mn_{2x}Se_3$ layers with increasing Mn content measured at 7 K. A clear Dirac cone is observed for x_{Mn} = 0% and a gap opening with increasing Mn content. The red lines represent the normal emission spectra.

Angular resolved photoemission maps are shown in Fig. 1, revealing n-type carriers of ~10^{18}cm^{-3}, i.e., Fermi level in the conduction band, which decreases with increasing Mn content. As indicated by the dotted lines, a gap is opened at the Dirac point which increases up to about 100 meV for x_{Mn} = 8%. However, temperature dependent measurements reveal that this band gap is independent of temperature and persists up to 300K. This unexpected behavior indicates that the breaking-up of the topological surface state is not caused by magnetism. Instead, we propose that this effect is caused by strong impurity scattering [4] that locally destroys the protection of the Dirac state.

[1] X.L. Qi, S.C. Zhang, Rev. Mod. Phys. 83, 1057(2011); M.Z. Hasan, C.L. Kane, *ibid.* 82, 3045(2010).
[2] Y.L. Chen et al., Science 329, 5992 (2010), and S. Y. Xu et al., Nature Phys. 8, 616 (2012).
[3] M. R. Scholz, et al., PRL 108, 256810 (2012). L. A. Wray, et al., Nat. Phys 7, 32 (2010).
[4] Z. Alpichshev et al., PRL 108, 206402(2012); A.M. Black-Schaffer et al. PRB 85, R121103 (1012).

Local and tunable geometric phase of Dirac fermions in a topological junction

S.-J. Choi[1], S. Park[1], and H.-S. Sim[1]

[1] *Department of Physics, Korea Advanced Institute of Science and Technology, Daejeon 305-701, Korea*

Electrons in graphene and a surface of topological insulators behave as Dirac fermions (DFs). They have the interesting property of spin-momentum locking that their spin rotates following the change of the spatial momentum. Massless DFs acquire the Berry phase of π in the spatial motion along a closed trajectory on a plane, as their spin rotates along a great circle on Bloch sphere. This special value π causes topological phenomena [1, 2, 3] such as the half-integer quantum Hall effect and weak antilocalization.

When DFs become massive, they can have the other possible values of Berry phase of spin 1/2. The continuous values of Berry phase give rise to the modification of the known effects of Berry phase π. They may also result in new interesting effects, together with unusual transport of DFs, and will offer a way of experimentally detecting Berry phase of spin 1/2 in a controlled fashion.

We theoretically show that DFs acquire geometric phase as a scattering phase shift in a *local and nonadiabatic scattering* event of reflection or transmission at a junction with mass gap (See Fig. 1). The geometric phase of spin 1/2 is an electronic analogue of polarized light in optics [4, 5, 6]. The Pancharatnam-Berry phase has new roles in solids. It carries the information of the Chern number of the insulator side of a metal-insulator junction of DFs. This implies a new type of bulk-edge correspondence for a *metal-insulator* junction, which is different from the conventional version of the correspondence with gapless edge states between *two insulators* with different Chern numbers. The Pancharatnam-Berry phase also modifies the quantization rule of DFs. This suggests *geometric-phase devices* with nontrivial charge and spin transport such as a topological wave guide and a topological field effect transistor.

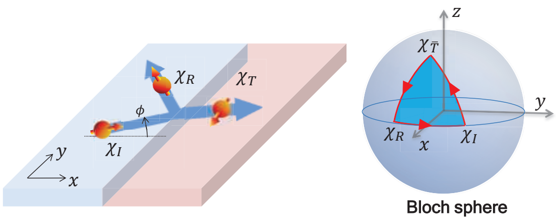

Figure 1: (left) Scattering of DFs at a junction with mass gap. A plane wave with a spin state χ_I incident from the left side is reflected to a wave with a spin state χ_R or transmitted to a wave with a spin state with χ_T. (right) The reflection coefficient of the scattering is shifted by geometric phase which amount is given by $-\Omega_{I\bar{T}R}/2$. $\Omega_{I\bar{T}R}$ is the solid angle of the *geodesic* polygon on the Bloch sphere which sequentially connects the vertices representing spin states χ_I, $\chi_{\bar{T}}$, χ_R, where $\chi_{\bar{T}}$ denotes the spin state orthogonal to χ_T.

[1] K. S. Novoselov *et al.*, Nature **438**, 197 (2005).
[2] Y. Zhang, Y.-W. Tan, H. L. Stormer, and P. Kim, Nature **438**, 201 (2005) .
[3] V. I. Fal'ko, *et al.*, Solid State Commun. **143**, 33 (2007).
[4] S. Pancharatnam, Proc. Indian Acad. Sci. A**44**, 247 (1956).
[5] M. V. Berry, J. Mod. Opt. **34**, 1401 (1987).
[6] J. Anandan, Nature **360**, 307 (1992).

Magnetic field pecularities of three distinct excitation regimes of a quantum-well microcavity

J. Fischer[1], I. Lederer[1], A. Chernenko[2], S. Brodbeck[1], A. Rahimi-Iman[1], M. Amthor[1], C. Schneider[1], M. Kamp[1], and S. Höfling[1]

[1] *Technische Physik, Physikalisches Institut, Universität Würzburg and Wilhelm Conrad Röntgen Research Center for Complex Material Systems, Universität Würzburg, Am Hubland, 97074 Würzburg, Bavaria, Germany*

[2] *Institute of Solid State Physics, Russian Academy of Sciences, Chernogolovka, 142432 Russia*

In this work we investigate three distinct working regimes of a GaAs multi-quantum well microcavity by exploiting an external magnetic field applied in Faraday configuration. By exciting the sample off-resonantly, we investigate uncondensed exciton-polaritons, the polariton-condensate and cavity mediated photon-lasing at high excitation densities.

We study the Zeeman splitting and the diamagnetic shift of the exciton-polaritons and fundamental resonances of the microresonator. In the uncondensed case we measured both quantities for a wide detuning range from about δ=-10 meV to δ=+3 meV. We observe a clear dependence of the Zeeman splitting and the diamagnetic shift on the excitonic fraction $|X(\delta,B)|^2$ (the excitonic Hopfield coefficient), in agreement with previous works [1]. For the other two working regimes of the microcavity, we chose a detuning of δ=-6.5 meV for which we can observe polariton condensation and photonic lasing on the same sample position. Fig. 1 depicts the mode-splitting for the three different regimes at $P=0.1P_{th}$ (a), $P=1.6P_{th}$ (b) and $P\approx 20P_{th}$ (c) for magnetic fields up to B=5T. Below the polariton-condensation threshold P_{th}, the Zeeman splitting increases linearly with the magnetic field and results in a splitting of ΔE=23µeV at B=5T. In the condensate case we observe strong indications of the "spin-Meissner"-effect [2,3,4] and an unexpected sign reversal of the Zeeman splitting (ΔE(5T)= -146µeV). At high excitation powers above the Mott density of excitons in the quantum-wells, both the Zeeman splitting and the diamagnetic shift are completely absent (Fig. 1 (c)).

We believe that this characterization method can be used to clearly and unambiguously distinguish between polaritons in the linear regime, polariton condensates and photonic lasers.

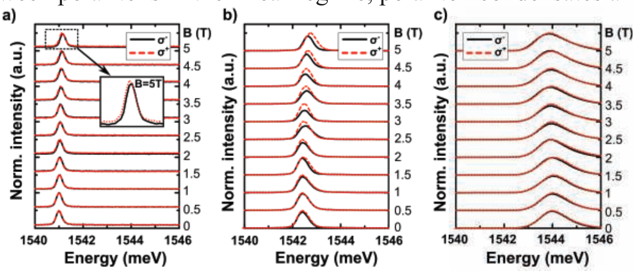

Fig. 1: Polarization resolved measurements of the ground state emission for (a) P=0.1Pth, (b) P=1.6Pth and (c) P≈20Pth. The black line indicates the σ^-- and the red dashed line the σ^+-component. In the photonic regime (c) the emission is not affected by the magnetic field.

[1] A. Rahimi-Iman et al, Phys. Rev. B **84**, 165325 (2011).
[2] Y. G. Rubo et al., Physics Letters A **358**, 227 (2006).
[3] A. V. Larionov et al, Physical Review Letters **105**, 256401 (2010).
[4] P. Walker et al, Physical Review Letters **106**, 257401 (2011).

Ultrastrong light-matter coupling with multisubband plasmons

Benjamin Askenazi[1], Aymeric Delteil[1], Angela Vasanelli[1], Yanko Todorov[1], Grégoire Beaudoin[2], Isabelle Sagnes[2] and Carlo Sirtori[1]

[1] *Univ. Paris Diderot, Sorbonne Paris Cité, Laboratoire MPQ, UMR7162, 75013 Paris, France*
[2] *CNRS-Laboratoire de Photonique et Nanostructures, Route de Nozay, 91460 Marcoussis, France*

Intersubband polaritons are quasi-particles arising from the strong interaction between an excitation of a two-dimensional electron gas and a cavity optical mode [1]. The strength of the interaction, measured by the ratio between the vacuum field Rabi splitting E_R and the intersubband excitation energy E_{ISB} [2], can be optimized by reducing the cavity mode volume and increasing the light-matter interaction oscillator strength. An ultra-subwavelength confinement of the optical mode is provided by Double Metal Cavities (DMCs) [3], while high oscillator strength can be obtained by exploiting Coulomb interaction in highly doped quantum wells. Indeed, it has been recently demonstrated [4] that, in a quantum well with several occupied subbands, all the intersubband transitions can be phase locked by dipole-dipole Coulomb interaction, giving rise to a single sharp absorption resonance. This resonance, which concentrates the whole oscillator strength of the system, is associated to a collective excitation of the electron gas, the *multisubband plasmon* (MSP). In this work we demonstrate the ultrastrong coupling between a MSP in a single quantum well and a DMC mode, with E_R/E_{ISB}=*70%* at room temperature.

Our sample consists of a single highly doped (7 x 10^{18} cm^{-3}) GaInAs/AlInAs quantum well, 148nm thick. Transmission measurements at Brewster angle show a single sharp resonance (ΔE/E=6%), as presented in the inset of Fig.1. DMCs were realized, with patch widths ranging from 0.5µm to 8µm, and reflectivity measurements were performed at room temperature. The main panel of Fig. 1 shows the energy position of the reflectivity minima as a function of the cavity mode energy. Thanks to the very strong light-matter coupling, reflectivity minima are observed in a wide energy range, spanning the mid and far infrared. The upper and lower polariton branches are separated by a 36meV gap, characteristic of the ultra-strong coupling dispersion. A coupling of the lower branch with optical phonons is also visible in the graph. A Rabi energy of 81meV is deduced from the data, corresponding to 70% of the multisubband plasmon resonance.

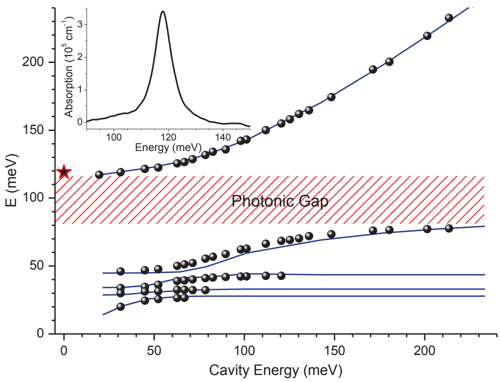

Fig.1. Main panel: Polaritonic dispersion extracted from reflectivity measurements at 300K (symbols) on gratings of different patch widths. Solid lines represent the simulated dispersion. Inset: Absorption coefficient measured at Brewster angle at 300K.

[1] D. Dini *et al.*, Phys. Rev. Lett. **90**, 116401 (2003).
[2] C. Ciuti *et al.*, Phys. Rev. B **72**, 115303 (2005).
[3] Y. Todorov *et al.*, Opt. Exp. **13**, 13886-13907 (2010).
[4] A. Delteil *et al.*, Phy. Rev. Lett. **109**, 246808 (2012).

Implementation of an *AND* gate with Bose-Einstein polariton condensates

C. Antón,[1] G. Tosi,[1] M.D. Martín,[1] Z. Hatzopoulos,[2,3] G. Konstantinidis,[2] P. Eldridge,[2] P.G. Savvidis,[2,3] and L. Viña[1]

[1]*Depto. Física de Materiales, Universidad Autónoma de Madrid, 28049 Madrid, Spain*
[2]*FORTH-IESL, P.O. Box 1385, 71110 Heraklion, Crete, Greece*
[3]*Dept. Physics, University of Crete, 71003 Heraklion, Crete, Greece*

The use of polariton condensates in all optical logic devices has been the subject of intense research in recent years, promising ultrafast switching times, low losses, spin information transport and low power consumption.[1,2] In this communication we report on the realization of a novel *logic AND gate* mediated by **propagating Bose-Einstein exciton-polariton condensate bullets** in a quasi-1D semiconductor microcavity.

The combination of two 2 ps-long, quasi-resonant light pulses [dubbed A and B, separated by a distance of 50 μm and delayed by 80 ps, see Fig. 1(i)] *optically controls* the switch response. The system dynamics is fully studied both in momentum and real space, and at different emission energies, obtaining a complete account of the velocities [Figs. 1(a-c)] and positions [Figs. 1(i-iii)] of the polariton bullets as well as of their energy relaxation. The operation of a related switch, using the same sample, has been published recently.[3]

The ON state of the gate is constituted by a long-lived (~200 ps) trapped polariton condensate at the border of the ridge [Fig. 1(iii)]. The ignition of this state is mediated by the parametric scattering between two oscillating polariton bullets that are enclosed in a half-parabolic potential [Fig. 1(ii)]. This potential is sculpted by the border of the ridge and the photo-generated excitonic barrier of pulse B.[4] Our data also reveal the amplification of the polariton bullets intensity, arising from stimulated relaxation of reservoir excitons into the polariton condensate. Finally, coherent interference phenomena between polariton bullets, in real and momentum spaces, are evidenced [Figs. 1(b,ii)].

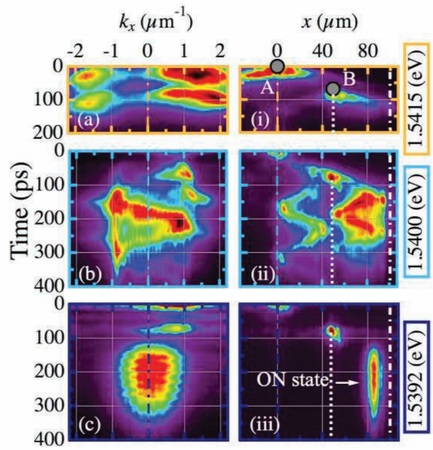

Figure 1. Emission in momentum/real space along the k_x/x-axis parallel to the ridge versus time in the left/right column for different energies. The grey dots in (i) mark the coordinates of the laser beams. In the right column the vertical lines depict the positions of the barriers created by the pulsed laser A, B and by the edge of the ridge, respectively. The upper row shows the movement of short-lived hot polaritons. The S-shaped profiles (ii) arise from the oscillation of these bullets bounded by the barriers. The oscillations are also seen in momentum space (b); mutual coherence between bullets propagating at the same speed is demonstrated by the appearance of interference fringes. The bottom row shows the ON state of the *AND* gate constituted by a trapped condensate (iii), which weakly oscillates at the bottom of the half-parabolic potential (c).

[1] A. Amo *et al.*, Nat. Photon. **4**, 361 (2010).
[2] T.C.H. Liew *et al.*, Phys. Rev. Lett. **101**, 016402 (2008).
[3] T. Gao *et al.*, Phys. Rev. B **85**,235102 (2012); C. Anton *et al.*, Appl. Phys. Lett. **101**,261116 (2012).
[4] E. Wertz *et al.*, Nat. Phys. **6**, 860 (2010).

INVITED

Fluids of polariton condensates: from a drop in a quantum pond to optical gates

L. Dominici[1,2], D. Ballarini[1,2], M. De Giorgi[1,2], E. Cancellieri[3], A. Bramati[3], G. Gigli[1,2], F.P. Laussy[4], D. Sanvitto[1,2]

[1]*CBN, Istituto Italiano di Tecnologia, 73010 Lecce, Italy.*
[2]*NNL, Istituto Nanoscienze – CNR, 73100 Lecce, Italy.*
[3]*LKB, ENS et CNRS, 75005 Paris, France.*
[4]*Universidad Autonoma de Madrid, 28049 Madrid, Spain.*

In this talk we will review some of the striking physical phenomenology associated with the dynamics of a quantum flow of polariton condensates.

Due to their intrinsic dissipative nature and strong non-linearities, polariton condensates display an incredibly span of behaviours ranging from the manifestation of superfluid-like flow [1,2] and quantized circular currents [3] to a complex dynamics of vortex formation and migration [4].

In particular we will show how it is possible to manipulate and control the polariton flow dynamics, with the formation of solitonic rings, expanding shock waves and a resolution-limited long-lived backjet when a drop of polaritons is suddenly created in a previously unperturbed state.

Furthermore, given their strong non-linearities and very high propagation velocities, polariton fluids are particularly attractive for their potential use as optical switches in integrated circuits. Among other applications, we will demonstrate the possibility to realize a polariton-based transistor for logic operations made out of polariton fluids [5].

[1] A. Amo, D. Sanvitto, F. P. Laussy, et al. Nature 457, 291 (2009).
[2] A. Amo, J. Lefrère, S. Pigeon, et al., Nat. Phys. 5, 805 (2009).
[3] D. Sanvitto, F. M. Marchetti, M. H. Szymanska, et al., Nat. Phys. 6, 527 (2010).
[4] D. Sanvitto, S. Pigeon, A. Amo et al. Nat. Phot. 5, 610 (2011).
[5] D. Ballarini, M. De Giorgi, et al. Nature Comm. 4 1778 (2013).

Part of this work was realized under the *POLAFLOW ERC project*

2 July (Tuesday)

Grunwaldzki Bridge

2 July (Tuesday)

EP2DS Session 1

9.00 – 9.30 **TuIE1**

Philip Kim (*Department of Physics, Columbia University*)
Electron transport in van der Waals heterostructures

9.30 – 9.45 **TuOE4**

W. Jaskólski[1], M. Pelc[1], L. Chico[2], A. Ayuela[3]
([1]*Nicolaus Copernicus University, Toruń, Poland;* [2]*CSIC Madrid, Spain;* [3]*CSIC-UPV/EHU, San Sebastian, Spain*)
Octagonal defect lines in graphene nanoribbons and carbon nanotubes

9.45 – 10.00 **TuOE2**

T. Szkopek[1], J. Guillemette[1], S.S. Sabri[1], B. Wu[1], K. Bennaceur[1], P.E. Gaskell[1], M. Savard[1], P.L. Lévesque[2], F. Mahvash[1,3], A. Guermoune[1,3], M. Siaj[3], R. Martel[2], G. Gervais[1]
([1]*McGill University;* [2]*Université de Montréal;* [3]*Université du Québec, Canada*)
Quantum Hall effect in hydrogenated graphene

10.00 – 10.15 **TuOE3**

V.E.Calado, S. Zhu, G.C.A.M. Janssen, L.M.K. Vandersypen
(*TU Delft, The Netherlands*)
Ballistic transport in CVD graphene

10.15 – 10.30 **TuOE1**

J.A. Alexander-Webber[1], A.M.R. Baker[1], T.J.B.M. Janssen[2], A. Tzalenchuk[2], S. Lara-Avila[3], S. Kubatkin[3], R. Yakimova[4], B.A. Piot[5], D.K. Maude[5], R.J. Nicholas[1]
([1]*University of Oxford, UK;* [2]*National Physical Laboratory, Teddington, UK;* [3]*Chalmers University of Technology, Sweden;* [4]*Linkoping University, Sweden;* [5]*LNCMI-CNRS, Grenoble, France*)
Phase -space of the breakdown of the quantum Hall effect in epitaxial graphene

MSS Session 1

9.00 – 9.15 **TuOM1**

N. Balakrishnan[1], G. Pettinari[1,5], O. Makarovsky[1], L. Turyanska[1], M.W. Fay[1], M. De Luca[3], A. Polimeni[3], M. Capizzi[3], F. Martelli[4], S. Rubini[4], A. Patanè[1]
([1]*The University of Nottingham, UK;* [3]*Sapienza Università di Roma, Italy;* [4]*TASC-IOM-CNR, Trieste, Italy;* [5]*IFN-CNR, Roma, Italy*)
Laser writing of hydrogen containing III-N-Vs

9.15 – 9.30 **TuOM2**

J.A. Alexander-Webber[1], C. Faugeras[2], P. Kossacki[2,3], M. Potemski[2], X. Wang[1], H.D. Kim[1], S.D. Stranks[1], R.A. Taylor[1], R.J. Nicholas[1] ([1]*Oxford University, UK;* [2]*LNCMI-CNRS, Grenoble, France;* [3]*University of Warsaw, Poland*)
High magnetic field imaging and spectroscopy of bound excitons in individual carbon nanotubes

9.30 – 9.45 **TuOM3**

Kanji Yoh, Tomotsugu Ishikura (*Hokkaido University, Sapporo, Japan*)
Spin injection into InAs heterostructures beyond fundamental limit

9.45 – 10.00 **TuOM4**

Fei Pei, Edward Laird, Gary Steele, Leo Kouwenhoven
(*Delft University of Technology, The Netherlands*)
Valley-spin qubit in a carbon nanotube

10.00 – 10.30 **TuIM1**

W. Pfaff[1], H.Bernien[1], B. Hensen[1], G. Koolstra[1], M.S. Blok[1], L. Robledo[1], T.H. Taminiau[1], M. Markham[2], D.J. Twitchen[2], L. Childress[3], R. Hanson[1]
([1]*Delft University of Technology, Netherlands;* [2]*Element Six Ltd., UK;* [3]*McGill University, Montreal, Canada*)
Quantum networks with spins in diamond

EP2DS Session 2

11.00 – 11.30 **TuIE2**
T. Jullien[1], J. Dubois[1], P. Roulleau[1], F. Portier[1], P. Roche[1], Y. Jin[2], A. Cavanna[2], W. Wegsheider[3], D. C.hristian Glattli[1]
([1]*SPEC, CEA Saclay, France;* [2]*CNRS, Marcoussis, France;* [3]*ETH Zürich, Switzerland*)
Demonstration of quiet on-demand injection of electrons using Lorentzian voltage pulses

11.30 – 11.45 **TuOE5**
F.D. Parmentier[1], S. Jezouin[1], M. Albert[2], A. Anthore[1], U. Gennser[1], A. Cavanna[1], I. Safi[2], F. Pierre[1] ([1]*CNRS Marcoussis;* [2]*CNRS Orsay*)
Tomonaga-Luttinger physics in electronic quantum circuits

11.45 – 12.00 **TuOE6**
J.D. Fletcher[1], M. Kataoka[1], H. Howe[2], M. Pepper[2], P. See[1], S. P. Giblin[1], J.P. Griffiths[3], G.A.C. Jones[3], I. Farrer[3], D.A. Ritchie[3], T.J.B.M. Janssen[1]
([1]*National Physical Laboratory, Teddington, Middlesex;* [2]*University College London;* [3]*University of Cambridge, UK*)
Measuring the size of single-electron wavepackets using a beam-chopping technique

12.00 – 12.15 **TuOE7**
E. Bocquillon[1], V. Freulon[1], J.-M Berroir[1], P. Degiovanni[2], B. Placais[1], A. Cavanna[3], Y. Jin[3], G. Feve[1] ([1]*CNRS Paris;* [2]*Universite de Lyon;* [3]*CNRS - Laboratoire de Photonique et de Nanostructures*)
Electron quantum optics in quantum Hall edge channels

12.15 – 12.30 **TuOE8**
H. Ito1, S. Mamyouda[1], Y. Shibata[1], Y. Ootuka[1], S. Nomura[1], S. Kashiwaya[2], M. Yamaguchi[3], H. Tamura[3], T. Akazaki[3]
([1]*University of Tsukuba;* [2]*National Institute of Advanced Industrial Science and Technology;* [3]*NTT Basic Research Laboratories, Japan*)
Imaging of spin-resolved quantum Hall edge states by near-field scanning optical microscopy

MSS Session 2

11.00 – 11.15 **TuOM5**
C. Maissen[1], G. Scalari[1], F. Valmorra[1], M. Beck[1], C. Reichl[2], W. Wegscheider[2], D. Hagenmuller[3], S. De Liberato[3], C. Ciuti[3], J. Faist[1] ([1]*Hochschule Zurich, Switzerland;* [2]*Technische Hochschule Zurich, Switzerland;* [3]*Universite Paris Diderot and CNRS, Paris, France*)
Study on the ultrastrong coupling of the cyclotron transition of two dimensional electron gases to THz split ring resonators

11.15 – 11.30 **TuOM6**
E. Cerda-Méndez[1], D. Sarkar[2], D.N. Krizhanovskii[2], S. Gavrilov[3], K. Biermann[1], M.S. Skolnick[2], P.V. Santos[1] ([1]*Paul Drude Institut für Festkörperelektronik, Germany;* [2]*University of Sheffield, UK;* [3]*Institute of Solid State Physics, Chernogolovka, Russia*)
Polaritonic two-dimensional nonlinear crystals

11.30 – 11.45 **TuOM7**
M. Sich[1], F. Fras[1], J. K. Chana[1], D.V. Skryabin[2], A.V. Gorbach[2], E.A. Cerda-Méndez[3], K. Biermann[3], R. Hey[3], P.V. Santos[3], M.S. Skolnick[1], D. N. Krizhanovskii[1]
([1]*University of Sheffield, UK;* [2]*University of Bath, UK;* [3]*Paul-Drude-Institut für Festkörperelektronik, Berlin, Germany*)
Bright polariton soliton trains in a semiconductor microcavity

11.45 – 12.00 **TuOM8**
G. Grosso, G. Nardin, Y. L´eger, F. Morier-Genoud, B. Deveaud
(*EPFL, Switzerland*)
Dynamics of formation and decay of oblique dark solitons in polariton quantum fluids

12.00 – 12.30 **TuIM2**
C. Hopfmann[1], F. Albert[2], E. Stock[1], M. Lermer[2], C. Schneider[2], S. Höfling[2], A. Forchel[2], M. Kamp[2], S. Reitzenstein[1]
([1]*Technische Universität Berlin;* [2]*Universität Würzburg, Germany*)
On-chip quantum optics using electrically driven quantum dot - micropillar cavities

EP2DS Session 3

14.00 – 14.30 **TuIE3**
S. A. Studenikin, J. Thorgrimson, G. Poulin-Lamarre, P. Zawadski, G.C. Aers, A.S. Sachrajda
(*National Research Council of Canada, Ottawa, Canada*)
The three spin system

14.30 – 14.45 **TuOE9**
A. Mavalankar, C.G. Smith, S.J. Chorley, J. P. Griffiths, G. A. C. Jones, I. Farrer, D. A. Ritchie
(*Semiconductor Physics Group, Department of Physics, JJ Thomson Avenue, Cambridge, UK*)
Thermometry and refrigeration using quantum dots

14.45 – 15.00 **TuOE10**
B. Brun[1] , F. Martins[2], S. Faniel[2], B. Hackens[2], V. Bayot[1,2], S. Huant[1], U. Gennser[4], D. Mailly[4], M. Sanquer[3], H. Sellier[1]
([1]*CNRS/UJF, Grenoble;* [2]*UCL, Louvain-la-Neuve;* [3]*CEA, Grenoble;* [4]*CNRS, Marcoussis, France*)
Scattering gate interferometry at a quantum point contact

15.00 – 15.15 **TuOE11**
Tobias Kraehenmann, Clemens Roessler, Simon Burkhard, Thomas Ihn, Klaus Ensslin, Christian Reichl, Werner Wegscheider
(*ETH Zurich, Switzerland*)
Ballistic electron transfer between quantum dots

MSS Session 3

14.00 – 14.15 **TuOM9**
H. Sellier[1], M. Pala[2], S. Baltazar[2], P. Liu[1], B. Hackens[3], F. Martins[3], X. Wallart[4], L. Desplanque[4], V. Bayot[1,3], S. Huant[1]
([1]*CNRS & Université Joseph Fourier, Grenoble;* [2]*IMEP-LAHC, Grenoble INP;* [3]*IMCN/NAPS, Louvain-la-Neuve;* [4]*IEMN, UMR CNRS 8520, UST Lille, France*)
A novel mesoscopic phenomenon: An analog of the Braess paradox in 2DEG networks

14.15 – 14.30 **TuOM10**
E.J.H. Lee[1], X. Jiang[2], M. Houzet[1], R. Aguado[3], S. De Franceschi[1]
([1]*SPSMS, CEA-INAC/UJF-Grenoble, France;* [2]*Harvard University, Cambridge, USA;* [3]*Instituto de Ciencia de Materiales de Madrid, Spain*)
Spin-resolved Andreev levels in hybrid superconductor-semiconductor nanowire devices

14.30 – 14.45 **TuOM11**
H.J. Krenner[1], S.S. Kapfinger[1], D.A. Fuhrmann[1], A. Wixforth[1], S.M. Thon[2], H. Kim[2], D. Bouwmeester[2], P.M. Petroff[3], R. Blattmann[4], P. Hänggi[4], S. Kohler[5]
([1,4]*Universität Augsburg, Germany;* [2,3]*University of California, Santa Barbara, USA;* [5]*Instituto de Ciencia de Materiales de Madrid, Spain*)
Acousto-mechanical tuning of photonic crystal nanocavity modes for quantum gate applications

14.45 – 15.15 **TuIM3**
H. Sanada[1], Y. Kunihashi[1], H. Gotoh[1], K. Onomitsu[1], M. Kohda[2], J. Nitta[2], P.V. Santos[3], T. Sogawa[1] ([1]*NTT Corporation, Japan;* [2]*Tohoku University, Sendai, Japan; 3 Paul-Drude-Institut für Festkörperelektronik, Berlin, Germany*)
Magnetic-field-free electron spin resonance in winding GaAs channel

EP2DS Session 4

15.45 – 16.15 **TuIE4**
Harold Y. Hwang
(*Stanford University; SLAC, USA*)
Unconventional electronic and magnetic states at the $LaAlO_3/SrTiO_3$ interface

16.15 – 16.30 **TuOE12**
J. Falson[1], D. Maryenko[2], D. Zhang[3], B. Friess[3], Y. Kozuka[1], A. Tsukazaki[4], J.H. Smet[3], M. Kawasaki[1,2] ([1]*University of Tokyo, Japan;* [2]*RIKEN, Wako, Japan;* [3]*Max Planck Institute for Solid State Research, Stuttgart, Germany;* [4]*University of Tokyo, Kashiwa, Japan*)
Even denominator and higher Landau level fractional quantum Hall states in ZnO

16.30 – 16.45 **TuOE13**
P. Tonndorf[1,4], R. Schmidt[1,4], P. Böttger[1], X. Zhang[1], J. Börner[2], A. Liebig[1], M. Albrecht[1], C. Kloc[3], O. Gordan[1], D.R.T. Zahn[1], S. Michaelis de Vasconcellos[1,4], R. Bratschitsch[1,4]
([1,2]*Chemnitz University of Technology, Germany;* [3]*Nanyang Technological University, Singapore;* [4]*Westfälische-Wilhelms Universität Münster, Germany*)
Raman and photoluminescence spectroscopy of atomically thin MoS_2, $MoSe_2$, and WSe_2

16.45 – 17.00 **TuOE14**
Philip W. Adams
(*Louisiana State University, USA*)
Spin-resolved tunneling studies of the exchange field in ferromagnetic/ superconducting bilayers

17.00 – 17.15 **TuOE15**
R. S. Sundaram[1], A. Lombardo[1], M. Engel [2], A.L. Eiden[1], U. Sassi[1], R.Krupke[3], Ph. Avouris[4], M. Steiner[4], A.C. Ferrari
([1]*University of Cambridge, UK;* [2]*Karlsruhe Institute of Technology, Germany;* [3]*Technische Universität Darmstadt, Germany;* [4]*IBM Thomas J. Watson Research Center, New York, USA*)
Photodection and electroluminescence in single layer MoS_2

MSS Session 4

15.45 – 16.00 **TuOM12**
R. Trotta[1,2], C. Ortix[3], E. Zallo[2], O.G. Schmidt[2] and A. Rastelli[1,2]
([1]*Johannes Kepler University Linz,Austria;* [2,3]*IFW Dresden, Germany*)
Erasing the exciton fine structure splitting in semiconductor quantum dots

16.00 – 16.15 **TuOM13**
M. Syperek[1], M. Baranowski[1], G. Sęk[1], J. Misiewicz[1], A. Löffler[2], S. Höfling[2], S. Reitzenstein[2,3], M. Kamp[2], A. Forchel[2]
([1]*Wrocław University of Technology, Poland;* [2]*Universität Würzburg, Germany;* [3]*Institut für Festkörperphysik,Berlin, Germany*)
Atypical thermally-induced carrier relaxation processes in self-assembled $In_{0.3}Ga_{0.7}As/GaAs$ quantum dots

16.15 – 16.30 **TuOM14**
K. Müller, R. Ripszam, T. Kaldewey, M. Bichler, G. Koblmüller, G. Abstreiter, J.J. Finley
(*TU München, Garching, Germany*)
Resonant optical initialization, control and readout of a spin qubit with near unity fidelity

16.30 – 17.00 **TuIM4**
Evgeny Chekhovich
(*University of Sheffield, UK*)
Using nuclear magnetic resonance to explore the physics of nuclear spins in semiconductor quantum dots

TuIE1

INVITED

Electron Transport in van der Waals Heterostructures

Philip Kim

Department of Physics, Columbia University

The recent advent of atomically thin 2-dimensional materials such as graphene, hexa boronitride, layered transition metal chalcogenide and many strongly correlated materials, has provided a new opportunity of studying novel quantum phenomena in low dimensional systems and their heterostructures utilizing them for novel electronic devices. With a strong built-in anisotropy in their components, vdW materials often show a quasi-low dimensionality leading to strongly correlated electron behaviors. Moreover, combination of different layered constituents may produce heterogeneous and functional materials. In this lecture, we will discuss to develop the method of transferring two-dimensional atomic layers of van der Waals solids to build functional heterostacks. We will discuss novel electron transport phenomena can occur across the heterointerfaces of designed quantum stacks to realize exotic charge transport phenomena in atomically controlled quantum heterostructures.

Octagonal defect lines in graphene nanoribbons and carbon nanotubes

W. Jaskólski [1], M. Pelc [1], L. Chico [2] and A. Ayuela [3]

[1] *Institute of Physics, Faculty of Physics and Astronomy, Nicolaus Copernicus University, Grudziadzka 5, Torun, Poland*
[2] *Instituto de Ciencia de Materiales de Madrid, CSIC, C/ Sor Juana Ines de la Cruz 3, 28049 Madrid, Spain*
[3] *Donostia International Physics Center (DIPC) and Centro Mixto CSIC-UPV/EHU, Departamento de Física de Materials E20018 San Sebastian, Spain*

Experimental techniques allow nowadays to pattern graphene into nanometer size ribbons with well controlled size and shape of the edges [1]. Graphene ribbons can be connected by introducing topological defects at their interfaces and it concerns also junctions between carbon nanotubes. Such junctions are interesting because they reveal localized states of magnetic nature at Fermi energy. Junctions between carbon nanotubes are usually realized by pentagon/heptagon topological defects, which strongly mix the graphene sublattices and therefore cannot yield localized states at the Fermi energy. Interfaces between graphene ribbons form one-dimensional grain boundaries, where octagons may also happen. It has been recently shown [2] that such grain boundaries can act as one-dimensional metallic wires.

We study several graphene systems containing octagonal defect lines. All the calculations are performed within the π-electron tight binding approximation. The electron interaction effects are taken into account by means of the Hubbard model. We show that contrary to pentagon/heptagon defects, octagonal defects give rise to localized states at Fermi energy even if the graphene sublattices are mixed. We prove that the localization along chains of octagons is a consequence of the zigzag nature of graphene edges forming the defect lines.

First, we study zigzag graphene ribbon containing defect lines made of octagons only. Although such a system is not a pure graphene structure, there is no sublattice mixing in this case. Four flat bands appear at Fermi energy: two of them are localized at zigzag edges of the ribbon and the additional pair is localized at the line of octagonal defects. The inclusion of electron-electron interaction effects reveals that such a system has spontaneous magnetization of 2 Bohr magnetons.

Next, we consider a system in which every second octagon in the defect line is reconstructed into a pair of pentagons. Such system has been very recently studied experimentally [2]. The presence of pentagons mixes locally both sublattices. Consequently, only one flat band at the Fermi level is localized at the octagonal defect lines. Spontaneous magnetization survives, but drops down to 0.6 Bohr magnetons.

We have studied also rolled-up systems, i.e., carbon nanotubes with octagonal defect lines along the tube axis or at junctions between tubes. We have shown that localization at octagons with energies at the Fermi level is robust and present in all the system considered, independently whether the graphene sublattices are mixed or not. It suggests that octagonal defects can indicate reactivity sites in graphene. Finally, we show that the appearance of localized flat bands at the Fermi energy may be explained using the hybridization rules introduced in Ref. [3] for graphene ribbons with arbitrary edges.

[1] X. Jia, M. Hofmann, V. Meunier, et al., Science **323,** 1701 (2009).
[2] J. Lahiri, Y. Lin, P. Bozkurt, I. I. Oleynik, and M. Batzill, Nature Nanotech. **5**, 326 (2010).
[3] W. Jaskólski, A. Ayuela, M. Pelc, H. Santos, and L. Chico, Phys. Rev. B **83**, 235424 (2011).

Quantum Hall Effect in Hydrogenated Graphene

T. Szkopek[1], J. Guillemette[1], S.S. Sabri[1], B. Wu[1], K. Bennaceur[1], P.E. Gaskell[1], M. Savard[1], P.L. Lévesque[2], F. Mahvash[1,3], A. Guermoune[1,3], M. Siaj[3], R. Martel[2] and G. Gervais[1]

[1] McGill University, Montréal, Canada
[2] Université de Montréal, Montréal, Canada
[3] Université du Québec à Montréal, Montréal, Canada

The quantum Hall effect (QHE) is observed in a two-dimensional electron gas formed in millimeter-scale hydrogenated graphene [1], with a mobility less than 10 cm^2/Vs and corresponding Ioffe-Regel disorder parameter $(k_F\lambda)^{-1} \sim 500$. Our observations with hydrogenated graphene push the limit of disorder where the QHE can still be attained in a strong magnetic field, suggesting that the QHE might be robust to arbitrarily large disorder.

Disordered graphene samples were prepared from pristine, large-area, monolayer graphene samples grown by chemical vapour deposition (CVD) on Cu foils. Disorder was controllably introduced into the graphene by exposure to a beam of atomic hydrogen in a UHV chamber. *In-situ* measurement shows an exponential growth in graphene sheet resistance versus hydrogen dose. We find hydrogenated graphene to exhibit a strong temperature dependent resistance consistent with variable range hopping. We measured the 2-point resistance of hydrogenated graphene at low temperatures in magnetic fields of up to 45T, Fig. 1. A colossal negative magnetoresistance was observed, with a dramatic transition from a highly resistive state of $R_{2pt} = 250\ h/e^2$ at zero field to a quantized resistance $R_{2pt} = 12\ 962\Omega$ at 45T, which is within 0.5% of $h/2e^2$. The quantized resistance corresponds to a QHE state with $\nu=-2$ filling factor, $R_{2pt} \approx |R_{xy}| = h/2e^2$, and $R_{xx} = 0$. The high field resistance versus charge carrier density is consistent with the opening of an impurity-induced gap in the density of states of graphene.

The mean spacing between point defects induced by hydrogenation was estimated to be $\lambda_D = 4.6 \pm 0.5$ nm via Raman spectroscopy. The rapid collapse of resistance and emergence of a QHE state is observed to occur when the magnetic length $\ell_B = (\hbar/eB)^{1/2}$ is comparable to the mean point defect spacing λ_D. The interplay between electron localization by defect scattering and magnetic confinement in two-dimensional atomic crystals will be discussed.

[1] J. Guillemette et al., arXiv:1301.1257 [cond-mat.mes-hall]

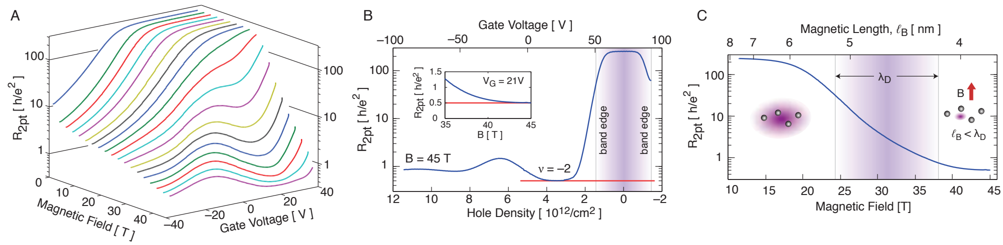

Fig. 1: A) The two-point resistance of a hydrogenated graphene sheet versus magnetic field and gate voltage. All data were taken at a temperature of 575±25 mK. B) At 45T, the resistance versus gate voltage and hole density, with the red line indicating a Hall plateau at $R_{2pt} = h/2e^2$. C) Resistance of the hydrogenated graphene versus both the magnetic field B and magnetic length $\ell_B = (\hbar/eB)^{1/2}$. The shaded region indicates the estimated point defect spacing extracted from the Raman spectra.

Ballistic transport in CVD graphene

V.E.Calado[1], S. Zhu[2], G.C.A.M. Janssen[2] and L.M.K. Vandersypen[1]

[1] *Kavli Institute of Nanoscience, TU Delft, 2600 GA Delft, The Netherlands*
[2] *Micro and Nano Engineering Laboratory, Precision and Microsystems Engineering, TU Delft, 2628 CD Delft, The Netherlands*

Chemical vapor deposition (CVD) synthesis of graphene is a scalable and controllable method for the production of single layer graphene (SLG). This has been intensively studied during last few years with a strong focus on improving its electronic and structural quality in order to match that of exfoliated graphene.

Here we report the synthesis of SLG by CVD that has the electronic quality of exfoliated graphene, which shows ballistic quantum transport. The synthesis is done with well-defined conditions in a home-made ultra clean furnace. This is ultimately necessary to allow fine tuning of the growth parameters. While doing that, we have achieved a nucleation density down to ~ 1 mm^2, which in turn leads to large (~ 0.5 mm) single crystals. We have developed a dry transfer method that minimizes the contamination (i.e. from water in case of wet transfer methods). With this method we transferred SLG crystals onto hexagonal boron nitride substrates (hBN). The hBN was exfoliated onto SiO_2/Si substrates and acts as an ultra-clean and atomically flat substrate for graphene [1].

Transport measurements were done on Hall bar shaped geometries in a liquid He cryostat. At room temperature we measured a field effect mobility of 17.000 cm^2/Vs which increased to 50.000 cm^2/Vs at 4K. For the first time, ballistic transport over 1 μm in CVD graphene was observed by transverse magnetic focusing between neighboring contacts [2]. Atomic force microscopy confirms that wrinkles in CVD graphene breaks down ballistic transport. By reducing or even eliminating them the quality could be improved even further.

We conclude that CVD graphene that has been grown and transferred with our method maintains its high electronic quality that matches (or potentially exceeds) that of exfoliated graphene. With this growth and transfer method it is now possible to grow mm sized crystals that show ballistic transport on a micron scale, and can replace exfoliated graphene in both fundamental research and future devices..

[1] C. R. Dean et al., Nature Nanotechnol. **5**, 722-726 (2010).
[2] T. Taychatanapat et al., Nature Phys. **AOP**, (2013).

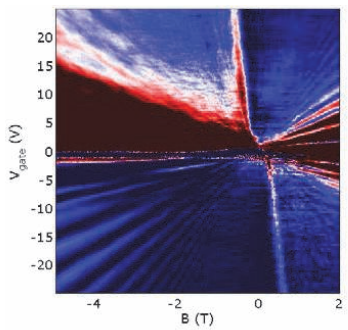

Fig. 1: Resistance between neighboring contacts in CVD graphene plotted as function of gate voltage and magnetic field. The square root line is due to transverse magnetic focusing, which is the evidence of ballistic transport.

Phase-space of the breakdown of the quantum Hall effect in epitaxial graphene

J.A. Alexander-Webber[1], A.M.R. Baker[1], T.J.B.M. Janssen[2], A. Tzalenchuk[2], S. Lara-Avila[3], S. Kubatkin[3], R. Yakimova[4], B.A. Piot[5], D.K. Maude[5], and R.J. Nicholas[1]

[1] Department of Physics, University of Oxford, Clarendon Laboratory, Parks Rd. Oxford, U.K.
[2] National Physical Laboratory, Hampton Road, Teddington, U.K.
[3] Department of Microtechnology and Nanoscience, Chalmers University of Technology, Goteborg, Sweden
[4] Department of Physics, Chemistry and Biology (IFM), Linkoping University, Linkoping, Sweden
[5] LNCMI-CNRS, Grenoble, 38042 Cedex 9, France

Keywords: Graphene, Magnetotransport, Quantum Hall effect, Hot electrons, Breakdown, SiC

Charge carriers in graphene behave as massless Dirac fermions, which leads to a large cyclotron energy gap when a perpendicular magnetic field is applied. As such, some signs of the quantum Hall effect (QHE) are observable even up to room temperature at high enough magnetic fields [1]. However, to characterise the true phase-space in which the quantum Hall regime is observed we must consider the dissipationless state where ρ_{xx}=0 and ρ_{xx}=h/νe^2 within measurement noise levels. We report the phase-space defined by the QHE in polymer gated epitaxial graphene on SiC as a function of temperature, current, carrier density and magnetic field up to 30T. At T=2K we have observed extremely high breakdown currents of over 200μA in a 5μm wide device at 25T, corresponding to a current density (40A/m) almost two orders of magnitude greater than in even the most well optimised GaAs devices. With increasing temperature the critical current decreases with the behaviour seen previously in GaAs 2DEGs [2]; $Ic(T) = Ic(0)(1 - \left(\frac{T}{Tc}\right)^2)$, where Tc is a critical temperature (fig. 1b). At the highest carrier densities at 29T the QHE persists with ρ_{xx}=0 up to a remarkably high temperature of Tc>45K, with a superlinear increase in Tc with magnetic field (fig. 1c).

Upon further reduction of the carrier density such that the Fermi energy approaches the Dirac point, magnetotransport shows remarkable behaviour as the device reaches the ν=2 quantised Hall plateau at fields as low as 1T remaining quantised up to at least 19T. The magnetic field dependence of the breakdown current (fig. 1a) suggests that, in addition to the strong pinning to ν=2 observed previously [3], the carrier density remains strongly field dependent above the field of peak breakdown. Measurements of thermal activation into n=0 along the plateau reveals that the Fermi energy is pinned to a constant energy of 40meV. Breakdown currents at 2K of over 100μA are observed at just 5T in a 35μm wide device. These measurements demonstrate that graphene on SiC is a very promising material to engineer a high precision quantum Hall resistance standard with readily accessible magnetic fields and temperatures.

References:
[1] K.S. Novoselov, et al. Science **315,** 1379 (2007).
[2] L. Rigal, et al., Physical Review Letters **82**, 1249 (1999).
[3] T.J.B.M Janssen, et al. Phys. Rev. B **83**, 233402 (2011).

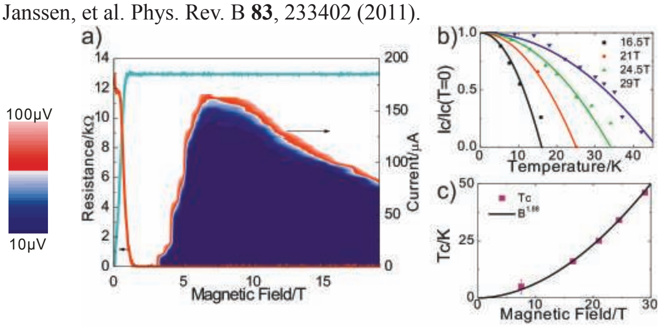

Fig. 1: a) Magnetotransport (ρ_{xy}[light blue] and ρ_{xx} [red]) data and corresponding I-V_{xx}-B contour plot for a 35μm wide device at T=1.5K. The dark blue region of the contour plot is at the level of noise in our setup (10μV) and represents QHE phase-space in which ρ_{xx}=0. b) Normalised temperature dependence of the peak breakdown current at several magnetic fields up to 29T. Also shown is the fit for each field. d) The magnetic field dependence of Tc, with a best fit line.

Laser writing of hydrogen containing III-N-Vs

N. Balakrishnan [1], G. Pettinari [1,5], O. Makarovsky [1], L. Turyanska [1], M.W. Fay [2], M. De Luca [3], A. Polimeni [3], M. Capizzi [3], F. Martelli [4], S. Rubini [4] and A. Patanè [1]

[1] *School of Physics and Astronomy, The University of Nottingham, Nottingham NG7 2RD, UK*
[2] *Nottingham Nanotechnology and Nanoscience Centre, The University of Nottingham NG7 2RD, UK*
[3] *Dipartimento di Fisica, Sapienza Università di Roma, Piazzale A. Moro 2, 00185 Roma, Italy*
[4] *TASC-IOM-CNR, Area Science Park, S.S. 14, Km. 163.5, 34149 Trieste, Italy*
[5] *IFN-CNR, via Cineto Romano 42, 00156 Roma, Italy*

The incorporation of a small concentration of N-atoms into the anion sublattice of a III-V compound induces a large reduction of the band gap energy. On the other hand, H-atoms tend to neutralize the electronic activity of N by forming N-H complexes [1]. Here we exploit these unique properties and a focused laser beam to profile the band gap of III-N-Vs [2-3].

We show that the N-H complex can be dissociated by light due to a resonant photon absorption. This is a local process that depends on the photon energy (Fig. 1a) and can be activated at temperatures as low as 4.2 K, significantly smaller than those required for thermal dissociation (> 200 °C). The photon-assisted N-H dissociation provides a means of profiling the band gap energy of a III-N-V alloy: nanoscale light emitting spots in the visible and near infrared region are laser-activated in Ga(AsN), (InGa)(AsN) and Ga(PN); profiles of different shapes are patterned in the growth plane with submicron spatial resolution and high energy accuracy (Fig. 1b). Moreover, the patterned profiles are erasable and the samples can be re-hydrogenated making any nanoscale in-plane band gap profile rewritable (Fig. 1c).

The versatility of hydrogen makes this laser writing technique of general interest and relevant to the development of fast fabrication approaches to nanotechnologies. Non-thermal (photonic) laser writing may also offer an alternative route to non-destructive band gap profiling of temperature sensitive material systems.

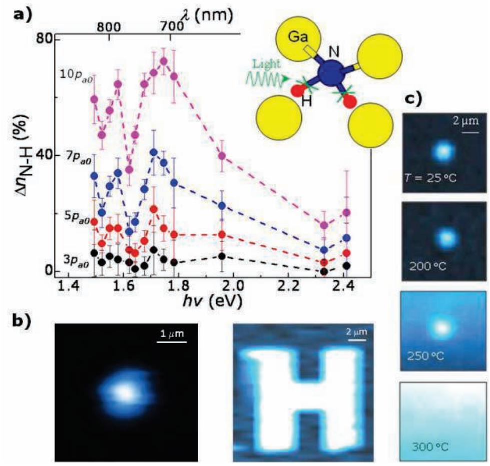

Figure 1. (a) Percentage change in the concentration of N-H complexes, Δn_{N-H}, dissociated by laser in a Ga(AsN) quantum well (QW) versus photon energy, $h\nu$, and wavelength, λ, at various power densities, p_a (p_{a0} = 10^5 W cm^{-2}). The inset sketches the photon-assisted dissociation of a di-hydrogen N-H complex. **(b)** Micro-photoluminescence maps of dot-like (left) and H-shaped (right) profiles at T = 300 K for an hydrogenated Ga(AsN) QW created by a focused laser beam. **(c)** Light emitting dots created by laser writing in Ga(AsN) and mapped following an annealing in a furnace at T = 200 °C, 250 °C, 300 °C for 1 hr.

[1] R. Trotta et al., *Adv. Funct. Mat.* **22**, 1782 (2012).
[2] N. Balakrishnan et al., *Phys. Rev.* B **86**, 155307 (2012).
[3] N. Balakrishnan et al., *Appl. Phys. Lett.* **99**, 021105(2011).

High magnetic field imaging and spectroscopy of bound excitons in individual carbon nanotubes

J.A. Alexander-Webber[1*], C. Faugeras[2], P. Kossacki[2,3], M. Potemski[2], X. Wang[1], H.D. Kim[1], S.D. Stranks[1], R.A. Taylor[1], and R.J. Nicholas[1$]

[1]*Department of Physics, Oxford University, Clarendon Laboratory, Parks Rd. Oxford OX1 3PU, U.K.*
[2]*LNCMI-CNRS, Grenoble, 38042 Cedex 9, France*
[3]*Institute of Experimental Physics, University of Warsaw, Warsaw, Poland*
* *j.alexander-webber1@physics.oc.ac.uk*
$ *r.nicholas1@physics.ox.ac.uk*

We report low temperature (4.2K) micro-photoluminescence (μPL) studies of high-purity semiconducting individual single walled carbon nanotubes (CNTs) in magnetic fields up to 30T. We observe ultra-narrow emission linewidths with a FWHM<80μeV. Using these narrow linewidths we study in detail the effects of high magnetic fields on the exciton fine structure. In pristine CNTs the dark exciton is clearly resolved at B<1T with a consistent zero-field splitting of Δ_x=2meV between the dark and bright spin-singlet exciton for (8,6) tubes (Fig.1a). Upon high intensity laser irradiation the optical properties of the CNTs are dramatically transformed. An additional dark-bright pair of exciton states is created (Fig.1b). We attribute these new states to bound spin-singlet excitons with an increased zero-field splitting of Δ_x^{bound}=6meV. This may explain the apparent variability of Δ_x observed within single chiralities in early individual CNT magnetospecroscopy [1,2].

In addition, the magnetic field alters the spatial distribution of the emission, causing emission from previously dark regions with a different spectral response. We observe strong magnetic brightening accompanied by significant shifts in the spatial distribution along the tube (Fig. 1d,e). The spatial dependence of the emission spectrum suggests that the presence of defect states at different points along the nanotube can be detected due to magnetic field induced localisation.

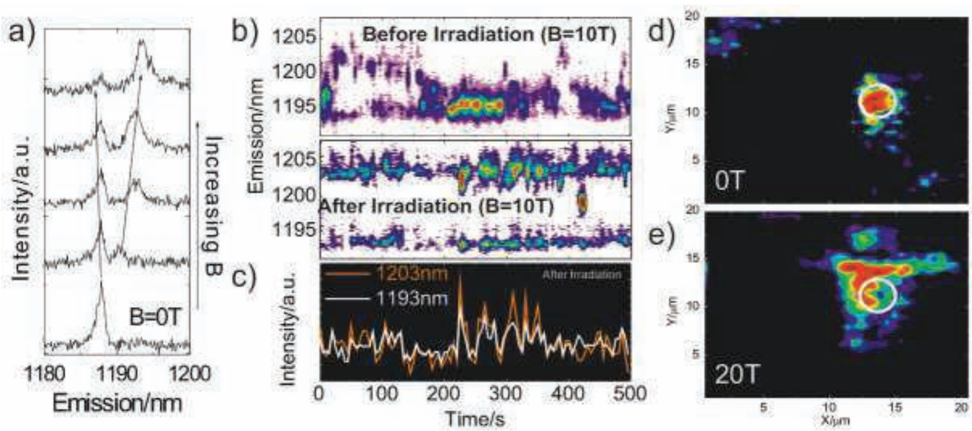

Figure 1. a) Bright-dark transition in a pristine (8,6) CNT. b) Emission time-series before and after high intensity irradiation at 10T, a new dark-like exciton is observed. c) Time-series showing the correlation between the two emission states after irradiation. Spatial mapping of single CNT emission at (d) 0T and (e) 20T.

References

[1] A. Srivastava, H. Htoon, V.I. Klimov, and J. Kono, Phys. Rev. Lett. **101,** 87402 (2008).

[2] R. Matsunaga, K. Matsuda, and Y. Kanemitsu, Phys. Rev. Lett. **101**, 147404 (2008).

Spin injection into InAs heterostructures beyond fundamental limit

Kanji Yoh and **Tomotsugu Ishikura**

Research Center of Integrated Quantum Electronics, Hokkaido University, Sapporo, Japan

Electrical spin injection into semiconductors is the key technology for practical spintronics devices. Spin injection through tunnel barrier has become popular to obtain high spin injection effect to avoid the so-called conductivity mismatch[1]. On the other hand, tunnel barrier greatly introduce contact resistance resulting in reduced injection current density. So, it is desirable to have less tunnel barrier for spin transistor applications as long as efficient spin tunneling is guaranteed. The InAs inverted heterostructure is ideal for that purpose because surface pinning position is in the conduction band together with high spin-orbit interaction[2][3]. We have fabricated spin valve devices with and without MgO tunnel barrier to compare spin injection efficiency in InAs/InGaAs/InAlAs inverted HEMT structure.

The 4.1 nm InAs channel layer of the HEMT is buried in the middle of InGaAs sub-channel layer to confirm mobility. The structure consist of 300/800 nm of InP/ $In_{0.52}Al_{0.48}As$ buffer layer, $1.2\times10^{12}cm^{-2}$ of Si δ-doping, 10 nm of $In_{0.52}Al_{0.48}As$ spacer layer, 5.6 nm of $In_{0.53}Ga_{0.47}As$ sub-channel, 4.1 nm of InAs main channel, 1.8 nm of $In_{0.53}Ga_{0.47}As$ sub-channel, 50 nm of $In_{0.52}Al_{0.48}As$ barrier layer and $In_{0.53}Ga_{0.47}As$ 10 nm cap-layer. The electrical transport parameters were characterized by Hall measurement, yielding 20,000 cm^2/Vs of mobility, 1.5×10^{12} cm^{-2} of carrier density and 300 Ohm/□ of sheet resistance at 1.4 K. MgO samples were subjected to post-anneal at 250°C for 40min to obtain better crystal quality.

The spin transport lengths were estimated at 1.4K to be 1.62 μm in nonlocal set-up as shown in Fig.1. The spin polarization were estimated to be 6.93 % (No annel) and 8.93% (annealed at 250°C) in the interface of $Ni_{81}Fe_{19}$/MgO/InAs. Local spin valve measurement on barrier-less sample (Fig.2.b) exhibited MR characteristics comparable to samples with MgO tunnel barrier (Fig.2a). The estimated spin injection efficiency of 5.3% was obtained without tunnel barrier, which is comparable to samples with tunnel barriers (Fig.3). The present high spin injection efficiency makes remarkable contrast with conductivity mismatch calculation ($\eta \approx 8\mathrm{x}10^{-7}$) [1]. This result is consistent with optical measurements [4], and first principle calculations [5]. The role of ballistic nature during spin injection will be discussed.

[1] G. Schmidt, et al, Phys. Rev. B **62**, R4790 (2000). [2] H. C. Koo, et al, Science **325,** 1515 (2009). [3] M. Ohno and K. Yoh, Phys. Rev. B **75,** 241308(R) (2007). [4] K.Yoh et al, Semi.Sci.Technol. 19,pp.1-4 (2004). [5] Wunnicke et al, J.Supercond./Novel Magn.16,171 (2003).

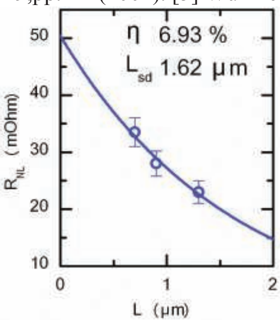

Fig.1 Non-local spin injection measurement result of NiFe/MgO/InAs I-HEMT structure

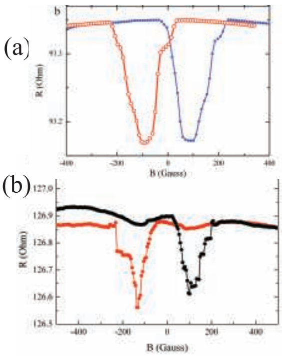

Fig.2 Local spin injection measurement results. (a)with MgO (b)Without MgO

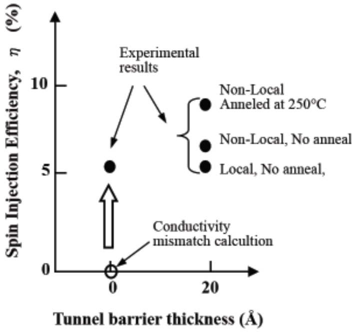

Fig.3 Spin injection efficiency comparison between samples with and without MgO tunnel barrier.

Valley-spin qubit in a carbon nanotube

Fei Pei [1], Edward Laird [1], Gary Steele [1] and Leo Kouwenhoven [1]

[1] *Kavli Institute of Nanoscience, Delft University of Technology, The Netherlands*

Compared with spin qubits realized in III-V materials, carbon nanotubes are a particularly attractive host material, because of the much lower concentration of nuclear spins. In this work, we realize a nanotube qubit in a double quantum dot. The qubit is encoded in two valley-spin states, with coherent manipulation via electrically driven spin resonance (EDSR) mediated by a bend in the nanotube. Readout is performed by measuring the current in Pauli blockade. We also find a spin-orbit coupling in multiple devices that is an order of magnitude larger than previously measured. This work is enabled by a novel fabrication technique with a controlled transfer of individual ultra-clean nanotubes by stamping [1] [2] [3].

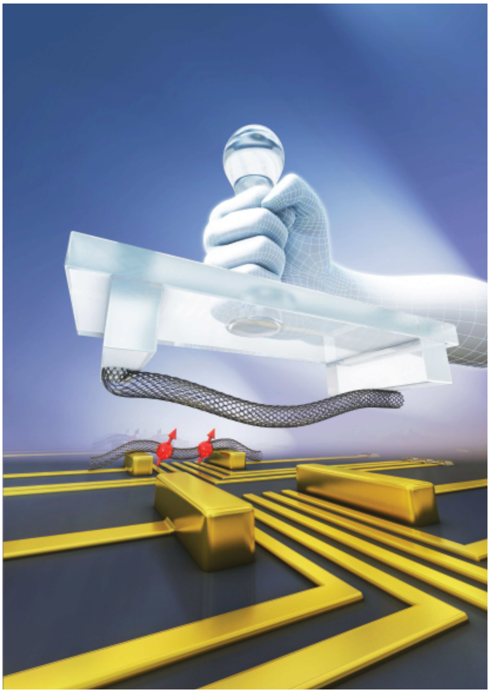

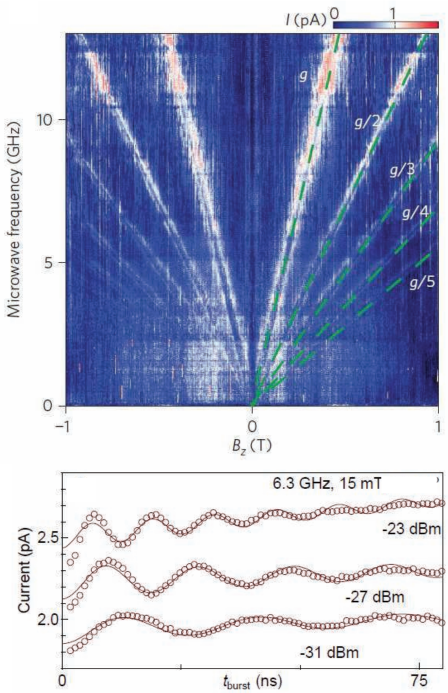

[1] F. Pei, E.A. Laird, G.A. Steele & L.P. Kouwenhoven, Nat. Nanotechnol. **7**, 630-634 (2012)
[2] E.A. Laird, F. Pei & L.P. Kouwenhoven, Arxiv 1210.3085 (2012)
[3] G.A. Steele, F. Pei, E.A. Laird, J.M. Jol, H.B. Meerwaldt & L.P. Kouwenhoven, Nat. Commun. **4**, 1573 (2013)

TuIM1

INVITED

Quantum networks with spins in diamond

W. Pfaff,[1] H.Bernien,[1] B. Hensen,[1] G. Koolstra,[1] M.S. Blok,[1] L. Robledo,[1] T.H. Taminiau,[1] M. Markham,[2] D.J. Twitchen,[2] L. Childress,[3] and R. Hanson[1]

[1] *Kavli Institute of Nanoscience Delft, Delft University of Technology, P.O. Box 5046, 2600 GA Delft, The Netherlands*
[2]*Element Six Ltd., Kings Ride Park, Ascot, Berkshire SL5 8BP, United Kingdom*
[3]*McGill University Department of Physics, 3600 Rue University, Montreal, QC H3A 2T8, Canada*

Entanglement between spatially separated objects is one of the most intriguing phenomena in physics. Besides being of fundamental interest, entanglement is also a valuable resource in quantum information technology enabling secure quantum communication networks and distributed quantum computing.

Here we present our recent results towards the realization of quantum networks with solid-state qubits. We have entangled two spin qubits in diamond, each associated with a nitrogen vacancy center [1]. The two diamonds reside in separate setups three meters apart. With no interaction between the two spins to mediate entanglement, we make use of a scheme based on quantum measurements: we perform a joint measurement on photons emitted by the NV centers that are entangled with the spins. The detection of the photons projects the spins into an entangled state. We verify the generated entanglement by single-shot readout of the spins in different bases.

The entanglement reported here can in principle be combined with recently achieved initialization, readout and entanglement operations [2, 3] on local long-lived nuclear spin registers, enabling deterministic long-distance teleportation, quantum repeaters and extended quantum networks.

[1] H. Bernien et al., Nature (2013; in press); preprint at arXiv:1212.6136.
[2] L. Robledo et al., Nature **477**, 574 (2011).
[3] W. Pfaff et al., Nature Physics **9**, 29 (2013).

INVITED

Demonstration of quiet on-demand injection of electrons using Lorentzian voltage pulses

Thibaut Jullien [1], Julie Dubois [1] , Preden Roulleau [1], Fabien Portier [1], Patrice Roche[1], Y. Jin [2], A. Cavanna [2], W. Wegsheider [3], and D. Christian Glattli [1]

[1] *Nanoelectronics, SPEC, CEA Saclay, France.*
[2] *Laboratoire de Photonique et nanostructures, CNRS, Marcoussis, France.*
[3] *Laboratory for Solid State Physics, ETH Zürich, CH-8093 Zürich, Switzerland.*

Injecting a controlled number of electrons in a quantum conductor opens the way to new quantum experiment. Here we consider the injection of n electrons using a short time voltage pulse with $\int eV(t)dt = nh$. When the voltage pulse has a Lorentzian shape, L. Levitov et al. [1] have shown that the n-electron injection is free of extra neutral electron-hole pairs and is a minimal excitation state that we will call a "Leviton". We present the first implementation. Using periodic voltage pulses applied on a contact of a 2DEG, a coherent train of n-electron Levitons is send to a QPC which acts as an electron beam splitter. By measuring the shot noise resulting from the partitioning of all excitations we demonstrate that Lorentzian voltage pulses give minimal excitation states, i.e. Levitons. This is complemented by energy domain study of the excitations using shot noise spectroscopy and by a time-domain study using shot noise in a Hong-Ou-Mandel like n-electron collision experiment. The ERC Advanced grant 228273 MeQuaNo is acknowledged.

[1] H-W Lee & L. Levitov, cond-mat: 9312013; J. Keeling, I. Klich, and L. Levitov, Phys. Rev. Lett. 97, 116403 (2006).
[2] J. Dubois, T. Jullien, P. Roulleau, F. Portier, P. Roche, Y. Jin, A. Cavanna, W. Wegscheider and D.C. Glattli, submitted.

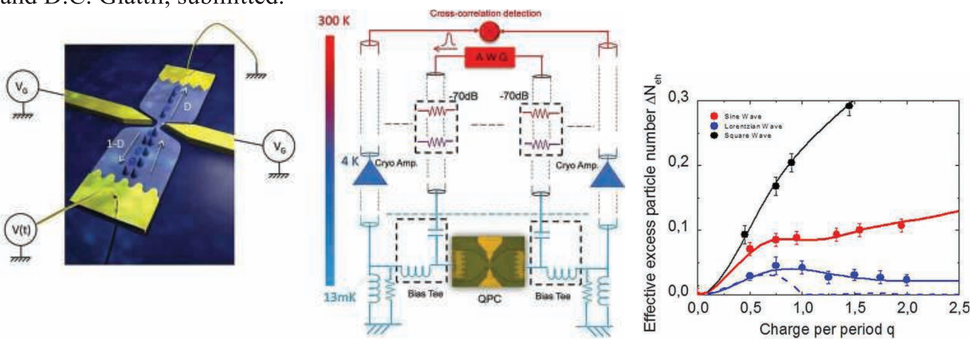

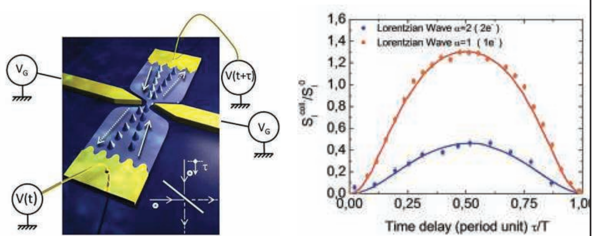

Upper figures : schematic injection of voltage pulses (left); experimental set-up (center); excess shot noise for various pulses shapes carrying charge q : Levitons show less than 2% extra excitations per electron (right).
Lower figures: Hong Ou Mandel correlation: collision of electron pulses time-shifted by ***t.*** The HOM noise reveals the shape of Leviton wavepackets.

Tomonaga-Luttinger physics in electronic quantum circuits

F. D. Parmentier[1], S. Jezouin[1], M. Albert[2], A. Anthore[1], U. Gennser[1], A. Cavanna[1], I. Safi[2], and F. Pierre[1]

[1] *CNRS / Univ Paris Diderot (Sorbonne Paris Cité), Laboratoire de Photonique et de Nanostructures, Marcoussis, France*

[2] *CNRS / Univ Paris Sud, Laboratoire de Physique des Solides, Orsay, France*

In one-dimensional conductors, electron-electron interactions result in correlated electronic systems markedly different from conventional Fermi liquids. At low energy, a hallmark signature of the so-called Tomonaga-Luttinger liquids (TLL) is the universal conductance scaling curve in presence of an impurity. A seemingly different problem is that of the quantum laws of electricity when distinct quantum conductors are assembled in a circuit. In particular, the conductance across a quantum conductor embedded in a dissipative circuit is suppressed at low energy, a phenomenon called dynamical Coulomb blockade (DCB).

Here, we present an experimental investigation of the DCB on a single-channel quantum conductor realized by a quantum point contact in a two-dimension electron gas, and demonstrate a proposed link to TLL physics [1].

A remarkable feature in the data implies a phenomenological expression for the conductance of a single-channel quantum conductor embedded in an arbitrary linear circuit [2]. Its validity is further established experimentally using a wide range of circuits, including data obtained with a carbon nanotube at Duke University [3].

In the particular case of a pure resistance in series with the single-channel conductor, theory predicts a mapping between DCB and the transport across a TLL with an impurity [4]. By confronting both the data and the phenomenological expression with the TLL universal conductance scaling curve, we demonstrate experimentally this mapping.

The powerful TLL framework advances our understanding of the laws governing quantum transport with distinct quantum components. Reciprocally, the demonstrated mapping provides a new test-bed for TLL predictions.

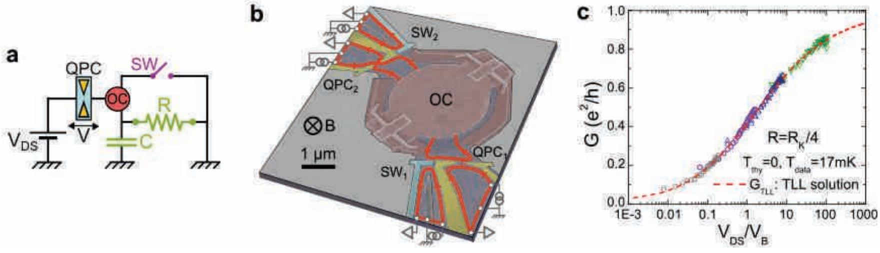

Fig. 1: **a**, Schematics of the samples. **b**, Sample micrograph. **c**, Comparison between experimental data and the TLL universal conductance curve.

[1] S. Jezouin *et al.*, arXiv:1301.4159 (2013).
[2] F.D. Parmentier *et al.*, Nature Physics **7,** 935-938 (2011).
[3] H. T. Mebrahtu *et al.*, Nature **488,** 61 (2012).
[4] I. Safi and H. Saleur, Phys . Rev. Lett. **93,** 126602 (2004)

TuOE6

Measuring the size of single-electron wavepackets using a beam-chopping technique

J. D. Fletcher [1], M. Kataoka [1], H. Howe [2], M. Pepper [2], P. See [1], S. P. Giblin [1], J. P. Griffiths [3], G. A. C. Jones [3], I. Farrer [3], D. A. Ritchie [3], and T. J. B. M. Janssen [1]

[1] *National Physical Laboratory, Hampton Road, Teddington, Middlesex TW11 0LW, UK*
[2] *London Centre for Nanotechnology, and Department of Electronic & Electrical Engineering, University College London, Torrington Place, London, WC1E 7JE, UK*
[3] *Cavendish Laboratory, University of Cambridge, J. J. Thomson Avenue, Cambridge CB3 0HE, UK*

Single electron sources defined in confined semiconductor systems allow precise charge transfer rates [1]. The ability to control the emission time of single electron excitations allows us to mimic the interferometers and probes of quantum optics, and perhaps even use electrons as carriers of quantum information [2]. The electron energy and emission time distributions are key features of clock-controlled electron sources, but are yet to be established and controlled. We have developed a time-domain 'beam chopping' probe of single electron excitations from a two-gate electron pump, defined in GaAs 2DEG [1] (Fig. 1a). We operate at high magnetic field (B = 12 T) in the quantum Hall regime where electrons can travel ballistically along edge channels with reduced inelastic scattering [3]. Three microns away from the pump we use a third barrier to probe the electronic distribution in the time-domain, modulating this barrier at the pump frequency, but with an adjustable phase shift (Fig 1b). The current passing the detector barrier I_c depends on the overlap of the electronic excitations with the time dependent transmission probability. By studying the variation of I_c with delay time (Fig 1c) and assuming a model electronic distribution we estimate the wavepacket length (which includes both emission broadening and dispersion) to be only 80 ps. We show that this is actually short enough that multiple electrons emitted in the same pump cycle can be distinguished and routed into different device leads.

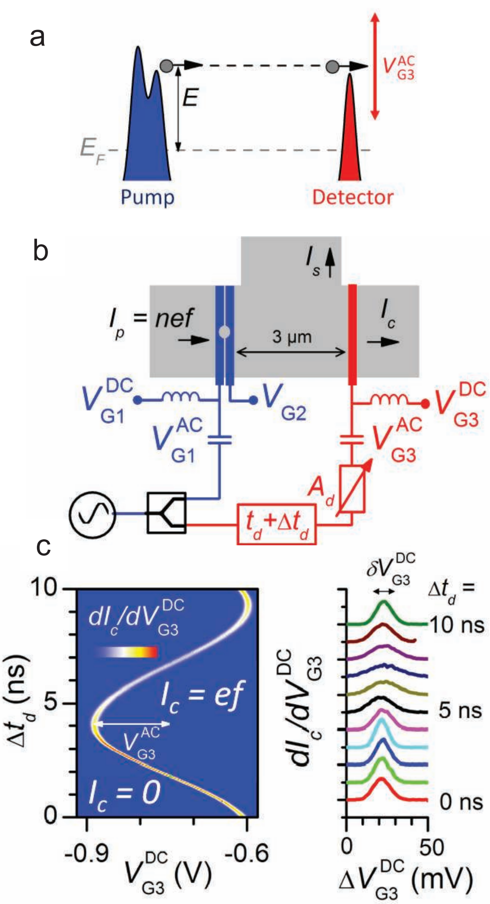

Fig 1.

[1] S. P. Giblin *et al.* Nat. Comm. **3**, 930 (2012).
[2] E. E. Bocquillon Phys. Rev. Lett. **108**, 196803 (2012).
[3] D. Taubert *et al.*, Phys. Rev. B **83**, 235404 (2011).

TuOE7

Electron quantum optics in quantum Hall edge channels

E. Bocquillon,[1] V. Freulon,[1] J.-M Berroir,[1] P. Degiovanni,[2] B. Plaçais,[1] A. Cavanna,[3] Y. Jin,[3] G. Fève[1]

[1] *Laboratoire Pierre Aigrain, Ecole Normale Supérieure, CNRS (UMR8551), Université Pierre et Marie Curie, Université Paris Diderot*
[2] *Université de Lyon, Fédération de Physique André Marie Ampère, CNRS - Laboratoire de Physique de l'Ecole Normale Supérieure de Lyon*
[3] *CNRS - Laboratoire de Photonique et de Nanostructures*

The ballistic propagation of electronic waves along the quantum Hall edge channels of a two dimensional electron gas bears strong analogies with photon optics, inspiring a whole set of experiments [1, 2] and providing an efficient tool to understand the electronic propagation in quantum conductors. I will present optics-like experiments [3, 4] with electrons that push these analogies down to the single particle scale, where a single electronic excitation is emitted on-demand in the conductor.

In particular, using two independent on-demand electron sources, we trigger the emission of two single-electron wavepackets at different inputs of an electronic beamsplitter. Whereas classical particles would be randomly partitioned by the splitter, we observe two-particle interferences [4] resulting from quantum exchange in this electronic analog [5, 6] of the optical Hong-Ou-Mandel [7] experiment. Both electrons, emitted in indistinguishable wavepackets with synchronized arrival time on the splitter, exit in different outputs as recorded by the low frequency current noise. Full random partitioning is recovered when the arrival of one electron is delayed with respect to the other. This two-electron interference experiment demonstrates the possibility to generate on-demand coherent and indistinguishable single-electron wavepackets for quantum information processing in quantum conductors.

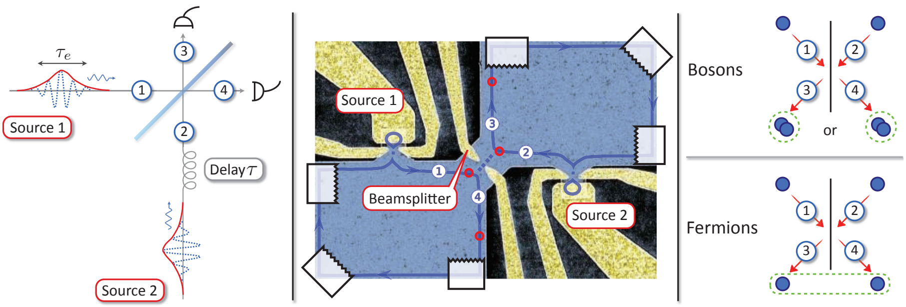

Figure 1: Two single particle wavepackets of width τ_e are emitted at inputs 1 and 2 and interfere on the splitter. Whereas photons bunch and exit in the same output, we observe antibunching of indistinguishable electrons due to Fermi statistics

[1] Henny et al., Science **284**, 296 (1999).
[2] Ji et al., Nature **422**, 415 (2003).
[3] Bocquillon et al., Physical Review Letters **108**, 196803 (2012).
[4] Bocquillon et al., Science DOI: 10.1126/science.1232572 (2013).
[5] Ol'khovskaya et al., Physical Review Letters **101**, 166802 (2008).
[6] Jonckheere et al., Physical Review B **86**, 125425 (2012).
[7] Hong et al., Physical Review Letters **59**, 2044 (1987).

TuOE8

Imaging of spin-resolved quantum Hall edge states by near-field scanning optical microscopy

H. Ito, [1] **S. Mamyouda,** [1] **Y. Shibata,** [1] **Y. Ootuka,** [1] **S. Nomura,** [1] **S. Kashiwaya,** [2] **M. Yamaguchi,** [3] **H. Tamura** [3] **and T. Akazaki** [3,*]
[1] *Division of Physics, University of Tsukuba*
[2] *National Institute of Advanced Industrial Science and Technology*
[3] *NTT Basic Research Laboratories*

The Hall conductance is closely related to the topological invariant Chern number [1] and the low energy excitations in the edge state characterize topological quantum liquids through the bulk-edge correspondence [2]. Thus the edge states are closely related to the bulk property, and for this reason the edge states have received much attention recently, for example, to clarify the symmetry of pair potential of a topological superconductor [3]. The chiral edge states in the integer quantum Hall effect is the simplest but most useful system to investigate the topological nature of quantum liquids. An optical approach was demonstrated to be a strong tool for the measurement of spin polarizations of the electrons in the edge states [4]. There are several reports on mappings of the quantum Hall edge states, but direct spin-resolved mappings of the quantum Hall edge states have not been reported.

Here we report on Hall photovoltage mappings of the spin-resolved quantum Hall chiral edge states using a near-field scanning optical microscope (NSOM) [5]. Spatial profiles of the photovoltage are investigated depending on the sign of magnetic field (B) and the circular polarizations of the incident beam. The sample was a standard Hall-bar structure of a GaAs/AlGaAs modulation-doped single heterojunction with a mobility of 178 m^2/Vs. A tunable laser beam was irradiated on the sample surface through the NSOM probe aperture at the excitation power of less than 1 nW. The polarization of the incident beam was controlled by a Berek compensator and a polarizer located close to the dilution refrigerator.

Figure 1 shows B dependence of a mapping of the spatial derivative of the photovoltage (dV/dx) at the excitation energy of E_p=1.5194 eV irradiated with an unpolarized beam. The position with large dV/dx (red) corresponds to the position of the incompressible strips. In-between the incompressible strips with even local filling factor (ν_L), the photovoltage signals due to odd ν_L are clearly observed at around B=3.50, 2.62, and 2.06 T. Circular polarization dependence of the photovoltage signals has been investigated at odd and even ν_L at E_p=1.5120 eV near the onset of the absorption at B and $-B$. The obtained scanning photovoltage mappings clearly indicate that the degree of circular polarization is large at odd ν_L in the vicinity of the edge. Our results open up a novel method to investigate spin selective mappings of the edge states of topological quantum liquids. This work was partly supported by Kakenhi Nos. 20104005, and 20221007 and 21340076.

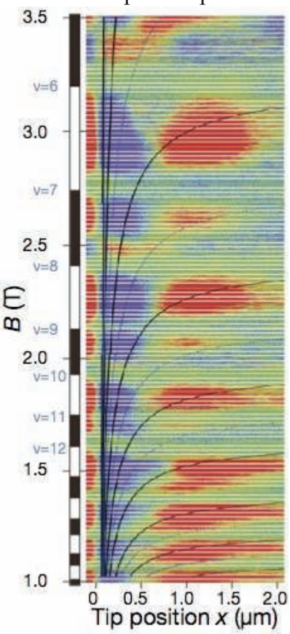

Fig. 1 Magnetic field dependence of a mapping of dV/dx at E_p=1.5194 eV at T = 250 mK.

* Present address: Kochi National College of Technology

[1] D.J. Thouless et al., Phys. Rev. Lett. **49**, 405 (1982).
[2] Y. Hatsugai, Phys. Rev. Lett. **71**, 3697 (1993).
[3] S. Kashiwaya et al., Phys. Rev. Lett. **107**, 077003 (2011).
[4] S. Nomura et al., Phys. Rev. Lett. **93**, 096803 (2004).
[5] H. Ito et al., Phys. Rev. Lett. **107**, 256803 (2011).

Study on the ultrastrong coupling of the cyclotron transition of two dimensional electron gases to THz split ring resonators

C. Maissen[1], **G. Scalari**[1], **F. Valmorra**[1], **M. Beck**[1], **C. Reichl**[2], **W. Wegscheider**[2], **D. Hagenmüller**[3], **S. De Liberato**[3], **C. Ciuti**[3], **and J. Faist**[1]

[1] *Institute of Quantum Electronics, Eidgenössische Technische Hochschule Zürich, Switzerland*
[2] *Laboratory for Solid State Physics, Eidgenössische Technische Hochschule Zürich, Switzerland*
[3] *Laboratoire Matériaux et Phénomènes Quantiques, Université Paris Diderot-Paris 7 and CNRS, Paris, France.*

Semiconductor heterostructures have been widely used to study the interaction of electronic transitions with light. The collective character of electronic excitations in semiconductor nanostructures allowed to reach strong light-matter interaction.

Interest in the ultrastrong coupling regime increased recently as new QED-phenomena are expected to appear [1]. We demonstrated ultrastrong coupling between the cylotron transition of two dimensional electron gases (2DEGs) and split ring resonators (SRRs) reaching a normalized Rabi frequency of $\frac{\Omega}{\omega_c} = 0.58$ [2].

The cyclotron transition has a huge electric dipole which scales as $d \sim el_0\sqrt{\nu}$, where $l_0 = \sqrt{\hbar/eB}$ is the magnetic length and $\nu = \rho_{2DEG}2\pi l_0^2$ the filling factor [3]. The transition frequency can be tuned by the magnetic field applied perpendicular to the 2DEG plane as $\omega_c = eB/m^*$. On the other side, SRRs exhibit a LC resonance with strongly subwavelength mode confinement which further enhances the coupling strength. We investigated in more detail the predicted scaling of the normalized Rabi frequency $\frac{\Omega}{\omega_{res}} \sim \sqrt{n_{QW}\nu}$ by optimizing the SRR design. Observations of the polariton frequencies in dependence of the carrier density and number of quantum wells agree well with predictions. In this process we could push the normalized Rabi frequency to $\frac{\Omega}{\omega_{res}} = 0.72$, limited at this stage by the depth of the cavity mode.

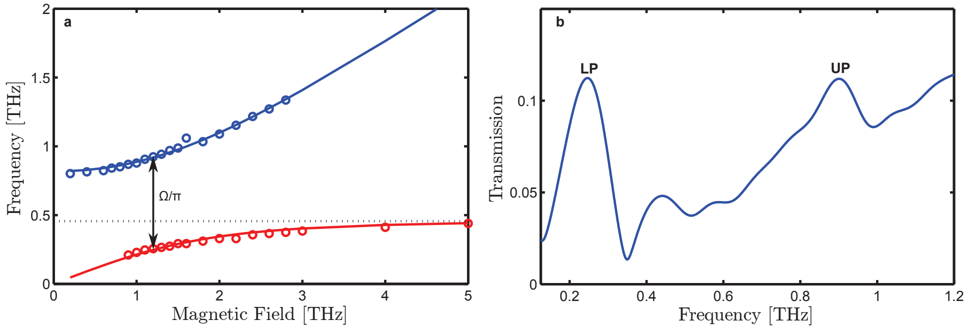

Figure 1: **a**) Transmission maxima (open circles) and best fit (solid line) (as described in [2]) yielding $\Omega/\omega_{res} = 0.72$. The dashed line indicates the frequency of the unperturbed cavity mode. **b**) Transmission spectrum at resonance (B = 1.2 T). The lower and upper polariton (LP,UP) are clearly visible.

[1] C. Ciuti, G. Bastard, and I. Carusotto, Phys. Rev. B **72**, 115303 (2005).
[2] G. Scalari, C. Maissen, D. Turcinkova, D.Hagenmuller, S. de Liberato, C. Ciuti, C. Reichl, D. Schuh, W. Wegscheider, M. Beck, and J. Faist, Science **335**, 1323 (2012).
[3] D. Hagenmüller, S. De Liberato, and C. Ciuti, Phys. Rev. B **81**, 235303 (2010).

Polaritonic two-dimensional nonlinear crystals

E. Cerda-Méndez[1], D. Sarkar[2], D.N. Krizhanovskii[2], S. Gavrilov[3], K. Biermann[1], M. S. Skolnick[2] and P.V. Santos[1]

[1]Paul Drude Institut für Festkörperelektronik, Berlin, Germany
[2]Department of Physics and Astronomy, University of Sheffield, Sheffield, United Kingdom
[3]Institute of Solid State Physics, Chernogolovka, Russia

Exciton-polaritons are bosonic quasiparticles resulting from the strong coupling of light and matter (excitons) in a semiconductor microcavity. Polaritons may form metastable macroscopic coherent phases (MCP) with properties such as Bose-like condensation and superfluidity. Also, the excitonic dipole provides strong nonlinearity through repulsive particle-particle interactions. The periodic modulation of such a nonlinear system may thus give rise to interesting phenomena, such as spatial wave localization. In particular, states localized within the gap of the band structure induced by the periodic modulation, termed gap solitons, have been the subject of widespread attention and were demonstrated in atomic and photonic systems. The study of solitonic phenomena in polaritons has been limited to homogeneous media and one dimensional periodic potentials.

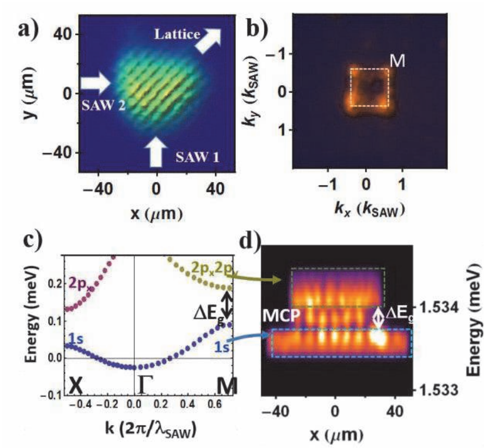

Figure 1. a) Real space image of the polariton MCP under the 2D SAW potential. b) k-space map of the emission of the polariton MCP, showing the preferential emission at the M points of the Brillouin Zone (white lines). c) Calculated 2D lattice band structurec) d) Spatially resolved spectra of the MCP where the low and high energy emission regions (boxes) show that the MCP is located within the gap ΔEg between the s- and p-states of the lattice (the region in the rectangles has been amplified by 100).

In this work, we show nonlinear polariton MCP features consistent with gap-solitonic behavior [1] in a two dimensional (2D) polaritonic crystal. The MCP is resonantly pumped in an (Al,Ga)As microcavity under a 2D periodic potential created by surface acoustic waves (SAWs) (Fig. 1a). The lattice introduces a band structure with energy band gaps ΔEg at the edges of the Brillouin Zone (BZ) (Fig. 1c). [2] Under the lattice, the MCP forms at the negative effective-mass M-points of the BZ at $\mathbf{k}=(\pm k_{SAW},\pm k_{SAW})/2$ (Fig. 1b), and within the gap ΔEg between the low density s- and p-like dispersion branches (Fig. 1d). The threshold for formation of the MCP in the 2D crystal is lower than for an unmodulatedMCP, which we attribute to the efficient accumulation of particles at the anomalous dispersion M-points. Also, the reduction of the MCP coherence length with the potential amplitude shows that the state is localized in space. These features are consistent with a model predicting the formation of a soliton within the band gap ΔEg. This work opens the possibility for the study of complex solitonic phenomena in polaritons as well the possibility for implementation for modulable robust polaritonic components for optical information processing.

[1] E. A. Ostrosvskaya and Yuri S. Kivshar, Phys. Rev Lett. 90, 160407 (2003)
[2] E. Cerda-Méndez et al., Phys. Rev. B., 86, 100301(R) (2012)

Bright polariton soliton trains in a semiconductor microcavity

M. Sich[1], F. Fras[1], J. K. Chana[1], D. V. Skryabin[2], A. V. Gorbach[2], E. A. Cerda-Méndez[3], K. Biermann[3], R. Hey[3], P. V. Santos[3], M. S. Skolnick[1] and D. N. Krizhanovskii[1]

[1] *Department of Physics and Astronomy, University of Sheffield, Sheffield, S3 7RH, UK*
[2] *Department of Physics, University of Bath, Bath, BA2 7AY, UK*
[3] *Paul-Drude-Institut für Festkörperelektronik, Hausvogteiplatz 5-7, 10117, Berlin, Germany*

Microcavity polaritons are two-dimensional composite bosons arising from strong exciton-photon coupling in semiconductor microcavities. Polariton-polariton interactions enable polariton superfluidity, non-equilibrium condensation as well as formation of dark and bright polariton solitons – localised wavepackets stabilised by nonlinearities. Polariton soliton trains – arrays of consecutive solitons, are an important step towards exploration of fundamental properties of the polariton system such as pattern formation and soliton-soliton interactions. Soliton trains may open a path towards ultrafast all-optical digital information processing.

Solitons form due to the combination of the natural negative effective mass of the lower polariton branch at large k-vectors (Fig. 1(a)) and polariton-polariton repulsive interactions [1]. For a large pump spot (~80 μm), the soliton results from local switching within the bistable area from the lower to the upper state locally in a region of a few microns by a trigger pulsed writing beam (w.b.), as shown on Fig. 1(b).

The size and spacing of solitons inside the train are determined by the polariton healing length (~5 μm) – a fundamental characteristic of inteparticle interactions in high density states and superfluids. Triggering of the soliton train therefore requires an elongated profile of the w.b. (30 μm x 7 μm). Trains consisting of up to four solitons were reliably observed (Fig. 1(c)). Individual solitons are ~5 μm in size and are equally spaced by ~5 μm.

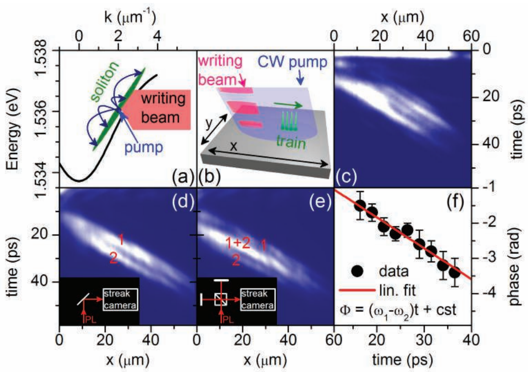

Fig. 1. (a) Dispersion (energy–momentum) diagram of the lower-branch polaritons and schematic representation of the soliton spectrum and excitation scheme. (b) Schematic of soliton train excitation in the microcavity structure. (c) A Streak camera image of a four-soliton train. Streak camera images of a two-soliton train without (d) and with (e) Michelson interferometer in imaging path (see insets). (f) Resolved phase difference between the two solitons, here '0' is arbitrary.

Phases of harmonics in the soliton spectrum are derived from the phase of the w.b. and are related through scattering processes. A single trigger pulse ensures coherence of different solitons within one train. Fig. 1(d) shows a streak camera image of a soliton train consisting of two solitons. Interfering emission from the first soliton with the second at different times (Fig. 1(e)) allowed for reconstruction of the phase difference between harmonics of the two solitons (Fig. 1(f)) as a function of time. The energy difference of ~50 μeV of the detected spectra of the two consecutive solitons is deduced from the linear trend. It results from the complex soliton-soliton interactions which manifest themselves as a redistribution of scattering inside individual solitons.

[1] M. Sich *et al.*, Nature Photon. **6**, 50-55 (2012).

Dynamics of formation and decay of oblique dark solitons in polariton quantum fluids

G. Grosso *, G. Nardin, Y. L´eger, F. Morier-Genoud, and B. Deveaud

Laboratoire d'Optoèlectronique Quantique, Ècole Polytechnique Fèdèrale de Lausanne (EPFL), Switzerland

* *corresponding author: gabriele.grosso@epfl.ch*

The demonstration of polariton superfluidity [1] has underlined the huge potential of semiconductor microcavities for studying the physics of quantum fluids. As in everyday fluids, waves and turbulence are also expected at the quantum scale. Similar to a boat sailing across calm waters, an obstacle flowing a quantum fluid can leave turbulences in its wake and generate waves. A large variety of quantum hydrodynamic effects are expected to appear in a polariton fluid at the breakdown of superfluidity under different perturbations [2, 3]. Presently, there is growing interest around solitons, especially in condensed matter systems [4]. Solitons are solitary waves, which propagate in the medium while maintaining their shape. The stability of their shape is the result of the exact compensation of the dispersion by the interparticle interactions. For the case of repulsive interaction, dark solitons may appear, having the shape of density depressions in the fluid. Nucleation and stability of dark solitons depend on particular conditions which are basically set out by the density and the velocity of the fluid, together with the nature of the obstacle that provides the perturbation.

In our experiments we create dark solitons by perturbing a polariton quantum fluid with an engineered attractive potential called mesa. Using a time and phase resolved setup we image the formation dynamics [5] of hydrodynamically nucleated dark solitons and their eventual decay and breaking into vortex streets [6].

We assess quantitatively the formation and the decay process of dark solitons and our results are scaled against parameters such as the formation speed as well as the fluid density during the hydrodynamic transient. The variation of the formation velocity and the stability conditions are quantified and traced back to an effect of the local density distribution of the fluid. We propose an explanation in terms of the conditions for the convective instability of dark solitons.

[1] A. Amo, et al.. *Nature Phys*., **5**, 805 (2009).
[2] S. Pigeon, I. Carusotto and C. Ciuti. *Phys. Rev*. **B**, **83**, 144513 (2011).
[3] G. Nardin, et al. *Nature Phys*., **7**, 635 (2011).
[4] M. Sich, et al., *Nat. Photon*., **6**, 50 (2011).
[5] G. Grosso, et al. *Phys. Rev*. B, **86**, 020509(R) (2012).
[6] G. Grosso, et al. *Phys. Rev. Lett*., **107**, 245301 (2011).

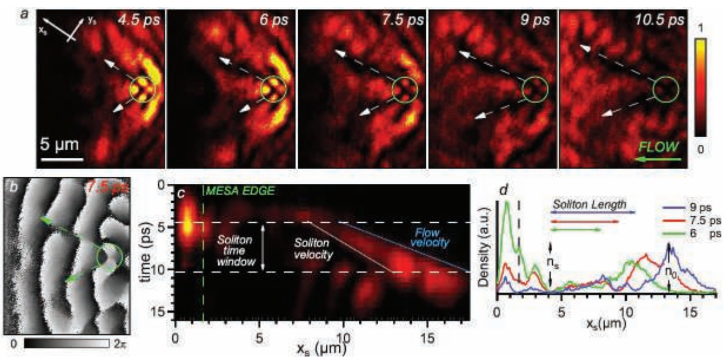

Fig.1: a- Time evolution of the density of a polariton wavepacket scattering on an engineered circular obstacle (green circle). Dark solitons (white arrows) are visible few picoseconds after the polaritons injection and are characterized by dark straight lines in the density and a phase shift (b). The velocity of formation of dark soliton can be extracted from the time evoulution of the polariton density along the soliton grow direction (c). d- Density of dark solitons ns with respsct to the polairotn fluid n0 at different times.

INVITED

On-Chip Quantum Optics using Electrically Driven Quantum Dot - Micropillar Cavities

C. Hopfmann[1], F. Albert[2], E. Stock[1], M. Lermer[2], C. Schneider[2], S. Höfling[2], A. Forchel[2], M. Kamp[2], S. Reitzenstein[1]

[1]Institut für Festkörperphysik, Technische Universität Berlin, Berlin, Germany
[2]Technische Physik, Universität Würzburg, Würzburg, Germany

The prospect of studying quantum optics in the solid state and the quest for quantum light sources in the field of quantum communication has triggered enormous efforts in the development of micro- and nanocavity systems with embedded quantum dots (QDs). These structures exploit cavity quantum electrodynamics (cQED) effects and can act as efficient non-classical light sources and as high-β microlasers. Initially, QD-microcavities were exclusively excited optically by external lasers, while significant technological progress has enabled electrical pumping in advanced structures.
Here we report for the first time on an on-chip quantum optics experiment where an integrated microlaser excites a QD-micropillar cavity operating in the weak coupling regime of cQED. Our approach combines two very active but so far independent routes of cQED, namely high-β lasing and light-matter interaction at the quantum in a novel, integrated device concept. This concept is illustrated in Fig. 1(a) and relies on the fact that micropillar cavities allow for the localization of vertically emitting modes and laterally emitting whispering gallery modes (WGMs). We take advantage of these unique opportunity provided by the micropillar geometry to utilize an electrically pumped WGM micropillar as in-plane laser source. The integrated WGM microlaser resonantly excites radially displaced QD-micropillars. This specific configuration allows us to perform for the first time on-chip quantum optics in the cQED regime using an integrated coherent light source.

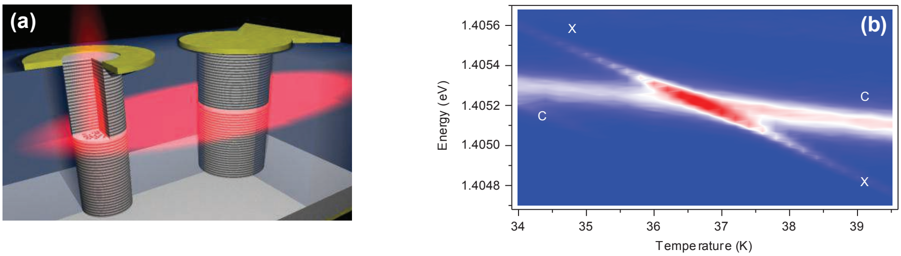

Figure 1. (a) Schematic view of device design for on-chip quantum optics (left panel). (b) Demonstration of Purcell enhancement of a QD–micropillar under resonant pumping via an electrically driven internal WGM microlaser.

The high quality electrically pumped WGM lasers were studied by means of micro-electroluminescence spectroscopy and show single mode emission, threshold currents below 10 µA and β-factors of about 0.1 at low temperature. Emission from such a WGM laser was used to resonantly excite a target quantum dot in an adjacent micropillar with a diameter of 2.5 µm via p-shell excitation. It is interesting to note, that resonant excitation schemes are crucial for generation of indistinguishable photons and are not feasible in conventional approaches for electrically driven quantum light sources based on simple pin-diodes.
Resonant p-shell pumping was then applied to excite a QD-micropillar system where a single QD exciton (X) was shifted through resonance with the fundamental cavity mode (C) by means temperature tuning (cf. Fig. 1 (b)). In this experiment, weak coupling associated with a Purcell factor of 4.1 was observed for the first time in a quantum device with an integrated coherent light source [1].

[1] E. Stock et al., Adv. Mat. 2012, DOI: 10.1002/adma.201202778.

Monday Tuesday Wednesday Thursday Friday

TuIE3

INVITED

The Three Spin System

S. A. Studenikin, J. Thorgrimson, G. Poulin-Lamarre, P. Zawadski, G. C. Aers, and A. S. Sachrajda

National Research Council of Canada, Ottawa, Canada

Double quantum dot circuits have been the focus of intense study over the last decade. Recently we have investigated the linear triple quantum dot system [1-4]. A variety of novel physics and applications have already emerged from these investigations. The isolation of the center quantum dot from leads, for example, has led to the discovery of quantum backaction via single phonon interferometery [2] as well as a new charge detection approach which significantly enhances the signal to noise for spin qubit readout [4]. The Pauli blockade double quantum dot rectification effect evolves to a full insulator phenomenon (spinsulator) in a triple quantum dot with a resonant leakage current which involves a non-intuitive spin busing via coherent superpositions of quantum states [3].

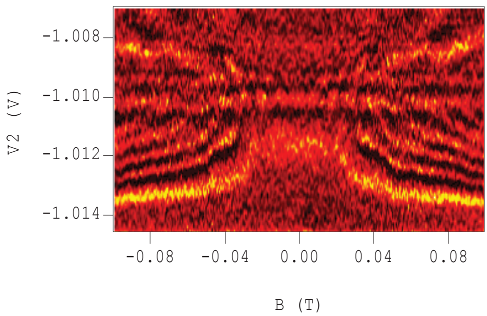

Coherent behavior of three spins has also been demonstrated with Landau-Zener-Stückleberg manipulation [1]. In this work we use the triple quantum dot circuit formed in GaAs/AlGaAs heterostructure by lateral gates to study the coherent properties of the three spin system in more detail. The two-spin singlets and triplets of the two spin system are replaced with doublets and quadruplets in the three-spin scenario. Our device enables us to tune the magnitude of the exchange couplings between the three spins and the relative strength of the exchange to the hyperfine interactions. By varying these experimental parameters as well as pulse shapes we are able to study the coherent behavior of pairs of different three-spin states. The figure shows an example of experimental data where disparate coherent oscillations between different pairs of the three-spin states are revealed. We find that such magnetic field plots are able to distinguish and identify different species of coherent oscillations, in particular, the all-exchange oscillations [5] are manifested as horizontal fringes as they are related to a field independent part of the energy spectrum. The all-exchange spin qubit does provide protection against global noise effects such as magnetic field fluctuations but we also find that coherent behavior between other three spin states have different attractive properties such as a reduced sensitivity to local charge noise.

[1] L. Gaudreau, G. Granger, A. Kam, G. C. Aers, S. A. Studenikin, P. Zawadzki, M. Pioro-Ladriere, Z. R. Wasilewski, and A. S. Sachrajda, *Nature Phys.* **8**, 54 (2012).
[2] G. Granger, D. Taubert, C. E. Young, L. Gaudreau, A. Kam, S. A. Studenikin, P. Zawadzki, D. Harbusch, D. Schuh, W. Wegscheider, Z. R. Wasilewski, A. A. Clerk, S. Ludwig, and A. S. Sachrajda, *Nature Phys.* **8**, 522 (2012).
[3] M. Busl, G. Granger, L. Gaudreau, R. Sanchez, A. Kam, M. Pioro-Ladriere,S. A. Studenikin, P. Zawadzki, Z. R. Wasilewski, A. S. Sachrajda, G. Platero, Nature Nanotechnol. 2013 (accepted).
[4] S. A. Studenikin, J. Thorgrimson, G. C. Aers, A. Kam, P. Zawadzki, Z. R. Wasilewski, A. Bogan, and A. S. Sachrajda, *App. Phys. Lett.*. **101**, 233101 (2012).
[5] D. P. DiVincenzo, D. Bacon, J. Kempe, G. Burkard, and K. B. Whaley, *Nature,* **408**, 339 (2000).

Monday
Tuesday
Wednesday
Thursday
Friday

Thermometry and Refrigeration using Quantum Dots

A. Mavalankar, C.G. Smith, S.J. Chorley, J. P. Griffiths, G. A. C. Jones, I. Farrer, and D. A. Ritchie
Semiconductor Physics Group, Department of Physics, JJ Thomson Avenue, Cambridge CB3 0HE
Email: am877@cam.ac.uk

The two-dimensional electron gas in GaAs/AlGaAs heterostructures has diverse applications at cryogenic temperatures, but is heated by noise in the measurement set up. Our work involves the fabrication of a quantum dot refrigerator which can cool the electron gas to below the ambient lattice temperature[1].

Lithographically defined Ti/Au gates patterned on the surface of a GaAs/AlGaAs heterostructure define three quantum dots (left, right, and top) of radius 150 nm, tunnel-coupled to an enclosed, macroscopic, two-dimensional reservoir of electrons 100μm^2 in area. The QDR uses the discrete energy levels of two quantum dots to cool the central electron reservoir (Fig 1). The third quantum dot (the 'thermometer') probes the temperature of the two dimensional reservoir being cooled (Fig 2, inset).

Our temperature measurement scheme consists of monitoring the charge distribution of the thermometer dot. This dot is open only to the enclosed reservoir whose temperature we want to extract. Changing the energy level of the dot through the Fermi-Dirac energy distribution of the enclosed reservoir results in the occupation probability of the dot being described by the same distribution. This is reflected in the current flowing through an adjoining quantum point contact. Fitting a Fermi-Dirac distribution to the measured current thus yields the temperature of the two-dimensional reservoir (Fig 2). We have demonstrated measuring electronic temperatures in the range 100 mK to 300 mK, with errors as low as 5 mK. The limits of this temperature measurement scheme still have to be explored. Using this scheme, we have also investigated the variation in the electron temperature as a function of the voltages on the top and right plunger gates. This variation is produced because the changing voltages on the plunger gates move the energy level of the entrance dot down through the Fermi level of the source while moving the level of the exit dot up through the Fermi level at the drain, thus changing the energy extracted from the reservoir. Our results agree qualitatively with the model of electron cooling developed by Edwards[2].

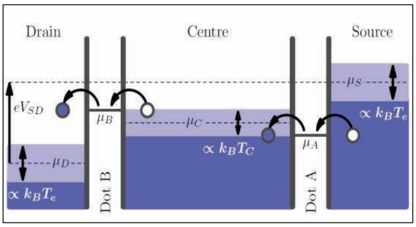

Fig 1: Energy level diagram of a Quantum Dot Refigerator in the cooling regime.

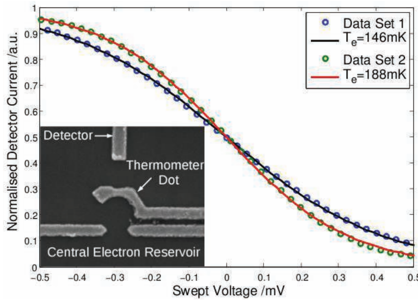

Fig 2: Fitting a Fermi-Dirac function to the detector current of the thermometer dot. Two measurements (for different voltages on the entrance and exit dots) are presented here, with the extracted electron temperatures differing by 40mK. Inset: Scanning Electron Micrograph of a quantum dot and the adjoining quantum point contact.

References

[1] J. R. Prance, C. G. Smith, J. P. Griffiths, S. J. Chorley, D. Anderson, G. A. C. Jones, I. Farrer, and D. A. Ritchie 2009 *Phys. Rev. Lett*. **102** 146602
[2] H. L. Edwards, Q. Niu, G. A. Georgakis, and A. L. de Lozanne 1995 *Phys. Rev. B* **52** 5714

Scattering Gate Interferometry at a Quantum Point Contact

B. Brun [1], F. Martins [2], S. Faniel [2], B. Hackens [2], V. Bayot [1,2], S. Huant [1], U. Gennser [4], D. Mailly [4], M. Sanquer [3] and H. Sellier [1]

[1] *Institut Néel (CNRS/UJF), 25 rue des Martyrs 38042 Grenoble*
[2] *Institut Matière Condensée et Nanonsciences, (UCL),Ch. du Cyclotron 2, Louvain-la-Neuve*
[3] *Institut Nanosciences et Cryogénie (CEA), 17 rue des Martyrs 38054 Grenoble*
[4] *Laboratoire de Photonique et de Nanostructures (CNRS), Route de Nozay 91460 Marcoussis*

Electron-electron interactions are widely considered to explain the puzzling 0.7 anomaly [1] in Quantum Point Contacts (QPCs). Motivated by the theory developed in Ref. [2], we are interested to see if we can measure the scattering of electrons in the QPC due to Friedel oscillations generated by a distant perturbative potential. Since this experiment will also produce single particle interferences, the more subtle interaction effects will appear as deviation from the single particle models used to analyze the data.

Pioneering Scanning Gate Microscopy (SGM) experiments have already revealed such single electron interferences superimposed to the electron streams imaged in real space [3]. Inspired by SGM technique, we designed a new type of interferometer where an additional sharp gate is designed in front of the QPC to act as a tunable perturbative back-scattering potential for electrons towards the QPC. The negative voltage (Vg3) applied on this gate allows us to move the scattering region towards the QPC and generate interferences.

Additionally to this interferometry study, we performed SGM on a QPC, at base temperature of 20 mK. We observed usual single particle interferences (red dashed line 1) Fig. 2), and compared it to what can be obtained with our interferometers. We studied contrast and phase of these oscillations as the QPC opens, and discovered surprising effects. The interferences are more contrasted on the QPC plateaus and at the 0.7 anomaly than in the crossover regions between the plateaus, and they show sharp phase shifts between each plateau and noticeably at the 0.7 anomaly.

Finally, we observed a new type of fringes in our SGM experiment (blue dashed line 2) Fig.2), exhibiting an increasing wavelength as the tip is moved away from the QPC, and more contrasted below the first plateau. These new oscillations are not due to interferences but to the direct tuning of a self-organized many-particle state inside the QPC channel. These observations shine a new light on the puzzling many-body effects underlying QPCs' physics.

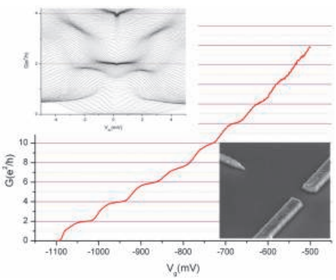

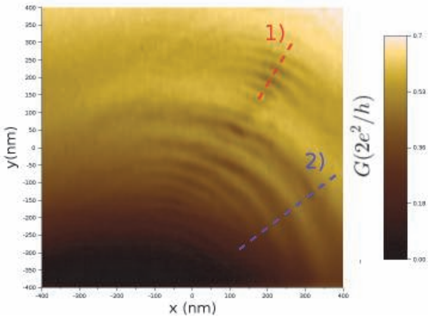

Fig.1 *(left): G(Vg) of the QPC. Insets: SEM image of the device and DC spectroscopy.*
Fig.2 *(right): SGM image showing interferences (line 1) and new oscillations (line 2)*

[1] K.J. Thomas *et al.*, Phys. Rev. Lett. **77**, 1 (1996).
[2] A. Freyn, I. Kleftogiannis, and J.L. Pichard, Phys. Rev. Lett **100**, 226802 (2008)
[3] M.A. Topinka *et al.*, Nature **410**, 183 (2001)

Ballistic electron transfer between quantum dots

Tobias Krähenmann[1], Clemens Rössler[1], Simon Burkhard[1], Thomas Ihn[1], Klaus Ensslin[1], Christian Reichl[1] and Werner Wegscheider[1]

[1]*Solid State Physics Laboratory, ETH Zürich, 8093 Zürich, Switzerland*

We observe ballistic transport of electrons from one quantum dot (QD) to another QD in Coulomb blockade. Our recent experimental efforts aim at realizing a weak-measurement protocol in a solid-state environment. The process of a quantum measurement and its resulting projection of the state vector on an eigenstate of the measurement Hamiltonian is a cornerstone of quantum mechanics. In 1988 Aharonov *et al.* [1] introduced the concept of a weak measurement. In a weak measurement the system is weakly coupled to the measuring device. In a second step a strong von Neumann measurement is performed to post-select the system. The introduced concept has since been successfully applied in a few experiments (e.g. [2, 3]).

Our system of choice is a top-gated GaAs/AlGaAs heterostructure. The sample consists of two double QDs with nearby quantum point contacts acting as sensitive charge detectors. A scanning electron micrograph of the sample is shown in Fig. 1. The two QDs can be tuned individually for selective energy filtering in the system.

An energy scheme describing the ballistic transport is shown in Fig. 2(a). The measurement data is shown in Fig. 2(b). The energy level of the detector dot is set to $\approx 200\ \mu eV$ above the Fermi level. Now the source level is swept together with the emitter dot level and the current through the detector dot is recorded. The red peak around $V_{\mathrm{emitter}} = -200\ \mu\mathrm{V}$ corresponds to ballistic transfer of electrons. The blue region at higher energies corresponds to electrons which are relaxed in the center reservoir. In the future we plan to implement a weak measurement protocol using one QD for the weak measurement while the post-selection will be done in the second QD.

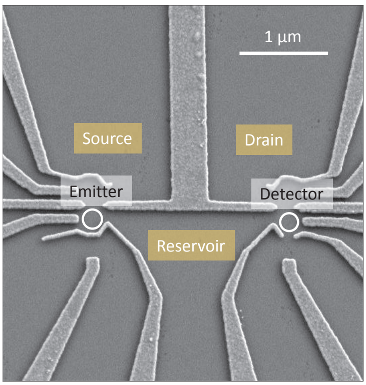

Figure 1: Scanning electron micrograph of a top gated AlGaAs heterostructure sample. The two quantum dots are indicated by circles.

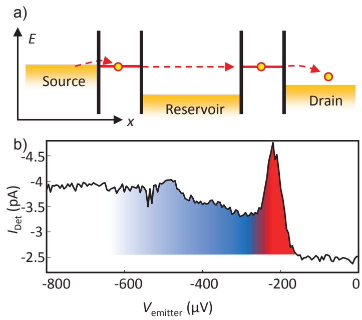

Figure 2: (a) Energy scheme describing the ballistic transport. (b) Detector current as a function of emitter voltage. A pronounced ballistic peak (red) and a region of energy relaxed electrons (blue) is observed.

[1] Y. Aharonov, D. Z. Albert, and L. Vaidman, Phys. Rev. Lett. **60**, 1351 (1988).
[2] N. W. M. Ritchie, J. G. Story, and R. G. Hulet, Phys. Rev. Lett. **66**, 1107 (1991).
[3] O. Hosten and P. Kwiat, Science **319**, 787 (2008).

Monday
Tuesday
Wednesday
Thursday
Friday

TuOM9

A novel mesoscopic phenomenon: An analog of the Braess paradox in 2DEG networks

H. Sellier [1], M. Pala [2], S. Baltazar [2], P. Liu [1], B. Hackens [3], F. Martins [3], X. Wallart [4], L. Desplanque [4], V. Bayot [1,3], and S. Huant [1]

[1] *Institut Néel, CNRS & Université Joseph Fourier, BP 166, F-38042 Grenoble*
[2] *IMEP-LAHC, Grenoble INP, Minatec, BP 257, F-38016 Grenoble*
[3] *IMCN/NAPS, UCLouvain, 2 chemin du cyclotron, B-1348 Louvain-la-Neuve*
[4] *IEMN, UMR CNRS 8520, UST Lille, BP 60069, F-59652 Villeneuve d'Ascq*

Aharonov-Bohm oscillations and universal conductance fluctuations are emblematic interference effects in mesoscopic nanostructures of two-dimensional electron gas (2DEG). While studying quantum networks with asymmetric parallel channels, we discovered a new phenomenon which is a mesoscopic analog of the classical Braess paradox [1]. This counter-intuitive effect was first described for congested road networks where adding a new road can paradoxically lead to a deterioration of the overall traffic situation. Known so far in classical situations only, including electrical and mechanical networks, we have extended the concept of the Braess paradox to mesoscopic semiconductor networks where electron transport is governed by quantum mechanics [2].

Our network has three branches connected asymmetrically with respect to source and drain contacts as shown in the figure. The vertical wires are narrower than the horizontal ones to behave as congested channels. Numerical simulations of quantum transport through this network show that the presence of the central wire decreases the overall conductance although intuition tells us that it should increase the conductance by adding extra channels. Remarkably, this phenomenon is robust with respect to Fermi level variations and cannot be reduced to previously known mesoscopic effects in nanostructures.

Then, we have considered scanning gate microscopy [3] as a versatile tool to control the transmission of the central channel with the sharp tip of a cryogenic AFM microscope that induces a local potential change in the 2DEG. Numerical simulations of the network transmission as a function of the tip position show that the transmitted current is increased, instead of decreased, when the tip is placed above the central channel with a negative voltage that depletes locally the 2DEG (see figure). This network has been fabricated in a high-mobility GaInAs/AlInAs heterostructure with dimensions that ensure ballistic and coherent transport at low temperature. Using a scanning gate microscope at 4.2 K, we have observed such a counter-intuitive Braess-like effect that can be distinguished from other mesoscopic effects. This mesoscopic analog of the classical Braess paradox raises fundamental questions that will be discussed and may find applications in future quantum devices.

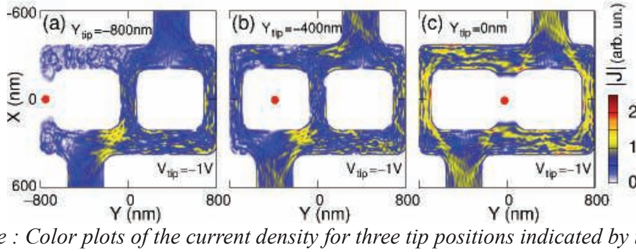

Figure : Color plots of the current density for three tip positions indicated by the red dots.

[1] D. Braess, Unternehmensforschung **12**, 258 (1968).
[2] M. Pala *et al.*, Phys. Rev. Lett. **108**, 076802 (2012); Nanoscale Res. Lett. **7**, 472 (2012).
[3] B. Hackens *et al.*, Nat. Phys. **2**, 826 (2006).

Spin-resolved Andreev levels in hybrid superconductor-semiconductor nanowire devices

Eduardo J. H. Lee[1], **Xiaocheng Jiang**[2], **Manuel Houzet**[1], **Ramón Aguado**[3] **and Silvano De Franceschi**[1]

[1]*SPSMS, CEA-INAC/UJF-Grenoble 1, 17 rue des Martyrs, 38054, Grenoble, France*
[2]*Harvard University, Department of Chemistry and Chemical Biology, Cambridge, MA, 02138, USA*
[3]*Instituto de Ciencia de Materiales de Madrid (ICMM-CSIC), Sor Juana Inés de la Cruz 3, 28049, Madrid, Spain*

The combination of superconductors and low-dimensional conductors embodies a rich, yet largely unexplored physics. In this hybrid system, macroscopic properties enforced by superconductivity can be controlled through electrically tunable microscopic degrees of freedom, inherent to a relatively small number of confined electrons. Here we consider the prototypical case of a quantum dot (QD) coupled strongly to a superconductor (S) and weakly to a normal-metal (N) tunnel probe. Specifically, we address devices based on individual InAs/InP core/shell nanowires electrically contacted by vanadium and gold, where a single QD is naturally formed in the nanowire section between the S and N leads. We investigate the magnetic properties of the lowest-energy, sub-gap states, which are governed by a competition between superconducting pairing and Coulomb repulsion. In a magnetic field, only when the ground state is a spin singlet, can the Zeeman splitting of the (excited) doublet be revealed by tunnel spectroscopy. The splitting is strongly influenced by a level-repulsion effect with the continuum of quasi-particle states; and it can induce a quantum phase transition (QPT) to a spin-polarized state [1]. Our experimental results, supported by theory, hold relevance for current research on quantum-information devices and Majorana fermions in hybrid nanostructures.

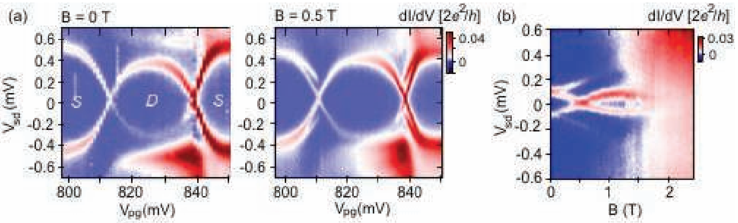

Figure 1: (a) Magnetic field-induced Andreev level splitting. The green (yellow) circles indicate the regions in which the ground state is a singlet (doublet). (b) Field-induced quantum phase transition from a singlet to a spin-polarized ground state. The QPT appears as a zero-bias peak.

[1] E. J. H. Lee, X. Jiang, M. Houzet, R. Aguado, C. M. Lieber and S. De Franceschi, arXiv:1302.2611.

Monday Tuesday Wednesday Thursday Friday

Monday Tuesday Wednesday Thursday Friday

Acousto-Mechanical Tuning of Photonic Crystal Nanocavity Modes for Quantum Gate Applications

H. J. Krenner[1], S. S. Kapfinger[1], D. A. Fuhrmann[1], A. Wixforth[1], S. M. Thon[2], H. Kim[2], D. Bouwmeester[2], P. M. Petroff[3], R. Blattmann[4], P. Hänggi[4], S. Kohler[5]

1. *Lehrstuhl für Experimentalphysik 1, Universität Augsburg, 86150 Augsburg, Germany*
2. *Physics Department, University of California, Santa Barbara, California 93106, USA*
3. *Materials Department, University of California, Santa Barbara, California 93106, USA*
4. *Lehrstuhl für Theoretische Physik 1, Universität Augsburg, 86150 Augsburg, Germany*
5. *Instituto de Ciencia de Materiales de Madrid, CSIC, E-28049 Madrid, Spain*

Recently we have shown that the mechanical deformation induced by radio frequency surface acoustic waves (SAWs) on a two-dimensional photonic crystal membrane (PCM) spectrally tunes the resonance frequency of nanocavities within the PCM at gigahertz frequencies [1]. Here we report the first direct experimental investigation of this tuning mechanism in the time domain. In Fig. 1 (a), we present a typical photoluminescence (PL) spectrum (dashed) of a nanocavity mode recorded under non-resonant excitation of an ensemble of quantum dots off-resonantly coupled to the mode. Turning the SAW on, leads to a clear, characteristic broadening of the spectrum (solid), with a tuning bandwidth of 100 GHz. To demonstrate that the applied SAW dynamically modulates the optical mode, we implemented a time-resolved detection scheme. The excitation laser pulses were actively phase locked to the SAW and the PL signal was detected with an avalanche photodiode with a temporal resolution of 50 ps. The transient of the unperturbed mode detected at n_0, is plotted for reference (grey line) in Fig. 1 (b). With a SAW of f_{SAW} of 850 MHz is applied, we set the laser repetition rate to $f_{\mathrm{SAW}}/11$ and detect the nanocavity emission at the blue end of the tuning range $\nu_{\mathrm{det}} = \nu_{\mathrm{blue}}$ marked in panel (a). The signal shows a clear beating, precisely given by the SAW period T_{SAW} = 1175 ps which is enveloped by the transient of unperturbed mode. For the solid black line, the phase relation between laser pulse and the SAW was set such that the system is pumped at the time when mode is tuned to the detection frequency, $\nu(t_{\mathrm{exc}} = t_0) = \nu_{\mathrm{blue}}$. Shifting the time of excitation by $T_{\mathrm{SAW}}/2$, we excite the system with the mode at $\nu(t_{\mathrm{exc}} = t_0 + T_{\mathrm{SAW}}/2) = \nu_{\mathrm{red}}$. Since the detection is performed at $\nu_{\mathrm{det}} = \nu_{\mathrm{blue}}$, the beating of the transient (dotted grey) is offset in time also by $T_{\mathrm{SAW}}/2$. To resolve the full dynamics of our tuning mechanism we keep $\nu(t_{\mathrm{exc}} = t_0 + T_{\mathrm{SAW}}/2) = \nu_{\mathrm{red}}$ and tune ν_{det}. The recorded transients are plotted in grayscale representation in Fig. 1 (c). In this data the dynamic tuning and mode decay is monitored and clearly resolved over the full spectral tuning bandwidth.

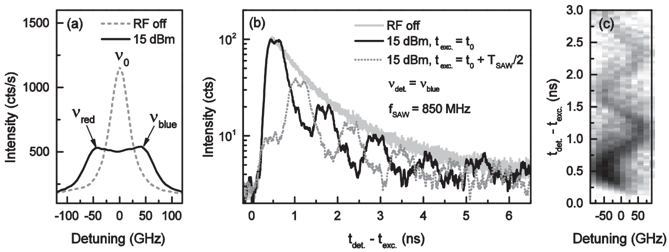

Fig. 1 (a) Time integrated spectrum of the cavity mode with no fixed phase relation between SAW and excitation laser (b) Time resolved traces of the modulated mode

Finally we elaborate strategies to extend our approach for controlled entanglement generation in this prototype solid-state cavity quantum electrodynamics system using Landau-Zener-Stückelberg transitions. For our theoretical modelling we consider a realistic dissipative system being at or above the threshold to the strong coupling. Our first calculations predict for cavity quality factors $Q \geq 60000$ a concurrence of $C \sim 0.7$ when driving the coupled quantum dot-nanocavity system at SAW frequencies up to 3 GHz.

[1] D. A. Fuhrmann *et al.*, Nature Photonics **5**, 605 (2011)

Magnetic-field-free electron spin resonance in winding GaAs channel

Haruki Sanada[1], Yoji Kunihashi[1], Hideki Gotoh[1], Koji Onomitsu[1], Makoto Kohda[2], Junsaku Nitta[2], Paulo V. Santos[3], and Tetsuomi Sogawa[1]

[1] *NTT Basic Research Laboratories, NTT Corporation, Atsugi, Japan*
[2] *Department of Materials Science, Tohoku University, Sendai, Japan*
[3] *Paul-Drude-Institut für Festkörperelektronik, Berlin, Germany*

Electron spin resonance (ESR) has the potential for use in manipulating individual spins for quantum information technologies. In general, ESR requires two external magnetic fields: a static field ($\mathbf{B}_0$) and oscillating one ($\mathbf{B}_1$). However, approaches relying on real magnetic fields, which are generated in much broader spaces than the size of individual electrons, are energetically inefficient for spin-information processing on a chip. Here we demonstrate magnetic-field-free ESR achieved by using spin-orbit interaction (SOI) [1]. Because a moving electron experiences a spin-orbit effective magnetic field $\mathbf{B}^{SO}$ that depends on the moving direction, we expect both the static and oscillating fields needed for ESR to be replaced with effective fields ($\mathbf{B}_0^{SO}$ and $\mathbf{B}_1^{SO}$) by controlling the trajectory of travelling electrons [Fig. 1(a)].

The sample was an undoped 20-nm-thick GaAs/AlGaAs (001) quantum well. A surface acoustic wave (SAW) beam propagating along [-110] produces an array of potential wires moving with the velocity $v_{SAW} \sim 2.97$ km/s [2]. A Ti film with 3-μm-wide slits deposited on the wafer partially screens the piezoelectric field and produces moving dots that travel along the channels formed beneath the slits [Fig. 1(b)]. We performed Kerr microscopy to investigate spin transport along straight and winding channels, the latter of which was designed to be close to the resonance condition.

Figure 2 shows a Kerr image measured for the two channels in the absence of external magnetic field. The Kerr rotation is proportional to the spin density at the probe position. The oscillations observed for the straight channel [Fig. 2(a)] are attributed to the spin precession induced by $\mathbf{B}_0^{SO}$. The effects induced by $\mathbf{B}_1^{SO}$ appear in the data for the winding channel [Fig. 2(b)]; the spin precession phase inverts when the probe position crosses $y \sim 30$ μm. The Bloch simulations of the spin dynamics under $\mathbf{B}^{SO}$ well reproduce the experimental results, and this proves the feasibility of the magnetic-field-free ESR. This technique will provide an efficient and flexible approach for the coherent control of flying spin information in solid-state devices.

[1] H. Sanada *et al.*, Nature Physics, *to be published*.
[2] H. Sanada *et al.*, Phys. Rev. Lett. **106**, 216602 (2011).

This work was supported by JSPS KAKENHI (No. 24686004 and 23310097).

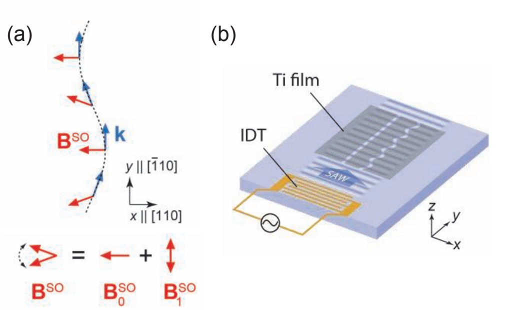

Fig. 1 (a) **k**-vectors and Dresselhaus fields ($\mathbf{B}^{SO}$) for electrons moving along a sinusoidal channel. The electrons experience static ($\mathbf{B}_0^{SO}$) and oscillating ($\mathbf{B}_1^{SO}$) fields. (b) Sample schematic. The winding channel has a sinusoidal shape with a period of 23 μm and amplitude of 2 μm.

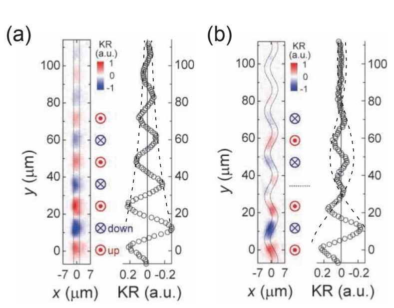

Fig. 2 Kerr images of the straight (a) and winding (b) channels. The same data averaged along the x axis are plotted on the right side of each image. The dashed lines are guides to the eyes.

Monday
Tuesday
Wednesday
Thursday
Friday

INVITED

Unconventional Electronic and Magnetic States at the $LaAlO_3/SrTiO_3$ Interface

Harold Y. Hwang [1,2]

[1] *Dept. of Applied Physics, Stanford University, USA*
[2] *Dept. of Photon Science, SLAC National Accelerator Laboratory, USA*

The nature and control of the electronic structure at oxide heterointerfaces is an emerging research opportunity, enabled by modern atomic-scale growth and probe techniques for creating and studying new artificial interface states. Among the many issues that arise, the electrostatic boundary conditions that occur at heterointerfaces are often a very important determinant of the interface properties. This has been extensively studied for the (100) oriented $LaAlO_3/SrTiO_3$ interface, a novel 2D system exhibiting both magnetism and superconductivity. After introducing this system, we will focus on recent x-ray spectroscopic studies [1] demonstrating d_{xy} ferromagnetism on the interface titanium, which has a number of potential implications for the superconducting state.

[1] J.-S. Lee, Y. W. Xie, H. K. Sato, C. Bell, Y. Hikita, H. Y. Hwang, & C.-C. Kao, *Nature Mater.* DOI: 10.1038/NMAT3674 (2013).

Even denominator and higher Landau level fractional quantum Hall states in ZnO

J. Falson,[1] D. Maryenko,[2] D. Zhang,[3] B. Friess,[3] Y. Kozuka,[1] A. Tsukazaki,[4] J. H. Smet[3] and M. Kawasaki[1,2]

[1] *Department of Applied Physics and Quantum-Phase Electronics Center (QPEC), The University of Tokyo, Tokyo, Japan*
[2] *RIKEN Center for Emergent Matter Science (CEMS), Wako, Japan*
[3] *Max Planck Institute for Solid State Research, Stuttgart, Germany*
[4] *Department of Advanced Materials Science, The University of Tokyo, Kashiwa, Japan*

The ZnO two-dimensional electron system has recently emerged as an alternative platform for investigating 2D correlation physics. Advances in growth techniques now allow the realisation of samples with electron mobilities exceeding $\mu = 700{,}000\ \mathrm{cm}^2/\mathrm{Vs}$ [1], enabling the observation of an extensive series of fractional quantum Hall states (FQHS) in the lowest Landau level [2].

In this work, we present low temperature magnetotransport data focusing on the higher Landau level physics of the system. Figure 1 displays the magnetotransport, where a rich variety of FQHS are revealed for $\nu > 2$ at base $T \approx 20$mK. Most notable is the clear quantisation of the even denominator $\nu = 7/2$ FQHS; the first observation of an even denominator state outside of the GaAs electron system. While this state is stable, the $\nu = 5/2$ FQHS is curiously absent. Rather, the $\nu = 5/2$ region presents as asymmetric, with the observation of FQHS $\nu = 8/3$, 13/5 and 18/7 on the low field side contrasted by a complete absence of FQHS on the high field side. Instead, a single reentrant integer quantum Hall state (RIQHS) is revealed at *higher* temperature. Such results suggest that ZnO allows the exploration of new and unique facets of 2D electron correlation physics.

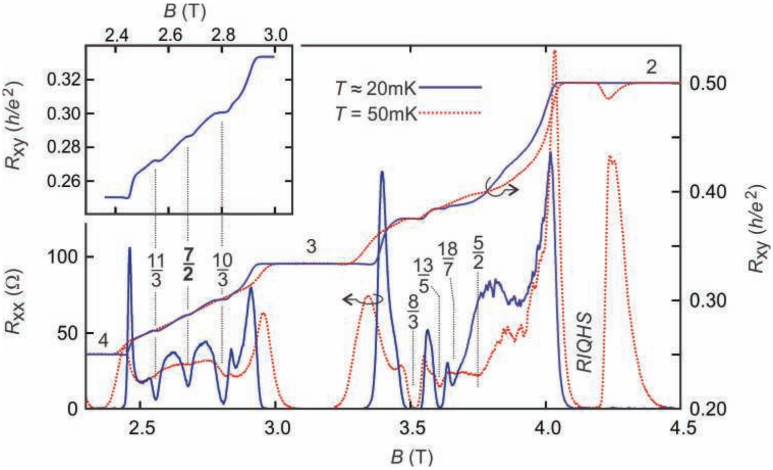

Figure 1: Magnetotransport at $T \approx 20$mK (blue, solid) and 50mK (red, dotted) for $4 > \nu > 2$ with notable quantised states, and the location of $\nu = 5/2$ indicated. The inset displays a close-up of the quantised Hall resistance for $4 > \nu > 3$.

[1] J. Falson *et al.*, *Appl. Phys. Express* **4**, 091101 (2011).
[2] D. Maryenko *et al.*, *Phys. Rev. Lett* **108**, 186803 (2012).

TuOE13

Raman and photoluminescence spectroscopy of atomically thin MoS_2, $MoSe_2$, and WSe_2

Philipp Tonndorf [1,4], Robert Schmidt [1,4], Philipp Böttger [1], Xiao Zhang [1], Janna Börner [2], Andreas Liebig [1], Manfred Albrecht [1], Christian Kloc [3], Ovidiu Gordan [1], Dietrich R. T. Zahn [1], Steffen Michaelis de Vasconcellos [1,4] and Rudolf Bratschitsch [1,4]

[1] *Institute of Physics, Chemnitz University of Technology, Germany*
[2] *Institute of Chemistry, Chemnitz University of Technology, Germany*
[3] *School of Materials Science & Engineering, Nanyang Technological University, Singapore*
[4] *Physikalisches Institut, Westfälische-Wilhelms Universität Münster, Germany*

Atomically thin molybdenum and tungsten dichalcogenides are of considerable interest due to their usability in fabricating electronic devices. Recently, photoluminescence (PL) of monolayer MoS_2 has been reported [1], which renders these materials also interesting for optical and optoelectronic applications. Light emission is due to the formation of a direct bandgap in monolayer material compared to an indirect bandgap of the bulk crystal.
We investigate photoluminescence, transmission, and vibrational properties of few- down to monolayer samples of MoS_2, $MoSe_2$ and WSe_2 [2], which are prepared by mechanical exfoliation from single crystals onto SiO_2/Si substrates. Raman spectroscopy shows that the energy, width, and amplitude of the vibrational modes strongly depend on the thickness of the flakes. As for MoS_2 we find for $MoSe_2$ that the Raman signal shows a characteristic softening (stiffening) of the A_{1g} (E^1_{2g}) mode with decreasing thickness of the material, respectively. Our high experimental resolution allows us to observe a Davydov splitting of the A_{1g} line for the first time. Starting from one Raman line for mono- and bilayer $MoSe_2$ it splits into two for three and four layer material. For five layers, three Raman lines appear. This effect is due to the presence of more than one $MoSe_2$ molecule in the unit cell. For $MoSe_2$ and WSe_2 we find that the B^1_{2g} mode, which is normally Raman inactive, becomes Raman active for a bilayer and is decreasing in intensity for thicker few-layer material.

PL emission of few- and monolayer $MoSe_2$, WSe_2, and MoS_2 is investigated with a confocal micro-PL setup. The observed PL intensity maxima for monolayer materials are in excellent agreement with the known direct A exciton in the corresponding bulk material. This observation corroborates recent model calculations for other transition metal dichalcogenides, which show that the indirect gap increases in energy, while the direct gap at the K point stays at about the same energy when decreasing the thickness from bulk to monolayer material. The PL intensity of monolayer $MoSe_2$ is 10 - 20 times stronger than that of the bilayer material. The emission intensity from the trilayer decreases again by one order of magnitude as compared to the bilayer. Interestingly, the PL intensity of the WSe_2 bilayer is only reduced by a factor of 4 compared to the monolayer. To gain insight into the efficiency of the PL emission process we investigate the role of absorption for each monolayer material. The retrieved values for A_{MX2} are similar for the three monolayer materials. In contrast, the PL emission is always brightest for WSe_2 and faintest for naturally grown MoS_2, differing by at least an order of magnitude, which might be due to a different quantum yield. This observation paves the way for optoelectronic devices based on this exceptional material.

[1] K. F. Mak, C. Lee. J. Hone, J. Shan, and T. F. Heinz, Phys. Rev. Lett. **105**, 136805 (2010).
[2] P. Tonndorf, R. Schmidt, P. Böttger, X. Zhang, J. Börner, A. Liebig, M. Albrecht, C. Kloc, O. Gordan, D. R. T. Zahn, S. Michaelis de Vasconcellos, and R. Bratschitsch, Optics Express **4**, 4908-4916 (2013).

Spin-Resolved Tunneling Studies of the Exchange Field in Ferromagnetic/Superconductor Bilayers

Philip W Adams

Department of Physics and Astronomy
Louisiana State University, Baton Rouge, LA, USA

I will give an overview of our spin-resolved studies of the exchange field produced in ferromagnetic/superconductor bilayers [1, 2, 3, 4]. In particular, we are using spin-resolved electron tunneling to probe the exchange field in the Al component of EuS/Al bilayers, in both the superconducting and normal-state phases of the Al. Contrary to expectation, we have found that the exchange field is a non-linear function of applied field, even in applied fields that are well beyond the EuS coercive field. Ours results suggest that interface mechanism that produces the exchange field is not well understood.

We have also incorporated a gate onto our EuS/Al bilayer structures in order to apply an electric field to the EuS-Al interface. The idea is to modulate the interface coupling with an electric field in order to produce a gate-controlled exchange field. So far we have had reasonable success. Below is a plot of the parallel critical field transition in a EuS/Al bilayer where the Al is superconducting, $T_c = 2.7$ K. The data was taken at 0.6 K and the transition occurs when the total internal magnetic field is about 5.5 T. So the exchange field in this case was about 3 T. The two curves in the figure represent the critical field transitions with gate voltages of 5V and -5V respectively. Note that the critical field transition is shifted, indicating that the gate is affecting the exchange field. In the inset we show the resistance of the Al component as a function of gate voltage at the midpoint of the critical field transition. In this case the gate voltage was a triangle wave with a magnitude of 5 V. I will discuss our ongoing efforts to optimize this gating effect, with the goal of producing a gate-controlled superconducting switch.

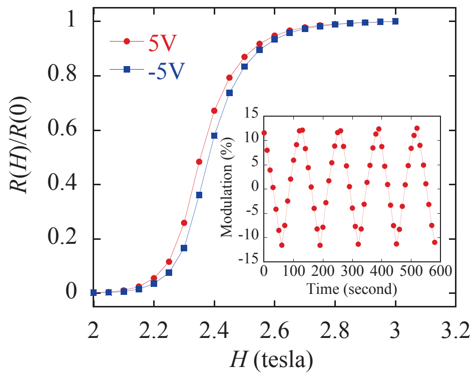

[1] G. Catelani, Y.M. Xiong, X.S. Wu, and P.W. Adams, Phys. Rev. B **80**, 054512 (2009)
[2] Y.M. Xiong, S. Stadler, P.W. Adams, and G. Catelani, Phys. Rev. Lett. **106**, 247001 (2011).
[3] T.J. Liu, J. C. Prestigiacomo, Y.M. Xiong, and P.W. Adams, Phys. Rev. Lett. **109**, 147207 (2012).
[4] T.J. Liu, J.C. Prestigiacomo, and P.W. Adams, submitted.

TuOE15

Photodetection and electroluminescence in single layer MoS2

R. S. Sundaram[1], A. Lombardo[1], M. Engel [2], A.L. Eiden[1], U.Sassi[1],R.Krupke[3], Ph. Avouris[4], M. Steiner[4], A.C. Ferrari

[1] *Cambridge Graphene Centre, Department of Engineering, University of Cambridge, CB3 0FA, Cambridge. United Kingdom*

[2] *Institute of Nanotechnology, Karlsruhe Institute of Technology, 76021 Karlsruhe, Germany*

[3] *Institut für Materialwissenschaft, Technische Universität Darmstadt, 64287 Darmstadt, Germany*

[4] *IBM Thomas J. Watson Research Center, Yorktown Heights, New York 10598, USA*

Molybdenum disulphide (MoS_2), a layered quasi-2 dimensional (2d) chalcogenide material[1-3], is subject of intense research because of its electronic[4] and optical properties[5], such as strong photoluminescence (PL)[5, 6], controllable valley and spin polarization[7, 8]and a large on-off ratio in field effect transistors (FETs)[4]. This combination of electrical and optical properties suggests that 1L-MoS_2 is a promising candidate for novel optoelectronic devices, such as 2d photodetectors[9, 10], and light-emitting devices. Here, we study photodetectors fabricated based on 1L-MoS_2[11]. Using spatially resolved photocurrent measurements we characterize the active areas of photodetection. Devices fabricated with Au source and drain electrodes show zero net photocurrent under zero bias conditions with charge separation occurring in the vicinity of the contacts. However, a strong built in potential within the channel is observed in devices fabricated with asymmetric drain-source contacts using thermally evaporated Au and Pt. This results in a net photocurrent at zero bias. Furthermore, we exploit the direct band gap of 1L-MoS_2 to demonstrate electrically excited luminescence in devices made of 1L-MoS_2 and study the underlying emission mechanism. We find that the electroluminescence occurs via hot carrier processes and is localized in the region of the contacts. The observed photoluminescence and electroluminescence arise from the same excited state at 1.8eV. Our results show that single layer MoS_2 is promising for novel optoelectronic devices, such as 2-dimensional light detectors and emitters.

[1] R. F. Frindt, J. Appl. Phys. ,**37**, 1928 (1966)..
[2] X. Zhang, W. P. Han, J. B. Wu, S. Milana, Y. Lu, Q. Q. Li, A. C. Ferrari, P. H. Tan; Phys. Rev. B **87**, 013113,(2012).
[3] F. Bonaccorso, A. Lombardo, T. Hasan, Z. Sun, L. Colombo, A. C. Ferrari; Materials Today **15**, 564 (2012)
[4] Radisavljevic B., Radenovic A., Brivio J., Giacometti V., and Kis A., Nature Nano **6**, 147 (2011)..
[5] K. F. Mak, C. Lee, J. Hone, J. Shan, and T. F. Heinz, Phys. Rev. Lett., **105**, 136805 (2010).
[6] A. Splendiani, L. Sun, Y. Zhang, T. Li, J. Kim, C.-Y. Chim, G. Galli, and F. Wang, Nano Lett., **10**, 1271 (2010).
[7] K. F. Mak, K. He, J. Shan, and T. F. Heinz, Nature Nano, **7**, 494 (2012).
[8] H. Zeng, J. Dai, W. Yao, D. Xiao, and X. Cui, Nature Nano, **7**, 490 (2012).
[9] Yin, Z.; Li, H.; Li, H.; Jiang, L.; Shi, Y.; Sun, Y.; Lu, G.; Zhang, Q.; Chen, X.; Zhang, H. ACS Nano, **6**, 74 (2011).
[10] H. S. Lee, S.-W. Min, Y.-G. Chang, M. K. Park, T. Nam, H. Kim, J. H. Kim, S. Ryu, and S. Im, Nano Lett. 12, 3695 (2012).
[11] R. S. Sundaram, M. Engel, A. Lombardo, R. Krupke, A. C. Ferrari, Ph. Avouris, M. Steiner; Nano Lett. **13,**1416, (2013).

Erasing the exciton fine structure splitting in semiconductor quantum dots

R. Trotta [1,2], C. Ortix [3], E. Zallo [2], O. G. Schmidt [2] and A. Rastelli [1,2]

[1] *Institute of Semiconductor and Solid State Physic, Johannes Kepler University Linz, Altenbergerstr. 69, A-4040 Linz*

[2] *Institute for Integrative Nanosciences, IFW Dresden, Helmholtzstr. 20, 01069 Dresden, Germany*

[2] *Institute for Theoretical Solid State Physics, IFW Dresden, Helmholtzstr. 20, 01069 Dresden, Germany*

Despite the remarkable progress achieved in the growth and fabrication of semiconductor nanostructures, real semiconductor quantum dots (QDs) usually do not show any structural symmetry. This induces a coherent coupling of the two bright excitonic states and leads to an energetic separation between them, the well-known fine structure splitting (*FSS*). When the *FSS* is larger than the radiative linewidth of the transitions (~ 1 μeV) the fidelity of the entangled photons emitted during the cascade biexciton-exciton-ground state is strongly reduced and the possibility to use QDs in advanced quantum optics experiments is severely hampered. For more than a decade researchers have struggled to find a reproducible way to suppress the FSS and the idea to use external perturbations (such as magnetic, electric, and strain fields) has been explored [1, 2]. However, recent results [3] have raised fundamental doubts about the success of these attempts in QDs with low structural symmetry.

In this presentation [4], we will show that the coupling between the bright excitons, and hence the *FSS*, can be always erased by the simultaneous application of large strain (up to 0.4%) and electric fields (up to 250 kV/cm) provided by a novel device where diode-like nanomembranes are integrated on top of piezoelectric substrates [5]. In particular, we will show that the energetic degeneracy between the bright excitons can be restored when one of the external perturbations is used to align the polarization of the exciton emission along the axes of application of the second perturbation, which is then able to suppress completely the energetic splitting between the states. The experimental results are supported by a theoretical model valid for every QD, regardless of its properties of symmetry. Our findings highlight the importance of having at hand two independent and broad-band tuning knobs for creating artificial atoms meeting the stringent requirements imposed by advanced quantum optics experiments. Finally, new concepts enabling the demonstration of tunable sources of entangled photons will be discussed.

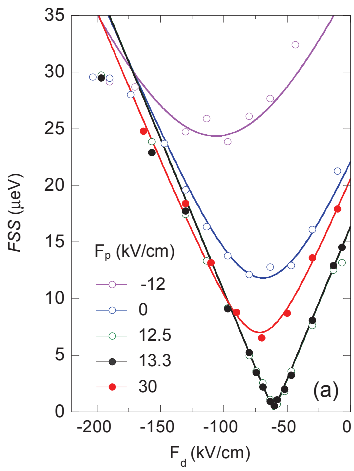

Figure. Exciton fine structure splitting (symbols) as a function of the electric field across the diode (F_d) and the piezoelectric substrate (F_p). The lines are the result of a theoretical analysis of the experimental data.

[1] A. J. Bennett, et al. Nature Phys. **6**, 947 (2010).
[2] J. D. Plumhof et al., Phys. Rev. B **83**, 121302 (2011).
[3] R. Singh et al., Phys. Rev. Lett. **104**, 196803 (2010).
[4] R. Trotta et al., Phys. Rev. Lett. **109**, 147401 (2012).
[5] R. Trotta et al., Adv. Mater. **24**, 2668 (2012).

TuOM13

Monday Tuesday Wednesday Thursday Friday

Atypical thermally-induced carrier relaxation processes in self-assembled $In_{0.3}Ga_{0.7}As/GaAs$ quantum dots

M. Syperek[1)], M. Baranowski[1)], G. Sęk[1)], J. Misiewicz[1)], A. Löffler[2)], S. Höfling[2)], S. Reitzenstein[2) 3)], M. Kamp[2)], and A. Forchel[2)]

[1)] Institute of Physcis, Wrocław University of Technology, Wybrzeże Wyspiańskiego 27, 50-370 Wrocław, Poland

[2)] Technische Physik, Universität Würzburg and Wilhelm Conrad Röntgen Research Center for Complex Material Systems, Am Hubland, D-97074 Würzburg, Germany

[3)] Present address: Technische Universität Berlin, Institut für Festkörperphysik, Hardenbergstr. 36, D-10623 Berlin, Germany

Due to their unusual optical and electronic properties $In_{0.3}Ga_{0.7}As/GaAs$ quantum dots (QDs) are excellent objects for the study of quantum optical effects at low temperatures. This particular QD system is an exemplary target system for optoelectronic devices utilizing cavity quantum electrodynamics effects. Its peculiar properties like low QD surface density and enhanced transition oscillator strength can lead to the development of dot-in-cavity structures characterized by a superior photon extraction efficiency, highly directed emission, tunable photon emission rate. Moreover, they facilitate the observation of strong coupling in micropillar cavities.[1] These are related to at least a few applications starting from single dot lasers and photon emitters, quantum information processing devices based on single QDs or QD molecules.[2]

Hereby, we focus on the carrier dynamics in such QDs pointing out at the important role of the wetting layer (WL) in the carrier relaxation scheme. Temperature dependent macro- and micro- photoluminescence experiments of the WL emission suggest the existence of a large density of zero-dimensional (0D) states, efficiently acquiring carriers at low temperatures. At elevated temperatures, the carriers are released from the 0D WL states and redistributed between QDs in the vicinity of the two-dimensional (2D) WL channel. This process is predominantly controlled by rising phonon bath and enhancement of carrier-phonon interaction.

Time-resolved photoluminescence reveals the complexity of the above-mentioned carrier relaxation scheme. Instead of a monotonic decrease of the ground state PL rise time with temperature typical for QDs, for these dots the PL rise time atypically increases from ~100 to ~200 ps in the temperature range of 10 - 45 K, and then decreases at higher temperatures.

To analyze the aforementioned effect qualitatively we propose a multi-level rate equation model in which we assume a thermal hoping transport between two types of energetically and spatially separated 0D density of states (namely 0D WL and QDs) in the vicinity of 2D mobility channel (2D WL). Results of simulations show that the observed increase in the carrier density population build-up time of the fundamental states in the ensemble of QDs can be achieved only when the density of 0D WL states exceeds significantly the density of QDs. Thus, the elongated QD PL rise time is related to time-consuming, acoustic phonon mediated carrier migration within the 0D WL density of states in the presence of 2D WL mobility edge.

[1] J.P. Reithmeier et al. Nature **432**, 197 (2004); **[2]** T. Heindel et al., Appl. Phys. Lett. **96**, 011107 (2010), S. Reitzenstein et al. Appl. Phys. Lett. **89**, 051107 (2006); D. Press et al. Phys. Rev. Lett. **98,** 117402 (2007), S. M. Ulrich et al. **98,** 043906 (2007).

Resonant optical initialization, control and readout of a spin qubit with near unity fidelity

K. Müller[1], R. Ripszam[1], T. Kaldewey[1], M. Bichler[1], G. Koblmüller[1], G. Abstreiter[1] and J.J. Finley[1]

[1] *Walter Schottky Institut and Physik Department, TU Muenchen, Garching, Germany*

Ultrafast photocurrent spectroscopy provides exquisite sensitivity to probe charge and spin dynamics as well as coherence properties of individual quantum dot nanostructures [1-2]. Here, we demonstrate how a precisely timed sequence of three monochromatic ultrafast (~2-5 ps) optical pulses with a well-defined polarization can be used to (i) prepare an arbitrary superposition of exciton spin states in an individual InGaAs quantum dot photo-diode, (ii) arbitrarily control of the spin-wavefunction without an applied magnetic field and (iii) read-out with high fidelity the quantum state in an arbitrary basis simply by detecting a strong (~2-10 pA) electric current flowing in an external circuit [3]. The results obtained show that the combined preparation, control and read-out of the spin quantum state can all be performed with a near-unity (>97%) fidelity.

Due to the finestructure splitting of self-assembled quantum dots, the neutral exciton forms a spin qubit with two energy eigenstates that can be addressed using the linear optical polarizations H and V (inset figure 1). Therefore, arbitrary superposition spin states can be initialized by directly mapping the polarization of a resonant ps-duration laser pulse to the exciton spin Bloch sphere. In pump-probe spectroscopy experiments this exciton spin can be read out by either the spin selectivity of the conditional absorption of the biexciton transition (2X) or the spin-selectivity of the stimulated emission (X). As an example we present in figure 1(a) pump-probe spectra for pumping the exciton with R polarized light and probing the spin state with R and L polarizations and in (b) the temporal evolution of the peaks. Clearly, the spin selectivity of the conditional absorption of 2X and stimulated emission of X can be seen in (a) and fully modulated antiphased oscillations resulting from the spin precession in (b). In this contribution we present the arbitrary initialization of an exciton spin and the projection readout along arbitrary axis.

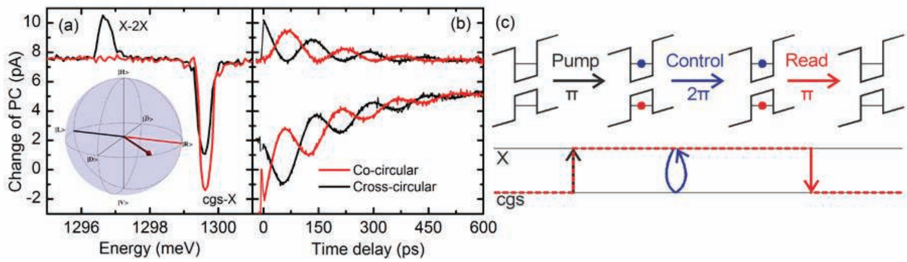

Arbitrary, high fidelity coherent optical control is achieved by applying an additional 2π-pulse with a precisely defined polarization in resonance with X between initialization and readout (figure 1c). This control pulse does not affect the population of the X state but induces precise rotations of the exciton spin state. We demonstrate arbitrary coherent control of the exciton spin state using a single resonant ps-duration laser pulse. Thereby, the fidelity of the control is again near unity, limited to >97% by the ~100fA readout noise in the photocurrent signal. Our methods are fully applicable to other optically addressable quantum emitters and have strong potential for scaling to more complex systems such as molecules and spin-chains.

[1] K. Müller et al. Phys. Rev. Lett. 108, 197402 (2012)
[2] K. Müller et al. Phys. Rev. B 85, 241306(R) (2012)
[3] K. Müller et al arXiv:1212.2993 (2012)

INVITED

Using nuclear magnetic resonance to explore the physics of nuclear spins in semiconductor quantum dots.

E. A. Chekhovich[1]

[1] *Department of Physics and Astronomy, University of Sheffield, Sheffield S3 7RH, UK*

When semiconductor quantum dots (QDs) are considered in the context of implementing solid-state quantum computer, it is inevitable that hyperfine interaction (HI) has to be considered. [1, 2]. The most important model system associated with HI is the so called "central spin" problem that describes single electron or hole spin (trapped in a QD) interacting via HI with a large (10^4-10^6) number of nuclear spins, which also interact with each other via dipole-dipole interaction. The key challenge is to understand how HI affects the coherence of the central spin, and find the conditions under which electron spin coherence can be significantly extended. Although all Hamiltonians of the central spin problem are well known, when realistic properties of a QD are taken into account (e.g. inhomogeneous strain and finite electron wavefunction confinement) it becomes almost impossible to solve. As a result many aspects of nuclear spin physics in QDs still lack understanding.

In this talk I will discuss the use of nuclear magnetic resonance (NMR) as a tool for studying nuclear spin system in semiconductor QDs (with a particular focus on III-V dots). In the first part of the talk I will demonstrate the unique capacity of NMR by reviewing some recent results obtained with this technique. For example the recent measurement of the hole hyperfine constants with chemical-element sensitivity enabled observation of a considerable contribution of the *d*-symmetry orbitals into the valence band states, which significantly modifies hole hyperfine Hamiltonian, making HI non spin-conserving [3]. Furthermore we have demonstrated that NMR on QDs can be used as a powerful structural analysis tool making it possible to probe chemical composition and elastic strain distribution within the volume of a single QD in a noninvasive manner [4].

In the second part of my talk I will present the results of the most recent experimental work done in Sheffield. I will show how NMR can be used to study nuclear-nuclear interactions in self-assembled QDs. Such interactions are responsible for random fluctuations of the nuclear field acting on the central spin and thus set an upper limit on the coherence time of the central spin [1]. For strain free GaAs (bulk, quantum wells and lattice matched GaAs/AlGaAs QDs) the timescale of the dipole-dipole interaction can be easily estimated as ~200 μs which agrees well with experiment [1, 2] However, for self-assembled QDs (e.g. InGaAs/GaAs) the task of predicting nuclear spin bath dynamics is much more complex, due to the presence of strong inhomogeneous quadrupole effects [1]. Here we were able to measure the intrinsic coherence time of the nuclear spins in individual QDs: we found $T_2 \sim 2$ ms for ^{71}Ga spins and $T_2 \sim 5.5$ ms for ^{75}As. Such pronounced increase of the nuclear T_2 is attributed to the effect of quadrupole interaction that leads to partial freezing of the flip-flops between nuclear spins. Our results suggest that millisecond-scale electron spin coherence is possible in principle in strained QDs, setting up a new milestone on the road towards scalable solid-state quantum computer.

[1] B. Urbaszek, Rev. Mod. Phys. **85**, 79 (2013).
[2] E. A. Chekhovich *et al*, Nature Materials **12**, 494 (2013).
[3] E. A. Chekhovich *et al*, Nature Physics **9**, 74 (2013).
[4] E. A. Chekhovich *et al*, Nature Nanotechnology **7**, 646 (2012).

3 July (Wednesday)

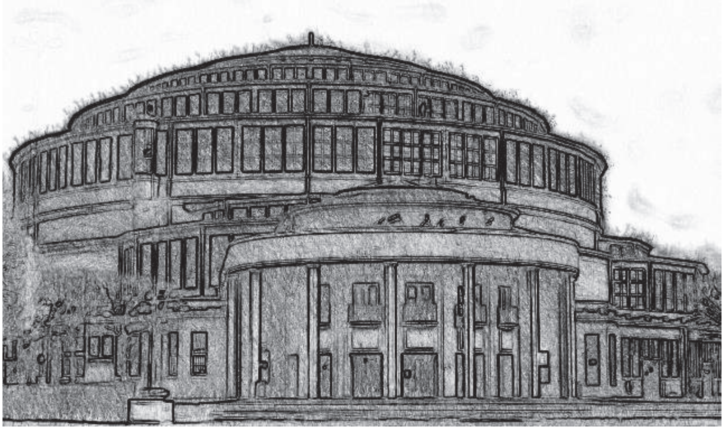

Centennial Hall

3 July (Wednesday)

EP2DS Session 1

9.00 – 9.30 **WeIE1**
Clement Faugeras (*LNCMI, CNRS-UJF-UPS-INSA, Grenoble, France*)
Interaction effects in the magneto-Raman scattering response of graphene

9.30 – 9.45 **WeOE1**
S.A.Tarasenko[1], C.Drexler[2], P.Olbrich[2], J.Karch[2], M.Hirmer[2], F.Müller[2], M.Gmitra[2], J. Fabian[2], R.Yakimova[3], S. Lara-Avila[4], S.Kubatkin[4], M.Wang[5], R.Vajtai[5], P.M.Ajayan[5], J.Kono[5], S.D.Ganichev[2]
([1]*Ioffe, St. Petersburg, Russia;* [2]*University of Regensburg, Germany;* [3]*Linköping University, Sweden;* [4]*Chalmers University of Technology, Sweden;* [5]*Rice University, Houston, USA*)
Ratchet transport of carriers in graphene

9.45 – 10.00 **WeOE2**
Klaus Ziegler (*Universität Augsburg, Germany*)
Electronic transport and optical properties of graphene near instabilities

10.00 – 10.15 **WeOE3**
R.G. Mani[1], J. Hankinson[2], C. Berger[2], W. de Heer[2]
([1]*Georgia State University;* [2]*Georgia Institute of Technology, Atlanta, USA*)
Resistively detected spin resonance and zero-field pseudo spin splitting in epitaxial graphene

10.15 – 10.30 **WeOE4**
F. Chiappini[1], S. Wiedmann[1], K.S. Novoselov[2], A.K. Geim[2], R.V. Gorbachev[2], J.C. Maan[1], U.Zeitler[1]
([1]*Radboud University Nijmegen, NL;* [2]*University of Manchester, UK*)
Single-layer graphene on h-BN in tilted magnetic fields

MSS Session 1

9.00 – 9.15 **WeOM1**
C.L. Yu[1], M.T. Deng[1], P. Caro[1], H.Q. Xu[1,2]
([1]*Lund University, Sweden;* [2]*Peking University, China*)
Kondo correlation and spin-orbit interaction in an InSb nanowire quantum dot coupled to the Nb contacts

9.15 – 9.30 **WeOM2**
V.S. Pribiag[1], S. Nadj-Perge[1], J. W.G. van den Berg[1], S.M. Frolov[1], I. van Weperen[1], S.R. Plissard[2], E.P.A.M. Bakkers[1,2], L.P. Kouwenhoven[1] ([1]*Delft University of Technology;* [2]*Eindhoven University of Technology, The Netherlands*)
Electrical control of electron and hole spins in InSb nanowire quantum dots

9.30 – 9.45 **WeOM3**
T. Fujisawa[1], S. Sharmin[1], K. Muraki[2]
([1]*Tokyo Institute of Technology;* [2]*NTT Corporation, Atsugi, Japan*)
Complete lifting of spin blockade under unstable electron-nuclear dynamics

9.45 – 10.00 **WeOM4**
D. Dunker[1], J. Debus[1], T.S. Shamirzaev[2], D.R. Yakovlev[1,3], K.S. Zhuravlev[2], M. Bayer[1]
([1]*Technische Universität Dortmund, Germany;* [2]*Russian Academy of Sciences, Novosibirsk, Russia;* [3]*Ioffe, St. Petersburg, Russia*)
Spin properties of the indirect exciton in indirect band-gap (In,Al)As/AlAs quantum dot ensembles

10.00 – 10.30 **WeIM1**
W. Gao, P. Fallahi, E. Togan, A. Deteil, A. Imamoglu
(*ETH Zurich, Switzerland*)
Spin-photon quantum interface in quantum dots

EP2DS Session 2

11.00 – 11.30 **WeIE2**
Koji Muraki
(*NTT Corporation; Japan Science and Technology Agency*)
NMR probing of fractional quantum Hall liquid and Wigner solid phases

11.30 – 11.45 **WeOE5**
B. Frieß[1], V. Umansky[2], L. Tiemann[1], K. von Klitzing[1], J. Smet[1]
([1]*Max Planck Institute for Solid State Research, Stuttgart, Germany;* [2]*Weizmann Institute of Science, Rehovot, Israel*)
Probing the stripe phase at filling factor 5/2 by NMR

11.45 – 12.00 **WeOE6**
Y. Liu, S. Hasdemir, M. Shayegan, L.N. Pfeiffer, K.W. West, K.W. Baldwin
(*Princeton University, Princeton, USA*)
Evidence for a nematic fractional quantum Hall state at $\nu = 5/2$ in parallel magnetic field

12.00 – 12.15 **WeOE7**
John J. Quinn
(*University of Tennessee, USA*)
Method of constructing trial wavefunctions for quantum Hall states

12.15 – 12.30 **WeOE8**
D. Kamburov, Y. Liu, M. Shayegan, L.N. Pfeiffer, K.W. West, K.W. Baldwin
(*Princeton University, USA*)
Anisotropic Fermi contour of composite fermions in tilted magnetic fields

MSS Session 2

11.00 – 11.15 **WeOM5**
Toshihiro Kubo[1], Yasuhiro Tokura[1,2]
([1]*University of Tsukuba;* [2]*NTT Corporation, Japan*)
Probing spins in spin interferometer with superconducting lead

11.15 – 11.20 **WeOM6**
T.-M. Chen[1], M. Pepper[2], I. Farrer[3], G.A.C. Jones[3], D.A. Ritchie[3]
([1]*National Cheng Kung University, Tainan, Taiwan;* [2]*University College London, UK;* [3]*Cavendish Laboratory, Cambridge, UK*)
All-electrical spin injection from a quantum point contact

11.30 – 11.45 **WeOM7**
N. Ares[1], V.N. Golovach[1,2], G. Katsaros[1,2], M. Stoffel[3], F. Fournel[4], L.I. Glazman[5], O.G. Schmidt[2], S. De Franceschi[1]
([1]*SPSMS, CEA-INAC/UJF-Grenoble, France;* [2]*IFW Dresden, Germany;* [3]*UMR CNRS, Vandoeuvre-les-Nancy, France;* [4]*CEA, LETI, MINATEC, Grenoble, France;* [5]*Yale University, New Haven, USA*)
SiGe self-assembled nanostructures for quantum spintronics

11.45 – 12.00 **WeOM8**
M. Oltscher, M. Ciorga, M. Utz, D. Schuh, D. Bougeard, D. Weiss
(*University of Regensburg, Germany*)
Spin injection into a high mobility 2DEG system

12.00 – 12.30 **WeIM2**
Alberta Bonanni
(*Johannes Kepler University, Linz , Austria*)
Modulated semiconductor structures of magnetically doped nitrides

16.30 – 19.00

Special session on recent progress and future perspectives in the search for Majorana fermions in condensed matter

Majorana1

Sankar Das Sarma (*University of Maryland, College Park, USA*)
Majorana in semiconductors

Majorana2

Leo Kouwenhoven (*Delft University of Technology, The Netherlands*)
Majorana's in InSb nanowires

Majorana3

Moty Heiblum (*Braun Center for Submicron Research, Weizmann Institute of Science, Israel*)
Zero-bias peaks and splitting in an Al–InAs nanowire

Majorana4

Piet W. Brouwer (*Freie Universität Berlin, Germany*)
Disordered Majorana Wires

Majorana5

Leonid Rokhinson (*Purdue University, West Lafayette, USA*)
Observation of fractional ac Josephson effect: the signature of Majorana particles

Majorana6

Charles M. Marcus (*University of Copenhagen, Denmark*)
(Title not available)

INVITED

Interaction effects in the magneto-Raman scattering response of graphene

C. Faugeras [1]

[1] LNCMI, CNRS-UJF-UPS-INSA, 25, avenue des Martyrs, 38042 Grenoble, France

Magneto-Raman scattering studies of graphene-like locations on the surface of bulk graphite will be reported. The high electronic quality of this system allows for the direct observation of inter Landau level electronic excitations [1] up to 5000 cm^{-1} from the laser line, which can be tuned, due to the use of high magnetic fields, over most of the phonon features visible in the Raman scattering response of graphene. A detail investigation of the Raman scattering response of this system reveals new effects of electron-phonon interaction, which imply not only the E_{2g} phonons (magneto-phonon resonance [2,3]), but also K-point phonons as well as 2Γ point phonons. Resonant electron-phonon interaction with these three phonon modes is evidenced in magnetic field highlighting the role of combined excitations and the one of multiple phonon scattering as an important electron relaxation process. These results are analyzed in the frame of multimode interaction involving up to three distinct excitations.

In a second part, I will present the magneto-Raman scattering response of a graphene on BN hybrid structure. Such structures present high electronic quality with a Fermi level close to charge neutrality point. The magneto-phonon resonance in this quasi neutral system will be discussed together with the presentation of its response due to purely electronic excitations.

[1] C. Faugeras et al., Phys Rev. Lett. 107 (2011) 036807
[2] C. Faugeras et al., Phys. Rev. Lett. 103 (2009) 186803
[3] J. Yan et al., Phys. Rev. Lett. 105 (2010) 227401

Ratchet transport of carriers in graphene

S.A. Tarasenko[1], C. Drexler[2], P. Olbrich[2], J. Karch[2], M. Hirmer[2], F. Müller[2], M. Gmitra[2], J. Fabian[2], R. Yakimova[3], S. Lara-Avila[4], S. Kubatkin[4], M. Wang[5], R. Vajtai[5], P.M. Ajayan[5], J. Kono[5], and S.D. Ganichev[2]

[1] *Ioffe Physical-Technical Institute, St. Petersburg, Russia*
[2] *Terahertz Center, University of Regensburg, Germany*
[3] *Linköping University, Sweden,* [4] *Chalmers University of Technology, Sweden*
[5] *The Richard E. Smalley Institute, Rice University, Houston, USA*

Monday Tuesday Wednesday Thursday Friday

Free carriers driven by an alternating electric field can exhibit a directed motion facilitated by thermal or quantum fluctuations. Here, we report on theoretical and experimental study of such ratchet effects of Dirac fermions in graphene demonstrating that the ratchets can be downscaled to one-atom thick crystals. We show that the single-layer graphene samples subjected to an in-plane magnetic field rectify ac electric current converting it into a dc electric signal. The ac electric field, in our experiments provided by terahertz (THz) radiation, pushes electrons back and forth in the graphene plane while the static magnetic field acts as a valve letting the electrons move in one direction and suppressing the oppositely directed motion.

The ratchet current is proportional to the square of the amplitude of the ac electric field, scales linearly with the static magnetic field magnitude, and reverses its direction by switching the magnetic field polarity [1]. We show that it is generated for both linearly polarized as well as rotating ac electric field. For linear polarization, the current depends on the angle between the electric field polarization and the static magnetic field. For the rotating field, the current reveals a helicity-sensitive component reversing its sign by switching the rotation direction of the electric field.

Ratchets effects are only possible in systems with broken space inversion symmetry. Therefore, the observation of electronic ratchet demonstrates that the spatial symmetry of graphene layers, nominally centrosymmetric two-dimensional crystals with the honeycomb lattice, is broken due to substrate or chemisorbed adatoms on the graphene surface. We present a microscopic theory of the quantum ratchet effect and show that the dc current stems from the asymmetry of scattering of Dirac fermions in graphene, which is caused by the mixing of π- and σ-band states in the in-plane magnetic field. The developed theory is in a good agreement with the experiment describing the observed dependence of the ratchet current on the static magnetic field, ac electric field amplitude and polarization. The results suggest that the ratchet current can be calibrated to nondestructively measure the strength of the structure inversion asymmetry.

The experiments were carried out on single-layer graphene samples grown on the Si-terminated face of a 4H-SiC(0001) semi-insulating substrate or synthesized by chemical vapor deposition (CVD) on Si/SiO2. The samples (5 x 5 mm^2 with ohmic contacts) were placed into an optical cryostat with crystal quartz windows and split-coil superconducting magnet providing magnetic fields up to 7 Tesla. The THz radiation is generated by an optically pumped ammonia laser. The dc current generated in the unbiased graphene sample was measured via the voltage drop across a load resistor.

[1] C. Drexler, S.A. Tarasenko, P. Olbrich et al., Nat. Nanotechnol. **8**, 104 (2013).

Electronic transport and optical properties of graphene near instabilities

K. Ziegler
Institut für Physik, Universität Augsburg, D-86135 Augsburg, Germany

Graphene, a genuine two-dimensional material formed by carbon atoms, has remarkable electronic and optical properties. It is a transparent semimetal with a minimal conductivity and it is colorless because its optical properties are independent of the frequency of the transmitted light. This is very different from the conventional Drude-type behavior of other materials. All these properties are strongly related to the existence of a quasiparticle spectrum which consists of two bands that touch each other at two Dirac nodes. This structure is associated with a number of interesting features, such as Klein tunneling and electron-hole pair creation. Recent experimental studies have revealed that the sublattice symmetry of the honeycomb lattice of graphene can be broken by chemical doping or by external gates in the case of bilayers. Here we will discuss the role of broken symmetries due to structural instabilities. This can lead to a random gap in the quasiparticle spectrum which may cause an insulating behavior. We discuss the gap opening and the related transition from a semimetal to an insulator in the case of disordered mono- and bilayers graphene and the effect of Coulomb and electron-phonon interaction on the gap formation. The discussion includes the role of dynamical symmetries and spontaneous symmetry breaking, and scaling laws in the form of a generalized Drude formula.

[1] K. Ziegler, Phys. Rev. Lett. **97**, 266802 (2006).
[2] K. Ziegler, Phys. Rev. Lett. **102**, 126802 (2009); Phys. Rev. B **79**, 195424 (2009).
[3] K. Ziegler et al., Phys. Rev. B **84**, 073407 (2011); K. Ziegler, E. Kogan, EPL **95**, 36003 (2011).
[4] A. Sinner, K. Ziegler, Phys. Rev. B 86, 155450 (2012).

WeOE3

Resistively detected spin resonance and zero-field pseudo spin splitting in epitaxial graphene

Ramesh G. Mani [1], John Hankinson [2], Claire Berger[2], and W. de Heer[2]

[1] *Dept. of Physics & Astronomy, Georgia State University, Atlanta, GA 30303 U.S.A*
[2] *School of Physics, Georgia Institute of Technology, Atlanta, GA 30332 U.S.A.*

Graphene[1] is an appealing material for electron-spin quantum computing (QC) and spintronics, due to the expected weak spin-orbit interaction, and the scarcity of nuclear spin in natural carbon. Due to QC and spintronics, the electrical detection and microwave control of spin have become topics of interest, now in graphene nanostructures, where the small number of spins limits the utility of traditional spin resonance. This work reports the resistive detection of spin resonance in epitaxial graphene, and ESR based measurements of the g-factor, the spin relaxation time, and the pseudo-spin (valley - degeneracy)-splitting at zero-magnetic-field.[2]

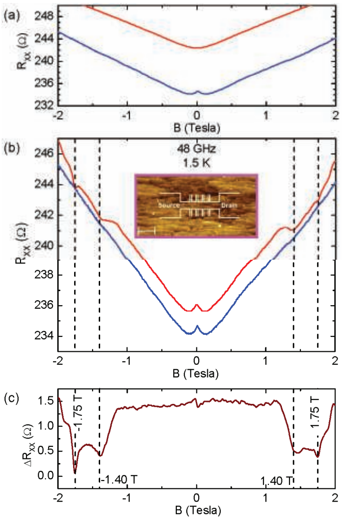

Figure 1) Resistively detected microwave-induced spin-resonance at f = 48 GHz in a three layer epitaxial graphene specimen. (a) The diagonal resistance, R_{xx}, is exhibited vs. the magnetic field, B, at temperatures T = 90K (red trace) and T = 1.5 K (blue trace). (b) R_{xx} is exhibited vs. B without microwave excitation (blue trace), and under constant f = 48 GHz microwave excitation at P = 4 mW (red trace), at T = 1.5 K. Resonant reductions in the R_{xx} are observed in the vicinity of B = ± 1.4 T and B = ± 1.75 T. Inset: An AFM image of the EG/SiC surface. (c) The change in the diagonal resistance, ΔR_{xx}, between the photo-excited and dark conditions in panel (b), i.e., $\Delta R_{xx} = R_{xx}$ (4 mW) - R_{xx} (dark), is exhibited vs. B.

Transport studies were carried out in the B ⊥ c-axis configuration on p-type epitaxial graphene Hall bar specimens. The epitaxial graphene (EG) was realized by the thermal decomposition of insulating 4H silicon carbide (SiC),[127] and the c-face of the EG/SiC chip was processed by e-beam lithography into micron-sized Hall bars with Pd/Au contacts. The specimens were immersed in pumped liquid Helium, and irradiated with microwaves over the frequency range $10 \leq F \leq 50$ GHz, at a source-power $0.1 \leq P \leq 10$ mW.

Figure 1(a) exhibits the diagonal resistance, R_{xx}, vs. B, for a trilayer sample at 90K (red) and 1.5K (blue). These data indicate $dR_{xx}/dT > 0$ at B = 0 Tesla. Fig. 1(b) illustrates the influence of microwave-excitation at f = 48 GHz. Here, for B < 1 Tesla, microwave-excitation produces a positive displacement of the photo-excited R_{xx} (red curve, Fig. 1(b)) relative to the dark trace (blue curve, Fig. 1(b)), akin to increasing the temperature. However, at B > 1 Tesla, R_{xx} exhibits resistance-valleys as the photo-excited curve approaches the dark curve. Fig. 1(c) shows two noteworthy features in $\Delta R_{xx} = R_{xx}$ (4 mW) - R_{xx}(dark): a high magnetic field resonance at |B| = 1.75 Tesla, and a low magnetic field feature at |B| = 1.4 Tesla. The high B-field resonances of Fig. 1 followed the relation f(GHz) = 27.2 B(T) vs. the microwave frequency, while the low-B resonances followed f(GHz) = 10.76 + 26.9 B(T), with a non-zero intercept, f_0 = 10.76 GHz. The observed slopes, for the low (high) field resonance correspond to spin resonances with $g_{//} = 1.92 \pm 0.028$ ($g_{//} = 1.94 \pm 0.014$). The non-zero intercept is associated with a zero-field pseudo spin splitting.

[1] S. Das Sarma, S. Adam, E. H. Hwang, and E. Rossi, Reviews in Modern Physics 83, 407 (2011).
[2] R. G. Mani, J. Hankinson, C. Berger, and W. de Heer, Nature Communications 3, 996 (2012).

Single-layer graphene on h-BN in tilted magnetic fields

F. Chiappini[1], S. Wiedmann[1], K.S. Novoselov[2], A.K. Geim[2], R.V. Gorbachev[2], J.C. Maan[1] and U.Zeitler[1]

[1] High Field Magnet Laboratory and IMM, Radboud University Nijmegen, NL
[2] School of Physics and Astronomy, University of Manchester, UK;

We have measured the Landau level structure of high-mobility graphene positioned on h-BN by means of magneto-transport experiments in magnetic fields up to 30 T. For the best quality sample (sample B) we observe a full splitting of the four-fold Landau level degeneracy in agreement with recent results by the Kim group [1].

We performed our experiments on two single-layer graphene devices placed directly on h-BN on top of an *n*-Si/SiO_2 wafer, acting as a back gate. In particular, using tilted magnetic fields, we investigated the spin polarization of individual quantum-Hall states and, more specifically, the competition between a bare Zeeman splitting [2,3] due to the total magnetic field and an exchange-driven splitting dependent on the perpendicular field component.

Already in sample A filling factors ν= -1 and ν= -4 appear. Keeping the perpendicular component constant while increasing the total magnetic field, the resistance minima become more pronounced for both filling factors indicating a (partial) spin polarization of these quantum-Hall states. Using temperature dependent experiments, we extract the gaps for ν= -1 (in perpendicular magnetic field 30 T) and ν= -4 (at θ = 66.4 °, B_{TOT} = 30 T): Δ_{-1}= 93±2 K and Δ_{-4}= 32±2 K. The size of Δ_{-4} is in agreement with the Zeeman energy at 30 T whereas Δ_{-1} is considerably larger pointing towards an interaction-driven enhancement [4].

[1] A. F. Young *et al.*, Nat. Phys. **8**, 550 (2012).
[2] A.J.M. Giesbers *et al.* Phys. Rev. B **80**, 241411(R) (2009);
[3] E.V. Kurganova *et al*., Phys. Rev. B **84**, 121407(R) (2011).
[4] Y. Zhang *et al.* Phys. Rev. Lett. **96**, 136806 (2006).

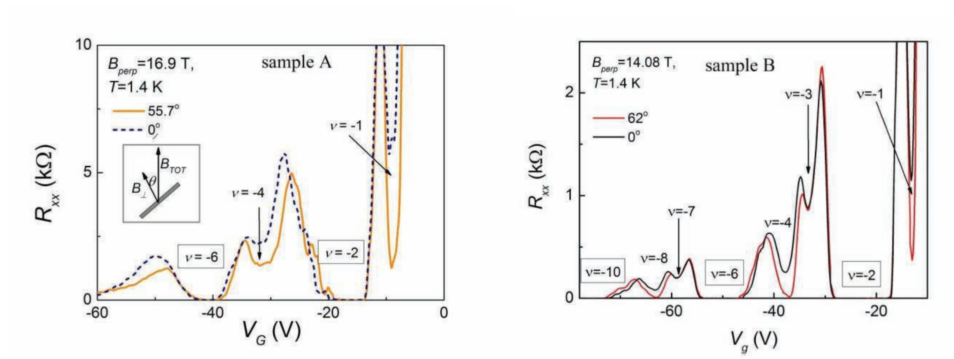

Fig. 1: Splitting of the three lowest hole Landau levels in (tilted) magnetic fields. The perpendicular component of the magnetic field i is $B_\perp$ =16.90 T for sample A and $B_\perp$ =14.08 T for sample B.
The well-pronounced filling factors ν = -2, -6 and -10 separate the four-fold degenerate Landau levels, which become partly split in sample A and fully split in sample B.
The inset in (A) sketches the tilt configuration.

Kondo correlation and spin-orbit interaction in an InSb nanowire quantum dot coupled to the Nb contacts

C.L. Yu[1], M.T. Deng[1], P. Caroff[1] and H.Q. Xu[1,2]

[1] *Division of Solid State Physics, Lund University, Box 118, S-221 00 Lund, Sweden*
[2] *Department of Electronics and Key Laboratory for the Physics and Chemistry of Nanodevices, Peking University, Beijing 100871, China*

We report the fabrication and electrical measurements of Kondo correlation and spin-orbit interaction in a Nb-InSb nanowire quantum dot-Nb hybrid device. Our work is motivated by recent proposals [1, 2] for the realization of Majorana fermions in semiconductor nanowires with strong spin-orbit interaction coupled to s-wave superconductors and encouraging experimental results [3, 4]that show the signatures of Majorana fermions . Through the transport measurements to the device, Kondo effects and spin-orbit interaction are investigated in the presence of a proximity effect induced superconducting energy gap in the Nb-covered InSb nanowire segments.

The device is fabricated from an InSb segment of an epitaxially grown InAs/InSb heterostructure nanowire. Two Nb-based superconductor thin film contacts with a spacing of 120 nm between them are defined by electron beam lithography and magnetron sputtering. A quantum dot is naturally formed in the nanowire segment between the two contacts. Transport measurement is performed in a dilution refrigerator at a base temperature of 25 mK.

At low temperature, the Nb-covered InSb nanowire segments turn to be superconductors with a superconducting energy gap Δ in the order of 0.25 meV due to the proximity effect [5]. Between the two superconducting segments, a Josephson-quantum dot junction structure is formed together with the InSb nanowire quantum dot. Although in the presence of the proximity effect induced superconducting energy gap, the conventional Kondo effect induced conductance enhancement at zero magnetic field and the integer-spin Kondo effect induced conductance enhancement at finite magnetic fields are observed. In the strong coupling regime, the Kondo effect induces a zero-bias conductance peak in the form of Cooper pair cotunneling enhancement. However, the integer-spin Kondo effect causes two conductance peaks at finite bias voltages and shows an anti-crossing behaviour in the magnetic field evolution due to the existence of spin-orbit interaction. We have deduced the spin-orbit interaction energy Δ_{so} from the anti-crossing and compared it to the values that determined by the anti-crossing behaviour of quasi-particle cotunneling through excited states of the quantum dot [6].

[1] R. M. Lutchyn, J. D. Sau, S. Das Sarma, Phys. Rev. Lett. 105, 077001 (2010);
[2] Y. Oreg, G. Refael, F. von Oppen, Phys. Rev. Lett. 105, 177002 (2010).
[3] V. Mourik, Z. Zuo, S.M. Frolov, S.R.Plissard, E.P.A.M. Bakkers, L.P. Kouvwenhoven. Science 336, 1003 (2012).
[4] M.T. Deng, C.L. Yu, G.Y. Huang, M. Larsson, P. Caroff, and H.Q. Xu Nano Lett. 12 (12), 6414-6419 (2012).
[5] H. A. Nilsson, P. Samuelsson, P. Caroff, and H.Q. Xu. Nano Lett. 12, 228-233 (2012).
[6] H. A. Nilsson, P. Caroff, C. Thelander, M. Larsson, J.B. Wagner, L.-E Wernersson, L. Samuelson, and H.Q. Xu. Nano Lett. 9, 3151-3156 (2009).

Electrical control of electron and hole spins in InSb nanowire quantum dots

V. S. Pribiag[1], S. Nadj-Perge[1], J. W. G. van den Berg[1], S. M. Frolov[1], I. van Weperen[1], S. R. Plissard[2], E. P. A. M. Bakkers[1,2] and L. P. Kouwenhoven[1]

[1] *Kavli Institute of Nanoscience, Delft University of Technology, The Netherlands*
[2] *Department of Applied Physics, Eindhoven University of Technology, The Netherlands*

The spin-orbit interaction enables fast all-electrical control of individual spins in quantum dots. The presence of very large spin-orbit coupling thus makes InSb nanowires a highly promising platform for spin-based qubits. We rely on electric dipole spin resonance (EDSR) to demonstrate single electron spin rotations, measure the strength of the spin-orbit coupling and extract the anisotropic g-factor. Fast Rabi oscillations in excess of 100 MHz are demonstrated [1]. This is considerably faster than typical Rabi frequencies for GaAs qubits, however the coherence times are relatively short (T_{echo} ~35 ns).

A promising approach to enhancing qubit coherence is to use hole spins as qubits instead of electron spins, since hole spins have weaker hyperfine coupling. Here we take advantage of the small bandgap of InSb to readily gate-tune our nanowire devices between few-electron and few-hole quantum dots [2]. In the few-hole regime we demonstrate rotation of single hole spin states via EDSR and use this to extract the hole g-factors. Thanks to the high tunability of these devices we are able to compare important properties of electrons and holes, such as effective masses, g-factors and spin-blockade anisotropies. The ability to control and read out hole spin states paves the way for more coherent, all-electrical hole-spin qubits.

[1] J. W. G. van den Berg et al., Phys. Rev. Lett. **110**, 066806 (2013).
[2] V. S. Pribiag et al., Nature Nanotechnology DOI:10.1038/NNANO.2013.5 (2013).

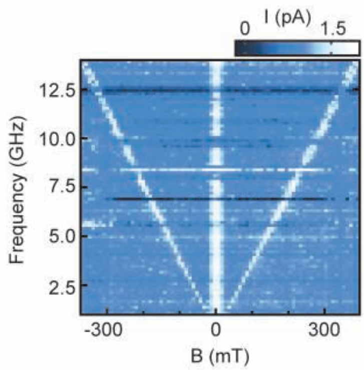

Figure 1. Electric Dipole Spin Resonance of a hole spin state in an InSb nanowire quantum dot.

Complete lifting of spin blockade under unstable electron-nuclear dynamics

Toshimasa Fujisawa [1], **Sonia Sharmin** [1], **and Koji Muraki** [2]

[1] *Department of Physics, Tokyo Institute of Technology, Tokyo, Japan.*
[2] *NTT Basic Research Laboratories, NTT Corporation, Atsugi, Japan.*

Current suppression in the Pauli spin-blockade regime of a double quantum dot (DQD) is associated with triplet states orthogonal to the singlet state allowed for transport [1]. Here we report that such spin-blockade effect is completely lifted even in a conventional measurement, where dynamic nuclear spin polarization (DNP) gives rise to vanishing orthogonal spin states to the singlet. Unstable dynamics causing this unusual situation is studied by evaluating current levels and noise characteristics consistent with model calculations [2].

A two-electron DQD fabricated in AlGaAs/GaAs heterostructure shows typical spin-blockade characteristics with high non-blockaded current I_H (~ 800 fA in our device) in the reverse bias and lowest spin-blockaded current I_L (~ 30 fA) in the forward bias. Figure 1(c) shows a current trace at a forward bias (usually spin-blockade) during a slow sweep of energy detuning ε between (1,1)S and (0,2)S from negative ε, where (1,1) charge configuration is the ground state, to positive ε, where (0,2)S state is the ground state. The current increases stepwise at ε ~ -25 μeV and more dramatically at ε ~ -5 μeV reaching to the non-blockaded current level of I_H, which indicates the complete lifting of spin blockade. This behavior can be understood with highly non-linear DNP with nuclear spin polarization vectors $\vec{p_L}$ and $\vec{p_R}$ in the left and right dot, respectively. When significantly different Overhauser fields in both magnitude and direction are accumulated as shown in Fig. 1(a), the total fields $\vec{F} = g\mu_B\vec{B} + A_{HF}\vec{p}$ (thick arrows) of the two dots are no longer parallel. This is the case where all four eigenstates of the (1,1) charge states involve spin-singlet components, and thus spin blockade is lifted as illustrated in Fig. 1(b). Stability of the electron-nuclear feedback against its own statistical fluctuation plays an essential role in reaching this situation. In the case of negative ε, balanced polarization ($\vec{p_L} = \vec{p_R}$) is unstable, and DNP takes place dominantly only in one dot (assumed to be the left) to cancel the external magnetic field as shown in the left and central insets of Fig. 1(c). Further increase of ε triggers off another unstable dynamics causing significant transverse component of $\vec{p_L}$ (the right inset). This is consistent with the calculated DNP flow [small arrows in Fig. 1(d)] and current indicating the complete lifting of spin blockade.

[1] K. Ono et al., Science 312, 1634 (2002). [2] S. Sharmin et al., to be submitted.

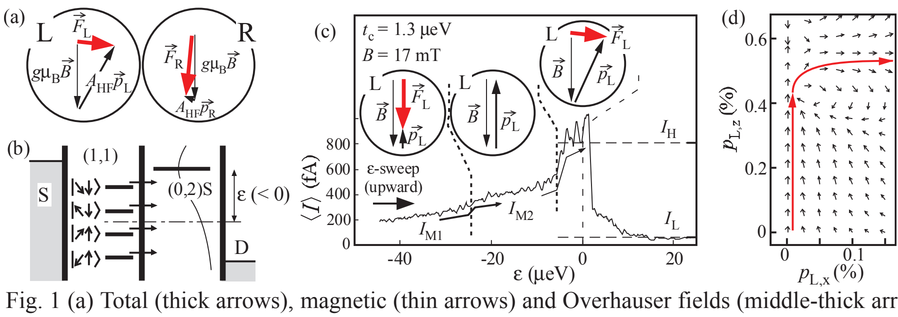

Fig. 1 (a) Total (thick arrows), magnetic (thin arrows) and Overhauser fields (middle-thick arrows) in the two dots. (b) Schematic energy diagram with non-orthogonal spin states to the singlet (0,2)S. (c) Current trace with complete lifting of Pauli-spin blockade ($I > I_H$). The developing fields in the left dot are shown in the insets. (d) DNP flow (small arrows) and a schematic trajectory (large arrows).

Spin properties of the indirect exciton in indirect band-gap (In,Al)As/AlAs quantum dot ensembles

D. Dunker[1], J. Debus[1], T. S. Shamirzaev[2], D. R. Yakovlev[1,3], K. S. Zhuravlev[2], and M. Bayer[1]

[1]*Experimentelle Physik 2, Technische Universität Dortmund, 44227 Dortmund, Germany*
[2]*A. V. Rzhanov Institute of Semiconductor Physics, Siberian Branch of the Russian Academy of Sciences, 630090 Novosibirsk, Russia*
[3]*Ioffe Physical-Technical Institute, RAS, 194021 St. Petersburg, Russia*

While semiconductor quantum dots (QDs) have been established as efficient light emitters or detectors in optoelectronics, other applications are only perspective so far. A particular example in this respect is their implementation in spin electronics or quantum information technology. For that purpose, the QDs are typically loaded with resident carriers whose spins are rather well protected from relaxation by the three-dimensional confinement. In this context, exciton complexes have been used up to now for manipulation of the spin of resident carriers, but are considered as less prospective as information carriers. This reservation is primarily related to their limited lifetime in the order of a nanosecond, which would most likely not allow enough coherent manipulations, either by microwave or optical techniques, to be of interest for quantum information. This situation may change if the exciton lifetime could be extended significantly.

Interesting, but technologically challenging in this respect is the placement of QDs in photonic crystals by which their radiative decay could be prevented. Another possibility is the realization of QDs with a band gap which is indirect in either real or momentum space or both. Here, we focus on self-assembled (In,Al)As/AlAs QDs, for which dependent on the dot size a crossover between the conduction-band ground states of the Γ-valley and X-valley occurs, as reflected by the lifetime of the lowest-energy exciton. This exciton is formed by a Γ-valley heavy-hole and a mixed electron contributed by the Γ- and X-valley, whereby both carriers are located within the QD. Besides the advantage of this indirect exciton to be optically addressable, its lifetime lasts hundreds of μs [1], which may be sufficient for a large number of coherent manipulations in this time range.

We report on spin properties of the indirect exciton in undoped (In,Al)As/AlAs quantum dots under influence of magnetic fields, studied by stationary and time-resolved photoluminescence. The application of high fields ($B \leq 10$ T) allows us to identify the dominant role of one-acoustic-phonon processes in the exciton spin relaxation [2]. The longitudinal spin relaxation time follows a B^{-5}-dependence from, e.g., 200 μs at 4 T to 1 μs at 10 T for a temperature of 1.8 K, and is rather robust against temperature changes. An approach for modeling the circular polarization of the photoluminescence induced by magnetic field is suggested for an ensemble of excitons with a considerable dispersion of lifetimes. At low fields in the mT-range, a high optical orientation degree for the indirect exciton is found under quasi-resonant excitation. It ranges around 80% at 50 mT depending strongly on the excitation and detection energies. Moreover, it sensitively responses to the optical excitation density as well as even weak variations in the magnetic field strength. Electron-nuclear hyperfine and exciton-exchange interactions are discussed for the low-field spin properties of the indirect exciton.

[1] T. S. Shamirzaev, J. Debus, D. S. Abramkin, et al., Phys. Rev. B **84**, 155318 (2011).
[2] D. Dunker, T. S. Shamirzaev, J. Debus, et al., Appl. Phys. Lett. **101**, 142108 (2012).

WeIM1

INVITED

Spin-photon quantum interface in quantum dots

W. Gao[1], P. Fallahi[1], E. Togan[1], A. Deteil[1] and A. Imamoglu[1]
[1]*Institute of Quantum Electronics, ETH zurich, HPT G12, 8093 Zurich, Switzerland*
e-mail: *imamoglu@phys.ethz.ch*

Realization of a quantum interface between flying photonic qubits and stationary spin qubits is expected to play a key role, both in quantum repeaters and realization of quantum networks. Thanks to their superior optical properties and the possibility of integration in photonic nanostructures, semiconductor quantum dots confining a single spin are particularly well suited for this purpose. In this talk, I will describe the observation of spin-photon entanglement [1]. I will also describe our ongoing experiments aimed at transferring quantum information from a propagating photonic qubit onto a single solid-state spin qubit.

References

[1] W. B. Gao, P. Fallahi, E. Togan, J. Miguel-Sanchez & A. Imamoglu, *Nature* **491**, 426–430 (2012)

INVITED

NMR probing of fractional quantum Hall liquid and Wigner solid phases

Koji Muraki [1,2]

[1] *NTT Basic Research Laboratories, NTT Corporation*
[2] *ERATO Nuclear Spin Electronics Project, Japan Science and Technology Agency*

Nuclear magnetic resonance (NMR) has played a decisive role in elucidating various spin-related physics in the quantum Hall regime. In this talk, I will present resistively detected NMR (RD-NMR) measurements performed in the millikelvin temperature regime on a high-mobility two-dimensional electron system confined to a GaAs quantum well. The wide range of density tunability provided by the back gate allows us to explore both the first and second Landau levels (LLs), from full depletion to $\nu = 8/3$, at a constant magnetic field of 6.4 T.

Measurements of spin polarization as a function of filling factor via the Knight shift reveal markedly different behavior in the first and second LLs. In contrast to the first LL, where the spin polarization oscillates with ν, the second LL remains fully polarized independent of ν, including not only the quantized Hall states at $\nu = 5/2$, 7/3, and 8/3 but also the non-quantized states between them [1]. The implications of the different behavior is discussed in terms of the composite fermion model.

Furthermore, I will show that NMR can be a sensitive probe of not only the spin, but also the charge degree of freedom in the electron system. This is demonstrated in the fractional as well as integer regime, where striking anomalies in the Knight shift and spectral lineshape appear at low partial filling. Numerical simulations incorporating a spatially varying density landscape resulting from the formation of a Wigner solid reproduce the observed anomalies remarkably well. Our RD-NMR spectra uncover the evolution of quantum electron solids manifested by local density fluctuations that grow as the transition to the liquid phase is approached.

K. M. thanks L. Tiemann, T. D. Rhone, G. Gamez, N. Kumada, and N. Shibata for their collaboration in this work.

[1] L. Tiemann, G. Gamez, N. Kumada, and K. Muraki, Science **335**, 828 (2012).

Probing the stripe phase at filling factor 5/2 by NMR

B. Frieß [1], V. Umansky [2], L. Tiemann [1], K. von Klitzing [1] and J. Smet [1]

[1] *Max Planck Institute for Solid State Research, Stuttgart, Germany*
[2] *Braun Centre for Semiconductor Research, Department of Condensed Matter Physics, Weizmann Institute of Science, Rehovot, Israel*

The appearance of periodic charge modulations as charge density waves is currently of strong interest in a variety of fields, such as high T_c superconductors and two dimensional electron systems in the quantum Hall regime. In the latter case electrons are believed to arrange into two dimensional “bubble” phases as well as unidirectional “stripe” phases for certain ratios of the electron density and magnetic field. A prominent example for such a potential stripe phase formation is the 5/2 state in tilted magnetic fields. As shown in Fig. 1, the 5/2 state disappears when tilting the sample with respect to the external magnetic field. This behavior had initially been interpreted to indicate an unpolarized 5/2 state [1], but in view of the strong transport anisotropy has later been revised as a signature of the emergence of a stripe-like phase [2]. However, beyond this indication by transport measurements alone, little is known about the stripe formation itself.

We have employed a technique called resistively detected NMR to probe the electron spin distribution at various filling factors between ν=2 and ν=3 when tilting the sample with respect to the external magnetic field. The resonance frequency of the nuclei has been shown to be a sensitive detector for changes in the electron spin polarization [3]. Starting from a single peak at ν=2 we observe the development of a prominent second peak, which ultimately evolves back into a single peak when approaching ν=3. Our measurements strongly suggest the emergence of separate regions with two different electron spin densities in the filling factor range displaying large transport anisotropy. In addition, by modeling the electron distribution as well as the corresponding NMR response across the filling factor range we are able to draw conclusions about the microscopic details of the stripe pattern.

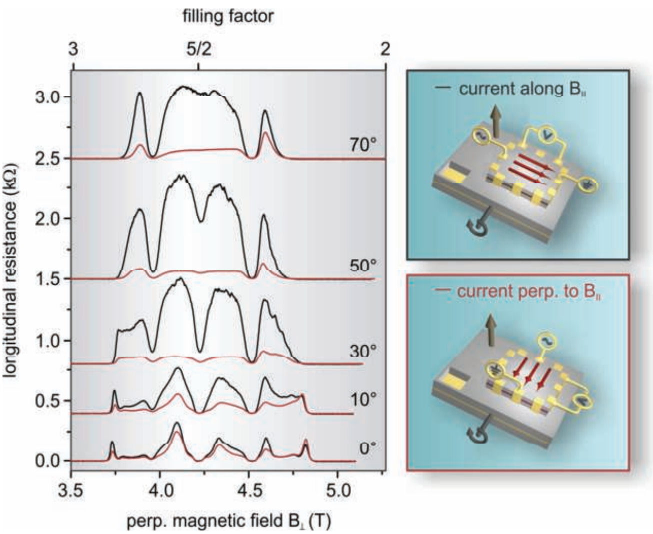

FIG. 1: Longitudinal resistance as a function of perpendicular magnetic field for different tilt angles (offset for clarity). Current flow along $B_{||}$ (black) and perpendicular to $B_{||}$ (red).

[1] J. P. Eisenstein *et al.*, Phys. Rev. Lett. **61**, 997 (1988).
[2] M. P. Lilly *et al.*, Phys. Rev. Lett. **83**, 824 (1999). W. Pan *et al.*, Phys. Rev. Lett. **83**, 820 (1999).
[3] L. Tiemann *et al.*, Science **335**, 828 (2012). O. Stern *et al.*, Phys. Rev. B **70**, 075318 (2004).

Evidence for a Nematic Fractional Quantum Hall State at ν = 5/2 in Parallel Magnetic Field

Yang Liu, S. Hasdemir, M. Shayegan, L. N. Pfeiffer, K. W. West and K. W. Baldwin

Department of Electrical Engineering, Princeton University, Princeton, New Jersey, USA

The origin and properties of the fractional quantum Hall (FQH) state at Landau level filling factor ν = 5/2 have become of tremendous current interest, thanks to the possibility that this state might be non-Abelian and be useful topological quantum computing. We study the ν = 5/2 FQH state as a function of parallel magnetic field ($B_{||}$), applied in the sample plane, in a very high-quality 2D electron system. We find that the application of $B_{||}$ leads to a strong transport anisotropy as the resistance along $B_{||}$ becomes more than 30 times larger than in the perpendicular direction. Despite the enormous transport anisotropy, the energy gap for this FQH state has the same magnitude along both directions. We interpret our data in terms of a FQH nematic phase.

Figure 1 highlights our main findings. The data were taken in a 30-nm-wide GaAs quantum well, and $B_{||}$ is introduced via tilting the sample in magnetic field by an angle θ. The longitudinal resistances are measured parallel (R_{xx}) and perpendicular (R_{yy}) to $B_{||}$. At low temperatures (T < 0.1 K), both R_{xx} and R_{yy} decrease monotonically with decreasing T. At a given θ, the resistance anisotropy ratio remains constant over a relatively large T range so that the energy gaps we extract from the T-dependence of the resistances are the same for both directions. However, the resistance anisotropy increases tremendously as θ is increased (Fig. 1). Above about 0.12 K, R_{xx} starts to decrease as T is increased, signaling that transport is becoming less anisotropic.

Our transport measurements reveal that the application of $B_{||}$ leads to a ν = 5/2 FQH state whose in-plane longitudinal resistance is highly anisotropic and yet the energy gap deduced from the low-temperature data is the same for both transport directions. These observations are generally consistent with a FQH nematic phase [2], although other explanations might be possible [1]. Regardless of the interpretations, our results attest to the very rich and yet not fully understood nature of the enigmatic ν = 5/2 FQHS.

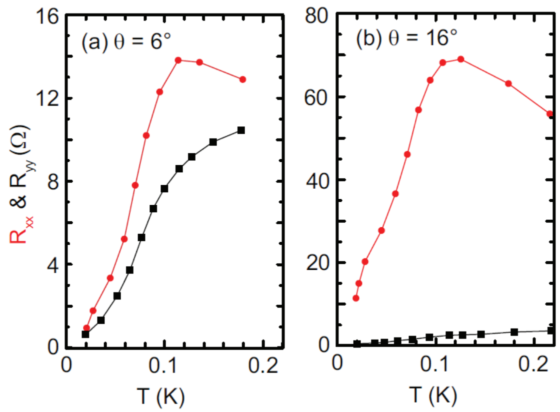

Fig. 1. Longitudinal magneto-resistances vs. temperature (T), measured parallel (R_{xx}) and perpendicular (R_{yy}) to the direction of the in-plane magnetic field $B_{||}$. θ denotes the angle between the total field and the normal to sample plane. The data were taken on a 2D electron system confined to a 30-nm-wide GaAs quantum well, at density 3.05 x 10^{15} m^{-2} and mobility 2,500 m^2/Vs. In both plots, the resistance decreases monotonically at lower temperatures. However, the low-temperature R_{xx}/R_{yy} anisotropy ratio increases from about unity at 6° to about 15 at 16°.

[1] Yang Liu, S. Hasdemir, M. Shayegan, L.N. Pfeiffer, K.W. West and K.W. Baldwin, cond-mat: 1302.6386 (2013).

[2] M. Mulligan, C. Nayak, and S. Kachru, Phys. Rev. B **84**, 195124 (2011).

WeOE7

Method of Constructing Trial Wavefunctions for Quantum Hall States

J. J. Quinn

Department of Physics, University of Tennessee, Knoxville, Tennessee 37996, USA

Numerical studies indicate that incompressible quantum Hall states occur when the relation between the single particle angular momentum ℓ and the number N of electrons in the partially filled Landau level is $2\ell = \nu^{-1}N - c_\nu$. Here, ν is the filling factor and c_ν is a "finite size shift". The values of c_ν found numerically depend on correlations, and for $\nu = n/q < 1/2$ are given by $c_\nu = q + 1 - n$. This finite size shift points the way to constructing electronic trial wavefunctions. A trial wavefunction can always be written $\Psi = FG$, where $F = \Pi_{i<j} z_{ij}$ and $G(z_{ij})$ is a symmetric correlation function caused by interactions. For the Moore-Read state, $G_{\mathrm{MR}}(z_{ij})$ is a product of F and the antisymmetric Pfaffian. Another choice is the quadratic function, $G_Q = S\{\Pi_{i<j\in g1} \Pi_{k<l\in g2} (z_{ij}z_{kl})^2\}$, where S is a symmetrizing operator, and g_1 and g_2 each contain $N/2$ particles resulting from a partition of N into two sets. For the Jain states with $\nu = n/q < 1/2$, the N particles can be partitioned into n subsets, $g_1, g_2, \ldots, g_n$, each containing two particles more than the preceding one. For example, for $n = 3$, g_1; g_2, and g_3 contain N/3 – 2, N/3, and N/3 + 2 electrons, respectively. Choosing different correlations among particles within different subsets, and between particles belonging to different subsets can result in the maximum power of z_i in the antisymmetric wavefunction equal to $2\ell = \nu^{-1}N - c_\nu$, with $c_\nu = q + 1 - n$. The choice of correlation functions is not necessarily unique. Exact diagonalization studies of small systems are being carried out to compare different choices.

Anisotropic Fermi Contour of Composite Fermions In Tilted Magnetic Fields

D. Kamburov, Y. Liu, M. Shayegan, L. N. Pfeiffer, K. W. West, K. W. Baldwin

Department of Electrical Engineering, Princeton University, USA

The composite fermion (CF) formalism provides an extremely powerful yet very simple description of the fractional quantum Hall. In the CF picture, an even number of flux quanta pair up with each carrier at high magnetic field to form quasi-particles which, at filling factor ν = ½, occupy a Fermi sea with a well-defined Fermi contour. The existence of a CF Fermi contour raises the question whether fermionization preserves any low-field Fermi contour anisotropy.

In the study presented here we employ the commensurability of the CF semi-classical orbits with a unidirectional periodic potential modulation [1] in a high-mobility (001) GaAs 2D hole system to extract the Fermi contour anisotropy created by parallel magnetic field, $B_{\|}$. We measure the magnetoresistance along two perpendicular arms of an L-shaped Hall bar, shown in Figs. 1(a) and (b), at different tilt angles (θ) of the sample. The periodic modulation produces strong CF commensurability resistance minima near filling factor ν = ½. When the magnetic field is purely perpendicular (θ = 0), as shown in the bottom traces of the Fig. 1 panels, the observed positions of the minima agree with the positions anticipated for a circular CF Fermi contour (dashed green lines in Fig. 1) [2]. As the sample is tilted to increase $B_{\|}$, the minima move *away* (Fig. 1a) or *toward* (Fig. 1b) the magnetic field at ν = ½ position, depending on the orientation of the Hall bar. These shifts are a direct measure of the changes in the size of the CF Fermi contour wave vectors along and perpendicular to $B_{\|}$.

Our results provide stimulus for future studies to address the role of anisotropy in interacting carrier systems.

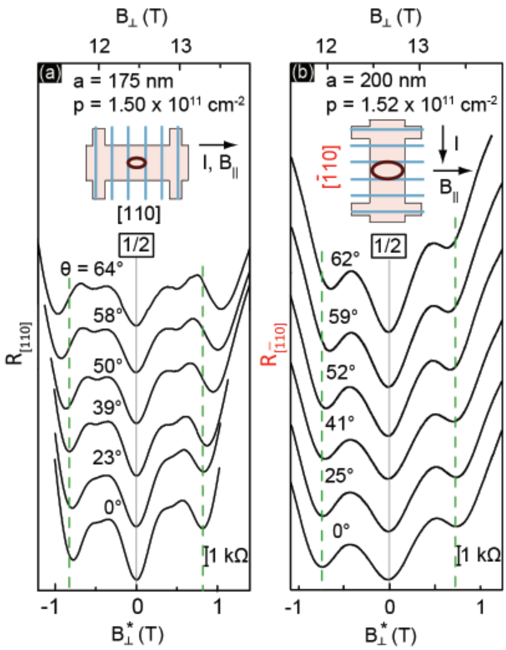

FIG. 1: CF commensurability minima near ν = ½ measured along the two arms of an L-shaped Hall bar. $B^*_\perp$ is the effective magnetic field felt by the CFs. As the sample is tilted at an angle θ to introduce $B_{\|}$ along [110], the resistance minima for the [110] Hall bar (a) move away from ν = ½ ($B^*_\perp = 0$) while those in the [$\bar{1}$10] Hall bar (b) move towards ν = ½.

References:

[1] D. Kamburov *et al*., arXiv:1302.2540.
[2] D. Kamburov *et al*., Phys. Rev. Lett. **109**, 236401 (2012).

Probing spins in spin interferometer with superconducting lead

Toshihiro Kubo [1] **and Yasuhiro Tokura** [1,2]

[1] *Graduate School of Pure and Applied Sciences, University of Tsukuba*
[2] *NTT Basic Research Laboratories, NTT Corporation*

Recently the spin-orbit interaction (SOI) in semiconductors has attracted great attention as it plays a very intriguing role in semiconductor spintronics. SOI can couple the spin degree of freedom of electrons to their orbital motion and vice versa, therefore giving a useful handle for manipulating and controlling the electron spin by external electric field or gate voltages [1]. In general, SOI is very strong in narrow gap semiconductors such as InAs and InSb [2].

In this work, using the superconducting lead, we study the relation between the asymmetric Andreev bound state and a spin current generated by the SOI in an interferometer containing a quantum dot (QD) as shown in Fig. 1. It is argued that the spin current is generated under the condition when the SOI is finite, a QD has an on-site Coulomb interaction, and an interferometer is out of equilibrium [3,4]. We employ the Schwinger-Keldysh nonequilibrium Green's function method based on Nambu-Gor'kov formalism. First we consider the situation without superconducting lead, namely t_S=0 in Fig. 1, and discuss the mechanism of spin current generation. We show that the generated spin current depends on whether the nonequilibrium situation is created by the source-drain bias voltage or thermal gradient applied to two normal leads (L,R). Depending on the condition for the QD energy level and the strength of SOI, even for finite thermal gradient, we may have no spin current. On the contrary, for finite source-drain bias voltage, the spin current always occurs. Next we discuss the detection scheme of the spin current using the superconducting lead whose voltage is zero. The local density of states (LDOS) in the system shows the peak splitting corresponding electron and hole in an Andreev bound state. When the spin current is not generated, those peaks in the LDOS are symmetric with respect to energy. As the source-drain bias voltage, on-site Coulomb interaction, or SOI increase, those peaks become asymmetric. This result shows that there is the relation between a finite spin current and the asymmetry in LDOS. This property in LDOS appears in the tunneling current from the left lead to right lead through a QD. Therefore, we can detect the spin current generation from the transport property through a QD.

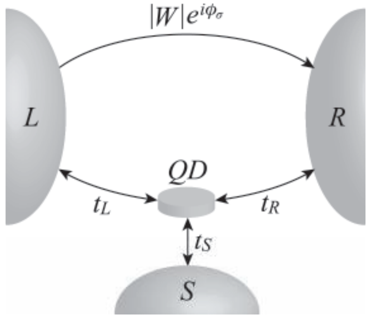

Figure 1: Schematic diagram of an interferometer containing a QD which couples to two normal leads (L,R) and a superconducting lead (S). $\phi_\sigma=\sigma\phi_{SO}$ is spin-dependent phase due to SOI, where ϕ_{SO} is proportional to the strength of the Rashba SOI. t_v is the tunneling amplitude between the QD and the reservoir v and W indicates the direct transmission between two normal leads.

[1] J. Nitta, T. Akazaki, and H. Takayanagi, Phys. Rev. Lett. **78**, 1335 (1997).
[2] S. Takahashi, R. S. Deacon, K. Yoshida, A. Oiwa, K. Shibata, K. Hirakawa, Y. Tokura, and S. Tarucha, Phys. Rev. Lett. **104**, 246801 (2010).
[3] Qing-feng Sun and X. C. Xie, Phys. Rev. B **73**, 235301 (2006).
[4] N. Taniguchi and K. Isozaki, J. Phys. Soc. Jpn. **81**, 124708 (2012).

All-electrical spin injection from a quantum point contact

T.-M. Chen[1], M. Pepper[2], I. Farrer[3], G. A. C. Jones[3], D. A. Ritchie[3]

[1] *Department of Physics, National Cheng Kung University, Tainan 701, Taiwan*
[2] *Department of Electronic and Electrical Engineering, University College London, London WC1E 7JE, United Kingdom*
[3] *Cavendish Laboratory, J J Thomson Avenue, Cambridge CB3 0HE, United Kingdom*

There is considerable interest in being able to control the spin dynamics because this could lead to the development of a range of spintronic devices that in principle are much faster and use less energy than their electronic counterparts. In order to develop successfully such concepts it is necessary to controllably generate, manipulate, and detect spin currents by electrical means and so minimize, or eliminate, the use of ferromagnetic contacts or external magnetic fields. Most research towards the implementation of this electrical approach has focused on using the spin-orbit interaction to induce spin polarized transport, as reported in various nanostructures including quantum point contacts[1, 2]. However, it is essential to develop a more general approach in which materials with a strong intrinsic spin-orbit coupling are no longer necessary, and consequently a longer spin dephasing (relaxation) time will be obtained, of crucial importance for quantum information processing.

In this work we demonstrate on-chip spin polarizing or filtering actions by driving the gate-defined quantum point contact, one of the simplest geometries for integrated quantum devices, away from the conventional Ohmic regime. We have utilized a technique of electron focusing [3, 4] to directly measure the degree of spin polarization of the current. The height of a focusing signal V_c quantifies the degree of spin polarization of the emitted current $P_e = (I_\downarrow - I_\uparrow)/(I_\downarrow + I_\uparrow)$ and the spin selectivity of the collector $P_c = (T_\downarrow - T_\uparrow)/(T_\downarrow + T_\uparrow)$, given by the following relation: $V_c \propto (1 + P_e P_c)$. Our results show that the focusing signal doubles in value only when both the emitter and collector point contacts were set to the 0.25 anomaly[4, 5], indicating that point contacts are fully spin polarized. In addition, the electrons retain their spin polarization as they bend around in the circular orbit. This illustrates that there is an appreciable spin coherence length and that the spin polarization can be transmitted over considerable lengths by purely electrical means. We furthermore demonstrate that an electrical configuration of gates and applied voltages can give rise to spin injection with a tunable spin polarization between 0 to 100%, which has implications for the development of spintronic devices and future quantum information processing.

[1] P. Debray, S. M. S. Rahman, J. Wan, R. S. Newrock, M. Cahay, A. T. Ngo, S. E. Ulloa, S. T. Herbert, M. Muhammad , and M. Johnson, Nature Nanotechnology **4**, 759 (2009).

[2] C. H. L. Quay, T. L. Hughes, J. A. Sulpizio, L. N. Pfeiffer, K. W. Baldwin, K. W. West, D. Goldhaber-Gordon, and R. de Picciotto, Nature Physics **6**, 336 (2010).

[3] R. M. Potok, J. A. Folk, C. M. Marcus, and V. Umansky, Phys. Rev. Lett. **89**, 266602 (2002).

[4] T.-M. Chen, M. Pepper, I. Farrer, G. A. C. Jones, and D. A. Ritchie, Phys. Rev. Lett. **109**, 177202 (2012).

[5] T.-M. Chen, A. C. Graham, M. Pepper, I. Farrer, and D. A. Ritchie, Appl. Phys. Lett. **93**, 032102 (2008).

WeOM7

SiGe self-assembled nanostructures for quantum spintronics

N. Ares,[1] V. N. Golovach,[1, 2] G. Katsaros,[1, 2] M. Stoffel,[3] F. Fournel,[4] L. I. Glazman,[5] O. G. Schmidt,[2] and S. De Franceschi[1]

[1] *SPSMS, CEA-INAC/UJF-Grenoble 1, 17 Rue des Martyrs, F-38054 Grenoble Cedex 9, France*
[2] *Institute for Integrative Nanosciences, IFW Dresden, Helmholtzstr. 20, D-01069 Dresden, Germany*
[3] *Universit´e de Lorraine, Institut Jean Lamour, UMR CNRS 7198, Nancy-Universit´e, BP 239, F-54506 Vandoeuvre-les-Nancy, France*
[4] *CEA, LETI, MINATEC, 17 Rue des Martyrs, F-38054 Grenoble Cedex 9, France*
[5] *Department of Physics, Yale University, New Haven, Connecticut 06520, USA*

Quantum spintronics aims at utilizing the quantum nature of individual spins to bring new functionalities into logic circuits. Here we investigate a new route to quantum spintronics based on p-type SiGe nanostructures. This system combines weak hyperfine interaction, which is a favourable property for long spin coherence, with strong spin-orbit coupling, which can enable fast spin manipulation. We shall present tunneling and co-tunneling spectroscopy experiments on single quantum-dot devices. Our measurements reveal a variety of spin-related properties of the confined hole states. In particular, we find large g-factor anisotropies as well as pronounced spin-orbit related asymmetries in the non-linear transport characteristics [1,2]. In addition, we report a giant non-monotonic modulation of the hole g-factors induced by an external electric field [3]. Implications and schemes for electrically-driven spin coherent manipulation and readout are discussed.

[1] G. Katsaros, P. Spathis, M. Stoffel, F. Fournel, M. Mongillo, V. Bouchiat, F. Lefloch, A. Rastelli, O. G. Schmidt, and S. De Franceschi, *Nature Nanotechnology* **5**, 458 (2010).
[2] G. Katsaros, V.N. Golovach, P. Spathis, N. Ares, M. Stoffel, F. Fournel, O.G. Schmidt, L.I. Glazman, and S. De Franceschi, *Phys. Rev. Lett*. **107**, 246601 (2011).
[3] N. Ares, V.N. Golovach, G. Katsaros, M. Stoffel, F. Fournel, L.I. Glazman, O.G. Schmidt and S. De Franceschi, Phys. Rev. Lett. **110**, 046602 (2013).

Spin injection into a high mobility 2DEG system

M. Oltscher, M. Ciorga, M. Utz, D. Schuh, D. Bougeard, and D. Weiss

Institute for Experimental and Applied Physics, University of Regensburg, Regensburg, Germany

Electrical generation and control of electron spins in semiconductors is the central theme in semiconductor spintronics and of big importance for device prospects. In particular spin injection into two-dimensional (2D) electron systems would allow for many new functionalities in future devices, with a Datta-Das spin field effect transistor [1] being a primary example. Building on successful realization of spin injection into bulk GaAs employing the diluted magnetic semiconductor (Ga,Mn)As as a ferromagnetic material [2] we extended our work into heterostructures containing 2D electron gases (2DEG). We investigate two types of systems: 2DEG confined in a InGaAs quantum well structure and high mobility 2DEG confined in an inverted AlGaAs/GaAs heterojunction.

Experiments were performed on lateral devices consisting of a 2D channel of 50 μm width with four ferromagnetic (FM) spin injecting/detecting contacts placed about 200 nm above the channel. FM contacts consist of a (Ga,Mn)As/GaAs Esaki diode structure, similar to the one used in experiments on bulk devices [2]. The doping profile and the layer layout of the used MBE-grown wafer were carefully designed in order to assure that: (i) a sufficiently large charge current flows from the Esaki diode down to the 2D system to generate spin accumulation; (ii) after etching away the layers forming a diode structure from the region between the contacts, a lateral transport occurs exclusively within the 2D layer. Magnetotransport measurements confirmed the formation of a high quality 2DEG in both investigated systems with mobility reaching $\mu=5\times10^5$ cm^2/Vs for the inverted AlGaAs/GaAs heterojunction. We observe clear nonlocal spin-valve signals in both systems, with typical results for AlGaAs/GaAs structure shown in Fig.1. We discuss in details a peculiar bias dependence of the spin signal observed for the high mobility structure, with unusually high values of spin injection efficiency obtained for a certain range of negative bias values.

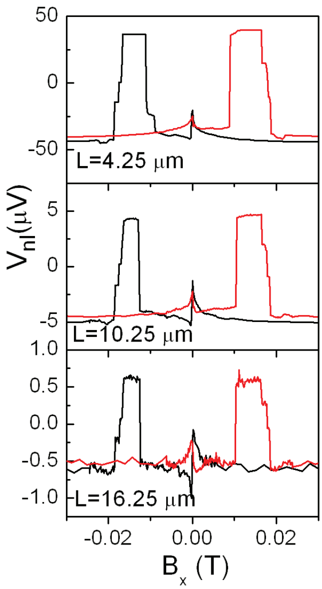

Fig. 1 Non-local spin valve signal (after removing the background) for three different values of injector–detector separation L observed for the AlGaAs/GaAs structure for an injection current of I=–20μA at T=4.2K.

The work was supported by German Science Foundation (DFG) through the project SFB689.

[1] S. Datta and B. Das, Appl. Phys. Lett. **56**, 665 (1990).
[2] M. Ciorga *et al.*, Phys. Rev. B **79**, 165321 (2009)

WeIM2

INVITED

Modulated semiconductor structures of magnetically doped nitrides

Alberta Bonanni

Institut für Halbleiter- und Festkörperphysik, Johannes Kepler University, Linz - Austria

We discuss the surprising interplay between the distribution of magnetic ions and shallow impurities in group III nitrides, that allows to control the magnetic and optical properties in these systems, including the activation of a strong broad-band infrared emission [1]. In particular, we summarize how - by exploiting also synchrotron-radiation and high-resolution microscopy techniques - we have unraveled a number of non-anticipated features of these systems, like the nature of superexchange ferromagnetic interactions and the self-aggregation of magnetic cations and impurity complexes driven by fabrication parameters and co-doping [1-6].

Furthermore, we introduce the architecture and epitaxy of nitride-based spin filtering magnetic-insulator/semiconductor quantum layered structures.

[1] T. Devillers et al., Sci. Rep. **2**, 722 (2012).
[2] A. Bonanni et al. Phys. Rev. B **84**, 035206 (2011).
[3] J. Suffczyński et al., Phys Rev. B. **83**, 094421 (2011).
[4] A. Navarro-Quezada et al., Phys. Rev. B **84**, 155321 (2011).
[5] M. Sawicki et al., Phys. Rev. B **85**, 205204 (2012).
[6] A. Navarro-Quezada et al., Appl. Phys. Lett. **101**, 981911 (2012).

Monday
Tuesday
Wednesday
Thursday
Friday

Majorana in semiconductors

Sankar Das Sarma

University of Maryland, USA

Majorana2

Majorana's in InSb nanowires

L. P. Kouwenhoven

Kavli Institute of Nanoscience, Delft University of Technology
2600 GA Delft, The Netherlands

A year ago we reported in Science magazine our experiment on “Signatures of Majorana fermions in Hybrid Superconductor-Semiconductor Nanowire Devices”. Since then the data has been reproduced and extended by others and also by ourselves. Theoretical analyses have pointed at both alternative explanations as well as strengthening the Majorana interpretation. Also new experimental checks have been proposed including the ultimate check in terms of a minimal scheme for braiding to demonstrate non-Abelian statistics. I will give an overview and an outlook. Background information and published work can be found at kouwenhovenlab.tudelft.nl.

Zero-bias peaks and splitting in an Al–InAs nanowire

Moty Heiblum

Braun Center for Submicron Research, Department of Condensed Matter Physics, Weizmann Institute of Science, Rehovot 76100, Israel

I present initial experimental studies of a system composed of an aluminum superconductor in proximity to an indium arsenide nanowire, with the latter possessing strong spin-orbit coupling and Zeeman splitting. In the ideal case, an induced one-dimensional topological superconductor, supporting Majorana fermions at both ends of the nanowire, is expected to form. We concentrate on the characteristics of a distinct zero bias conductance peak (ZBCP) and its splitting in energy – both appearing only with a small magnetic field applied along the wire. The ZBCP was found to be robustly tied to the Fermi energy over a wide range of system parameters. While not providing a definite proof of a Majorana state, the presented data and the simulations support its existence.

Majorana4

Disordered Majorana Wires

Piet W. Brouwer

Dahlem Center for Complex Quantum Systems and Fachbereich Physik, Freie Universität Berlin, Arnimallee 14, 14195 Berlin, Germany

A one dimensional spinless p-wave superconductor may may be in a topological nontrivial state, in which it has a zero energy Majorana bound state at each end. Such a system can be realized in spin-orbit coupled nanowire with proximity-induced pairing from a nearby s-wave superconductor. In this talk, I will discuss how non-idealities, such as potential disorder and deviations from a strict one-dimensional limit, affect the topological phase and its signatures in a current-voltage measurement. In particular, I'll argue that the topological phase can persist at weak disorder and that a multichannel spinless p-wave superconductor goes through an alternation of topologically trivial and nontrivial phases upon increasing the disorder strength, the number of phase transitions being equal to the channel number N.

[1] P.W. Brouwer, M. Duckheim, A. Romito, and F. von Oppen, Phys. Rev. Lett. **107**, 196804 (2011).
[2] G. Kells, D. Meidan, and P.W. Brouwer, Phys. Rev. B **85**, 060507 (2012).
[3] M.T. Rieder, P.W. Brouwer, and I. Adagideli, arXiv:1302.2071.

Observation of fractional ac Josephson effect: the signature of Majorana particles

Leonid P. Rokhinson[1], Xinyu Liu[2], and Jacek K. Furdyna[2]

[1] *Department of Physics, Department of Electrical and Computer Engineering, Purdue University, West Lafayette, Indiana 47907 USA*

[2] *Department of Physics, University of Notre Dame, Notre Dame, Indiana 46556 USA*

In 1928 Dirac reconciled quantum mechanics and special relativity in a set of coupled equations which became the cornerstone of quantum mechanics[1]. Its main prediction that every elementary particle has a complex conjugate counterpart – an antiparticle – has been confirmed by numerous experiments. A decade later Majorana showed that Dirac's equation for spin-1/2 particles can be modified to permit real wavefunctions[2]. The complex conjugate of a real number is the number itself, which means that such particles are their own antiparticles. The most intriguing feature of Majorana particles is that in low dimensions they obey non-Abelian statistics and can be used to realize quantum gates that are topologically protected from local sources of decoherence[3]. While the search for Majorana fermions among elementary particles is still ongoing, excitations sharing their properties may emerge in electronic systems. Specifically, it has been predicted that Majorana excitations may be formed in some unconventional states of matter[4, 5, 6, 7, 8, 9]. We report the observation of the fractional ac Josephson effect in a hybrid semiconductor/superconductor InSb/Nb nanowire junction, a hallmark of topological matter [10]. When the junction is irradiated with rf frequency f_0 at zero external magnetic field, quantized voltage steps (Shapiro steps) with a height $\Delta V = hf_0/2e$ are observed, as is expected for conventional superconductor junctions where the supercurrent is carried by charge-$2e$ Cooper pairs. At high fields the height of the first Shapiro step is doubled to hf_0/e, suggesting that the supercurrent is carried by charge-e quasiparticles. This is a unique signature of Majorana fermions, elusive particles predicted *ca.* 80 years ago.

[1] Dirac, P. A. M., Proc. R. Soc. Lond. A 117,610 (1928).
[2] Majorana, E., Nuovo Cimento **14**, 171 (1937).
[3] Kitaev, A. Y., Ann. Phys. **303**, 2 (2003).
[4] Read, N. and Green, D., Phys. Rev. B **61**, 10267 (2000).
[5] Kitaev, A. Y., Physics-Uspekhi **44**, 131 (2001).
[6] Fu, L. & Kane, C., Phys. Rev. Lett. **100**, 096407 (2008).
[7] Sau, J., Lutchyn, R., Tewari, S. & Das Sarma, S. Phys. Rev. Lett. **104**, 040502 (2010).
[8] Lutchyn, R. M., Sau, J. D. & Sarma, S. D., Phys. Rev. Lett. **105**, 077001 (2010).
[9] Oreg, Y., Refael, G. & von Oppen, F., Phys. Rev. Lett. **105**, 177002 (2010).
[10] Rokhinson, L. P. , Liu, X. and Furdyna, J. K. Nature Physics **8**, 795 (2012)

Majorana6

(Title not available)

Charles M. Marcus

The Niels Bohr Institute, Condensed Matter Physics, University of Copenhagen, Denmark

4 July (Thursday)

Wrocław Town Hall

4 July (Thursday)

EP2DS Session 1

9.00 – 9.30 **ThIE1**
Michael Fuhrer
(*Monash University, Australia; University of Maryland, College Park, USA*)
Surface conduction of topological Dirac electrons in bulk insulating Bi_2Se_3

9.30 – 9.45 **ThOE1**
Paolo Michetti, Björn Trauzettel
(*University of Würzburg, Germany*)
Devices with electrically tunable topological insulating phases

9.45 – 10.00 **ThOE2**
Kyoichi Suzuki, Yuichi Harada, Koji Onomitsu, Koji Muraki
(*NTT Basic Research Laboratories, NTT Corporation*)
Edge transport in InAs/GaSb topological insulating phase

10.00 – 10.15 **ThOE3**
S. Wolgast[1], Y.S. Eo[1], Ç. Kurdak[1], K. Sun[1], J.W. Allen[1], D.-J. Kim[2], Z. Fisk[2]
([1]*University of Michigan, Ann Arbor, USA;* [2]*University of California at Irvine, USA*)
Discovery of a 3D topological insulator: samarium hexaboride

10.15 – 10.30 **ThOE4**
Yuval Baum, Ady Stern
(*Weizmann Institute of Science, Rehovot, Israel*)
Density waves instability and a skyrmion lattice on the surface of strong topological insulators

MSS Session 1

9.00 – 9.15 **ThOM1**
T. Kümmell[1], W. Quitsch[1], O. Fedorych[1], A. Gust[2], C. Kruse[2], D. Hommel[2], G. Bacher[1]
([1]*Universität Duisburg-Essen;* [2]*Universität Bremen, Germany*)
Single photon sources for room temperature operation based on CdSe/ZnSSe/MgS quantum dots

9.15 – 9.30 **ThOM2**
M. Goryca[1], M. Koperski[1], P. Wojnar[2], T. Smoleński[1], T. Kazimierczuk[1], A. Golnik[1], P. Kossacki[1] ([1]*University of Warsaw, Poland;* [2]*Polish Academy of Sciences, Warsaw, Poland*)
Coherent oscillations of a single Mn^{2+} spin in a CdTe quantum dot

9.30 – 9.45 **ThOM3**
G. Reithmaier, S. Lichtmannecker, T. Reichert, P. Hasch, M. Bichler, R. Gross and J.J. Finley
(*Technische Universität München, Germany*)
On-chip time resolved detection of quantum dot emission using integrated superconducting single photon detectors

9.45 – 10.00 **ThOM4**
I. Schwartz, L. Gantz, E.R. Schmidgall, E. Bordo, D. Cogan, Y. Kodriano, E. Poem, D. Gershoni (*Technion, Haifa, Israel*)
Entanglement between a dark exciton and a single photon

10.00 – 10.30 **ThIM1**
P.L. McMahon[1], K. De Greve[1,2], Leo Yu[1], J. Pelc[1], C. Jones[1], C.M. Natarajan[1], N.Y. Kim[1], E. Abe[1], S. Maier[3], C.Schneider[3], M. Kamp[3], S. Höfling[3], R. Hadfield[4], A. Forchel[3], M.M. Fejer[1], Y. Yamamoto[1,5]
([1]*Stanford University, USA;* [2]*Harvard University, USA;* [3]*Universität Würzburg, Germany;* [4]*Heriot-Watt University, Scotland;* [5]*National Institute of Informatics, Japan*)
High-fidelity spin-photon entanglement generation using self-assembled InAs quantum dots

EP2DS Session 2

11.00 – 11.30 **ThIE2**
Jurgen H. Smet
(*Max-Planck-Institut für Festköperforschung, Stuttgart, Germany*)
Fractional quantum Hall physics in graphene

11.30 – 11.45 **ThOE5**
M.A. Zudov[1], P.D. Martin[1], A.T. Hatke[1], J.D. Watson[2,3], M.J. Manfra[2,3], L.N. Pfeiffer[4], K.W. West[4]
([1]*Univ. of Minnesota, Minneapolis;* [2,3]*Purdue Univ., West Lafayette;* [4]*Princeton Univ., USA*)
Giant photoresistance and a new class of microwave-induced resistance oscillations in GaAs/AlGaAs quantum wells

11.45 – 12.00 **ThOE6**
Thomas Stegmann, Dietrich E. Wolf, Axel Lorke
(*University of Duisburg-Essen and CENIDE, Germany*)
Magnetotransport along a boundary: From coherent electron focusing to edge channel transport

12.00 – 12.15 **ThOE7**
Y. Shilo[1], K. Cohen[1], R. Rapaport[1], S. Lazić[2], A. Violante[2], R. Hey[2], P.V. Santos[2], K. West[3], L. Pfeiffer[3]
([1]*The Hebrew University of Jerusalem, Israel;* [2]*Paul-Drude-Institut für Festkörperelektronik, Berlin, Germany;* [3]*Princeton University, USA*)
Observation of quantum and classical correlation regimes in cold dipolar exciton fluids

12.15 – 12.30 **ThOE8**
P. Rickhaus, M. Weiss, L. Marot, and C. Schönenberger
(*University of Basel, Switzerland*)
Quantum Hall effect in graphene with superconducting electrodes

MSS Session 2

11.00 – 11.15 **ThOM5**
P. Scarlino[1], E. Kawakami[1], M. Shafiei[1], L.M.K. Vandersypen[1], W. Wegscheider[2] ([1]*TU Delft, Netherlands;* [2]*ETH Zurich, Switzerland*)
Spin-orbit anisotropy and relaxation of GaAs single electron spin qubits

11.15 – 11.30 **ThOM6**
O. Drachenko[1], D. Kozlov[2], A. Ikonnikov[2], K. Spirin[2], V. Gavrilenko[2], H. Schneider[1], M. Helm[1], J. Wosnitza[3]
([1]*Institute of Ion-Beam Physics and Materials Research, Dresden, Germany;* [2]*Institute for Physics of Microstructures, Nizhny Novgorod, Russia;* [3]*Dresden High Magnetic Field Laboratory, Germany*)
Extra-long hole spin relaxation time in InGaAs/GaAs quantum wells probed by cyclotron resonance spectroscopy

11.30 – 11.45 **ThOM7**
F. Nagasawa[1], D. Frustaglia[2], H. Saarikoski[3], M. Kohda[1,4], K. Richter[3], J. Nitta[1] ([1]*Tohoku University, Sendai, Japan;* [2]*Universidad de Sevilla, Spain;* [3]*Universität Regensburg, Germany;* [4]*PRESTO, Saitama, Japan*)
Controlling of the geometric phase of electron spin in a semiconductor ring device

11.45 – 12.00 **ThOM8**
A. Hernandez-Minguez, K. Biermann, R. Hey and P. V. Santos
(*Paul-Drude-Institut für Festkörperelektronik, Berlin, Germany*)
Electric control of spin lifetimes in GaAs (111) quantum wells

12.00 – 12.30 **ThIM2**
J. Sinova[1,2], T. Jungwirth[2,3], A.F. Ferguson[4]
([1]*Texas A&M University, College Station, USA;* [2]*Institute of Physics ASCR, Praha, Czech Republic;* [3]*University of Nottingham, UK;*[4]*Hitachi Cambridge Laboratory, UK*)
Anti-damping intrinsic spin-orbit torque in GaMnAs arising from Berry phase

EP2DS Session 3

14.00 – 14.30 **ThIE3**

B.N. Narozhny[1], M. Titov[2], M. Schütt[3], P.M. Ostrovsky[4,5], I.V. Gornyi[3,6], A.D. Mirlin[1,3,7], T. Tudorovskiy[2], M.I. Katsnelson[2]
([1,3]*Karlsruher Institut für Technologie, Germany;* [2]*Radboud University Nijmegen, NL;* [4]*Max-Planck-Institut für Festkörperforschung, Stuttgart, Germany;* [5]*L.D. Landau Institute for Theoretical Physics RAS,Moscow, Russia;* [6]*Ioffe,St. Petersburg, Russia;* [7]*Petersburg Nuclear Physics Institute, Russia*)
Giant magneto-drag in graphene at the charge neutrality

14.30 – 14.45 **ThOE9**

M. Mucha-Kruczyński[1,2], J.R. Wallbank[1], A.A. Patel[1,3], A.K. Geim[4], V.I. Fal'ko[1,5]
([1]*Lancaster University, UK;* [2]*University of Bath, UK;* [3]*Indian Institute of Technology Kanpur, India;* [4]*University of Manchester, UK;* [5]*University of Geneva, Switzerland*)
Electronic structure of monolayer and bilayer graphene on hexagonal substrates

14.45 – 15.00 **ThOE10**

Shaffique Adam
(*Yale-NUS College; National University of Singapore, Singapore*)
Magnetotransport in disordered graphene at charge neutrality

15.00 – 15.15 **ThOE11**

Pierre Delplace, Jian Li, Markus Büttiker
(*Université de Genève, Switzerland*)
Magnetic field induced localization in 2D topological insulators

MSS Session 3

14.00 – 14.15 **ThOM9**

N. Ubbelohde[1], C. Fricke[1], F. Hohls[1,2], R.J. Haug[1]
([1]*Leibniz Universität Hannover, Germany;* [2]*Physikalisch-Technische Bundesanstalt, Braunschweig, Germany*)
Spin-dependent shot noise enhancement in a quantum dot

14.15 – 14.30 **ThOM10**

M.P. Nowak, B. Szafran
(*AGH University of Science and Technology, Kraków, Poland*)
Spin blockade lifting due to phonon mediated spin relaxation and electric dipole spin resonance in nanowire quantum dots

14.30 – 14.45 **ThOM11**

R. Thalineau[1], A.D. Wieck[2], C. Bäuerle[1],L. Saminadayar[1], T. Meunier[1]
([1]*CNRS and Universite Joseph Fourier, Grenoble, France;* [2]*Ruhr-Universität Bochum, Germany*)
A few-electron quadruple quantum dot in a closed loop

14.45 – 15.15 **ThIM3**

T. Fujita [1], K. Morimoto[1], S. Teraoka[1], G. Allison[1,2], A. Ludwig[3], A.D. Wieck[3], A. Oiwa[1], S. Tarucha[1]
([1]*University of Tokyo, Japan;* [2]*Princeton University, USA;* [3]*Ruhr-Universität Bochum, Germany*)
Real-time spin detection of single photo-electrons with a double quantum dot in a g-factor engineered quantum well

EP2DS Session 4

15.45 – 16.15 **ThIE4**
Manfred Helm
(*Helmholtz-Zentrum Dresden-Rossendorf, Germany*)
Strong-field THz spectroscopy of low-dimensional semiconductor systems

16.15 – 16.30 **ThOE12**
J. Yoneda[1], T. Otsuka[1,2], T. Nakajima[1,2], T. Takakura[1], T. Obata[1], H. Lu[3], C. Palmstrøm[3], A.C. Gossard[3], S. Tarucha[1,2]
([1]*University of Tokyo, Japan;* [2]*RIKEN, Saitama, Japan;* [3]*University of California, Santa Barbara, USA*)
Coherent dynamics of a strongly driven single electron spin

16.30 – 16.45 **ThOE13**
M. Pakmehr[1], A. Stier[1], B.D. McCombe[1], C. Bruene[2], H. Buhmann[2], L. Molenkamp[2]
([1]*University at Buffalo, USA;* [2]*Universität Würzburg, Germany*)
THz magnetophotoresponse and spin-orbit effects in the 2DEG in a HgTe quantum well

16.45 – 17.00 **ThOE14**
Y. Okazaki, I. Mahboob, K. Onomitsu, S. Sasaki, H. Yamaguchi
(*NTT Basic Research Laboratories, NTT Corporation, Japan*)
Mechanical friction induced by single electron transport

MSS Session 4

15.45 – 16.00 **ThOM12**
D. Laroche[1,2], G. Gervais[1], M.P. Lilly[2], J.L. Reno[2]
([1]*McGill University, Montreal, Canada;* [2]*Sandia National Laboratories, Albuquerque, USA*)
Coulomb drag in vertically-integrated quantum wires

16.00 – 16.15 **ThP83**
B. Ganjipour[1], M. Ek[2], B.M. Borg[1], K.A. Dick[1,2], L-E Wernersson[3], L. Samuelson[1] and C. Thelander[1]
([1-3]*Lund University, Lund, Sweden*)
Electron-hole symmetry in GaSb/InAs core/shell nanowires

16.15 – 16.30 **ThOM14**
S. Takada[1], M. Yamamoto[1,2], S. Nakamura[1], K. Watanabe[1], C. Bauerle[3], A. D. Wieck[4], S. Tarucha[1]
([1]*Univ. of Tokyo, Japan;* [2]*ERATO-JST, Saitama, Japan;* [3]*CNRS and Universite Joseph Fourier, Grenoble, France;* [4]*Ruhr-Universität Bochum, Germany*)
Coherent control of a single electron in a tunnel-coupled wire driven by a surface acoustic wave

16.30 – 17.00 **ThOM13**
L.W. Smith[1], A.R. Hamilton[2], K.J. Thomas[3], M. Pepper[3], I. Farrer[1], J.P. Griffiths[1], G.A.C. Jones[1], D.A. Ritchie[1]
([1]*Cavendish Laboratory, Cambridge, UK;* [2]*University of New South Wales, Australia;* [3]*University College London, UK*)
Compressibility measurements of the 0.7 structure in a one-dimensional quantum wire

ThIE1

INVITED

Surface conduction of topological Dirac electrons in bulk insulating Bi_2Se_3

Michael S. Fuhrer [1,2]

[1] *School of Physics, Monash University, Monash, 3800 Victoria, Australia*
[2] *Center for Nanophysics and Advanced Materials, University of Maryland, College Park, MD 20742-4111 USA*

The three dimensional strong topological insulator (STI) is a new phase of electronic matter which is distinct from ordinary insulators in that it supports on its surface a conducting two-dimensional surface state whose existence is guaranteed by topology. I will discuss experiments on the STI material Bi_2Se_3, which has a bulk bandgap of 300 meV, much greater than room temperature, and a single topological surface state with a massless Dirac dispersion. Field effect transistors consisting of thin (3-20 nm) Bi_2Se_3 are fabricated from mechanically exfoliated from single crystals, and electrochemical and/or chemical gating methods are used to move the Fermi energy into the bulk bandgap, revealing the ambipolar gapless nature of transport in the Bi_2Se_3 surface states. The minimum conductivity of the topological surface state is understood within the self-consistent theory of Dirac electrons in the presence of charged impurities[1]. The intrinsic finite-temperature resistivity of the topological surface state due to electron-acoustic phonon scattering is measured to be ~60 times larger than that of graphene largely due to the smaller Fermi and sound velocities in Bi_2Se_3, which will have implications for topological electronic devices operating at room temperature[2]. As samples are made thinner, coherent coupling of the top and bottom topological surfaces is observed through the magnitude of the weak anti-localization correction to the conductivity[3], and in the thinnest Bi_2Se_3 samples (~3 nm) in thermally-activated conductivity reflecting the opening of a bandgap[4,5].

[1] "Surface conduction of topological Dirac electrons in bulk insulating Bi_2Se_3," Dohun Kim, Sungjae Cho, Nicholas P. Butch, Paul Syers, Kevin Kirshenbaum, Shaffique Adam, Johnpierre Paglione, Michael S. Fuhrer, *Nature Physics* **8**, 460 (2012).
[2] "Intrinsic Electron-Phonon Resistivity in Bi_2Se_3 in the Topological Regime," Dohun Kim, Qiuzi Li, Paul Syers, Nicholas P. Butch, Johnpierre Paglione, S. Das Sarma, Michael S. Fuhrer, *Phys. Rev. Lett.* **109**, 166801 (2012).
[3] "Coherent Topological Transport on the Surface of Bi_2Se_3," Dohun Kim, Paul Syers, Nicholas P. Butch, Johnpierre Paglione, Michael S. Fuhrer, *to appear in Nature Communications*. arXiv:1212.2665.
[4] "Insulating Behavior in Ultrathin Bismuth Selenide Field Effect Transistors," Sungjae Cho, Nicholas P. Butch, Johnpierre Paglione, and Michael S. Fuhrer, *Nano Letters* **11**, 1925 (2011).
[5] "Topological insulator quantum dot with tunable barriers," Sungjae Cho, Dohun Kim, Paul Syers, Nicholas P. Butch, Johnpierre Paglione, and Michael S. Fuhrer, *Nano Letters* **12**, 469 (2012).

Devices with electrically tunable topological insulating phases

Paolo Michetti[1] and Björn Trauzettel[1]

[1] *Institute for Theoretical Physics and Astrophsics,*
University of Würzburg, Am Hubland 97074 Würzburg

Topological insulators (TIs) are time-reversal symmetric phases characterized by a topological Z_2 invariant. The boundary between a normal and a topological insulator is signaled by the appearance of helical edge modes, with spin-momentum locking, where transport is topologically protected against the scattering on non-magnetic disorder. Solid-state topological insulating phases promise, therefore, a powerful route for spin and charge manipulation in electronic devices.

While a possible choice to control transport in the edge modes is through quantum interference, we argue that a most straightforward implementation of a device requires a material with an easily tunable TI phase. We focus on a HgTe/CdTe double quantum well device and show that a topological phase transition can be driven by an inter-layer bias voltage [1], even when the individual layers are non-inverted. This paves the way to the realization of tunable topological mass domains of desired shape using lithographic gates. Helical edge modes located on such domain lines [2] can therefore be easily manipulated.

We then introduce the concept of a topological field-effect-transistor [3], where charge and spin transport in the helical edge modes is controlled by electrically switching the TI phase. We analyze further application to a spin battery [3], which also realizes a set up for an all-electrical investigation of the spin-polarization dynamics in metallic islands.

[1] P. Michetti, J. C. Budich, E. G. Novik and P. Recher, Phys. Rev. B 85 (2012) 125309.
[2] P. Michetti, P. H. Penteado, J.C. Egues and P. Recher, Semicond. Sci. Technol. 27 (2012) 124007.
[3] P. Michetti and B. Trauzettel, Appl. Phys. Lett. 102 (2013) 063503.

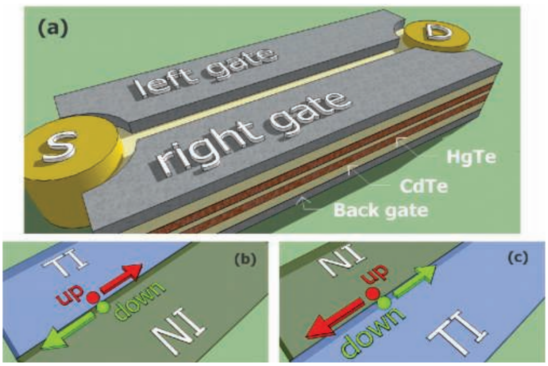

Fig. 1: Isometric sketch of a HgTe/CdTe DQW device with a back gate and two distinct top gates (left and right). In the ON state, top gates induce a gate-bias domain leading to a TI/NI interface (channel) where helical edge modes are found. Source (S) and drain (D) leads, placed along the interface between L and R top gates, collect charges from the edge modes. The lateral surface of the DQW is specifically treated to ensure negligible edge transport. (b) Schematic description of a TI/NI interface for direct gate polarization with indication of the helical spin transport of edge states. (c) Reverse gate polarization leading to opposite spin transport of the channel.

ThOE2

Edge Transport in InAs/GaSb Topological Insulating Phase

Kyoichi Suzuki, Yuichi Harada, Koji Onomitsu, Koji Muraki

NTT Basic Research Laboratories, NTT Corporation

We have investigated transport properties of InAs/GaSb heterostructure system [1,2], for which a topological insulating phase and thus quantum spin Hall effect (QSHE) are predicted. Although complete quantization has not been achieved, non-local resistance measurements provide compelling evidence that, for a sample with appropriate layer thicknesses, the current flow is governed by edge transport.

The samples studied are InAs (top)/GaSb (bottom) heterostructures sandwiched between $Al_{0.7}Ga_{0.3}Sb$ barriers with varying InAs layer thickness (w = 10, 12, and 14 nm). The Hall bars have six Ohmic contacts with a distance of 2 μm and a top gate. When the Fermi level is tuned in the band gap, a resistance maximum is observed for all the samples, with markedly different resistance values [Fig. (a)]. For the w = 10 nm sample, the peak resistance increases with decreasing temperature (T) and reaches several MΩ at 0.25 K, indicating that the system is a fully gapped normal insulator. In the w = 14 nm sample, the low peak resistance of only 2 kΩ and the absence of T dependence indicate a semimetallic band structure. In contrast, in the w = 12 nm sample, the peak resistance saturates at low T at a value quite close to $h/2e^2$, i.e., the quantized value expected for QSHE in the six-terminal geometry used.

Non-local resistance measured for the w = 12 nm sample showed resistance values comparable to $h/6e^2$ for all configurations, as expected for helical edge transport in a six-terminal device [Fig. (b), (c)]. Interestingly, despite the resistance fluctuations and deviations from $h/6e^2$ indicative of inelastic scattering processes, when we focus on the resistance ratio for adjacent contact pairs, in the gap region, the ratio is found to be identical for different current injection/ejection paths [boxed region in Fig. (d)], including the details of the fluctuations (inset). Similar results were confirmed for all combinations of adjacent contact pairs. As is seen in the p- and n-type regions (V_{FG} < 1.27 V and V_{FG} > 1.42 V), when bulk transport is dominant, the resistance ratio reflects the current distribution in the bulk and thus takes different values for different current paths. The observed perfect agreement in the gap region, in turn, clearly demonstrates that the current flows only between adjacent contacts along the sample edge. It is shown that, with our six-terminal non-local measurements, the resistances of all the individual edge channels can be deduced.

[1] Liu *et. al.*, Phys. Rev. Lett. **100**, 236601 (2008).
[2] Knez *et. al.*, Phys. Rev. Lett. **107**, 136603 (2011).

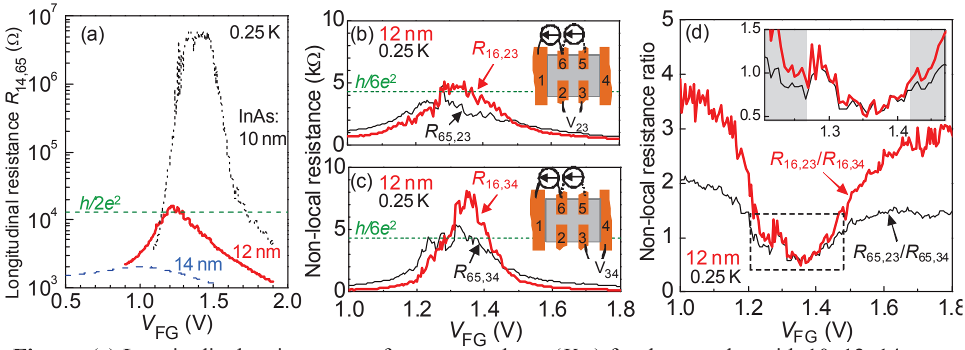

Figure. (a) Longitudinal resistance vs front gate voltage (V_{FG}) for the samples with 10, 12, 14 nm InAs. (b) and (c) Non-local resistances for the sample with 12 nm InAs. (d) Non-local resistance ratios between adjacent contact pairs, measured for different current injection/ejection paths.

Discovery of a 3D topological insulator: samarium hexaboride

Steven Wolgast [1], Yun Suk Eo [1], Çağlıyan Kurdak [1], Kai Sun [1], James W. Allen [1], Dae-Jeong Kim [2] and Zachary Fisk [2]

[1] *Dept. of Physics, University of Michigan, Ann Arbor, MI 48109, USA*
[2] *Dept. of Physics and Astronomy, University of California at Irvine, Irvine, CA 92697, USA*

One of the longest-studied mixed valent insulators, Samarium Hexaboride (SmB_6), exhibits a mysterious residual resistivity at low temperatures (T < 4 K), but at a value too high to explain within the framework of bulk conduction [1]. All efforts over the years to eliminate this resistivity have failed. The recently conjectured existence of a topologically protected surface state in SmB_6 [2] could resolve the long-standing mystery surrounding its low-temperature transport properties.

We developed a novel configuration (Fig. 1) designed to distinguish bulk-dominated conduction from surface-dominated conduction by exaggerating the geometric differences between the two conduction paths through contacts placed on both sides of a thin sample. The results of this experiment (Fig. 2) show that below 3 K, SmB_6 has a fully-insulating bulk and an intrinsic metallic surface with a remarkably high conductivity [3]. We argue that the robustness of the surface conductivity is a signature of the topological protection of the surface states. This discovery resolves the old mystery about the strange transport behavior of this material, and it provides a material in which 2D transport properties of a true topological state can be studied. We will also present some of our results from transport experiments using a Corbino geometry.

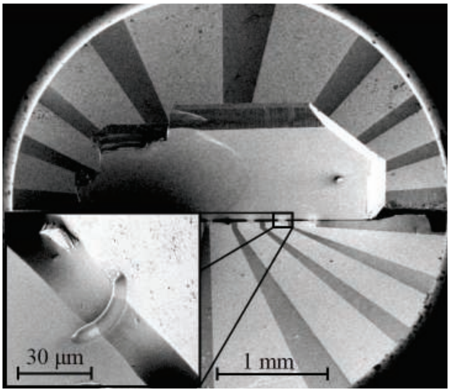

Figure 1 Picture of sample. A thin crystal of SmB_6 is sandwiched between two Si wafer pieces. Several Pt contacts connect both the front and back sides of the sample to Au contact pads on the Si pieces. **Inset** Close-up of a Pt contact.

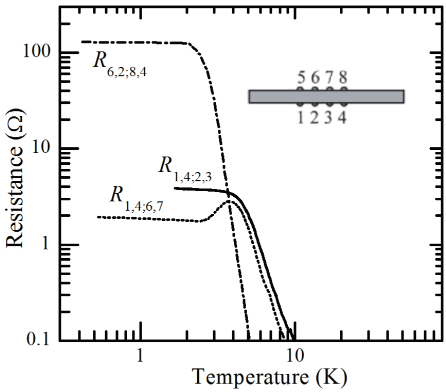

Figure 2 Various 4-terminal resistances plotted against temperature. The data shows a crossover from bulk conduction to surface conduction between 3 – 5 K. In the absence of a crossover, the resistances would differ only by constant scaling factors.

[1] J. W. Allen, B. Batlogg and P. Wachter, Phys. Rev. B **20**, 4807 (1979).
[2] M. Dzero, K. Sun, V. Galitski and P. Coleman, Phys. Rev. Lett. **104**, 106408 (2010).
[3] S. Wolgast, Ç. Kurdak, K. Sun, J. W. Allen, D. J. Kim and Z. Fisk, arXiv:1211.5104v2.

Density Waves Instability and a Skyrmion Lattice on the Surface of Strong Topological Insulators

Yuval Baum and Ady Stern

Department of Condensed Matter Physics, Weizmann Institute of Science, Rehovot 76100, Israel

The gapless surface states of strong topological insulators have drawn a great deal of attention over the past few years. In a previous work [1] it was shown that for a strong enough electron-electron interaction the surface of a strong topological insulator is unstable to the formation of spontaneous uniform magnetization.

In this work [2] we analyzed the instability conditions for spin-density-waves (SDW) formation on the surface of strong topological insulators. We find that for a certain range of energies the SDW instability is favored compared to the uniform one. We also find that the SDW are of spiral nature and for a certain range of parameters a Skyrmion-lattice is formed on the surface. We show that this phase may have a non trivial Chern-number even in the absence of an external magnetic field. Finally, we claim that a network of one-dimensional chiral channels may be established on the surface of a strong topological insulator.

[1] Y. Baum and A. Stern, Phys. Rev. B **85**, 121105(R)(2012).
[2] Y. Baum and A. Stern, Phys. Rev. B **86**, 195116 (2012).

Single photon sources for room temperature operation based on CdSe/ZnSSe/MgS quantum dots

Tilmar Kümmell [1], Wolf Quitsch[1], Oleh Fedorych[1], Arne Gust[2], Carsten Kruse[2], Detlef Hommel[2], Gerd Bacher[1]

[1] *Werkstoffe der Elektrotechnik and CENIDE, Universität Duisburg-Essen, Bismarckstr. 81, 47057 Duisburg, Germany*
[2] *Institut für Festkörperphysik, Universität Bremen, Otto-Hahn-Allee, 28359 Bremen, Germany*

Solid state single photon sources play a central role in quantum information technology. The challenges for a versatile, compact source are twofold: On the one hand, an electrically driven device is highly desirable; on the other hand, operation under ambient conditions up to room temperature is required. This joint goal has been achieved only partially during the recent years: In colloidal quantum dots and in color centers in diamond, high-quality optically driven single photon sources up to room temperature have been implemented, but a straightforward electrical operation remains a difficult task. In contrast, epitaxially grown semiconductor quantum dots based on GaInAs, GaN or GaP, provide excellent electrically driven single photon sources, but have failed to exhibit single photon emission at room temperature.

In this contribution, we show that single photon sources consisting of single, epitaxially grown CdSe/ZnSSe/MgS quantum dots can meet *both* requirements. Wide-bandgap II-VI single quantum dots generally provide a higher carrier confinement than III-V-based structures, and by additional MgS barriers virtually no loss of quantum efficiency can be detected between T = 4 K and T = 300 K [1].

In order to prove room temperature operation, single quantum dots were excited optically using a micro-photo-luminescence setup and lithographically defined metal nanoapertures. Photon correlation measurements were performed using a Hanbury-Brown-Twiss (HBT) setup. Under continuous wave excitation (λ = 457.9 nm), we observe antibunching behavior up to T = 300 K (Fig.1). Second-order correlation measurements exhibit a surprisingly low value of $g^{(2)}(\tau) = 0.16 \pm 0.15$ for zero time delay [2].

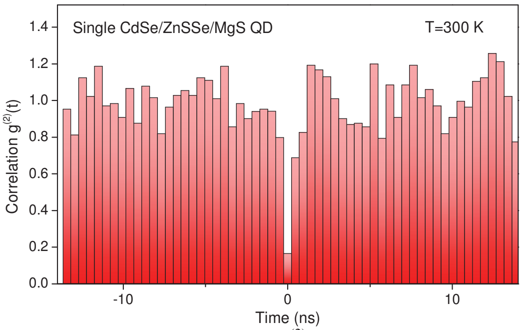

Fig. 1: Autocorrelation function $g^{(2)}(t)$ of CdSe/ZnSSe/MgS SQD emission at 300 K.

For electrically driven devices, these CdSe/ZnSSe/MgS quantum dots were embedded into p-i-n diode structures. Patterned Pd/Au contact layers serve as local current injectors to electrically address only a limited number of quantum dots. Single dot electroluminescence (EL) is collected at a DC voltage of 5.6 V by a Micro-EL setup. For the first time, low temperature photon correlation measurements reveal single photon emission from an electrically driven II-VI-based device. Obviously, the CdSe/ZnSSe/MgS quantum dot devices are ideally suited for future single photon sources that can be electrically driven and operated up to room temperature.

[1] R. Arians el al., Appl. Phys. Lett. 90, 101114 (2007)
[2] O. Fedorych et al., Appl. Phys. Lett. 100, 061114 (2012)

ThOM2

Coherent oscillations of a single Mn^{2+} spin in a CdTe quantum dot

M. Goryca [1], M. Koperski [1], P. Wojnar [2], T. Smoleński [1], T. Kazimierczuk [1], A. Golnik [1] and P. Kossacki [1]

[1] *Institute of Experimental Physics, Faculty of Physics, University of Warsaw, Warsaw, Poland*
[2] *Institute of Physics, Polish Academy of Sciences, Warsaw, Poland*

Semiconductor quantum dot (QDs) containing single magnetic impurity is a new form of diluted magnetic semiconductors which has recently attracted a lot of interest [1,2]. Not only is it a model system for investigation of many spin-related phenomena, but also a promising candidate for the building block of future information storage devices and a tool for quantum computation [3]. Particularly, the possibility to read and manipulate the electronic spin state of the magnetic ion has been shown in the case of CdTe quantum dots with a single isoelectronic Mn^{2+} impurity [4,5]. However, those experiments concerned only non-coherent phenomena, while application in quantum computing requires the ability to coherently manipulate and process the spin. Coherent measurements, including observation of Rabi oscillations and long coherence time, were performed on an ensemble of colloidal ZnO QDs containing many Mn^{2+} dopants [6]. Here we present a direct observation of coherent oscillations of a single Mn^{2+} spin embedded in a CdTe QD placed in magnetic field.

The sample used in the experiment contains a single layer of self-assembled CdTe/ZnTe QDs. The dots contain a low amount of Mn^{2+} ions, so that selection of single dots with exactly one magnetic ion is possible. In order to probe the spin state of the single Mn^{2+} impurity we performed a time-resolved measurement of the absorption of a QD containing such an ion. The QD was resonantly excited with two circularly polarized picosecond laser pulses. The energy of the photons was tuned to the transition energy of an exciton-Mn^{2+} complex with arbitrary chosen spin state of the magnetic ion. The absorption was detected by using the excitation transfer to a neighboring QD [5,7] and observation of the emission from this dot. The presence of a second, coupled QD not only enabled the detection of the absorption, it also assured a very short exciton lifetime in the absorbing QD, crucial for the temporal resolution of the experiment. The delay between the two pulses was precisely controlled so that the second pulse could probe the evolution of the investigated system after the first pulse.

The system under investigation was placed in a magnetic field applied in the Voigt configuration, parallel to the surface of the sample. Under such conditions the eigenstates of the Mn^{2+} ion depend on whether the exciton is present in the QD. Upon absorption of the first laser pulse the exciton-Mn^{2+} complex is created in a specific spin state, defined by the photon energy. However, when the exciton tunnels to the neighboring QD, the Mn^{2+} ion is no longer in the eigenstate due to the presence of magnetic field. Therefore the spin state of the magnetic impurity starts to oscillate and the probability of the absorption of the second pulse (of the same energy as the first one) depends on the delay between pulses. By observing the luminescence intensity of the neighboring QD we are able to reproduce those oscillations. We can also determine the dephasing time (T_2^*) of the Mn^{2+} ion, limited mainly by the hyperfine interaction and the crystal field originating from the strain of the QD material.

[1] L. Besombes et al., Phys. Rev. Lett. **93**, 207403 (2004).
[2] J. Fernandez-Rossier, Phys. Rev. B **73**, 045301 (2006).
[3] D. Loss et al., Phys. Rev. A **57**, 120–126 (1998).
[4] C. Le Gall et al, Phys. Rev. Lett. **102**, 127402 (2009).
[5] M. Goryca et al, Phys. Rev. Lett. **103**, 087401 (2009).
[6] S. T. Ochsenbein et al., Nature Nanotechnology **6**, 112 (2011).
[7] T. Kazimierczuk et al., Phys. Rev. B **79**, 153301 (2009).

On-chip time resolved detection of quantum dot emission using integrated superconducting single photon detectors

G. Reithmaier[1], S. Lichtmannecker[1], T. Reichert[1], P. Hasch[1], M. Bichler[1], R. Gross[2] and J. J. Finley[1]

[1]*Walter Schottky Institut, Technische Universität München, 85748 Garching, Germany*
[2]*Walther-Meißner-Institut, Technische Universität München, 85748 Garching, Germany*

Photonic information technologies using semiconductors are ubiquitous and are rapidly being pushed to the quantum limit where non-classical states of light can be generated and manipulated in nanoscale optical circuits [1]. Single photons can be generated on-chip and preferentially routed into waveguides by tailoring the local density of photonic modes experienced by the emitter [2]. Furthermore, effective interactions between photons can be induced by exploiting coherent light-matter couplings [3]. The ability to generate and detect single photons on-chip with near unity quantum efficiency and integrate sources and detectors with nanophotonic hardware would represent a major step towards the realization of semiconductor based quantum optical circuits. Superconducting nanowire single photon detectors (SNSPDs) provide high single photon detection efficiencies, low dark count rates, sensitivity from the visible to the infrared and ps timing resolution [4]. The possibility to integrate SNSPDs onto waveguides results in a drastic increase of the absorption length for incoming photons [5], pushing the single-photon detection efficiency towards unity. In this contribution we demonstrate the on-chip generation of light originating from optically pumped micro-ensembles of self-assembled InGaAs QDs, low loss guiding over ~ 0.5 mm along a GaAs-AlGaAs ridge waveguide and high efficiency detection via evanescent coupling to an integrated NbN SNSPD [6]. Fig 1a shows a schematic representation of a typical sample showing the QD loaded waveguide and integrated NbN SNSPD. A typical spatial dependence of the detector count rate as then excitation laser is scanned over the sample is presented in fig 1b for excitation above (λ_{exc} = 632.8 nm, main panel) and below (λ_{exc} = 940 nm, insets) the GaAs bandgap. By comparing measurements performed with optical excitation above and below the GaAs bandgap and exploring the temporal response of the system (fig 1c), we show that the detector signal stems from QD luminescence with a negligible background from the excitation laser. Power dependent measurements confirm the single photon sensitivity of the detectors and show that the SNSPD is two orders of magnitude more sensitive to waveguide photons than when illuminated in normal incidence [7]. The performance metrics of the SNSPD integrated directly onto GaAs nano – photonic hardware confirms the strong potential for on-chip few-photon quantum optical experiments on a semiconductor platform.

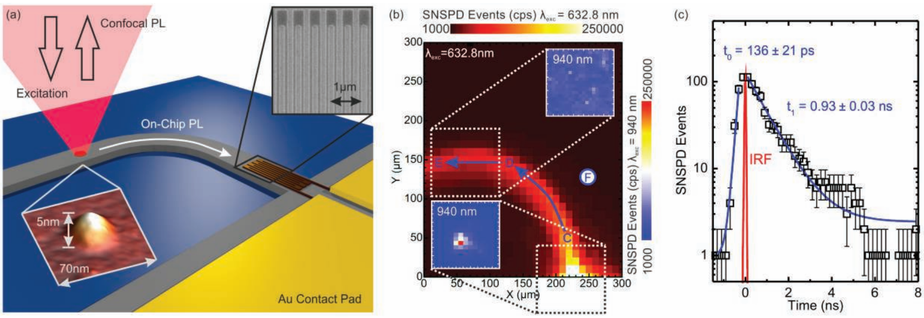

Figure 1 (a) Schematic of samples studied-QD loaded GaAs waveguide with integrated NbN SNSPD. (b) Spatial dependence of detector count rate when scanning the laser spot on sample with above and below gap excitation. (c) In-situ detected time resolved signal confirming the origin of the detector signal as arising from QD emission measured with a fast timing resolution of 72 ps.

[1] J. C. F. Matthews et. al., Nature Phot. **3**, 346 (2009)
[2] A. Laucht et al., Phys. Rev. X **2**, 011014 (2012)
[3] A. Reinhard et al., Nature Phot. **6**, 93 (2011)
[4] C. Natarajan et al., Sup. Sci. and Tech. **25**, 063001 (2012)
[5] W.Pernice et al., Nature Comm. **3**, 1325 (2012)
[6] G. Reithmaier et al., ArXiv:1212.2038 (2012)
[7] G. Reithmaier et al., ArXiv:1302.3807 (2013)

Monday Tuesday Wednesday Thursday Friday

ThOM4

Entanglement Between a Dark Exciton and a Single Photon

I. Schwartz [1], L. Gantz [1], E. R. Schmidgall[1], E. Bordo[1], D. Cogan[1], Y. Kodriano[1], E. Poem[1], and D. Gershoni [1]

[1] *Physics Department and The Solid State Institute, Technion, Haifa, 3200 Israel*

The building block for quantum information processing is a reliable two-level system - a 'qubit.' A candidate qubit must have a long lifetime and a long coherence time, in which its quantum state is not randomized by stochastic interactions with its environment. In addition, for networking, it is required to efficiently generate entanglement between stationary matter qubits such as spins in matter and propagating qubits such as photons[1-2]. Previously [3], we demonstrated that the spin of quantum dot-(QD) confined dark excitons (DE) has great potential as a matter qubit. The DE, which is formed from an electron-heavy-hole pair with parallel spins is optically inactive. Therefore, its lifetime is very long, 3-4 orders of magnitude longer than that of the optically-active bright exciton (BE). The DE is neutral, thus, unlike charge-carriers it is protected from dephasing by electrostatic fluctuations in its vicinity. In addition, the short range electron-hole exchange interaction removes the degeneracy between its two eigenstates even in the absence of an external magnetic field. Thus, the DE spin is protected also from dephasing induced by local fluctuations in the nuclear magnetic field. This is markedly different than charge-carrier spins, which are Kramers' degenerate.

Here we report on the first observation of quantum entanglement between the DE spin and the polarization of a propagating optical photon. Our demonstration of entanglement relies on the use of polarization sensitive single-photon detection, which allows us to project the photon into a superposition of two cross circular polarization states. The detection is temporally correlated with the detection of a polarized biexciton photon which heralds the generation of the DE in a well-defined coherent superposition of its two non-degenerate eigenstates. The DE spin then coherently precesses in time [3] in a relatively slow rate of ~3 nsec per period [3], since the short range exchange interaction amounts to 1.5 μeV only [3].

The scheme that we implement can generate nearly deterministic entangled DE spin–photon pairs at a rate determined by the high spontaneous recombination rate of the allowed transition from the biexciton state to the DE. The method provides a direct way for measuring the DE dephasing rate. Using pulsed, rather than cw excitation (Fig. 1), we straightforwardly obtained a lower limit of ~100nsec, for the coherence time of the DE.

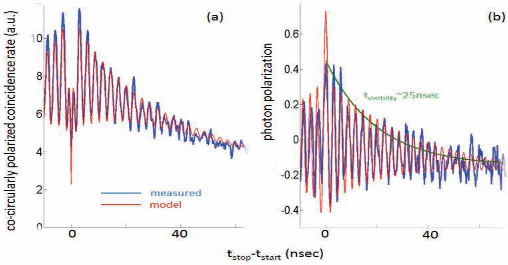

Fig. 1 a) Measured (blue) and calculated time resolved co circularly polarized autocorrelations of the biexciton spectral line which heralds the dark exciton, under resonant co-circularly polarized cw biexciton excitation. (b) Polarization degree of the emitted photon as a function of time after the DE is heralded. The polarization periodicity of ~3 nsec, demonstrates the entanglement between the emitted biexciton photon and the precessing spin of the DE in the QD. The polarization degree was obtained by subtracting from the measured signal in a) a similar measurement but for cross-circularly polarized photons. The degree of polarization is defined as $P=(I_{co}-I_{cross}) / (I_{co}+I_{cross})$ where I_{co} (I_{cross}) is the coincidence rate for co (cross) circularly polarized photons.

[1] W. B. Gao, et al., Nature, **491**, 426, (2012)
[2] K. De Greve et al., Nature **491**, 421 (2013)
[3] E.Poem, et al., Nature Physics **6**, 993-997, (2010

High-fidelity Spin-Photon Entanglement Generation using Self-Assembled InAs Quantum Dots

Peter L. McMahon[1,*], Kristiaan De Greve[1,2,*], Leo Yu[1], Jason Pelc[1], Cody Jones[1], Chandra M. Natarajan[1], Na Young Kim[1], Eisuke Abe[1], Sebastian Maier[3], Christian Schneider[3], Martin Kamp[3], Sven Hoefling[3], Robert Hadfield[4], Alfred Forchel[3], M.M. Fejer[1] and Yoshihisa Yamamoto[1,5]

[1] *Stanford University, USA*
[2] *Current affiliation: Harvard University, USA*
[3] *Universitaet Wuerzburg, Germany*
[4] *Heriot-Watt University, Scotland*
[5] *National Institute of Informatics, Japan*

[*] *Equal contribution.*

Self-assembled InAs quantum dots can trap a single electron, and this electron's spin states can be used to encode a quantum bit (qubit). The qubit can be optically initialized, controlled and measured. Measurements of the coherence time of such a qubit have shown that the time required to perform an arbitrary single operation (~50 ps) on the qubit is roughly five orders of magnitude smaller than the T_2 time (~3 μs) [1]. This partially makes electron spins in quantum dots appealing candidates as quantum memories.

Long-distance quantum cryptography will likely require the development of quantum repeaters. Charged quantum dots are an excellent candidate technology for building quantum repeaters, because they provide both a good stationary qubit (to be used as a memory), and a fast optical interface. One of the very first steps towards building a quantum repeater using quantum dots is to show that one can generate a photonic qubit that is entangled with a spin (memory) qubit.

In this talk, I will describe our recent demonstration of such entanglement. In particular, we generated and verified entanglement between the polarization state of a photon emitted by a single quantum dot, and the spin state of the electron in that quantum dot [2]. Atac Imamoglu's group at ETHZ concurrently demonstrated, in the same system, entanglement between the frequency of an emitted photon and the quantum dot electron's spin [3]. We have subsequently performed full-state tomography on our spin-photon qubit pair, and have measured a state fidelity in excess of 90% [4]. This measured fidelity rivals that of nearly all previous spin-photon entanglement results, including those from atomic physics groups, whose fidelities are often considered unachievable in solid-state systems.

[1] D. Press, *et al*., Nature Photonics **4**, 367 (2010).
[2] K. De Greve, L. Yu*, P.L. McMahon*, J. Pelc*, *et al*., Nature **491**, 421 (2012).
[3] W. Gao, *et al*., Nature **491**, 426 (2012).
[4] K. De Greve*, P.L. McMahon*, *et al*., accepted for publication.

INVITED

Fractional quantum Hall physics in graphene

Jurgen H. Smet

Max-Planck-Institut für Festköperforschung, Heisenbergstr. 1, D-70569 Stuttgart, Germany

Due to progress in graphene sample quality, rich interaction physics related to the fractional quantum Hall effect as well as the lifting of symmetries associated with the spin and pseudospin degrees of freedom of graphene's Fermi Dirac electrons starts to be disclosed. A key requirement to observe this fragile physics has so far been the fabrication of better quality samples. This has been accomplished by placing graphene on a flatter substrate, which is less prone to attract adsorbates, such as BN, or by suspending and in-situ current-annealing graphene. In the quest for observing even more fragile or novel incompressible states, probing a smaller area may circumvent the challenges of producing ever higher mobility samples, since the sample may be much cleaner on the nanometer scale. Here, we report two different approaches to locally access incompressible ground states:

Transport measurements normally provide a macroscopic, averaged view of the sample so that disorder prevents the observation of interaction-induced states. We demonstrate that transconductance fluctuations in a graphene field effect transistor reflect charge localization phenomena on the nanometer scale due to the formation of a dot network near incompressible quantum states. These fluctuations unveil higher order fractional quantum Hall states, although these states have remained hidden so far in conventional magnetotransport quantities.

Using a scanning single electron transistor to locally probe the compressibility is even more powerful, especially when combining the best of all worlds and performing such studies on a suspended and in-situ current annealed graphene flake. These experiments reveal for instance fractional quantum Hall states with unprecedented denominators for graphene. The observed sequence of fractional quantum Hall states partially deviates from the standard composite fermion sequence. Also phase transitions within fractional quantum Hall states abound.

The above experiments were carried out together with B. Feldman, A. Levin, D. Abanin, B. Halperin, A. Yacoby (Harvard University), D.-S. Lee, V. Skakalova, R.T. Weitz and K. von Klitzing (Max Planck Institute for Solid State Research).

Giant photoresistance and a new class of microwave-induced resistance oscillations in GaAs/AlGaAs quantum wells

Michael A. Zudov[1], **Peter D. Martin**[1], **Anthony T. Hatke**[1], **John D. Watson**[2,3], **Michael J. Manfra**[2,3], **Loren N. Pfeiffer**[4], **and Kenneth W. West**[4]

[1] *School of Physics and Astronomy, Univ. of Minnesota, Minneapolis, MN 55455, USA*
[2] *Department of Physics, Purdue Univ., West Lafayette, IN 47907, USA*
[3] *Birck Nanotechnology Center, School of Materials Engineering and School of Electrical and Computer Engineering, Purdue Univ., West Lafayette, IN 47907, USA*
[4] *Department of Electrical Engineering, Princeton Univ., Princeton, NJ 08544, USA*

We report on experimental study of microwave photoresistance in high-mobility two-dimensional electron systems in quantizing magnetic fields. As shown in Fig. 1(a), in addition to microwave-induced resistance oscillations [1], which persist to 20-th order, we observe a giant photoresistance effect which manifests itself as a series of narrow peaks [marked by ↓], occurring near the cyclotron resonance (cf. vertical line marked by 1). Some of these peaks are extremely strong, exceeding MIRO amplitude by more than an order of magnitude, and their relative strength depends on the sweeping direction of the magnetic field. Using lower radiation intensity allows to extend the measurements to considerably lower temperatures, a regime of strong Shubnikov-de Haas oscillations (SdHO). In contrast to higher-intensity, higher-temperature data shown in Fig. 1(a), giant photoresistance peaks are no longer observed [see Fig. 1(b)]. Instead, the data reveal strong suppression of the SdHO near the cyclotron resonance, and to a lesser extent, near its harmonics. Another interesting feature of the data in Fig. 1(b) is what at first glance appears as noise near the cyclotron resonance. However, this fine structure turned out to be highly reproducible and its strength was found to depend sensitively on microwave power. A closer look at this structure, presented in Fig. 1(c), reveals that it is a series of extrema, which are more pronounced near the SdHO maxima and are roughly equally spaced in magnetic field. In fact, there exist two series of radiation-induced minima; a series of "deep" minima, marked by vertical lines (separated by $\delta B = 0.26$ kG) and a series of "shallow" minima, marked by ↓, which appear roughly in the middle between the neighboring "deep" minima. Understanding the origin of these peculiar findings remains a subject of future experimental and theoretical studies.

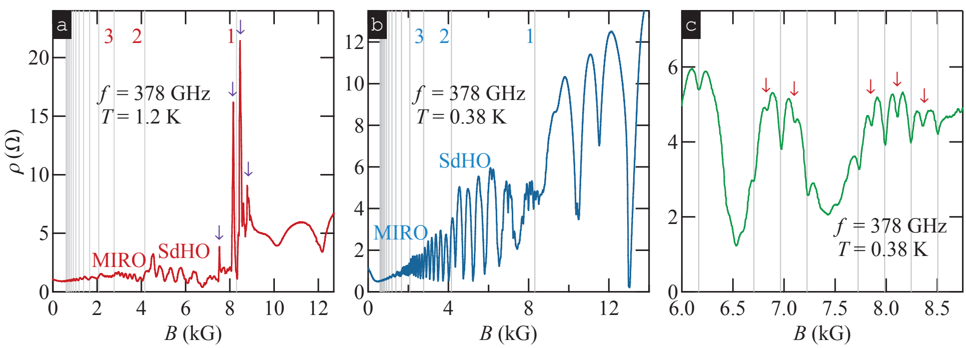

Figure 1: Magnetoresistivity $\rho(B)$ under microwave irradiation of frequency $f = 378$ GHz at (a) higher intensity and $T = 1.2$ K and (b,c) lower intensity and $T = 0.38$ K.

[1] M. A. Zudov, R. R. Du, J. A. Simmons, J. L. Reno, Phys. Rev. B **64**, 201311(R) (2001).

Magnetotransport along a boundary: From coherent electron focusing to edge channel transport

Thomas Stegmann, Dietrich E. Wolf, and Axel Lorke

Department of Physics, University of Duisburg-Essen and CENIDE, 47048 Duisburg, Germany

We study theoretically how electrons, coherently injected at one point on the boundary of a two-dimensional electron system, are focused by a perpendicular magnetic field B onto another point on the boundary, see the inset of Fig. 1. Using the non-equilibrium Green's function approach, we calculate the generalized 4-point Hall resistance $R_{xy} = (U_{P_1} - U_{P_2})/I_{SD}$ as a function of B.

In weak fields, R_{xy} (solid curve in Fig. 1) shows the characteristic equidistant peaks, which are observed in the experiment and which can be explained by classical cyclotron orbits specularly reflected at the boundary. These classical trajectories can be clearly seen in the local current and the local DOS of the injected electrons (Fig. 2a). In strong fields, the Hall resistance shows a single extended plateau $R_{xy} = h/2e^2$ reflecting the quantum Hall effect. The current is carried by a single edge channel straight along the boundary (Fig. 2c).

In intermediate fields, instead of lower Hall plateaus as in the case of a diffusive boundary (dashed curve in Fig. 1), we find [1] *anomalous oscillations*, which are neither periodic in $1/B$ (quantum Hall effect) nor periodic in B (classical cyclotron motion). These oscillations can be explained by the interference of the occupied edge channels causing beatings in R_{xy}. The Fig. 2b shows this interference between two occupied edge channels, which resembles also to some extent a cyclotron motion. Moreover, in this regime of two occupied edge channels, the beatings constitute a new commensurability between the magnetic flux enclosed within the edge channels and the flux quantum h/e. Introducing decoherence and a partially diffusive boundary shows that this new effect is quite robust.

[1] T. Stegmann, D. E. Wolf, A. Lorke, submitted to Phys. Rev. B, arXiv:1302.6178

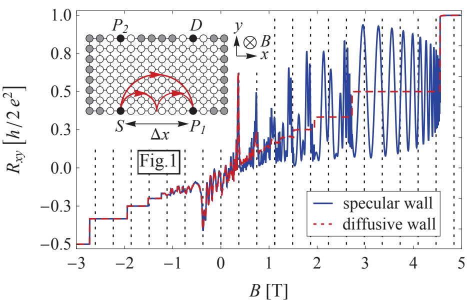

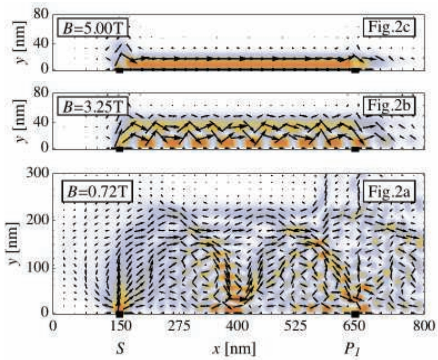

Observation of quantum and classical correlation regimes in cold dipolar exciton fluids

Yehiel Shilo, Kobi Cohen, Ronen Rapaport
The Racah Institute of Physics and the department of Applied physics, The Hebrew University of Jerusalem, Israel
Snežana Lazić, Adriano Violante, Rudolph Hey, Paulo V. Santos
Paul-Drude-Institut für Festkörperelektronik, Berlin, Germany
Ken West, Loren Pfeiffer
Electrical Engineering Department, Princeton University, Princeton, USA

Cold two-dimensional dipolar fluids are predicted to display a very rich phase diagram and intricate interaction induced particle correlations in both the classical and quantum regimes, far beyond the well studied weakly interacting quantum gases [1,2]. Therefore they are currently a major thrust in modern cold atoms and molecules research [1,3].

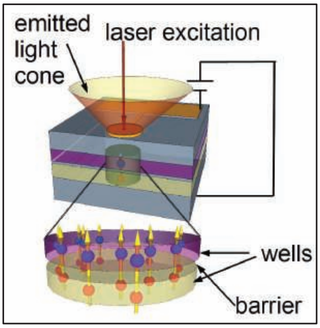

A dipolar exciton fluid in a semiconductor bilayer is a good system to study such physics directly [4-6]. Furthermore, these fluids can be transported, controlled, and manipulated over macroscopic distances via their interactions with externally applied potentials, a property that can be utilized for new types of coherent exciton based circuitry [10].

We will present experimental evidence for several many-body correlation regimes of a cold dipolar exciton fluid, created optically in a gated semiconductor bilayer trap. As the fluid temperature is lowered, the average interaction energy between the particles shows first a strong, temperature dependent reduction, which is an evidence for the onset of correlations *beyond the mean field model*. At lower temperatures, there is a clear transition to a temperature independent regime. We interpret this behavior as a transition from a classical to a quantum correlated dipolar fluid. At an even lower temperature, there is a sharp increase in the interaction energy of optically active excitons, accompanied by a strong reduction in their apparent population. This could be an evidence for a sharp macroscopic redistribution with the dark spin states [7] as was suggested theoretically [8]. We will also show experiments where the long-range character of the collective dipole of the exciton fluid is manifested by engineering and observing *remote* dipolar interactions between spatially separated fluids [9].

[1] Lahaye et al., Reports on Progress in Physics 72, 126401 (2009).
[2] Laikhtman, Rapaport, Phys. Rev. B 80, 195313 (2009).
[3] Pupillo et al., Phys. Rev. Lett. 104, 223002 (2010).
[4] Snoke, Science 298, 1368 (2002).
[5] Eisenstein, MacDonald, Nature 432, 691–694 (2004).
[6] High et al., Nature 483, 584–588 (2012).
[7] Shilo et al., Submitted (2012).
[8] Combescot, Betbeder-Matibet, Combescot, Phys. Rev. Lett. 99, 176403 (2007).
[9] Cohen, Rapaport, Santos, Phys. Rev. Lett. 106, 126402 (2011).
[10] Lazic et al., Submitted (2013)

Quantum Hall Effect in Graphene with Superconducting Electrodes

P. Rickhaus, M. Weiss, L. Marot, and C. Schönenberger

Department of Physics, University of Basel, Switzerland

We have realized an integer quantum Hall system with superconducting contacts by connecting graphene to niobium electrodes[1]. Below their upper critical field of 4 tesla, an integer quantum Hall effect coexists with superconductivity in the leads, but with a plateau conductance that is larger than in the normal state. We ascribe this enhanced quantum Hall plateau conductance to Andreev processes at the graphene-superconductor interface leading to the formation of so-called Andreev edge-states. The enhancement depends strongly on the filling-factor, and is less pronounced on the first plateau, due to the special nature of the zero energy Landau level in monolayer graphene.

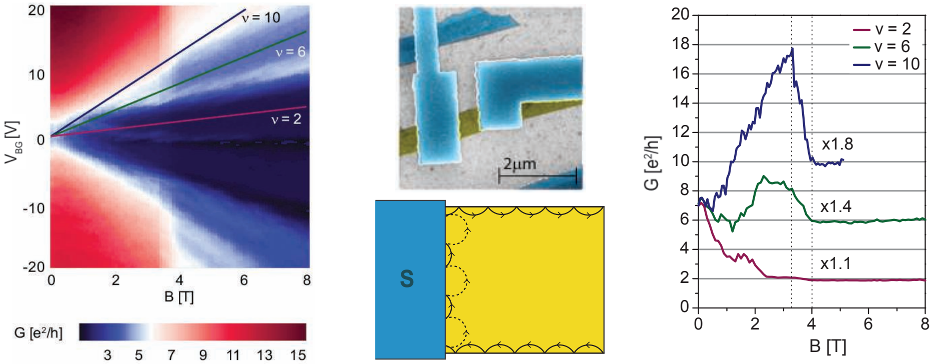

left: Conductance G as a function of magnetic field and gate voltage. middle: SEM picture of a typical device (top), quasiclassical illustration of chiral edge states along the sample border and an Andreev edge state along the N-S interface (bottom). right: conductance as a function of B for fixed filling factors ν=2,6, and 10.

[1] P. Rickhaus, M. Weiss, L. Marot, and C. Schönenberger, NanoLetters 12, 1942 (2012)

Spin-orbit anisotropy and relaxation of GaAs single electron spin qubits

P. Scarlino[1], E. Kawakami[1], M. Shafiei[1], L.M.K. Vandersypen[1], W. Wegscheider[2]

[1]Kavli Institute of Nanoscience, TU Delft, Lorentzweg 1, 2628 CJ Delft, The Netherlands

[2]Solid State Physics Laboratory, ETH Zurich, Schafmattstrasse 16, 8093 Zurich, Switzerland

In lateral quantum dots hosted in a semiconducture structure with lack of inversion symmetry the effect of Rashba (R) and Dresselhaus (D) spin-orbit (SO) interactions causes relaxation of the spin excited state, splitted in energy from the ground state due to the presence of an in plane static magnetic field. Considered together with a generic electric field fluctuation, that can come from external electrical noise or from phonons, the SO mediated spin mixture opens a spin decay channel [1]. The interplay of R and D spin-orbit coupling can result in a decay time with a striking anisotropy in the plane of the quantum well.

The study of the anisotropy in QDs has been realized looking at the hybridization between the ground and excited states with opposite spins [2]. When two different orbital states with opposite spin are tuned to a degeneracy the SO interaction causes an avoided crossing in the energy spectrum whose magnitude is twice the SO energy. This kind of experiment can be realized in quantum dots built in narrow gap semiconductors, where the SOI and the g-factor are quite high (hundreds of ueV). For GaAs-Qs, unfortunately, the SO energy will by barely visible from the anticrossing (being 10-20 ueV) and in the single electron regime, the magnetic field required to reach the hybridization region can be quite high due to its small g factor. A different approach to investigate the SO-anisotropy for single spin qubit in GaAs consists of measuring the spin excited state relaxation process as a function of the in-plane magnetic field orientation.

An experimental observation of such anisotropy in the relaxation time would be an unquestionable signature of the SO induced spin relaxation and could be used to extract information about the ratio R and D contibutions.

We measured the relaxation time (T1) for a single electron spin in a GaAs quantum dot with an all-electrical single shot readout technique [3] and found a clear 180 degree periodicity due to the interplay of R and D, as predicted by theory (see figure). Different from the theory for dots which are symmetrical in the plane, we find that the maxima in the T1 are not at a 45 degree angle respect to the [100] crystallografic direction. We speculate that this is related to the ellipticity and orientation of the single dot electrostatic confinement potential [4]. For the “magic” angle, the magnitude of the spin-orbit interaction is considerably quenched, allowing us to record an increase in T1 by one order of magnitude, reaching about 70 ms at 3 Tesla.

[1] PRL 93, 016601 (2004) ; **[2]** PRL 104, 246801 (2010), PRL 108, 166801 (2012) ;

[3] *Nature* 430, 431-435 (2004) ; **[4]** PRB 83, 245324 (2011) ;

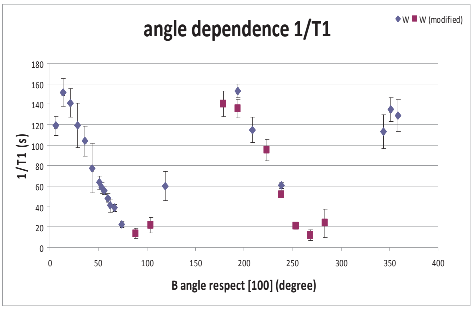

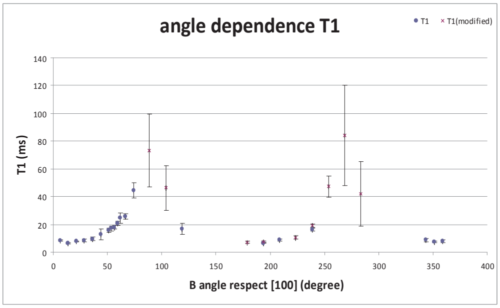

ThOM6

Extra-long Hole Spin Relaxation Time in InGaAs/GaAs Quantum Wells Probed By Cyclotron Resonance Spectroscopy

O. Drachenko[1], D. Kozlov [2], A. Ikonnikov[2], K. Spirin[2], V. Gavrilenko[2], H. Schneider[1], M. Helm[1], and J. Wosnitza[3]

[1] *Institute of Ion-Beam Physics and Materials Research, HZDR, D-01314 Dresden, Germany*
[2] *Institute for Physics of Microstructures, RAS, 603950 Nizhny Novgorod, Russia*
[3] *Dresden High Magnetic Field Laboratory, HZDR, D-01314 Dresden, Germany*

Strained InGaAs/GaAs heterostructures exhibit continuously growing attention, stimulated by the demonstration of efficient spin injection, circular-polarized electroluminescence in InGaAs/GaAs Schottky diodes, as well as the discovery of the anomalous Hall effect in Mn δ-doped InGaAs/GaAs quantum wells [1-3]. For spintronic applications a particularly crucial parameter is the carrier spin relaxation time, which desirably should be as long as possible. In the present work, we show the existence of an extralong, ms range, spin relaxation time of holes in strained InGaAs/GaAs quantum wells, using high-field cyclotron resonance (CR) spectroscopy.

The sample we have studied consists of fifty 7 nm wide $In_{0.14}Ga_{0.86}As$ quantum wells separated by 50 nm wide barriers, δ-doped with carbon. More detailed information about the sample can be found in our previous studies [4-5]. In our experiments, we have used two types of magnetic field coils: one delivers around 50 T with 12 ms rise-time (~100 ms total pulse duration), and another is able to produce 70 T with 35 ms rise-time (~150 ms total pulse duration). The details of our cyclotron resonance setup are given in Ref. 6. We found a strong hysteresis in the spectral weights of cyclotron resonance absorption when a rapidly changing magnetic field is used for the experiment (first magnetic-field coil type), while the hysteresis vanishes when a much slower changing magnetic field is used (second magnetic-field coil type). We argue that this behavior is caused by a long energy relaxation time between two lowest spin-split hole Landau levels, which is comparable with the magnetic field rise-time (~10ms). This implies a long hole spin relaxation time.

[1] Y. Ohno et al. Nature, London, **402**, 790 (1999).
[2] N. V. Baidus et al. Appl. Phys. Lett. **89**, 181118 (2006).
[3] B. A. Aronzon et al. JETP Lett. 85, **27** (2007).
[4] O. Drachenko et al., Phys. Rev. B, **79**, 073301 (2009).
[5] A. V. Ikonnikov et al., Semiconductors **44**, 1492 (2010).
[6] O. Drachenko et al., Rev. Sci. Instrum. **82**, 033108 (2011).

Controlling of the geometric phase of electron spin in a semiconductor ring device

F. Nagasawa[1], D. Frustaglia[2], H. Saarikoski[3], M. Kohda[1,4], K. Richter[3], and J. Nitta[1]

[1] Graduate School of Engineering, Tohoku University, Sendai 980-8579, Japan
[2] Departamento de Física Aplicada II, Universidad de Sevilla, E-41012 Sevilla, Spain
[3] Institut für Theoretische Physik, Universität Regensburg, 93040 Regensburg, Germany
[4] *PRESTO,* Japan Science and Technology Agency, Saitama 331-0012, Japan

Geometrical phases arise in time-dependent wave systems where the parameters of the wave function are cycled around a circuit. Such phase factors can be observed via interference of waves traversing different paths. Berry showed that the electron spin wave function in an adiabatic evolution acquires a geometric phase that depends only on the geometry of the traversed path in the parameter space. As a consequence the geometric phase is robust against dephasing. This is in contrast with the time-dependent dynamical phase of a particle. Experimentally, geometrical phase factors have been observed in various physical systems and previously reported for InGaAs rings [1]. However, a geometric phase of an electron spin wave function has not been directly observed and manipulated independently from the dynamical phase. Here we report measurement and manipulation of the geometric phase of an electron spin in a mesoscopic semiconductor device in which an array of rings forms interference paths. The observed geometrical phase is a non-adiabatic Aharonov-Anandan phase due to the Aharonov-Casher effect. A geometrical phase shift is induced with an in-plane magnetic field and measured in the interference pattern of the electron current. The measured oscillations in the conductance are consistent with theoretical calculations using the perturbation theory and the Recursive Green's Function method (see Figure). In the first order perturbation theory the phase shift is quadratic in magnetic field, which is in good agreement with experiments. Our findings show manipulation of the geometric phase independently of the dynamical phase without resorting to additional geometric phase factors such as the Aharonov-Bohm phase.

[1] F. Nagasawa, J. Takagi, Y. Kunihashi, M. Kohda, and J. Nitta, Phys. Rev. Lett. **108**, 086801 (2012)

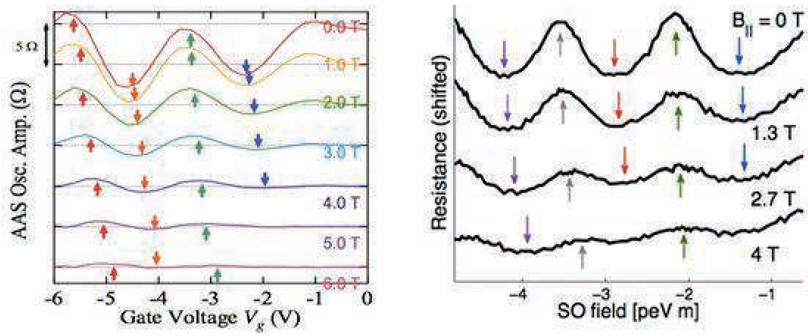

Figure : Interference of geometric phases causes oscillations in conductance through a semiconductor ring device. The oscillation period decreases with increasing in-plane magnetic field which is a sign of the geometric phase shift. Experiments to the left and Recursive Green's function calculations to the right.

Electric control of spin lifetimes in GaAs(111) quantum wells

A. Hernández-Mínguez, K. Biermann, R. Hey and P. V. Santos

Paul-Drude-Institut für Festkörperelektronik, Hausvogteiplatz 5-7, 10117 Berlin, Germany

Dyakonov-Perel, Elliot-Yafet and Bir-Aronov-Pikus spin dephasing mechanisms are the main processes limiting electron spin lifetimes in III-V semiconductors. In GaAs quantum wells (QWs), the most relevant one is Dyakonov-Perel (DP): spin-orbit-interaction (SOI) induces an effective magnetic field, $\mathbf{B}_{\mathrm{SOI}}$, whose magnitude and orientation depend on the in-plane electronic wave vector, $\mathbf{k}$. Polarized spins moving with different $\mathbf{k}$'s will precess with different Larmor frequency vectors, losing the initial spin polarization of the ensemble within a few nanoseconds.

In high quality GaAs QWs, $\mathbf{B}_{\mathrm{SOI}}$ is dominated by two terms: $\mathbf{B}_{\mathrm{BIA}}$, due to the intrinsic bulk inversion asymmetry of the III-V lattice, and $\mathbf{B}_{\mathrm{SIA}}$ or Rashba term, related to a structural inversion asymmetry induced, for instance, by an electric field applied perpendicular to the QW plane, E_z. GaAs(111) QWs are specially interesting because both $\mathbf{B}_{\mathrm{BIA}}$ and $\mathbf{B}_{\mathrm{SIA}}$ are, to first order on k, always parallel to each other. As a consequence, an electric field, E_c, fulfilling the condition $\mathbf{B}_{\mathrm{BIA}} + \mathbf{B}_{\mathrm{SIA}} = 0$, will efficiently suppress spin dephasing mechanisms associated with the SOI, leading to very long spin lifetimes [1].

The high value usually required for E_c, however, is the main obstacle to reach the BIA/SIA compensation. The field reduces the spatial overlap of the electron and hole wave functions, diminishing considerably the radiative recombination rate and, consequently, the yield of the polarization-resolved photoluminescence (PL) technique normally used for probing the spin dynamics.

In this contribution, we overcome this limitation by probing spins via a PL technique combining pulsed illumination and pulsed electric fields, enabling measurement of spin lifetimes in GaAs(111) QWs embedded in n-i-p diode structures over a wide range of electric fields across E_c. We show that the lifetime of optically injected, z-oriented spins initially increases with E_z, reaches a maximum, and then reduces for higher fields (cf. Fig. 1). This maximum is attributed to the transition between a BIA-dominated regime to another determined by the electrically induced SIA term: its observation provides a conclusive evidence of the SOI compensation mechanism. The long spin lifetimes around E_c, exceeding 100 ns [2], are among the highest reported for GaAs structures, making GaAs(111) QWs excellent candidates for spin-based quantum information processing.

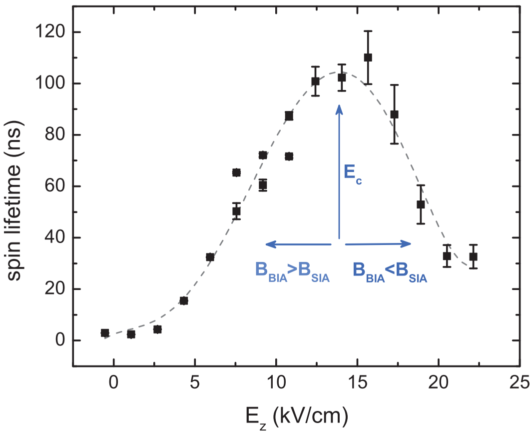

Fig. 1. Spin lifetime dependence on the electric field applied vertically to the quantum well plane.

[1] X. Cartoixà *et al.*, Phys. Rev. B. **71**, 045313 (2005).
[2] A. Hernández-Mínguez *et al.*, Phys. Rev. Lett. **109**, 266602 (2012).

INVITED

Anti-damping intrinsic spin-orbit torque in GaMnAs arising from Berry phase

Jairo Sinova [1,2], Tomas Jungwirth [2,3] and Andrew F. Ferguson [4]

[1] *Department of Physics and Astronomy, Texas A&M University, College Station, Texas 77843-4242*
[2] *Institute of Physics ASCR, v.v.i., Cukrovarnická 10, 162 53 Praha 6, Czech Republic*
[3] *School of Physics and Astronomy, University of Nottingham, Nottingham NG7 2RD, United Kingdom*
[4] *Hitachi Cambridge Laboratory, Cambridge CB3 0HE, United Kindgom*

Recent observations of in-plane-current induced magnetization switching at ferromagnet/normal-conductor interfaces have important consequences for future nonvolatile magnetic memory technology. In one interpretation, the switching originates from carriers with spin-dependent scattering time giving rise to a relativistic anti-damping spin-orbit torque (SOT), which the carriers exert on uniform magnets with broken spatial inversion symmetry. The alternative interpretation combines the relativistic spin Hall effect (SHE), which turns the normal-conductor into an injector of a spin-current, with the non-relativistic anti-damping spin-transfer torque (STT) acting on the ferromagnet. Remarkably, the SHE in these experiments originates from the Berry phase in the band structure of a clean crystal and the anti-damping STT is also based on a disorder independent transfer of spin angular momentum from carriers to the magnetization. In this paper we report the observation of an anti-damping relativistic SOT, which stems from an analogous Berry phase effect as the SHE. The SOT alone can therefore induce magnetization dynamics based on a scattering independent physical principle. In our combined theoretical and experimental study we focus on the ferromagnetic semiconductor (Ga,Mn)As which has a broken spatial inversion symmetry in the bulk crystal. This allows us to consider a bare ferromagnetic film without a symmetry breaking interface with another non-magnetic conductor, thus eliminating by design any SHE related contribution to the observed spin torque. The experimentally observed symmetry and amplitude of the anti-damping torque are consistent with the Berry phase origin for which we provide an intuitive physical picture as well as a numerical solution of the microscopic Kubo formula for the studied (Ga,Mn)As samples..

ThIE3

INVITED

Giant magneto-drag in graphene at the charge neutrality

B.N. Narozhny[1], M. Titov[2], M. Schütt[3], P.M. Ostrovsky[4, 5], I.V. Gornyi[3, 6], A.D. Mirlin[1, 3, 7], T. Tudorovskiy[2], and M.I. Katsnelson[2]

[1] Institut für Theorie der Kondensierten Materie and DFG Center for Functional Nanostructures, Karlsruher Institut für Technologie, 76128 Karlsruhe, Germany
[2] Radboud University Nijmegen, Institute for Molecules and Materials, NL-6525 AJ Nijmegen, The Netherlands
[3] Institut für Nanotechnologie, Karlsruhe Institute of Technology, 76021 Karlsruhe, Germany
[4] Max-Planck-Institut für Festkörperforschung, Heisenbergstr. 1, 70569, Stuttgart, Germany
[5] L.D. Landau Institute for Theoretical Physics RAS, 119334 Moscow, Russia
[6] A.F. Ioffe Physico-Technical Institute, 194021 St. Petersburg, Russia
[7] Petersburg Nuclear Physics Institute, 188350 St. Petersburg, Russia

Keywords: magneto-drag, Nernst-Ettingshausen effect, charge neutrality, hydrodynamic approach

Recent measurements [1] of frictional drag in graphene-based double-layer devices revealed the unexpected phenomenon of giant magneto-drag at the charge neutrality point: applying external magnetic fields as weak as 0.3 T results in the reversal of the sign and a dramatic enhancement of the amplitude (by orders of magnitude) of the drag resistance. If the device is doped away from the Dirac point, the effect of such a weak field on the drag resistance remains negligible. The observed effect is most pronounced at temperatures above 150 K and is apparent already at 50 mT. Moreover, the negative drag disappears in high magnetic fields and at low temperatures, hinting at the classical origin of the phenomenon.

Using the quantum kinetic equation framework [2], we derived a hydrodynamic description of transport in double-layer graphene-based devices [3] that accounts for the observed behavior. In the presence of disorder, the hydrodynamic equations provide a generalization of the standard Drude theory to the case of Dirac fermions in graphene [4]. Remarkably, already at this simplest level, the theory yields the giant negative magneto-drag at the neutrality point. At the same time, the theory predicts the existence of non-zero Hall drag in doped graphene in agreement with experiment [4].

Physically, the magneto-drag is intimately related to the anomalous Nernst-Ettingshausen effect in graphene. At the charge neutrality point, electrons and holes in different sub-bands experience a unidirectional drift in weak magnetic field which can be interpreted as a quasi-particle (or heat) flow in the direction perpendicular to the electric current. Such a mode is efficiently transferred by Coulomb interactions to the passive graphene layer where it induces a drag voltage by means of the inverse thermoelectric effect. Similar physics leads to the unusual Hall drag resistance.

References:

[1] R.V. Gorbachev, A.K. Geim, M.I. Katsnelson, K.S. Novoselov, T. Tudorovskiy, I.V. Grigorieva, A.H. MacDonald, S.V. Morozov, K. Watanabe, T. Taniguchi, and L.A. Ponomarenko, Nature Phys. 8, 896 (2012).
[2] M. Schütt, P.M. Ostrovsky, M. Titov, I.V. Gornyi, B.N. Narozhny, and A.D. Mirlin. Phys. Rev. Lett. 110, 026601 (2013).
[3] B.N. Narozhny, M. Titov, M. Schütt, P.M. Ostrovsky, I.V. Gornyi, A.D. Mirlin, T. Tudorovskiy, M.I. Katsnelson, in preparation.
[4] M. Titov, R.V. Gorbachev, B.N. Narozhny, M. Schütt, P.M. Ostrovsky, I.V. Gornyi, A.D. Mirlin, T. Tudorovskiy, M.I. Katsnelson, A.K. Geim, and L.A. Ponomarenko, in preparation.

Electronic structure of monolayer and bilayer graphene on hexagonal substrates

M. Mucha-Kruczyński[1,2], J. R. Wallbank[1], A. A. Patel[1,3], A. K. Geim[4], and V. I. Fal'ko[1,5]

[1] *Department of Physics, Lancaster University, Lancaster LA1 4YB, United Kingdom*
[2] *Department of Physics, University of Bath, Bath BA2 7AY, United Kingdom*
[3] *Department of Physics, Indian Institute of Technology Kanpur, Kanpur 208016, India*
[4] *Centre for Mesoscience and Nanotechnology, University of Manchester, Manchester M13 9PL, United Kingdom*
[5] *DPMC, University of Geneva, 24 Quai Ernest-Ansermet, CH1211 Genève 4, Switzerland*

The overlaying of two two-dimensional crystals with different periodicity leads to the creation of a moiré pattern, an ideal example being a heterostructure of graphene and hexagonal boron nitride (hBN) [1, 2, 3]. Due to the honeycomb lattice of graphene and hBN, the moiré pattern in this case has the form of a hexagonal lattice with a longer period for a perfect alignment of the two crystalline lattices. Outstanding quality and atomic-scale flatness of such layered structures make it possible for electrons in graphene to undergo coherent Bragg scattering on the moiré potential created by the hBN layer thus imposing a miniband structure on the electronic spectrum.

We develop a phenomenological, symmetry-based theory of monolayer [4] and bilayer [5] graphene placed on substrates with hexagonal Bravais symmetry, such as hBN, and investigate electronic spectra of such structures as a function of symmetry-allowed perturbation parameters. For monolayer graphene, we identify conditions at which the first moiré miniband is separated from the rest of the spectrum by either one or a group of three isolated mini Dirac points and is not obscured by dispersion surfaces coming from other minibands. In such cases the Hall coefficient exhibits two distinct alternations of its sign as a function of charge carrier density. We also show that for bilayer graphene the interplay between the directions of the supercell Brillouin zone and trigonal warping of the electronic spectrum plays an important role in forming the global features of the miniband spectrum. For no lattice misalignment between BLG and hBN, $\theta = 0$, trigonal warping leads to overlapping of different minibands for a considerable part of the perturbation parameter space. At the same time, for small misalignment angles $\theta \approx 0.5°$, the electronic spectrum of BLG on hBN is most likely to exhibit global gaps or secondary isolated Dirac points at the edge of the first moiré miniband. For the case of large misalignment angles, $\theta \gtrsim 1.2°$, the folded chiral bands cross the high-energy bands.

[1] M. Yankowitz et al., Nat. Phys. **8**, 382 (2012).
[2] L. A. Ponomarenko et al., arXiv:1212.5012 (2012).
[3] C. R. Dean et al., arXiv:1212.4738 (2012).
[4] J. R. Wallbank, A. A. Patel, M. Mucha-Kruczynski, A. K. Geim, and V. I. Fal'ko, arXiv:1211.4711 (2012).
[5] M. Mucha-Kruczynski, J. R. Wallbank, and V. I. Fal'ko, in preparation.

Magnetotransport in disordered graphene at charge neutrality

Shaffique Adam [1,2]

[1] *Yale-NUS College, 6 College Avenue East, Singapore 138614*

[2] *Graphene Research Center and Department of Physics, National University of Singapore, 2 Science Drive 3, Singapore 117551*

It is now reasonably well understood that for Dirac fermion systems including both graphene and topological insulators, close to charge neutrality the energy landscape becomes highly inhomogeneous, forming a sea of electron-like and hole-like puddles, that determine its properties at low carrier density [1]. The formation of these puddles and the corresponding electronic properties of the Dirac point provide an intriguing example of how the competing effects of disorder, electron-electron interactions, and quantum interference conspire together to give a surprisingly robust state whose properties can be described using semi-classical methods [2]. In the present work we study how this balance is altered in the presence of a moderate magnetic field. The limits of both strong magnetic fields and weak magnetic fields are somewhat understood: a large magnetic field forms quantized Landau levels and the corresponding quantum Hall effect; and in weak magnetic fields, a two-channel model has been effectively used to understand experiments [3]. However, the regime of intermediate magnetic fields has remained an enigma including the experimental observation of unusual insulating states at densities close to the Dirac point. We address this problem by studying three distinct effects of a magnetic field: (i) The magnetic field dependence of the polarizability function within the Random Phase Approximation; (ii) The magnetic field induced change in transmission across the Klein tunneling barrier formed at the boundary between the electron and hole puddles; and (iii) The generalization of the Landauer-Bruggeman effective medium theory for magnetotransport within the puddles. We find that the latter two effects contribute significantly to the transport properties in the presence of a magnetic field, and we compare our theory with available experimental data.

References:

[1] S. Das Sarma, S. Adam, E. H. Hwang, and E. Rossi, "*Electronic transport in two dimensional graphene*", Rev. Mod. Phys. **83**, 407 (2011).

[2] S. Adam, E. H. Hwang, V. M. Galitski, and S. Das Sarma, "*A self-consistent theory for graphene transport*", Proc. Nat. Acad. Sci. USA **104**, 18392 (2007).

[3] S. Adam, "*Graphene Carrier Transport Theory*", Graphene Nanoelectronics in NanoScience and Technology, edited by Hassan Raza, Springer, (2012)

ThOE11

Magnetic-Field-Induced Localization in 2D Topological Insulators

Pierre Delplace, Jian Li and Markus Büttiker

Département de Physique Théorique, Université de Genève, CH-1211 Genève, Switzerland

Localization of the helical edge states in quantum spin Hall insulators requires breaking time-reversal invariance. In experiments, this is naturally implemented by applying a weak magnetic field B [1,2]. We propose a model based on scattering theory that describes the localization of helical edge states due to coupling to random magnetic fluxes [3]. We find that the localization length is proportional to B^{-2} when B is small and saturates to a constant when B is sufficiently large. We estimate especially the localization length for the HgTe/CdTe quantum wells with known experimental parameters.

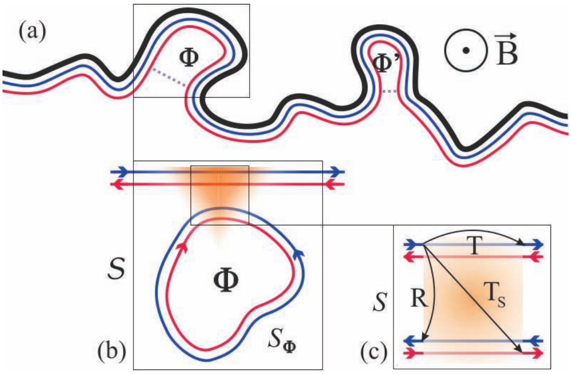

(a) Helical edge states in a disordered QSHI in a uniform magnetic field. Occasional occurrences of constrictions along the edge lead to Fabry-Perot-type loops where Aharonov-Bohm phases due to magnetic fluxes can accumulate. (b) The scattering of the helical edges by one of these loops, described by a scattering matrix S, can be divided into two parts: the scattering between two pairs of helical edge states (S), and the propagation of one of these pairs around the loop (S). (c) Three types of scattering probabilities, T, R and Ts, that are relevant to the scattering between two pairs of helical edge states.

[1] M. Konig, S. Wiedmann, C. Brune, A. Roth, H. Buhmann, L. W. Molenkamp, X.-L. Qi, and S.-C. Zhang, Science 318, 766 (2007)
[2] C.Brüne, A. Roth, H. Buhmann, E. M. Hankiewicz, L. W. Molenkamp, J. Maciejko, X.-L. Qi, and S.-C. Zhang, Nature Physics 8, 486 (2012)
[3] Pierre Delplace, Jian Li and Markus Büttiker, Phys. Rev. Lett. 109, 246803 (2012)

Monday Tuesday Wednesday Thursday Friday

Spin-dependent shot noise enhancement in a quantum dot

Niels Ubbelohde[1], **Christian Fricke**[1], **Frank Hohls**[1, 2] **and Rolf J. Haug**[1]

[1]*Institut für Festkörperphysik, Leibniz Universität Hannover, 30167 Hannover, Germany*
[2]*Physikalisch-Technische Bundesanstalt, 38116 Braunschweig, Germany*

Spin-dependent dynamics in the transport through quantum dots can be probed in a measurement of the electron shot noise. The time-dependent correlations of the current fluctuations provide additional information unavailable in a measurement of the time-averaged conductance.

The transfer of charges through quantum dots is correlated in comparison to the stochastic Poisson process of single barrier tunneling. For a single resonant level in the quantum dot shot noise becomes suppressed, while for a multi-level system competition between different transport channels results in an enhanced shot noise power [1]. A dependence of the blockade mechanism on the electron spin [2] can be induced by injecting electrons from spin-polarized leads [3]. This spin blockade effect has been observed for a quantum dot in magnetic field as a modulation of the Coulomb blockade peak amplitude or in the occurrence of negative differential conductance [3].

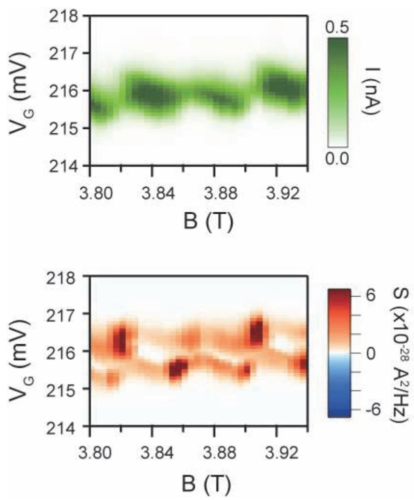

Fig. 1: Current and excess shot noise for a quantum dot in the spin blockade regime.

We present our measurements of the electron shot noise for a quantum dot in the spin blockade regime, where we observe super-Poissonian shot noise at the Coulomb blockade peak. The shot noise enhancement follows a regular pattern corresponding to the position and amplitude modulation of the Coulomb blockade peak in magnetic field. The complex internal level structure [4] of the quantum dot in this regime implies a dynamical blockade as the mechanism behind the observed enhancement. The periodic occurrence of peaks in the shot noise corresponds well to the alternating spin configuration of the quantum dot level system and is explained by the competition of transport channels with different spin giving rise to spin-dependent transport dynamics.

[1] O. Zarchin, Y. C. Chung, M. Heiblum, D. Rohrlich, and V. Umansky, Phys. Rev. Lett. **98**, 066801 (2007).
[2] A. Cottet, W. Belzig, and C. Bruder, Phys. Rev. B **70**, 115315 (2004).
[3] M. Ciorga, A. S. Sachrajda, P. Hawrylak, C. Gould, P. Zawadzki, S. Jullian, Y. Feng, and Z. Wasilewski, Phys. Rev. B **61**, R16315 (2000), M. Ciorga, M. Pioro-Ladriere, P. Zawadzki, P. Hawrylak, and A. S. Sachrajda, Applied Physics Letters **80**, 2177 (2002).
[4] M. C. Rogge, E. Räsänen, and R. J. Haug, Phys. Rev. Lett. **105**, 046802 (2010).

Spin blockade lifting due to phonon mediated spin relaxation and electric dipole spin resonance in nanowire quantum dots

M. P. Nowak, B. Szafran

AGH University of Science and Technology,
Faculty of Physics and Applied Computer Science,
al. Mickiewicza 30, 30-059 Kraków, Poland

Coherent electrical spin control is one of the prerequisites for creation of a solid-state quantum computer operating on spin qubits. Nanowire quantum dots have been demonstrated [1, 2, 4, 5, 6] as a good candidates to perform single spin rotations due to strong spin-orbit coupling that allows control the electron spin by electrical fields. The spin rotations are performed by electric dipole spin resonance where the electron is wiggled with frequency matching the Larmor frequency in a weak external magnetic field. The spin rotations allow for lifting the Pauli blockade of the single-electron current in the two-electron double-quantum dot. The electron-electron interaction leads to appearance of additional transitions due to exchange coupling between the adjacent spins [3, 7]. Lifting of the spin blockade is associated with phonon mediated relaxation from one of the spin antiparallel excited states in which electrons occupy separate dots to the singlet ground state with double occupancy of the single dot. However in the presence of spin-orbit coupling the spin-relaxation can occur as a concurrent process to electric dipole spin resonance lifting the blockade also from spin parallel states. We present theoretical description of the spin blockade lifting that incorporates both the electric dipole spin resonance and phonon mediated relaxation in two-electron coupled nanowire quantum dots. We find that the spin-nonconserving relaxation is possible provided the energy separation between initial and final states for the relaxation becomes small enough which leads to spontaneous lifting the blockade from one of the Zeeman split triplets. When the external magnetic field is increased the spin parallel triplet becomes the ground state which results in a restoration of the blockade from this state. This results in opening of an additional transition – related to the spin rotation accompanied by charge reconfiguration – which we identify in recent experimental results [4].

[1] S. Nadj-Perge, et al., Nature (London) **468**, 1084 (2010).
[2] M. D. Schroer, et al., Phys. Rev. Lett. **107**, 176811 (2011).
[3] S. Nadj-Perge, et al., Phys. Rev. Lett. **108**, 166801 (2012).
[4] S. M. Frolov, et al., Phys. Rev. Lett. **109**, 236805 (2012).
[5] K. D. Petersson, et al., Nature (London) **490**, 380 (2012).
[6] J. W. G. van den Berg, et al., Phys. Rev. Lett. **110**, 066806 (2013).
[7] M. P. Nowak, et al., Phys. Rev. B **86**, 125428 (2012).

A few-electron quadruple quantum dot in a closed loop

Romain Thalineau[1], Andreas D. Wieck[2], Christopher Bäuerle[1],Laurent Saminadayar, Tristan Meunier[1]

[1]*Institut Néel, CNRS and Université Joseph Fourier, 38042 Grenoble, France*
[2] *Lehrstuhl für Angewandte Festkörperphysik, Ruhr-Universität Bochum, Universitätsstrasse 150, 44780 Bochum, Germany*

Controlling the path of a single electron in semiconducting nanostructures is an interesting tool in the context of spin qubits systems. In particular, it opens the route towards the transport of quantum information on a chip and represents a potential strategy to scale up the number of spin qubits in interaction. In addition, in presence of spin-orbit interaction, it represents an interesting way to manipulate coherently the spin of a single electron[1]. Recently, fast and efficient single electron transport could be obtained by assisting the transport through a 1D-channel electrostatically defined with surface acoustic waves on AlGaAs heterostructures [2]. Nevertheless, such a technique is restricted to displacements on a straight line. To perform more complex displacements, engineering the path of the electron with series of quantum dots is a promising alternative. In this context, it has been demonstrated that topological spin manipulation can be obtained if the electron is transported adiabatically on a closed path under spin-orbit interaction [3].
We report the realization of a quadruple quantum dot device in a square-like configuration where a single electron can be transferred on a closed path free of other electrons [4]. By studying the stability diagrams of this system, we demonstrate that we are able to reach the few-electron regime and to control the electronic population of each quantum dot with gate voltages. This allows us to control the transfer of a single electron on a closed path inside the quadruple dot system. This work opens the route towards electron spin manipulation using spin-orbit interaction by moving an electron on complex paths free of electrons.

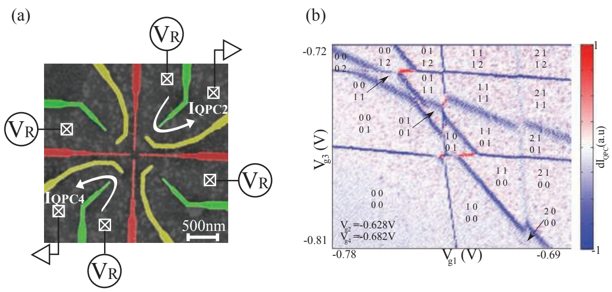

[1] K. C. Nowack, F. H. L. Koppens, Yu. V. Nazarov, and L. M. K. Vandersypen, Science **318**, 1430 (2007)
[2] S. Hermelin, S. Takada, M. Yamamoto, S. Tarucha, A. D. Wieck, L. Saminadayar, C. Bäuerle, and T. Meunier, Nature **477**, 435438 (2011)
[3] P. San-Jose, B. Scharfenberger, G. Schön, A. Shnirman, and G. Zarand, Phys. Rev. B **77**, 045305 (2008)
[4] R. Thalineau, S. Hermelin, A. D. Wieck, C. Baäuerle, L. Saminadayar, T. Meunier, Appl. Phys. Lett **101**, 103102 (2012).

INVITED

ThIM3

Real-time spin detection of single photo-electrons with a double quantum dot in a g-factor engineered quantum well

T. Fujita [1], K. Morimoto [1], S. Teraoka [1], G. Allison [1,2], A. Ludwig [3], A. D. Wieck [3], A. Oiwa [1] and S. Tarucha [1]

[1] *Department of Applied Physics, The University of Tokyo, Tokyo, Japan*
[2] *Department of Physics, Princeton University, Princeton, New Jersey, USA*
[3] *Lehrstuhl für Angewandte Festkörperphysik, Ruhr-Universität Bochum, Germany*

We present spin detection of single photo-electrons with a GaAs based double quantum dot (DQD) fabricated in a g-factor engineered quantum well (QW). We resonantly photo-excited single electron-light holes (or heavy holes) in the DQD and performed real-time detection of electron spin using Pauli spin blockade (PSB) in the DQD. This experiment gives insight into the spin relaxation dynamics of optically excited single electrons, which is an essential ingredient for the realization of quantum state transfer from single photons to single electron spins.

We chose a near zero electron g-factor wafer to prepare gate-defined DQDs. We used a nearby charge sensor to perform real-time detection of single photo-electrons [1] and measured the wavelength dependence of the single photo-electron absorption efficiency of the dot. Comparing the absorption efficiency spectrum with the photoluminescence result we have realized the capture of single photo-electrons resonantly generated in pairs with single electron-light holes (or heavy holes).

Next we setup the condition of PSB in the double dot at the (1,1)-(0,2) charge transition region. By fitting the magnetic field dependence of the leakage current of PSB-lifting we obtained the fluctuating hyperfine field of 23 mT. This value is much larger than that in conventional GaAs HEMT wafer QDs, reflecting the small g-factor of our QDs. In the time resolved inter-dot tunneling measurements we observed fast tunneling and slow tunneling, each resulting from anti-parallel and parallel spin configuration, as featured in a bi-exponential histogram of the tunneling event count. This result supports the proposal that the present setup can discriminate single photo-electron spins.

Finally, we performed single-shot detection of single photo-electron spins. We tuned the DQD to the (0,1) region and irradiated laser pulses to generate just one photo-electron to instantly reach the PSB condition. Then, as predicted from the above described inter-dot tunneling experiment, we could distinguish between the parallel and anti-parallel spins from the difference in the first inter-dot tunneling time, slow for parallel spin and fast for anti-parallel spin. This is an important step towards single photon to single spin coherent state transfer.

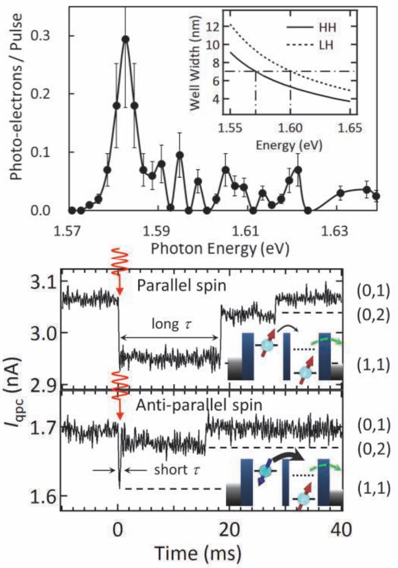

Figure: (Top) Determination of light and heavy hole excitation from single photo-electron detection efficiency. (Bottom) Single-shot single photo-electron spin detection.

[1] T. Fujita *et al*. (Submitted).

ThIE4

INVITED

Strong-field THz spectroscopy of low-dimensional semiconductor systems

Manfred Helm

Helmholtz-Zentrum Dresden-Rossendorf (HZDR), 01328 Dresden, Germany

Monday Tuesday Wednesday Thursday Friday

Many low-energy excitations in solids fall into the meV or THz range. Whereas linear spectroscopy is a valuable tool to obtain information on the linear response of these excitations, recent progress in THz sources also enables one to access their nonlinear and time-resolved behavior. To this end we use a free-electron laser to study intraexcitonic transitions in quantum wells and carrier dynamics in graphene.

Excitons possess a hydrogen-like internal excitation spectrum with a characteristic energy scale in the THz range. We pump the 1s-2p intraexcitonic transition in GaAs and InGaAs multiquantum wells with a THz free-electron laser and probe the induced changes in the absorption spectrum via interband absorption using a near-infrared femtosecond laser. We observe a splitting of the 1s exciton line, which can be explained by the Autler-Townes or AC Stark effect [1]. The behavior is, however, much more complex than for an ideal two-level system. Since for electric fields in the 10 kV/cm range the Rabi energy is of the same order of magnitude as the 1s-2p transition energy, we are in fact clearly beyond the validity of the rotating wave approximation. At the highest fields, when also the ponderomotive energy ($e^2F^2/4m\omega^2$) approaches the exciton binding energy, signatures of exciton field ionization are observed.

In graphene with its vanishing bandgap, interband excitations extend down to very low frequencies, where they compete with the free-carrier (intraband) absorption in lightly doped graphene (E_F ~13 meV). We have performed THz pump-probe experiments on multilayer graphene over a wide range of photon energies (10-250 meV) to investigate the carrier dynamics. Interestingly we observe a crossover from induced transmission (bleaching) for $\hbar\omega > 2E_F$ to induced absorption for $\hbar\omega < 2E_F$. At these photon energies interband transitions are initially blocked, but become possible after intraband free-carrier absorption and heating [2]. In a magnetic field the bands split up into non-equidistant Landau levels, which can be pumped and probed selectively. Using left- and right-circularly polarized light reveals some surprising behavior related to the importance of Auger scattering.

This work was done in collaboration with M. Teich, M. Wagner, M. Mittendorff, D. Stehr, S. Winnerl and H. Schneider (HZDR), S. Chatterjee, A.C. Klettke, M. Kira, and S.W. Koch (Univ. Marburg, Germany), M. Orlita and M. Potemski (LNCMI Grenoble, France), and T. Winzer, F. Wendler, E. Malic and A. Knorr (TU Berlin, Germany). The MQW samples were provided by A. M. Andrews and G. Strasser (TU Vienna, Austria), and by H.M. Gibbs and G. Khitrova (Univ. Arizona, Tucson, USA). The graphene samples were provided by M. Sprinkle, C. Berger and W. A. de Heer (Georgia Tech, Atlanta, USA).

[1] M. Wagner, H. Schneider, D. Stehr, S. Winnerl, A. M. Andrews, S. Schartner, G. Strasser, M. Helm, Observation of the intraexciton Autler-Townes effect in GaAs/AlGaAs semiconductor quantum wells, Phys. Rev. Lett. **105**, 167401 (2010).

[2] S. Winnerl, M. Orlita, P. Plochocka, P. Kossacki, M. Potemski, T. Winzer, E. Malic, A. Knorr, M. Sprinkle, C. Berger, W. A. de Heer, H. Schneider, M. Helm, Carrier relaxation in epitaxial graphene photoexcited near the Dirac point, Phys. Rev. Lett. **107**, 237401 (2011).

Coherent dynamics of a strongly driven single electron spin

J. Yoneda [1*], T. Otsuka [1,2*], T. Nakajima [1,2], T. Takakura [1], T. Obata [1], H. Lu [3], C. Palmstrøm [3], A. C. Gossard [3], and S. Tarucha [1,2]

[1] *Department of Applied Physics, University of Tokyo, Tokyo 113-8656, Japan*
[2] *RIKEN Advanced Science Institute, RIKEN, 2-1 Hirosawa, Wako, Saitama 351-0198, Japan*
[3] *Materials Department and Department of Electrical and Computer Engineering, University of California, Santa Barbara, CA 93106, USA*

Electron spin in quantum dots (QDs) is a distinguished platform for solid-state quantum computers (QCs), because of the relatively long coherence times and potential scalability. Recent experiments have demonstrated many of the prerequisite elements for QCs with realization of two single spin qubits [1] and two-qubit entanglement [2]. However, realizing sufficiently fast control over qubits compared with their couplings to the environment, a key ingredient of quantum gates, is still elusive, and this may hinder manipulations of pure spin states. In this work, we demonstrate single spin rotations on a timescale much shorter than the ensemble phase coherence time (T_2^*) via electron spin resonance (ESR) above 120 MHz in GaAs QDs, and report on the unconventional features in Rabi oscillations arising from a nearly pure spin state.

We used a double QD defined in a 2DEG of GaAs/n-AlGaAs by negatively-biased Schottky gates. A proximal Co micro magnet yields a slanting magnetic field at the double QD position and oscillating an electron inside the dot enables electrically driven ESR [1]. We have refined the magnet design and used a shallow (57 nm deep) 2DEG to raise the Rabi frequency (f_{Rabi}) by an order of magnitude or exceeding 120 MHz (the highest ever reported). The spin rotation time is now much shorter than $T_2^* > 50$ nsec. We found that in this regime the Rabi oscillations decay following an exponential-law with the initial phase shift of virtually zero, although it is usually reported that the initial phase is shifted by $\pi/4$ after averaging over nuclear spin statistics [3]. Note the fast Rabi oscillation can also decouple electron spin rotation from dynamical nuclear polarization. To capture the driven spin dynamics even more closely, we took magnetic field detuning dependence of Rabi oscillations, and the so-called "Chevron" interference pattern is clearly resolved in the detuning-time plane, consistent with the model of a single spin evolution within a pure state.

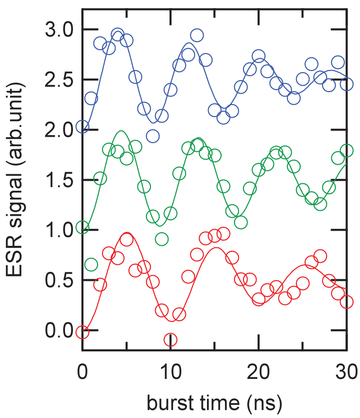

Figure: Fast Rabi oscillations. Extracted f_{Rabi} are 98, 113, 123 MHz for the bottom, middle, top traces, respectively. MW powers are attenuated by 6 dB from top to bottom. Solid lines are fit to an exponentially-damped sinusoidal function with no phase shift.

[1] M. Pioro-Ladrière et al. Nat. Phys. 4, 776 (2008).
[2] R. Brunner et al. Phys. Rev. Lett. **107**, 146801 (2011).
[3] F. H. L. Koppens, K. C. Nowack, L. M. K. Vandersypen, Phys. Rev. Lett. **100**, 236802 (2008).
* These authors contribute equally to this work.

THz Magnetophotoresponse and spin-orbit effects in the 2DEG in a HgTe quantum well

M. Pakmehr[1], A. Stier[1], B. D. McCombe[1], C. Bruene[2], H. Buhmann[2] and L Molenkamp[2]

[1] Department of Physics, University at Buffalo, SUNY, Buffalo, NY 14260, USA
[2] EP3, Universitaet Wuerzburg, D-97074 Wuerzburg, Germany

There is considerable current interest in HgTe because of its interesting "inverted" band structure and large spin-orbit interaction, and because it is a topological insulator under quantum confinement and shows a quantum spin Hall effect.[1] We have studied 6 nm

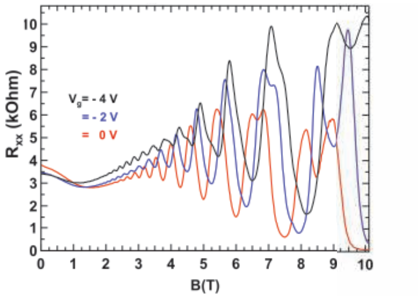

Fig. 1. Gate voltage dependence of Rxx at 4.2K.

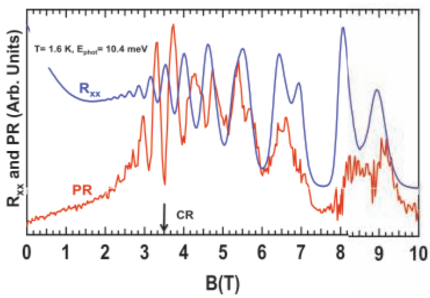

Fig. 2. PR (10.4 meV) and R_{xx} at 1.6 K

HgCdTe/HgTe quantum-well samples ("normal" band structure; n_s = 1.55 x 10^{12} cm^{-2}; μ = 1.64 x 10^5 cm^2 /V-sec) to measure effects of the (large) spin-orbit interaction. Application of electric fields via a gate creates an asymmetric potential in the growth direction that can result in a significant Rashba spin-splitting; gate bias also permits varying the electron density by up to 30%. Similar gated samples with the inverted band structure (larger wells) have shown extremely large Rashba spin splitting.[2] We have used photoresponse (PR) excited by several lines from an optically pumped THz laser (Fig 2) and R_{xx} (Fig. 1) and R_{xy} measurements to probe the high frequency and dc response of the Γ_6 conduction band electrons in fields up to 10 T. The R_{xx} oscillations show beating behavior at 4.2 K at large negative gate voltages indicative of Rashba spin splitting. Both R_{xx} and R_{xy} show complex behavior at 1.6 K at high fields. We find m* = 0.039m_e and g = -18 at V_g = 0 from a combination of transmission CR measurements and tilted field S-dH experiments. This is consistent with model fits to the PR vs. B, where we simulated the PR using the usual 2D expression for the oscillatory part of ρ_{xx} and a model of CR carrier heating. The difference between resonant heating (Lorentzian temperature profile – laser on) and a background (bath temperature - laser off) yields a difference (proportional to the PR) that exhibits the resonant absorption as an envelope of S-dH oscillations with a maximum that is close to the CR resonant field. The fits yield the carrier density, m*, scattering times and the g-factor (visibility of spin splitting is enhanced in the PR at low-intermediate fields). Attempts to measure electron spin resonance in the PR have thus far proven inconclusive. Detailed analyses of these results will be presented. Work was supported in part by NSF MWN DMR 1008138.

[1] M. Koenig, S. Wiedmann, C. Bruene et al., Science **318**, 766 (2007)
[2] J. Hinz, H Buhmann, M. Schaefer, et al., Semicond. Sci. Technol. **21**, 501 (2006)

Mechanical Friction Induced by Single Electron Transport

Y. Okazaki, I. Mahboob, K. Onomitsu, S. Sasaki, and H. Yamaguchi

NTT Basic Research Laboratories, NTT Corporation

Hybrid systems with mechanical and electronic degrees of freedom are a promising ingredient for quantum information devices owing to long-lived phonon states and accessible charge states [1]. Here, we investigate an electromechanical resonator embedded with a quantum dot (QD). The harmonic motion of the resonator can be regarded as a coherent phonon ensemble interacting with the charge states in the QD. The measured quality factor Q of the resonator shows enhancement and suppression on the sides of the Coulomb peak. Since Q characterizes mechanical damping of the resonator, our observation demonstrates variable mechanical friction induced by the single electron transport.

Figures (a) and (b) show our hybrid device. A doubly-clamped electromechanical resonator of 50 μm length is fabricated from a GaAs/AlGaAs heterostructure sustaining a two-dimensional electron gas (2DEG). At one clamping point of the resonator, the QD is defined in the 2DEG using negatively biased top gates [Fig. (b)]. The gate electrodes A and B at the other side are used to excite and detect the mechanical motion piezoelectrically. In this device, the charge states in the QD is mutually coupled with the resonator via a piezoelectric field associated with the mechanical motion.

The charge states in the QD can be controlled through gate voltage V_{g} and source drain bias V_{sd} as manifested by a typical Coulomb diamond [Fig. (c)]. On the other hand, the mechanical motion can be excited by applying ac voltage on gate A, and is detected through voltage spectral measurements on gate B. Figure (d) shows a typical power spectrum of a Lorentzian peak corresponding to the fundamental mechanical mode with the resonant frequency $f_0 \approx 1.67$ MHz. The quality factor Q can be determined from the peak width Δf ($Q = f_0/\Delta f$).

The measured Q on the left (right) hand side of the Coulomb peak [Fig. (e)] is enhanced (suppressed) to $Q \approx 2.8 \times 10^5$ ($Q \approx 2.0 \times 10^5$). This change is comparable to the intrinsic value $Q \approx 2.4 \times 10^5$ of the resonator. The enhancement (suppression) of Q originates from in-phase (out-of-phase) mechanical backaction from the QD to the resonator. This unique in-phase (out-of-phase) backaction serves as a negative (positive) friction, which amplifies (suppresses) the mechanical motion. The deviation of Q is observed only at $V_{\mathrm{sd}} \neq 0$ while it vanishes at $V_{\mathrm{sd}} = 0$, indicating that the single electron transport plays a vital role in causing additional friction in the electromechanical resonator.

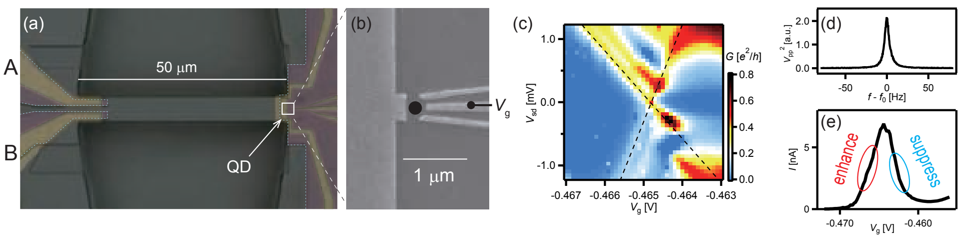

Fig.: (a) Optical and (b) electron micrographs of the device. (c) Coulomb diamond. (d) Power spectrum of the mechanical motion. (e) Coulomb peak at $V_{\mathrm{sd}} = 0.48$ mV.

[1] J.-M. Pirkkalainen *et al.* Nature **494**, 211 (2013).

ThOM12

Coulomb Drag in Vertically-Integrated Quantum Wires

D. Laroche[1,2], G. Gervais[1], M. P. Lilly[2] and J. L. Reno[2]

[1] *Department of Physics, McGill University, Montréal, Canada*
[2] *Sandia National Laboratories, Albuquerque, USA*

One of the challenges quantum circuitry is facing is to understand the mutual interactions between circuit elements closely-packed at the nanoscale. Due to the long-range nature of Coulomb interactions, driving an electrical current in such a circuit may have profound influences on the charge distribution of nearby circuit elements. To address these questions, we have fabricated independently-contacted and vertically-coupled quantum wires with a large degree of tunability and control over their electronic density, making them especially suited to study one-dimensional Coulomb drag between wires separated by only a few tens of nanometres. The wires are fabricated from a GaAs/AlGaAs double quantum well heterostructure with a 15 nm barrier separating the quantum wells.

We report here Coulomb drag measurements where both positive and negative signals are observed as the sub-band occupancy of each quantum wire is varied [1]. Peaks in the positive Coulomb drag signal are observed concomitant with the opening of 1D sub-bands in either wire. Negative Coulomb drag is also observed in two regimes: one at low electronic density when the drag wire is close to or beyond depletion, and one at a higher electronic density when the drag wire has one or more single 1D sub-band occupied. While both the positive and the low-density negative one-dimensional Coulomb drag regimes had been previously observed in horizontally-coupled quantum wires with a larger (~ 100 nm) inter-wire separation [2], we report here the first observation of negative one-dimensional Coulomb drag at high electronic density, *i.e.* when the drag wire is conducting.

The observation of a high-density negative Coulomb drag signal challenges the standard momentum-transfer model for Coulomb drag. However, negative Coulomb drag has been predicted to occur from a charge-fluctuation induced Coulomb drag model in asymmetric mesoscopic circuits[3, 4]. In addition, a fluctuation-induced model also predicts the presence of peaks in the positive Coulomb drag regime concomitant with the opening of 1D sub-bands, which is consistent with our observations. In order to assess the consistency of this fluctuation-induced model for Coulomb drag over the whole phase-space of the Coulomb drag measurement, the temperature dependence of drag signal in the various regimes will be presented, as well as the expectations from Luttinger liquid theory.

This work was performed, in part, at the Center for Integrated Nanotechnologies, a U.S. DOE, Office of Basic Energy sciences user facility. Sandia National Laboratories is a multi-program laboratory managed and operated by Sandia Corporation, a wholly owned subsidiary of Lockheed Martin Corporation, for the U.S. Department of Energy's National Nuclear Security Administration under contract DE-AC04-94AL85000. We also acknowledge funding from NSERC, FQNRT and CIFAR (Canada).

[1] D. Laroche, G. Gervais, M.P. Lilly, J.L. Reno, Nature Nanotech., **6**, 793 (2011); see also **News and Views** by M. Büttiker, R. Sánchez, Nature Nanotech **6** 757 (2011).
[2] M. Yamamoto, M. Stopa, Y. Tokura, Y. Hirayama, S. Tarucha, Science, **313**, 204 (2006).
[3] A. Levchenko, A. Kamenev, Phys. Rev. Lett. **101**, 216806 (2008).
[4] R. Sánchez, R. López, D. Sánchez, M. Büttiker, Phys. Rev. Lett. **104**, 076801 (2010).

Monday
Tuesday
Wednesday
Thursday
Friday

ThP83

Electron-hole symmetry in GaSb/InAs core/shell nanowires

Bahram Ganjipour[1], Martin Ek[2], B. Mattias Borg[1], Kimberly A. Dick[1,2], Lars-Erik Wernersson[3], Lars Samuelson[1] and Claes Thelander[1]

[1]Solid State Physics, Lund University, Box 118, SE-221 00 Lund, Sweden. [2]Polymer & Materials Chemistry, Lund University, Box 124, SE-221 00, Lund, Sweden. [3]Electrical & Information Technology, Lund University, Box 118, SE-221 00 Lund, Sweden.

The GaSb/InAs heterostructure has been investigated for various device implementations since the first pioneering work by Sakaki et al in the late 1970s [1]. In bulk, GaSb and InAs are among the semiconductors with the highest hole and electron motilities, respectively. The structures have shown promise for high speed electronic devices and photonic applications in the infrared region [2]. The heterostructure has recently gained a lot of interest as an important system for fundamental studies of quantum physics (e.g. recently in the search for Quantum Spin Hall effect and topological insulators) [3]. Theoretical and experimental studies show the presence of a hybridized mini-gap in GaSb/InAs heterostructure due to conduction and valance band overlap in InAs and GaSb, respectively. Novel quantum devices, such as 1D topological insulators, could be realized by combining the broken gap (semimetal) alignment of a GaSb/InAs heterostructure and the one-dimensional nature of a nanowire. We report on transport modulation in top-gated GaSb/InAs core/shell nanowire field-effect transistors. Comparing the transfer characteristics of the devices with different shell thicknesses it was found that the thickness of the shell had a strong effect on the semiconductor properties. We show that carrier concentrations and majority carrier type could be tuned, from *p* to *n* type, by varying the InAs thickness. A particularly interesting regime was found for nanowires with an InAs shell thickness in the range 4-6nm, which exhibit ambipolar conduction with a finite resistance at charge neutrality point at T= 4.2 K. At this point electrons and holes seem to coexist, which can be a signature of a negative band gap and electron-hole hybridization. However, nanowires with slightly thinner InAs shell show a small insulating region, which is a signature of a staggered band alignment, for which the resistance increases significantly when the Fermi level is positioned in the band gap. .

Figure 1: (a) transport properties of two different NWFETs with negative and normal band gap at 4.2 K. (b) Charge oscillations at V_{DS}= 1 mV, and T = 4.2 K for a device with electron- hole underlap, where the transport is tuned from single-hole tunneling, to single-electron tunneling

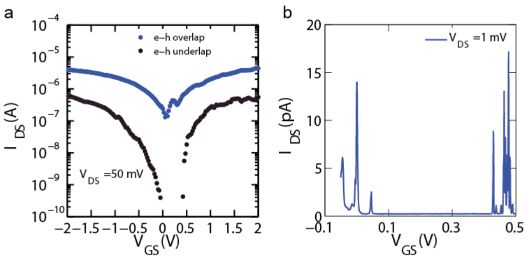

References:

[1] H. Sakaki, L.L. Chang, R. Ludeke, C.A. Chang, G.A. Sai-Halasz, L. Esaki, Appl. Phys. Lett. 31, 211 (1977).

[2] F. Fuchs, U. Weimer, W. Pletschen, J. Schmitz, E. Ahlswede, M. Walther, J. Wagner, and P. Koidl, Appl. Phys. Lett. 71, 3251 (1997), [3]I. Knez, R-R. Du and S. Gerard, PRL. 107, 136603 (2011)

Monday Tuesday Wednesday Thursday Friday

Coherent control of a single electron in a tunnel-coupled wire driven by a surface acoustic wave

S. Takada[1], M. Yamamoto[1,2], S. Nakamura[1], K. Watanabe[1], C. Bäuerle[3], A. D. Wieck[4] and S. Tarucha[1]

[1] *Department of Applied Physics, Univ. of Tokyo, Bunkyo-ku, Tokyo 113-8656, Japan*
[2] *ERATO-JST, Kawaguchi-shi, Saitama 331-0012, Japan*
[3] *Institut Néel - CNRS and Université Joseph Fourier, 38042 Grenoble, France*
[4] *Lehrstuhl für Angewandte Festkörperphysik, Ruhr-Universität Bochum, Universitätsstraße 150, 44780 Bochum, Germany*

Quantum electron optics is an attractive platform for building up coherent quantum systems in solid-state devices. In particular, flying electrons in depleted channels driven by surface acoustic waves (SAWs) are promising because quantum states of the electrons are decoupled from decoherence sources in their environment. Recent experiments have shown that single electrons are transferred as flying electrons trapped by SAWs and detected on demand [1, 2]. To realize quantum optics experiments with the single flying electrons, basic elements such as beam splitters and controllers of phase and interactions are required. Here we report on the realization of a coherent single electron beam splitter as well as coherent manipulation of the single electron charge states in a depleted tunnel-coupled wire driven by SAWs.

The device was defined in a GaAs /AlGaAs heterostructure by Schottky gates. An interdigital transducer (IDT) to generate SAWs is placed at the left side, about 1.2 mm apart from the beam splitter (Fig.1a). Electrons are injected one by one into the lower part of the depleted tunnel-coupled wire by the moving SAW potential. We tuned both tunnel-coupling energy and energy detuning between the upper and lower part of the wire by applying gate voltages Vg_c, Vg_U and Vg_L. We observed coherent oscillation of single electrons between the upper and lower part of the wire as a function of the tunnel-coupling energy or Vg_c (Fig.1b). The visibility was about 40% at the zero-energy detuning, which is most probably limited due to the geometry at the edges of the wire. As the detuning is increased, the oscillation period decreases with decreasing amplitude, which is a clear manifestation of the coherent charge oscillation (Fig.1b). Furthermore the visibility of the oscillation was almost constant from 0.3 K to 1 K. This implies that electrons transported by SAWs through a depleted quantum channel hardly decohere by the phonon bath. Our demonstration paves the way to perform various quantum electron-optical experiments and to realize coherent quantum systems.

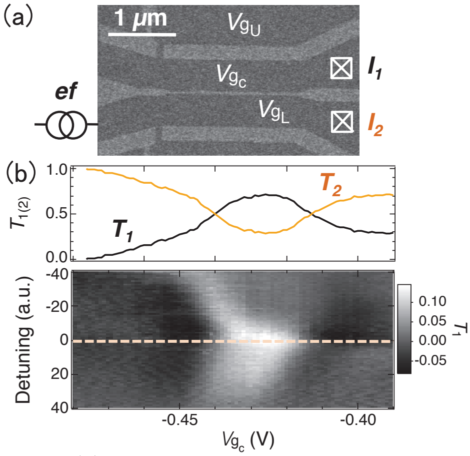

: Fig.1(a) A SEM picture of the relevant device. (b) Upper panel shows tunnel-coupling dependence of transmission probability $T_{1(2)} = I_{1(2)}/(I_1 + I_2)$ along the dashed line in the lower panel. Lower panel shows an intensity plot of T_1 as a function of tunnel-coupling energy (Vg_c) and energy detuning ($Vg_U - Vg_L$), where smoothed background is subtracted from raw data.

[1] S. Hermelin et al., Nature. **477**, 435 (2011).
[2] R. P. G. McNeil et al., Nature. **477**, 439 (2011).

INVITED

Compressibility measurements of the 0.7 structure in a one-dimensional quantum wire

L.W. Smith[1], A. R. Hamilton[2], K. J. Thomas[3], M. Pepper[3], I. Farrer[1], J. P. Griffiths[1], G. A. C. Jones[1], and D. A. Ritchie[1]

[1] *Cavendish Laboratory, J. J. Thomson Avenue, Cambridge, CB3 OHE, United Kingdom*
[2] *School of Physics, The University of New South Wales, Sydney 2052, Australia*
[3] *Department of Electronic and Electrical Engineering, University College London, London, WC1E 7JE, United Kingdom*

The conductance through a ballistic one-dimensional channel is quantised in units of $2e^2/h$. However, there is often also an extra conductance feature close to $0.7 \times 2e^2/h$, whose origins have been a subject of great debate. Many theories have been put forward to explain the so-called 0.7 structure, including spontaneous spin polarisation, the Kondo eect, and phenomenological spin-gap models, amongst others. The majority of experiments performed on 1D channels simply measure the conductance of the system, although notable exceptions include thermopower, shot noise, and scanning gate microscopy. All of these are inherently non-equilibrium measurements, unlike the thermodynamic compressibility. Very recently, high resolution measurements of the compressibility of a single 1D wire were performed, which for the first time were able to resolve magnetic field induced spin-splitting of subbands in the compressibility signal [1].

In this work we measure the compressibility signal due to the 0.7 structure for different temperatures and magnetic fields, and compare it with the predictions of various models. We show that compressibility measurements are a very powerful tool to probe the 0.7 structure, since models which predict very similar conductance characteristics give rise to very different responses in the compressibility.

[1] L.W. Smith, A. R. Hamilton, K. J. Thomas, M. Pepper, I. Farrer, J. P. Griffiths, G. A. C. Jones, and D. A. Ritchie, Phys. Rev. Lett. **107**, 126801 (2011).

5 July (Friday)

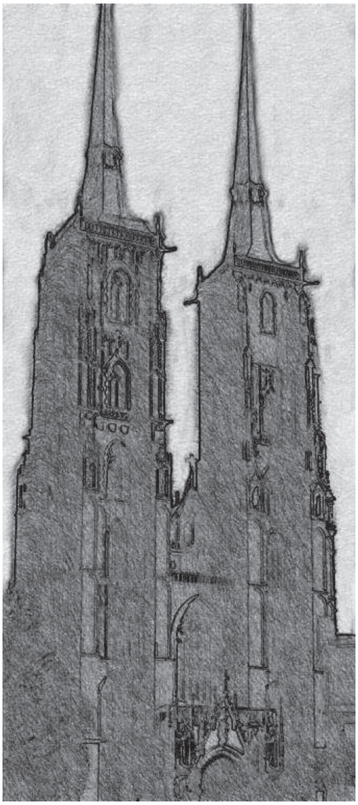

Wrocław Cathedral

5 July (Friday)

Plenary Session 1

9.00 – 9.45	**FriPlenary1** **Jacqueline Bloch** (*LPN/CNRS, Marcoussis, France*) Quantum fluids in semiconductor microcavities
9.45 – 10.30	**FriPlenary2** **Pawel Hawrylak** (*National Research Council of Canada, Ottawa, Canada*) Semiconductor and graphene quantum dots

Plenary Session 2

11.00 – 11.45	**FriPlenary3** **Tomasz Wojtowicz** (*Polish Academy of Sciences, Warsaw, Poland*) II-VI diluted magnetic semiconductor nanostructures for spintronic research
11.45 – 12.30	**FriPlenary4** **Konstantin S. Novoselov** (*University of Manchester, UK*) 2D atomic crystals and their heterostructures
12.30	Closing

Quantum fluids in semiconductor microcavities

Jacqueline Bloch

Laboratoire de Photonique et de Nanostructures,
LPN/CNRS, Route de Nozay, 91460 Marcoussis, France
Jacqueline.bloch@lpn.cnrs.fr

Semiconductor microcavities operating in the light-matter strong coupling regime provide a new system for fundamental studies of bosonic quantum fluids, and for the development of new devices for all optical information processing. Optical properties of semiconductor microcavities are governed by bosonic quasi-particles named cavity polaritons, which are exciton-photon mixed states. Cavity polaritons propagate like photons, but interact strongly with their environment via their matter component.
Our group at Laboratoire de Photonique and Nanostructures has developed these last years, state of the art microcavities and photonic circuits, where polariton condensates can be generated in fully engineered potential landscape.

After a general introduction on cavity polaritons, I will review recent experimental works illustrating the potential of this system. I will show how we can generate polariton flows which propagate over macroscopic distances (mm) while preserving their spatial and temporal coherence. These polaritons can be optically manipulated, trapped and re-amplified along their propagation. These properties are the basic ingredients for future development of polaritonic devices. I will describe recently implemented polariton devices: a polariton interferometer and a non-linear resonant tunneling polariton diode. Finally I will illustrate the crucial role of polariton interactions by presenting self-trapping experiments in coupled cavities.
I will conclude with perspectives opened by these polariton devices.

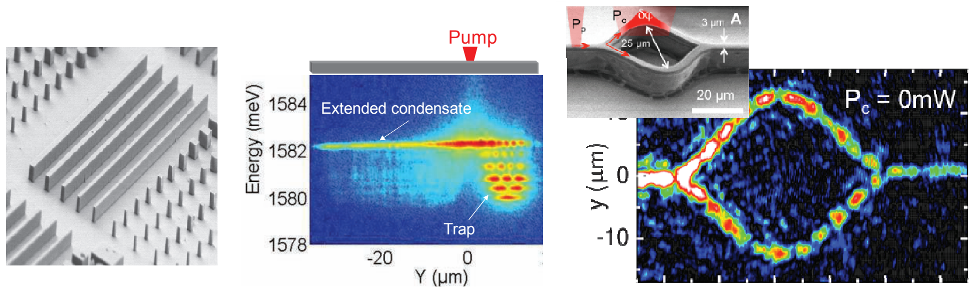

Figures : (left) Scanning electron microscopy image showing an array of photonic wires and micropillars; (centre) Emission of a 1D cavity showing an extended polarton condensate and optically trapped polaritons ; (right) Scanning electron microscopy image of a polariton interferometer; Spatially resolved emission measured on the polariton interferometer.

References

[1] E. Wertz, et al., Nat. Phys. 6, 860 (2010)
[2] L. Ferrier, et al., Phys. Rev. Lett. 106, 126401 (2011);
[3] D. Tanese, et al., Phys. Rev. Lett. 108, 036405 (2012)
[4] M. Galbiati, et al., Phys. Rev. Lett. 108, 126403 (2012);
[5] E. Wertz et al., Phys. Rev. Lett. 109, 216404 (2012)
[6] M. Abbarchi et al., Nature Physics 9, 275(2013)
[7] D. Tanese et al., Nature Communications 4, 1749 (2013)
[8] H-.S. Nguyen et al., Phys. Rev. Lett. to appear (arXiv:1305.5069)

FriPlenary2

Semiconductor and Graphene Quantum Dots

Pawel Hawrylak [1*]

[1] *Quantum Theory Group*
Emerging Technologies Division
National Research Council of Canada,
Ottawa, Ontario, Canada K1A 0R6

We describe here recent theoretical and experimental results on both lateral gated and self-assembled semiconductor quantum dots and on graphene quantum dots. Using LCHO-CI, extended Hubbard, CI and DMRG methods we describe lateral quantum dot molecules with controlled electron numbers in each dot and discuss potential use of such molecules as building blocks of a field effect transistor with a macroscopic quantum state based on artificial Haldane gap material, of a coded qubit based on chirality, GHZ maximally entangled state and Berry's phase generators[1]. We also describe topological phases driven solely by e-e interactions in a quadruple quantum dot molecule[2] and by spin orbit interaction in InAs [3] and HgTe based quantum dots[4]. We next turn to CdTe quantum dots containing single magnetic ions and discuss quantum interference and Kondo-like effects in fine structure of Mn ions interacting with excitons[5] and bi-excitons[6]. Finally, we describe one atom thick semiconductor quantum dots made of graphene and compare them with semiconductor quantum dots. Using a combination of DFT, tb, HF, CI and GW-BSE approaches we show that their electronic, optical and magnetic properties can be engineered by the size, shape, type of edge, topology and number of layers [7-11]. We focus on their optical and magnetic properties, and their control with external gate, carrier density, electric field and light. A possibility of realizing a fully integrated carbon-only quantum circuit will be discussed.

* in collaboration with Marek Korkusinski, Devrim Guclu, Pawel Potasz, Isil Ozfidan, Ania Trojnar, Yun-Pil Shim, Chang-Yu Hsieh and Marek Grabowski

[1] C-Y. Hsieh, Y.P. Shim. M. Korkusinski and P. Hawrylak, Rep. Prog. Phys. **75**, 114501 (2012).
[2] I.Ozfidan,A.Trojnar,M.Korkusinski and P.Hawrylak,(to be published).
[3] M. F. Doty, J. I. Climente, M. Korkusinski, M. Scheibner, A. S. Bracker, P. Hawrylak, and D. Gammon, Phys. Rev. Lett. **102**, 047401 (2009).
[4] M.Korkusinski and P.Hawrylak (to be published).
[5] A. Trojnar, M. Korkusi´nski, E. Kadantsev, P. Hawrylak, M.Goryca, T. Kazimierczuk, P. Kossacki, P. Wojnar, and M. Potemski, Phys. Rev. Lett. 107, 207403 (2011).
[6] A. H. Trojnar, M. Korkusinski, U.C. Mendes, M.Goryca, M. Koperski, T. Smolenski, P. Kossacki, P.Wojnar, and P.Hawrylak, Phys.Rev.B87, 205311 (2013).
[7] A.D. Guclu, P. Potasz, O. Voznyy, M. Korkusinski, P. Hawrylak, Phys.Rev.Letters, **103**, 246805 (2009).
[8] A. D. Güçlü, P. Potasz and P. Hawrylak, Phys. Rev. B 84, 035425 (2011).
[9] P. Potasz, A. D. Güçlü , A.Wojs and P. Hawrylak, Phys. Rev. B **85**, 075431 (2012).
[10] D.Guclu and P.Hawrylak, Phys. Rev**. B**87, 035425 (2013).
[11] D.Guclu, M.Grabowski and P.Hawrylak, Phys.Rev. **B**87, 035435 (2013).

Monday
Tuesday
Wednesday
Thursday
Friday

II-VI Diluted Magnetic Semiconductor Nanostructures for Spintronic Research

T. Wojtowicz

Institute of Physics, Polish Academy of Sciences, Al. Lotników 32/46, 02-668 Warsaw, Poland

Monday Tuesday Wednesday Thursday Friday

II-Mn-VIs are the best known and most thoroughly studied members of diluted magnetic semiconductors (DMSs) family, however, their modern applications in spintronic research was limited by the unavailability of appropriate nanostructures with sufficient quality. On the other hand one of the main advantages of II-Mn-VIs is that Mn in this class of materials is isoelectronic and does not lead to any drastic reduction of carrier mobility, as opposite to the case of III-Mn-Vs, where Mn in an acceptor.

In my talk I will review recent progress and present brief history of the spin related research performed on II-Mn-Te nanostructures produced in the Institute of Physics of the Polish Academy of Science in Warsaw. This will cover two-, one- and zero-dimensional nanostuctures based on ZnMnTe and CdMnTe DMSs.

I will start by shortly presenting the results on MBE technology and studies of CdMnTe self-assembled quantum dots and ZnMnTe-based nanowire structures produced with the use of gold-assisted vapor-liquid-solid growth mechanism [1].

Then I will concentrate on recent progress in MBE technology of telluride nanostructures containing two dimensional electron gas (2DEG) that lead to the observation of fractional quantum Hall effect not only in nonmagnetic CdTe quantum wells [2], but also for the first time ever in magnetic system (based on CdMnTe) [3]. This, interesting by itself, opens new perspective for the applications of such II-VI DMS nanostructures in both basic and applied research in the field of spintronics. After shortly describing the technological steps undertaken to bring the quality of MBE-grown CdMnTe nanostructures to the current level, I will discuss already demonstrated applications of such high mobility magnetic-2DEG for:

- THz and microwave radiation induced zero-bias generation of pure spin currents and very efficient magnetic field induced conversion of them into spin polarized electric current [4].
- Clear demonstration of THz radiation from spin-waves excited in DMS via efficient Raman generation process [5].
- Experimental demonstration of working principles of a new type of spin transistor based on controlling the spin transmission via tunable Landau-Zener transitions in spatially modulated spin-split bands [6].
- Unambiguous observation and quantitative determination of an enhancement of spin-orbit field in collective spin excitations [7].

The research was partially supported by National Centre of Science (Poland) grant DEC-2012/06/A/ST3/00247 and by the European Union within European Regional Development Funds, through the Innovative Economy Grant POIG.01.01.02-00-008/08.

[1] W. Zaleszczyk *et al.*, Nano Lett. **8**, 4061 (2008); P. Wojnar *et al.*, Nano Lett. **12**, 3404 (2012).
[2] B. A. Piot *et al.*, Phys. Rev. B **82**, 081307(R) (2010).
[3] C. Betthausen *et al.*, submitted.
[4] S. D. Ganichev *et al.*, Phys. Rev. Lett. **102**, 156602 (2009); C. Drexler *et al.*, Appl. Phys. Lett. **97**, 182107 (2010); P. Olbrich *et al.*, Phys. Rev. B **86**, 085310 (2012).
[5] R. Rungsawang *et al.*, Phys. Rev. Lett. **110**, 177203 (2013).
[6] C. Betthausen *et al.*, Science **337**, 324 (2012).
[7] F. Baboux *et al.*, Phys. Rev. B **87**, 121303(R) (2013).

FriPlenary4

2D atomic crystals and their heterostructures

Konstantin S. Novoselov

School of Physics & Astronomy, University of Manchester, Oxford Road, Manchester, M13 9PL, UK

Probably the most important "property" of graphene is that it has opened a floodgate of experiments on many other 2D atomic crystals: $NbSe_2$, TaS_2, MoS_2, etc. One can use similar strategies to those applied to graphene and obtain new materials by mechanical or liquid phase exfoliation of layered materials or CVD growth. An alternative strategy to create new 2D crystals is to start with an existing one (like graphene) and use it as an atomic scaffolding to modify it by chemical means (graphane and fluorographene are good examples). The resulting pool of 2D crystals is huge, and they cover a massive range of properties: from the most insulating to the most conductive, from the strongest to the softest.

If 2D materials provide a large range of different properties, sandwich structures made up of 2, 3, 4 … different layers of such materials can offer even greater scope. Since these 2D-based heterostructures can be tailored with atomic precision and individual layers of very different character can be combined together, - the properties of these structures can be tuned to study novel physical phenomena (Coulomb drag, Hostadter butterfly, metal-insulator transition, etc) or to fit an enormous range of possible applications, with the functionality of heterostructure stacks is "embedded" in their design (tunnelling or hot-electron transistors, photovoltaic devices).

Author Index

H

I